



TECHNISCHE UNIVERSITÄT MÜNCHEN

Lehrstuhl für Technische Mikrobiologie

**Interaction between *Lactobacillus hordei*, *Lactobacillus nagelii* and *Saccharomyces cerevisiae* isolates from water kefir**

Di Xu

Vollständiger Abdruck der von der Fakultät Wissenschaftszentrum Weihenstephan für Ernährung, Landnutzung und Umwelt der Technischen Universität München zur Erlangung des akademischen Grades eines

Doktors der Naturwissenschaften

genehmigten Dissertation.

Vorsitzender: Prof. Dr. Siegfried Scherer

Prüfer der Dissertation:

1. Prof. Dr. Rudi F. Vogel
2. Prof. Dr. Wolfgang Liebl

Die Dissertation wurde am 15.01.2019 bei der Technischen Universität München eingereicht und durch die Fakultät Wissenschaftszentrum Weihenstephan für Ernährung, Landnutzung und Umwelt am 18.03.2019 angenommen.

## **ACKNOWLEDGEMENTS**

This thesis was carried out under the supervision of Prof. Dr. Rudi F. Vogel and Dr. Jürgen Behr at the Lehrstuhl für Technische Mikrobiologie, Technische Universität München. I am most sincerely grateful to Prof. Dr. Rudi F. Vogel, who gave me an opportunity for achieving my PhD and a great number of supports in forming scientific thinking and writing. Thus, I benefit a lot for my future career and my life. Also, I would like to gratefully thank my supervisor Dr. Jürgen Behr who helped me a lot with the research design and provided many insightful discussions and suggestions about my research project throughout the doctoral period.

Many thanks to Dr. Frank Jakob for creating a cooperative study with Dr. Daniel Wefers from the Karlsruhe Institute of Technology and for their help in eventually publishing my first manuscript.

I would like to thank Julia Bechtner for the cooperation with manuscripts. Many thanks to Dr. Andreas J. Geißler and Lara Eisenbach for their help in processing my data of genomics and proteomics.

I would like to extend my thanks to Prof. Dr. Ludwig Niessen, Prof. Dr. Matthias Ehrmann, all my colleagues and technical assistants. Many thanks to Angela Seppour who is friendly to help on the daily routine. Special thanks to Jie Luo and Zhen Peng for their company when I arrived in Freising, and Roman Prechtel and Evelin Wigmann for the best company during the PhD period. Many thanks to Roman Prechtel for correcting the German summary in thesis as well.

In particular, I am most sincerely grateful to my parents for dual spiritual and financial support. It was their encouragement inspired me to achieve my PhD. Also, special thanks to Prof. Dr. Hua Wei and all my best friends, like Hui Wang, Xiang Lu, Dr. Xiuxiu Wu, Yue Li, Dr. Zhu Liu and Yuhong Mao etc. for your concern.

Gratefully thanks to China Scholarship Council for providing scholarship to afford four years in accomplishing my PhD thesis.

# CONTENT

<b>ACKNOWLEDGEMENTS .....</b>	<b>I</b>
<b>CONTENT.....</b>	<b>III</b>
<b>LIST OF PUBLICATIONS INCLUDED IN THIS THESIS.....</b>	<b>V</b>
<b>SUMMARY .....</b>	<b>VI</b>
<b>ZUSAMMENFASSUNG .....</b>	<b>IX</b>
<b>1. INTRODUCTION .....</b>	<b>1</b>
<b>1.1 Water kefir.....</b>	<b>1</b>
1.1.1 The origin of water kefir .....	1
1.1.2 The diversity of water kefir.....	1
<b>1.2 Metabolism of water kefir consortium .....</b>	<b>3</b>
<b>1.3 Polysaccharides of water kefir .....</b>	<b>6</b>
<b>2. MOTIVATION AND APPROACH.....</b>	<b>7</b>
<b>3. MATERIAL AND METHODS.....</b>	<b>9</b>
<b>3.1 Strains, medium and pre-culture condition.....</b>	<b>9</b>
3.1.1 Water kefir medium (WKM).....	10
3.1.2 Sucrose-MRS medium.....	10
3.1.3 Chemical defined medium (CDM).....	10
<b>3.2 Determination of cell growth and metabolites.....</b>	<b>11</b>
3.2.1 Viable cell counts .....	11
3.2.2 Chromatographic analysis of sugars and organic acids.....	12
3.2.3 Chromatographic analysis of amino acids .....	13
3.2.4 pH measurements .....	14
<b>3.3 Structural analysis of EPS .....</b>	<b>14</b>
3.3.1 EPS production activity test and isolation.....	14
3.3.2 Structural analysis of EPS via methylation analysis .....	15
3.3.3 Determination of molar mass and radius by AF4-MALS-UV.....	17
<b>3.4 Setting up a hydrophilic slide model mimicking physical contact in kefir granules.....</b>	<b>18</b>
<b>3.5 Genomics.....</b>	<b>19</b>
3.5.1 Genome sequencing.....	19
3.5.2 Genome assembly.....	19
3.5.3 Genome annotation and submission .....	20

3.5.4 Genomic statistics and visualization .....	21
<b>3.6 Proteomics.....</b>	<b>22</b>
3.6.1 Sample preparation for proteomic analysis .....	22
3.6.2 Liquid chromatography and mass spectrometry .....	23
3.6.3 Identification and quantification of peptides and proteins .....	24
<b>4. RESULTS (PUBLICATIONS BASED).....</b>	<b>25</b>
<b>4.1 Manuscript 1: <i>Lactobacillus hordei</i> dextrans induce <i>Saccharomyces cerevisiae</i> aggregation and network formation on hydrophilic surfaces.....</b>	<b>25</b>
<b>4.2 Manuscript 2: Lifestyle of <i>Lactobacillus hordei</i> isolated from water kefir based on genomic, proteomic and physiological characterization.....</b>	<b>35</b>
<b>4.3 Manuscript 3: Label-free quantitative proteomic analysis reveals the lifestyle of <i>Lactobacillus hordei</i> in presence of <i>Sacchromyces cerevisiae</i>.....</b>	<b>46</b>
<b>4.4 Manuscript 4: Comparative proteomic analysis of <i>Lactobacillus nagelii</i> and <i>Lactobacillus hordei</i> in the presence of <i>Saccharomyces cerevisiae</i> isolated from water kefir .....</b>	<b>87</b>
<b>5. MAIN FINDINGS .....</b>	<b>146</b>
<b>6. DISCUSSION .....</b>	<b>147</b>
6.1 Sugar transport and metabolism .....	147
6.2 Pyruvate and citrate metabolism.....	149
6.3 Peptide transport systems and peptidases, amino acids biosynthesis and metabolism.....	152
6.4 Acid tolerance by ADI pathway.....	155
6.5 Fatty acid biosynthesis and riboflavin metabolism .....	156
6.6 The role of <i>L. hordei</i> dextrans for granule formation.....	157
<b>LIST OF PUBLICATIONS DERIVED FROM THIS WORK .....</b>	<b>159</b>
<b>CURRICULUM VITAE .....</b>	<b>161</b>
<b>REFERENCES.....</b>	<b>162</b>

## LIST OF PUBLICATIONS INCLUDED IN THIS THESIS

**Di Xu**, Lea Fels, Daniel Wefers, Jürgen Behr, Frank Jakob, Rudi F. Vogel., 2018. *Lactobacillus hordei* dextrans induce *Saccharomyces cerevisiae* aggregation and network formation on hydrophilic surfaces. International Journal of Biological Macromolecules 115, 236–242.

**Di Xu**<sup>#</sup>, Julia Bechtner<sup>#</sup>, Jürgen Behr, Lara Eisenbach, Andreas J. Geißler, Rudi F. Vogel., 2019. Lifestyle of *Lactobacillus hordei* isolated from water kefir based on genomic, proteomic and physiological characterization. International Journal of Food Microbiology 290, 141–149.

**Di Xu**, Jürgen Behr, Andreas J. Geißler, Christina Ludwig, Rudi F. Vogel., 2019. Label-free quantitative proteomic analysis reveals the lifestyle of *Lactobacillus hordei* in presence of *Sacchromyces cerevisiae*. International Journal of Food Microbiology. Accepted.

Julia Bechtner<sup>#</sup>, **Di Xu**<sup>#</sup>, Jürgen Behr, Rudi F. Vogel., 2019. Comparative proteomic analysis of *Lactobacillus nagelii* and *Lactobacillus hordei* in the presence of *Saccharomyces cerevisiae* isolated from water kefir. Frontiers in Microbiology. Under review.

#joint first authorship

## SUMMARY

Water kefir is a slightly alcoholic and traditionally fermented beverage, which is generally fermented by lactic acid bacteria (LAB), acetic acid bacteria and yeasts. Homemade water kefir is usually prepared from sucrose, water, kefir grains, and dried or fresh fruits (e.g. figs) after 2-3 d of fermentation. *Lactobacillus (L.) hordei*, *L. nagelii* and *Saccharomyces (S.) cerevisiae* are respectively predominant and stable species of LAB and yeasts, which have been typically isolated from water kefir consortia. In contrast to sucrose, which is abundant in water kefir, amino- and fatty acids are lacking in this environment. Therefore, the lifestyles of *L. hordei* and *L. nagelii* were predicted and constructed via label-free quantitative proteomic analysis combined with genomic analysis and physiological characterization. Analysis of the genomic sequence of *L. hordei* TMW 1.1822 and *L. nagelii* TMW 1.1827 demonstrated that each strain contained three plasmids in addition to the chromosomal DNA. The sizes of the bacterial chromosomes were 2.42 Mbp and 2.41 Mbp, respectively, which lay in the typical range of LAB. Although the genome size was similar, *L. nagelii* TMW 1.1827 exhibited a total number of 2391 coding sequences (CDS), while *L. hordei* TMW 1.1822 featured 70 CDS more. Further, 1243 proteins of *L. nagelii* and 1474 proteins of *L. hordei* were respectively identified and quantified by proteomic analysis upon growth in water kefir medium. Thus, it provided the possibility of tracing metabolic activity of *L. hordei* and *L. nagelii*. Prediction of metabolic pathways of *L. hordei* and *L. nagelii* revealed the presence of all enzymes, which were required for the glycolytic Embden-Meyerhof (EMP) and phosphoketolase (PK) pathways. The genes encoding enzymes, which were involved in the metabolism of citrate, pyruvate and mannitol, were expressed as well. The

genomic analysis of *L. nagelii* revealed the prototrophy for 13 amino acids and auxotrophy for 7 amino acids. The same results were obtained for *L. hordei*, except for 3-deoxy-7-phosphoheptulonate synthase, which was additionally missing in this organism. Therefore, only *L. nagelii* was capable of producing tyrosine. Peptide transport system, arginine deiminase (ADI) pathway, and fatty acid synthesis were further predicted to enable the lifestyle of *L. hordei* and *L. nagelii*. Like *L. hordei*, *L. nagelii* also encoded the complete oligopeptide transport system OppABCDF. In the lack of FabB, unsaturated fatty acids may be therefore synthesized by predicted alternative enzymes of *L. hordei* TMW 1.1822. Also *L. nagelii* TMW 1.1827 appeared to be lacking in FabB and, additionally in FabA.

Since the growth of *L. hordei* and *L. nagelii* was improved in co-cultivation with *S. cerevisiae*, quantitative comparative proteomics was performed to investigate the interaction between LAB and yeast, and reveal real-time metabolic exchange in water kefir. In the presence of *S. cerevisiae*, 73 proteins were significantly differentially expressed (DE) in *L. nagelii* TMW 1.1827 as compared to 233 DE proteins in *L. hordei* TMW 1.1822. The down-regulated 3-phosphoglycerate mutase in *L. nagelii* indicates, that intermediates of early glycolytic steps may be used for other metabolic reactions or hexoses may rather enter PKP or PPP than EMP. However, the expression of glucose-6-phosphate dehydrogenase, which is part of the PKP and PPP, was significantly up-regulated in *L. hordei*. Thus, both microorganisms appeared to favor PKP over EMP. The changes in the carbohydrate metabolism revealed that *L. hordei* and *L. nagelii* displayed antidromic strategies to maintain  $\text{NAD}^+/\text{NADH}$  homeostasis after the metabolic switch



induced by *S. cerevisiae*. Furthermore, nine up-regulated enzymes involved in amino acid metabolism suggested that *S. cerevisiae* released glutamine, histidine, methionine and arginine, which were subsequently used by *L. nagelii* to ensure its survival in the water kefir consortia. However, up-regulation of the OppABCDF peptide transport system and sixteen enzymes involved in amino acid metabolism in *L. hordei* indicated enhanced peptide uptake, as well as the feeding of glutamate, glutamine, histidine, methionine, arginine, tryptophan and proline from *S. cerevisiae*. In addition, only the ADI pathway in *L. hordei* was significantly up-regulated, which alleviated acid stress and concomitantly protected *S. cerevisiae* against an acidic environment, which *L. hordei* generated in single culture. While *L. hordei* reacted with an enhanced utilization of citrate in co-culture with *S. cerevisiae*, *L. nagelii* profited from riboflavin, most likely secreted by the yeast.

Abundant sucrose in water kefir was consumed directly via parallel EMP and PK pathways, and was also extracellularly converted to glucan and fructose by a glucansucrase, leaving fructose as additional carbon source in *L. hordei* and *L. nagelii*. So far, factors, which promoted aggregation, i.e. formation of a specific glucan or bifunctional enzymes, were only detected in *L. hordei*. It induced the aggregation of *S. cerevisiae*, as well as the network formation on hydrophilic surfaces and was thus crucial for the stepwise growth of the water kefir granule. In summary, our study suggested *L. hordei* appeared to react more distinct to the presence of *S. cerevisiae* than *L. nagelii*.

## ZUSAMMENFASSUNG

Wasserkefir ist ein leicht alkoholisches und traditionell fermentiertes Getränk, das üblicherweise durch Milchsäurebakterien, Essigsäurebakterien und Hefen fermentiert wird. Selbst gemachter Wasserkefir wird gewöhnlich aus Saccharose, Wasser, Kefirkörnern und getrockneten oder frischen Früchten (z. B. Feigen) nach 2-3 Tagen Fermentation hergestellt. *Lactobacillus (L.) hordei*, *L. nagelii* und *Saccheromyces (S.) cerevisiae* sind jeweils vorherrschende Spezies von Milchsäurebakterien und Hefen, die typischerweise aus Wasserkefir-Konsortien isoliert werden. Im Gegensatz zu Saccharose, die im Überfluss vorhanden ist, enthält Wasserkefir jedoch kaum Amino- und Fettsäuren. Deshalb wurden die Lebensstile von *L. hordei* und *L. nagelii* durch markierungsfreie, quantitative Proteom-Analyse in Kombination mit einer Genomanalyse sowie physiologischer Charakterisierung vorhergesagt und konstruiert. Die Analyse der Genomsequenz von *L. hordei* TMW 1.1822 und *L. nagelii* TMW 1.1827 zeigte, dass jeder Stamm neben der chromosomalen DNA drei Plasmide enthielt. Die Größen der bakteriellen Chromosome lag mit 2,42 Mbp bzw. 2,41 Mbp in einem für Milchsäurebakterien typischen Bereich. Obwohl die Genomgrößen ähnlich waren, wies *L. nagelii* TMW 1.1827 eine Gesamtzahl von 2391 kodierenden Sequenzen auf, während *L. hordei* TMW 1.1822 70 weitere kodierende Sequenzen enthielt. Ferner wurden 1243 Proteine von *L. nagelii* und 1474 Proteine von *L. hordei* identifiziert und durch Proteomanalyse nach Wachstum in Wasserkefir Medium quantifiziert. Somit bot sich die Möglichkeit, die metabolische Aktivität von *L. hordei* und *L. nagelii* zu rekonstruieren. Die Vorhersage der metabolischen Stoffwechselwege von *L. hordei* und *L. nagelii* belegte die Anwesenheit aller Enzyme, die für den (glykolytischen) Embden-Meyerhof

(EMP)- und Phosphoketolase (PK)-Weg erforderlich sind. Darüber hinaus wurden auch diejenigen Gene exprimiert, die für Enzyme kodieren, die am Metabolismus von Citrat, Pyruvat und Mannit beteiligt sind. Die Genomanalyse von *L. nagelii* belegte außerdem die Prototrophie für 13 Aminosäuren, während für 7 Aminosäuren eine Auxotrophie bestand. Dies zeigte sich auch für *L. hordei*, wobei in diesem Organismus zusätzlich das Enzym 3-Desoxy-7-phosphoheptulonatsynthase fehlte. Daher war nur *L. nagelii* in der Lage, Tyrosin zu synthetisieren. Es wurde weiterhin vorhergesagt, dass das Peptid Transportsystem, der Arginin-Deiminase-Weg (ADI) und die Fettsäuresynthese den Lebensstil von *L. hordei* und *L. nagelii* ermöglichen. Wie *L. hordei* kodierte auch *L. nagelii* für das vollständige Oligopeptidtransportsystem OppABCDF. Ohne FabB können ungesättigte Fettsäuren daher durch vorhergesagte alternative Enzyme von *L. hordei* TMW 1.1822 synthetisiert werden. Auch *L. nagelii* TMW 1.1827 fehlten anscheinend die Enzyme FabB und zusätzlich FabA.

Da das Wachstum von *L. hordei* und *L. nagelii* bei der Co-Kultivierung mit *S. cerevisiae* verbessert wurde, wurden quantitative vergleichende Proteomik durchgeführt, um die Wechselwirkung zwischen Milchsäurebakterien und Hefe zu untersuchen und den Stoffwchelaustausch in Wasserkefir in Echtzeit aufzuzeigen. In Gegenwart von *S. cerevisiae* wurden in *L. nagelii* TMW 1.1827 73 Proteine signifikant unterschiedlich exprimiert, während in *L. hordei* TMW 1.1822 233 unterschiedlich exprimierter Proteine identifiziert wurden. In Gegenwart von *S. cerevisiae* wechselte *L. hordei* TMW 1.1822 vom EMP zum PK-Weg, wodurch Gluconat gebildet wurde, da die Expression von Glucose-6-phosphat-Dehydrogenase hochreguliert wurde. Die herunterregulierte 3-

Phosphoglycerat-Mutase in *L. nagelii* deutet darauf hin, dass Intermediate früher glykolytischer Schritte für andere Stoffwechselreaktionen verwendet werden können oder Hexosen eher in PKP oder PPP als EMP eintreten. Die Expression von Glucose-6-phosphat-Dehydrogenase, die Teil von PKP und PPP ist, wurde jedoch in *L. hordei* signifikant hochreguliert. Daher schienen beide Mikroorganismen PKP gegenüber EMP zu bevorzugen. Die Veränderungen im Kohlenhydratstoffwechsel, dass *L. hordei* und *L. nagelii* antidrome Strategien zeigten, um die  $\text{NAD}^+ / \text{NADH}$  Homöostase nach dem durch *S. cerevisiae* induzierten metabolischen Wechsel aufrechtzuerhalten. Darüber hinaus deuteten neun am Aminosäuremetabolismus beteiligte hochregulierte Enzyme an, dass *S. cerevisiae* Glutamin, Histidin, Methionin und Arginin freisetzt, die anschließend von *L. nagelii* verwendet wurden, um das Überleben in den Wasserkefir-Konsortien sicherzustellen. Die Hochregulierung des OppABCDF-Peptidtransport-Systems und von sechzehn Enzymen, die am Aminosäuremetabolismus von *L. hordei* beteiligt sind, zeigten jedoch eine erhöhte Peptidaufnahme sowie den Bezug von Glutamat, Glutamin, Histidin, Methionin, Arginin, Tryptophan und Prolin von *S. cerevisiae*. Darüber hinaus war nur der ADI-Weg in *L. hordei* signifikant hochreguliert, was den Säurestress abschwächte und gleichzeitig *S. cerevisiae* vor einer sauren Umgebung schützte, die *L. hordei* in einer Einzelkultur erzeugte. Während *L. hordei* in Co-Kultur mit *S. cerevisiae* Citrat verstärkt verstoffwechselte, profitierte *L. nagelii* von Riboflavin, das höchstwahrscheinlich von der Hefe abgegeben wurde.

Die reichlich vorhandene Saccharose in Wasser-Kefir wurde parallel mittels EMP- und PK-Weg verstoffwechselt und zudem extrazellulär durch eine Glucansucrase zu Glucan und Fruktose umgewandelt, wobei Fruktose als zusätzliche Kohlenstoffquelle für *L.*

*hordei* und *L. nagelii* diene. Bisher wurden Faktoren, die eine Aggregation fördern, d.h. die Bildung eines spezifischen Glucans und bifunktionelle Enzyme, nur in *L. hordei* nachgewiesen. Dies induzierte die Aggregation von *S. cerevisiae*, sowie die Netzwerkbildung auf hydrophilen Oberflächen und war somit entscheidend für das schrittweise Wachsen der Kefir-Granulen. Zusammenfassend verdeutlichte unsere Studie, dass *L. hordei* auf die Anwesenheit von *S. cerevisiae* unterschiedlicher zu reagieren schien als *L. nagelii*.

# **1. INTRODUCTION**

## **1.1 Water kefir**

### **1.1.1 The origin of water kefir**

Water kefir is a traditional fermented beverage, which is mostly made from sucrose, water, kefir grains, and dried or fresh fruits (e.g. figs). Traditionally, homemade water kefir is fermented for two or three days at room temperature, afterwards the kefir grains are removed by sieving. The supernatant results in slightly acidic, sweet and alcoholic drink with yellowish color and fruity aroma. However, the exact origin of water kefir grains remains unknown. First description of grains based beverage fermented with yeast and bacteria was called “Ginger-beer Plant”. It was brought to Europe by British soldiers from the Crimean war in 1855 (Ward, 1891). Another original description on the grains (called Tibi) was formed from the material called “Opuntia” which is a type of Mexican cacti (Lutz, 1899). Subsequently various grain beverages are emerged and known as “California bees”, “African bees”, “Tibi grains”, or “Sugary kefir grains” (Horisberger, 1969; Kebler, 1921; Pidoux, 1989). In the present study, the sugary kefir grains are called water kefir in order to differentiate them from milk kefir grains.

### **1.1.2 The diversity of water kefir**

Until now, most studies on water kefir focus on the microbial diversity of water kefir consortia. Different sources of water kefir display different species diversities, but the microbiota isolated from water kefir grains comprise a stable multispecies consortium, which generally consists of lactic acid bacteria (LAB), acetic acid bacteria (AAB) and yeasts (Gulitz et al., 2013; Gulitz et al., 2011; Laureys and De Vuyst, 2014; Marsh et al.,

2013; Martínez - Torres et al., 2017; Neve and Heller, 2002; Ward, 1891). In earlier studies, the bacterial population of sugary kefir grains were identified as lactobacilli, leuconostocs and sometimes pediococci, while yeast isolated from the sugary grains were mainly *Saccharomyces (S.) cerevisiae*, *S. florentinus*, *S. pretoriensis*, *Hanseniaspora valbyensis* (Galli et al., 1995; Leroi and Pidoux, 1993; Neve and Heller, 2002).

Recently, the microbial species diversity and community dynamics of water kefir fermentation have been well identified. The majority ecosystem present in homemade water kefir, in which grains were obtained from a private person, who cultivated water kefir at home in Ghent, Belgium, was found to be *Lactobacillus (L.) casei/paracasei*, *L. hilgardii*, *L. harbinensis*, *L. nagelii*, *L. hordei/mali* (in decreasing order), of which the first 3 species were most dominant LAB, besides *Bifidobacterium psychraerophilum/crudilactis*, *S. cerevisiae*, and *Dekkera bruxellensis* during 192 h fermentation (Laureys and De Vuyst, 2014). Meanwhile, a novel *Bifidobacterium aquikefiri* sp. was also isolated from a household water kefir in Belgium (Laureys et al., 2016). While a traditional Mexican water kefir grain indicated the presence of seven bacterial species, including *L. ghanensis*, *L. casei/paracasei*, *L. hilgardii*, *Pseudoarthrobacter chlorophenolicus*, *Acetobacter (A.) orientalis*, *A. tropicalis* and *A. okinawensis* as well as three yeasts, namely *S. cerevisiae*, *Candida (C.) californica* and *Pichia (P.) membranifacien*. *S. cerevisiae* was detected both in the supernatant with the populations of approximately  $10^5$ - $10^6$  CFU mL<sup>-1</sup> and in grains with approximately  $10^7$ - $10^8$  CFU g<sup>-1</sup>, while *L. hilgardii* was only isolated from water kefir grains (Martínez - Torres et al., 2017). In another study, the bacterial profile of water kefir was dominated by *Zymomonas* with a minor presence of *Acetobacter* and *Gluconacetobacter*, while the

yeast composition was constituted by *Dekkera*, *Hanseniaspora*, *Saccharomyces*, *Zygosaccharomyces*, *Torulaspota* and *Lachancea* based on 16S rRNA sequencing analysis from four water kefir sourced from UK, Canada and the United States (Marsh et al., 2013).

Gulitz et al (Gulitz et al., 2011) also analyzed the microbial consortia of three water kefir granules from different long-term traditional household preparations in Germany by 16S rRNA gene amplicon sequencing. The predominant bacterial genus in water kefir I and II was *Lactobacillus*, which accounted for 82.1 % in water kefir I and 72.1 % in water kefir II. More specifically, the most abundant species of *Lactobacillus* were *L. hordei* and *L. nagelii* followed by *L. casei*, *Leuconostoc (Lc.) mesenteroides*, *Lc. citreum* and *L. hilgardii*. In water kefir III, however, *Lc. mesenteroides*, *Lc. citreum* and *Acetobacter* species were more prevalent. While the predominant yeast in all three water kefir was *S. cerevisiae* and *Zygotorulaspota (Z.) florentina*. Further, the genus *Bifidobacterium* was found in all four water kefir obtained from home-made in Germany (Gulitz et al., 2013). According to the yeast diversity results from all different water kefir isolates, strains of *S. cerevisiae* were predominant in all studies. Strains of *L. hordei* and *L. nagelii* were among the most commonly isolated LAB from water kefir (Gulitz et al., 2011; Laureys and De Vuyst, 2014) which are further studied in this thesis.

## **1.2 Metabolism of water kefir consortium**

In contrast to milk kefir, which has been studied widely, the metabolism of LAB and other microorganisms in the water kefir consortium is restricted to a few recent studies.



As sucrose was the main nutrient of the water kefir medium, it turned out that it was completely converted after 24 h fermentation, which coincided with the production of polysaccharide. The major metabolites produced by the microbial dynamics during 192 h fermentation were lactic acid and ethanol. Glycerol, acetic acid, and mannitol were detected in low concentrations after 72 h of fermentation. Mannitol formation suggested the use of fructose not only as carbon source but also as electron acceptor by other members of the consortium. In addition, the most prevailing volatile aroma compounds were found to be ethyl acetate, isoamyl acetate, ethyl hexanoate, ethyl octanoate, and ethyl decanoate (Laureys and De Vuyst, 2014). Further, Laureys et al explored the water kefir fermentation respectively with dried figs, apricots and raisins as different nutrient source at different concentration and in the presence/absence of oxygen (Laureys et al., 2018).

Water kefir fermentation with raisins resembled fermentation in low nutrient concentration, which facilitated the growth of *L. hilgardii* and *Dekkera bruxellensis*. Whereas water kefir fermentation with fresh figs resembled fermentation in high nutrient concentration, which favored the growth of *L. nagelii* and *S. cerevisiae*. It is in accordance with the result showing that *L. nagelii* and *S. cerevisiae* dominate in water kefir with figs added as nutrient (Gulitz et al., 2011). Water kefir fermentation with dried apricots resembled fermentation under normal nutrient concentration. The presence of oxygen allowed the proliferation of AAB, resulting in high concentration of acetic acid.

Martínez-Torres et al reported on carbon utilization performed with ten bacteria (six *Acetobacter* spp., three *Lactobacillus* spp. and *Pseudoarthrobacter chlorophenicus*)

and twenty-two yeasts (nineteen *S. cerevisiae*, two *C. californica* and one *P. membranaefaciens*) during Mexican water kefir fermentation (Martínez - Torres et al., 2017). Three main metabolic products, namely lactic acid, acetic acid and ethanol were evaluated during a traditional 192 h fermentation. After 24 h, lactic and acetic acid were postulated to be initially generated by *L. hilgardii* and subsequently accumulated by *Acetobacter* spp., mainly *A. tropicalis*, while ethanol was mainly produced by *S. cerevisiae* but not by *C. californica* and *P. membranaefaciens*. Ethanol had been gradually diminished from 144 h to 192 h in water kefir fermentation and it was assumed to be oxidized to acetic acid by *Acetobacter* spp. Those previous studies investigated either the total dynamic metabolites of water kefir fermentation of microbial groups or inferred the contribution of one specific strain to water kefir fermentation via single cultivation in water kefir supernatants. However, it is difficult to reproduce the immediate and dynamic metabolic exchanges between specific species in complex water kefir community since metabolites produced by an organism are immediately consumed by another organism living in close proximity.

Stadie et al (Stadie et al., 2013) explored the metabolic interaction between LAB (*L. nagelii* and *L. hordei*) and yeasts (*S. cerevisiae* and *Z. florentina*), which were predominant in water kefir (Gulitz et al., 2011). The cell yield of each co-cultivated LAB and co-cultivated yeast was significantly increased compared with single-cultivation of each respective organism through a Transwell co-culture model system. Particularly, *Z. florentina* appreciated the pH decrease caused by the production of lactic acid, but not *S. cerevisiae*. This study suggested that the growth of *L. hordei* TMW 1.1822 should be improved by nutrients produced by yeast, such as amino acids for which *L. hordei* was

auxotrophic (isoleucine, leucine, methionine, phenylalanine, tryptophan, tyrosine and valine) as well as vitamin B6. Whereas the growth increase of *L. nagelii* TMW 1.1825 was referred to the release of amino acids which *L. nagelii* is auxotrophic for by the yeast, as well as additional arginine, which is released by *Z. florentina*. To elucidate the specific contributions of water kefir species at a molecular level, further investigations are still necessary due to the complexity of their communities and intrinsically dynamic nature.

### **1.3 Polysaccharides of water kefir**

Polysaccharides that are excreted extracellularly by many bacteria are called exopolysaccharide (EPS) usually with high molecular weight. The first description of microbial polysaccharides, which formed slimy structures grown on sucrose-containing medium, was made in 1839 (Jay, 1992). The kefir grains matrix is mainly constructed from EPS, which is produced by embedded microorganisms in water kefir fermentation. The backbone of this granule matrix has been suggested to be primarily made from dextran produced by *L. hilgardii* cells (Davidović et al., 2015; Fels et al., 2018; Horisberger, 1969; Neve and Heller, 2002; Pidoux et al., 1990; Waldherr et al., 2010). This dextran was a complex branched glucan generated by dextransucrases from sucrose. It contained consecutive  $\alpha$ -1,6-linkages between glucose molecules in its straight chains, which generally made up more than 50 % of the total linkages (Naessens et al., 2005; Neve and Heller, 2002; Tingirikari et al., 2014). Besides, it consisted of different portions of side chains, namely  $\alpha$ -1,3-,  $\alpha$ -1,4- and  $\alpha$ -1,2-branched linkages.

The EPS fraction of water kefir supernatant is predominantly composed of *O*<sub>3</sub>- and *O*<sub>2</sub>-branched dextrans as well as lower amounts of levans (Fels et al., 2018). In addition, some LAB species, such as *L. hordei*, *L. nagelii*, *Lc. mesenteroides/citreum* isolated from water kefir were able to produce EPS (Davidović et al., 2015; Gulitz et al., 2011). However, the structural composition of these EPS-producing LAB have not been analyzed yet. Still, it remains unknown how other bacteria (besides *L. hilgardii*) and yeasts become embedded into the kefir granule and formed this polysaccharide network.

## **2. MOTIVATION AND APPROACH**

In thesis the contribution of exopolysaccharide formation and metabolic interaction between lactobacilli and yeasts should be evaluated for the formation of the water kefir consortium and granule. Specifically the following working hypotheses should be tested:

- Exopolysaccharide formation played a major role in the physical interaction and establishment of space proximity of lactobacilli and yeasts.
- Specific exopolysaccharides can be found, which promote the network formation of *S. cerevisiae*.
- Lifestyle of *L. hordei* and *L. nagelii* can be predicted and constructed mainly in sugar transport, carbohydrate metabolism, peptidase transport system, amino-, and fatty acid metabolism.

- Symbiotic relationships and metabolic interaction (mutualism) between lactobacilli and yeasts can be predicted from quantitative proteomics.
- *L. hordei* and *L. nagelii* display different strategies to cope with the restrictions of the water kefir environment and the presence of *S. cerevisiae*.

The following methodical approach was taken to test these hypotheses:

- A simplified model system containing hydrophilic object slides was set up to mimic physical contact in kefir granules.
- Glycosidic linkages of these glucans were determined by methylation analysis, and their size distributions were investigated via asymmetric flow field-flow fractionation coupled to multi-angle laser light scattering and UV detector.
- Lifestyle of *L. hordei* and *L. nagelii* were predicted based on genomic, proteomic and chromatographic analysis.
- Metabolic traits of lactobacilli in the presence of yeast were predicted from label-free quantitative proteomic analysis combined with physiological characterization.

### 3. MATERIAL AND METHODS

#### 3.1 Strains, medium and pre-culture condition

Six strains of LAB (namely *L. hordei* TMW 1.1822, TMW 1.1821, TMW 1.1817, TMW 1.1907, *L. nagelii* TMW 1.1827, and *Lc. citreum* TMW 2.1194) and *S. cerevisiae* TMW 3.221 isolated from water kefir by Gulitz et al (Gulitz et al., 2011) from the Technische Mikrobiologie Weihenstephan (TMW) strain collection were used in this study. The LAB from a -80 °C stock were spread directly on modified MRS (mMRS) agar plates described by Stolz et al (Stolz et al., 1995) as shown in table 1 and incubated anaerobically at 30 °C for 2 d. A single colony was transferred into 10 ml liquid mMRS medium and cultivated anaerobically for 24 h at 30 °C. While *S. cerevisiae* TMW 3.221 from a -80°C stock was spread on YPG agar plates made of peptone from casein (10 g/L), yeast extract (5 g/l), glucose (20 g/l) and 1.5 % agar and cultivated aerobically for 24 h at 30 °C. A single colony was transferred into 10ml YPG medium and cultured anaerobically at 30 °C for 24 h.

**Table 1. Composition of mMRS medium**

Medium component	Concentration (g/l)
Yeast extract	5
Meat extract	5
Peptone from casein	10
Cysteine hydrochloride	0.5
NH <sub>4</sub> Cl	3
Tween 80	1
Maltose	10
Glucose	5
Fructose	5
KH <sub>2</sub> PO <sub>4</sub>	4
K <sub>2</sub> HPO <sub>4</sub> · 3 H <sub>2</sub> O	2.6
MgSO <sub>4</sub> · 7 H <sub>2</sub> O	0.2
MnSO <sub>4</sub> · H <sub>2</sub> O	0.038
Biotin	0.2
Folic acid	0.2
Nicotinic acid	0.2
Pyridoxal-5-phosphate	0.2
Thiamine	0.2

Riboflavin	0.2
Cobalamin	0.2
Pantothenic acid	0.2

---

### 3.1.1 Water kefir medium (WKM)

WKM was prepared as described by Stadie et al. (Stadie et al., 2013). 48 g dried figs (Seeberger, Ulm, Germany) were extracted in 100 ml still mineral water (Residenz Quelle naturell, Bad Winzheim, Germany) by shaking for 20 min. Big solids were removed by sieving and the smaller parts by centrifugation (15,000 g, 3 h) and sterile filtration by Nalgene™ Rapid-Flow™ sterile disposable bottle cap filter with PES membrane (0.2 µm, Thermo Scientific, New York, USA). 80 g sucrose was dissolved in 900 ml still mineral water and mixed with the prepared fig extract. Then WKM was adjusted to pH 6.5 and filtered by Nalgene™ Rapid-Flow™ sterile disposable bottle cap filter with PES membrane (0.2 µm).

### 3.1.2 Sucrose-MRS medium

Sucrose-MRS medium was made of 80 g/l sucrose, 10 g/l peptone, 2 g/l meat extract, 4 g/l yeast extract, 1 g/l tween 80, 2.5 g/l K<sub>2</sub>HPO<sub>4</sub>·3H<sub>2</sub>O, 2 g/l (NH<sub>4</sub>)<sub>2</sub>-citrate, 5 g/l Na-Acetate·3H<sub>2</sub>O, 0.2 g/l MgSO<sub>4</sub>·7H<sub>2</sub>O, 0.038 g/l MnSO<sub>4</sub>·H<sub>2</sub>O for the EPS production.

### 3.1.3 Chemical defined medium (CDM)

*L. hordei* TMW 1.1822, *L. nagelii* TMW 1.1827 and *S. cerevisiae* TMW 3.221 were respectively grown in CDM to obtain samples for chromatographic analysis of sugar, organic acids and amino acids. CDM was prepared as shown in table 2.

**Table 2. Composition of CDM**

Medium component	Concentration (g/l)	Medium component	Concentration (g/l)
sodium acetate	5	Xanthine	0.01
KH <sub>2</sub> PO <sub>4</sub>	3	<i>p</i> -aminobenzoic acid	0.01
K <sub>2</sub> HPO <sub>4</sub> · 3 H <sub>2</sub> O	3	Thiamin	0.001
MgSO <sub>4</sub> · 7 H <sub>2</sub> O	0.2	Riboflavin	0.001
MnSO <sub>4</sub> · H <sub>2</sub> O	0.04	Niacin	0.001
FeSO <sub>4</sub> · 7 H <sub>2</sub> O	0.02	Pantothenic acid	0.001
Tween 80	1	Pyridoxal	0.002
uracil	0.01	D-Biotin	0.01
adenine	0.01	Folic acid	0.001
thymine	0.01	Cobalamin	0.001
guanine	0.01	Orotic acid	0.01
inosine	0.01	Maltose	10
L-alanine	0.1	L-histidine	0.1
L-arginine	0.1	L-isoleucine	0.1
L-asparagine	0.2	L-leucine	0.1
L-aspartic acid	0.2	L-lysine	0.1
L-cysteine	0.2	L-methionine	0.1
glycine	0.1	L-phenylalanine	0.1
L-glutamine	0.2	L-proline	0.1
L- glutamic acid	0.2	L-serine	0.1
L-threonine	0.1	L-tyrosine	0.1
L-tryptophan	0.1	L-valine	0.1

## 3.2 Determination of cell growth and metabolites

### 3.2.1 Viable cell counts

*L. hordei* TMW 1.1822 and *L. nagelii* TMW 1.1827 were pre-cultivated anaerobically at 30 °C for 24 h in mMRS medium, while *S. cerevisiae* was pre-cultivated anaerobically at 30 °C for 24 h in YPG medium. Then 1% (v/v) pre-cultured *L. hordei*, *L. nagelii* and *S. cerevisiae* were separately inoculated into 40 ml WKM in replicate as single-culture, while 1% pre-cultured *L. hordei* plus 1% *S. cerevisiae*, and 1% pre-cultured *L. nagelii* plus 1% *S. cerevisiae* were simultaneously inoculated into 40 ml WKM in replicate as co-cultivation. 100 ul aliquots were respectively taken out from each samples for plate counting at the fermentation time point of 0, 2, 4, 5, 6, 7, 8, 12, 24, and 48 h. Single-cultivated LAB samples were plated in mMRS agar, whereas single-cultivated *S. cerevisiae* samples were plated in YPG agar. Meanwhile co-cultivated LAB and *S. cerevisiae* samples were not only plated in mMRS agar with added cycloheximide (final



concertation at 0.1 g/l) to inhibit the growth of yeast for counting LAB cells in co-cultivation but also plated in YPG agar with added chloromycetin (final concertation at 0.1 g/l) to inhibit the growth of bacteria for counting *S. cerevisiae* cells in co-cultivation at the same time point of 0, 2, 4, 5, 6, 7, 8, 12, 24, and 48 h.

### **3.2.2 Chromatographic analysis of sugars and organic acids**

Sugar consumption and production of organic acids by *L. hordei* TMW 1.1822, *L. nagelii* TMW 1.1827 and *S. cerevisiae* TMW 3.221 grown in CDM after 24 h were quantified by a Dionex UltiMate 3000 HPLC system (Dionex, Idstein, Germany) with Rezex ROA-Organic Acid H<sup>+</sup> column (Phenomenex, Aschaffenburg, Germany) and RI-101 detector (Shodex, München, Germany) as described by Geißler et al (Geißler, 2016). 1% pre-cultured *L. hordei*, *L. nagelii* and *S. cerevisiae* were respectively inoculated into 10 ml CDM in triplicate and incubated anaerobically at 30 °C for 24 h. 2 ml aliquots of each sample were respectively taken out for centrifugation to obtain the supernatant. The supernatant of each sample and CDM were treated with protein precipitation as follows. 1 ml of each sample in triplicate were added with 50 µl 70 % perchloric acid (v/v) (Sigma-Aldrich, St. Louis, USA) and vortexed for mixing. After 24 h, standing at 4 °C, the mixture was centrifuged (15,000 g, 10 min) to collect the supernatant. The supernatant was filtered by 0.2 µm Phenex<sup>TM</sup> Regenerated Cellulose Membrane (Phenomenex, Aschaffenburg, Germany) and ready for the analysis of organic acids and amino acids as below. For sugar analysis, 500 µl of each sample were mixed with 250 µl of a 10 % (w/v) ZnSO<sub>4</sub>·7H<sub>2</sub>O solution and afterwards added with 250 µl 0.5 M NaOH. After incubation for 20 min at 25° C, the supernatant was obtained by centrifugation and filtered as described above. Analytes were separated at a constant flow rate of 0.7 ml/min with

column temperature of 85 °C for 30 min. Sulfuric acid (Rotipuran, Roth, Karlsruhe, Germany) solution at a concentration of 5 mM was served as mobile phase.

### 3.2.3 Chromatographic analysis of amino acids

1 % pre-cultured *L. hordei*, *L. nagelii* and *S. cerevisiae* were separately inoculated into 10 ml CDM in triplicate and incubated anaerobically at 30 °C. After 24 h, 2 ml aliquots of each sample were taken out for centrifugation (13,000 g, 10 min). Likewise, 1mL supernatants of *L. hordei*, *L. nagelii*, *S. cerevisiae* cultures and CDM were respectively mixed with 50 ul of 70 % (v/v) perchloric acid (Sigma-Aldrich, St. Louis, USA) and standing overnight at 4 °C for protein precipitation. After centrifugation (15,000 rpm, 10 min), the supernatant was diluted 1:5 in 0.1M HCl. Samples were filtered as described above. Amino acids were analyzed on a Dionex Ultimate 3000 HPLC system (Dionex, Idstein, Germany) using a Gemini C18 column (Phenomenex, Aschaffenburg, Germany) with UV detection at 338 or 269 nm. Before separation, samples were performed to pre-column derivatisation with o-phthalaldehyde-3-mercaptopropionic acid (OPA) and 9-fluorenylmethyl chloroformate (FMOC) following Bartóak et al (Bartóak et al., 1994). The eluent A was comprised of 20 mM Na<sub>2</sub>HPO<sub>4</sub>, 20 mM NaH<sub>2</sub>PO<sub>4</sub> (Merck Millipore, Billerica, USA) and 0.8 % tetrahydrofuran (Roth, Karlsruhe, Germany) at pH 7.8; and eluent B was comprised of 30 % acetonitrile, 50 % methanol (Roth, Karlsruhe, Germany) and 20 % water (Macron, Avantor, Center Valley, USA). The gradient setting was 0 min 0 % B, 16 min 64 % B, 19 min 100 % B, 22 min 100 % B and 22.25 min 0 % B as described by Schurr et al (Schurr et al., 2013) with a flow rate of 0.8 mL/min and column temperature at 40 °C.

Quantification was executed employing calibration adjustment by external HPLC grade standards of at least three different concentrations in five repeating measurements and the Chromeleon software version 6.80 (Dionex, Idstein, Germany).

#### **3.2.4 pH measurements**

After 72 h fermentation in WKM, samples of single-cultivated *L. hordei* TMW 1.1822, single-cultivated *L. nagelii* TMW 1.1827, single-cultivated *S. cerevisiae* TMW 3.221, co-cultivated *L. hordei* and *S. cerevisiae* and co-cultivated *L. nagelii* and *S. cerevisiae* in triplicate were respectively performed on the pH measurement (761 pH-meter Calimatic, Knick, Germany).

### **3.3 Structural analysis of EPS**

#### **3.3.1 EPS production activity test and isolation**

Each LAB strain was spread onto sucrose-MRS agar plates and incubated anaerobically at 30 °C for 48 h to macroscopically observe EPS production activity. For isolation of EPS, 1 % (v/v) of the respective pre-cultured LAB strain was inoculated into 40 ml sucrose-MRS liquid medium and incubated at 30 °C for 24 h. The fermentation broth was centrifuged (8,000 g, 15 min) to collect the supernatant. The supernatant was precipitated with two sample volumes of ethanol for 24 h at 4 °C. Afterwards, the precipitate was recovered by centrifugation (10,000 g, 15 min) and the supernatant was discarded. Remaining ethanol was vaporized for 1 h at 60 °C. Subsequently, precipitated EPS were redissolved in water and dialyzed in dialysis tubings (3,500 Da MWCO; MEMBRA-CEL, Serva Electrophoresis GmbH, Germany) against 2 l water for 48 h at 4 °C with smooth

stirring. Deionized water was changed at least five times. The dialyzed EPS solution was finally vacuum freeze dried (FreezeZone 2.5 Plus, Labconco, USA) at -80 °C.

### **3.3.2 Structural analysis of EPS via methylation analysis**

The monosaccharide composition of the EPS was determined after a combination of methanolysis and TFA hydrolysis (De Ruiter et al., 1992; Wefers and Bunzel, 2015). Briefly, the polysaccharides were methanolized with 1.25 M methanolic HCl for 16 h at 80 °C. After evaporation, the methyl-glycosides were hydrolyzed with 2 M TFA for 1 h at 121 °C. After removal of the acid, the monosaccharides were analyzed by high performance anion exchange chromatography with pulsed amperometric detection (HPAEC-PAD) as described previously (Wefers and Bunzel, 2015).

Glycosidic linkages were determined by methylation analysis as described previously (Nunes et al., 2008; Wefers and Bunzel, 2015). In brief, the polysaccharides were permethylated by using finely ground sodium hydroxide and methyl iodide. The methylated EPS were extracted from the reaction mix by using dichloromethane. After drying, methylation was repeated once to ensure complete methylation. Subsequently, they were hydrolyzed with 2 M TFA for 90 min at 121°C. After evaporation of the acid, the partially methylated monosaccharides were reduced by using sodium borodeuteride. Following acetylation with acethanhydride, the partially methylated alditol acetates (PMAAs) were identified by GC-MS (GC-2010 Plus, GCMS-QP2010) (Shimadzu, Kyoto, Japan) equipped with a DB5-MS column (30 m × 0.25 mm i.d., 0.25 µm film thickness, Agilent Technologies, CA). The following conditions were used: initial column temperature, 140 °C, held for 2 min; ramped at 1 °C/min to 180 °C, held for 5

min; ramped at 10 °C/min to 300 °C, held for 5 min. The injection temperature was 250 °C and split injection with a split ratio of 30:1 was used. Helium was used as carrier gas at 40 cm/sec. The transfer line temperature was 275 °C and electron impact spectra were recorded at 70 eV. The portions of the PMAAs were determined by using a GC-FID system (GC-2010 Plus, Shimadzu) equipped with a DB5-MS column (30 m × 0.25 mm i.d., 0.25 µm film thickness, Agilent Technologies, CA) under the same conditions as described for the GC-MS analyses. A reduced split ratio of 10:1 was used, the FID temperature was 240 °C, and nitrogen was used as a makeup gas. Molar response factors were used for semiquantitative determination of the PMAAs (Sweet et al., 1975).

For chromatographic analysis of the enzymatically liberated oligosaccharides, the EPS were dissolved in bidistilled water (1 mg/ml) and *endo*-dextranase solution (from *Chaetomium erraticum*, EC 3.2.1.11, >100 KDU/g EPS) was added. Subsequently, the mixture was incubated at 30 °C for 24 h. The enzyme was inactivated by heating to 100 °C for 10 min and the liberated oligosaccharides were analyzed by HPAEC-PAD on an ICS-5000 system (Thermo Scientific Dionex, Sunnyvale, CA) equipped with a CarboPac PA200 column (250 mm × 3 mm i.d., 5.5 µm) (Thermo Scientific Dionex). A flow rate of 0.4 ml/min and a gradient composed of the following eluents was used at 25 °C: (A) bidistilled water, (B) 0.1 M sodium hydroxide, and (C) 0.1 M sodium hydroxide + 0.5 M sodium acetate. Before every run, the column was washed with 100 % C for 10 min and equilibrated with 90 % A and 10 % B for 20 min. 0-10 min, isocratic 90 % A and 10 % B; 10-20 min, from 90 % A and 10 % B linear to 100 % B; 20-45 min, from 100 % B linear to 80 % B and 20 % C; 45-55 min, from 80 % B and 20 % C linear to 100 % C; 55-60 min, isocratic 100 % C.

### 3.3.3 Determination of molar mass and radius by AF4-MALS-UV

To analyze the size distributions of isolated EPS, asymmetric flow field-flow fractionation (AF4) (Wyatt Technology, Germany) coupled to multi-angle laser light scattering (MALS) (Dawn Heleos II, Wyatt Technology, Germany) and UV detection (UV) as quantitative detector (Dionex) was used as previously described (Jakob et al., 2013; Ua-Arak et al., 2017). Each lyophilized EPS was redissolved in ddH<sub>2</sub>O at the concentration of 0.2 mg/ml, and 75 µl sample was automatically injected to the channel equipped with a 10 kDa regenerated cellulose membrane (Superon GmbH, Germany) for the separation. 50 mM NaNO<sub>3</sub> was used as eluent solution. Program settings were as follows: injection flow (0.2 ml/min), focus flow (1.5 ml/min) and cross flow (linear gradient from 3 ml/min to 0.1 ml/min within 10 min). The cross flow was kept at 0.1 ml/min for 15 min and finally reduced to 0 ml/min within 4 min. Finally, our data resulting from AF4-MALS-UV were computationally evaluated using the berry model, which works well for large molecules ( $M_w > 1 \times 10^6$  Da). A concentration series (0.5, 1, 2, 2.5, 5, and 10 mg/ml) of the respective isolated EPS was prepared, from which the UV extinctions at 400 nm were respectively measured using a FLOUstar Omega microplate reader (BMG Labtech, Ortenberg, Germany). The obtained values were used to calculate the specific extinction coefficients [mL/(mgcm)] of the respective EPS samples. For final molar mass determinations using ASTRA 6.1 software (Wyatt Technology, Germany), a refractive index increment (dn/dc) value of 0.1423 mL/g (Yuryev et al., 2006) for dextran was applied.

### **3.4 Setting up a hydrophilic slide model mimicking physical contact in kefir granules**

The slides (Fisherbrand™ Superfrost™ Excell™ Microscope Slides, Fisher Scientific GmbH, Germany), which have excellent uniform hydrophilic surface to adhere to bacterial cells, had been validated to set up our model to mimic the physical contact in the kefir granule in the easiest way. Firstly, the slides were sterilized with 70 % ethanol and dried under the clean bench. 20 ml WKM were filled into the petri dish (92×16 mm without cams, Sarstedt, Germany), followed by inoculation with 1 % (v/v) pre-cultured *S. cerevisiae* and respective each LAB strain as co-cultivation partner in triplicate. Meanwhile, single cultures were inoculated with 1 % of pre-cultured strain, and served as controls. Sterilized hydrophilic slides were immersed into the petri dishes, which had been filled with WKM with the coated side of slides upwards. The hydrophilic slide models were incubated at 30 °C, 70 rpm for 2 d. Afterwards the slides were taken out with sterilized tweezers, and put into new petri dishes containing 20 mL fresh WKM without any inoculation. These petri dishes were incubated for another 2 d at 30 °C, 70 rpm. After the second incubation, the slides were taken out, washed once gently with deionized water (ddH<sub>2</sub>O) and dried for 2 mins. Microscopic images were observed and taken under an Axiostar plus transmitted-light microscope with a coupled AxioCam digital camera (Zeiss, Germany) at the magnification of 400\* in which the network formation of *S. cerevisiae* and LAB cells could be seen although LAB cells were 4-10 times smaller in diameter than yeast cells (Kokkinosa et al., 1998; Yelin and Silberberg, 1999). The microscopic imaging of *S. cerevisiae* in the presence of *L. hordei* TMW 1.1822 were taken additionally under both 100× and 1000× magnification. For the isolated and added glucans of LAB strains upon cultivation with *S. cerevisiae* on the slide

model, the lyophilized EPS were added into WKM at a concentration of 1.67 mg/ml, respectively. This EPS concentration was determined when *L. hordei* TMW 1.1822 was cultivated in the slide model after 24 h. To check the possible role of sucrose and the concomitantly formed  $\alpha$ -glucans for *S. cerevisiae* biofilm formation in the presence of *L. hordei*, the sucrose in WKM was replaced by equimolar amounts of glucose and fructose (42.1 g/l, respectively) as performed as above.

### **3.5 Genomics**

#### **3.5.1 Genome sequencing**

*L. hordei* TMW 1.1822 and *L. nagelii* TMW 1.1827 were anaerobically cultivated in 15 ml liquid mMRS medium at 30 °C for 20 h for DNA isolation. Isolation of high molecular weight DNA was performed using the Genomic-tip 100/G kit (Qiagen, Venlo, Netherlands) according to the manufacturer. The isolation protocol was modified for the lysis time of proteinase K to overnight. Quality and quantity of isolated DNA were checked by NanoDrop (Thermo Fisher Scientific) and agarose gel electrophoresis. About 15  $\mu$ g of the isolated genomic DNA of *L. hordei* TMW 1.1822 and *L. nagelii* TMW 1.1827 at the respective concentration of 560 ng/ $\mu$ l and 372 ng/ $\mu$ l were sent to and sequenced by GATC Biotech (Konstanz, Germany) via PacBio Single Molecule Real Time (SMRT) sequencing (Eid et al., 2008; McCarthy, 2010).

#### **3.5.2 Genome assembly**

Genomic raw data were assembled according to SMRT Analysis (Version 2.2.0.p2, Pacific Biosciences, USA) and the hierarchical genome assembly process (HGAP) (Chin



et al., 2013). Manual curation of assembly was done as described by PacBio (<https://github.com/PacificBiosciences/Bioinformatics-Training/wiki/Finishing-Bacterial-Genomes>). Polished assemblies, obtained from assemblies using the RS\_HGAP\_Assembly\_3 protocol, were split into contigs using BioPerl (<http://www.bioperl.org>) and tested for their redundancy using NCBI BLAST (Altschul et al., 1990; Camacho et al., 2009). Each contig was checked for overlapping ends by the dotplot tool Gepard (Krumstiek et al., 2007) and coverage behavior and mapping quality with SMRT-View 2.30 (Pacific Biosciences, Menlo Park, USA). The accuracy of the genome assembly was evaluated by BridgeMapper (RS\_BridgeMapper), which is part of SMRT-Analysis software. Redundant or non-sense contigs were discarded, and all other contigs of chromosome and all plasmids were circularized using minimus2 (AMOS, <http://amos.sourceforge.net>) to generate a final fasta file. Further it was applied into SMRT-Analysis resequencing and repeated until the consensus accordance reached a value of 100%.

### **3.5.3 Genome annotation and submission**

The circularized genomes were annotated by the NCBI Prokaryotic Genome Annotation Pipeline ([https://www.ncbi.nlm.nih.gov/genome/annotation\\_prok](https://www.ncbi.nlm.nih.gov/genome/annotation_prok)) and RAST, which is a SEED-based prokaryotic genome annotation service using default settings (Aziz et al., 2008; Overbeek et al., 2013). For NCBI genome submission, a bioproject (PRJNA343197) was created including two single biosamples of *L. hordei* TMW 1.1822 and *L. nagelii* TMW 1.1827. The submission procedure was done as described online (<http://www.ncbi.nlm.nih.gov/genbank/genomesubmit>).

### 3.5.4 Genomic statistics and visualization

A genomic atlas was generated using Artemis and DNA plotter (<http://www.sanger.ac.uk/science/tools/artemis>) (Carver et al., 2008) by importing the whole genome GenBank file. Subcellular localization of proteins was predicted utilizing the tool PSORTb (Version 3.0.2, <http://www.psort.org/psortb/>) (Gardy et al., 2004; Yu et al., 2010). Functional analysis was accomplished using SEED categorization and SEED subsystem analysis (Subsystem and FIGfams Technology) based on RAST annotation (Aziz et al., 2008; Overbeek et al., 2013). The SEED subsystem analysis enables the assignment of predicted genes to a category, subcategory and subsystem. All the annotated EC and KO numbers, which were extracted from RAST fasta files, could be directly imported into iPath 3.0 (<https://pathways.embl.de/ipath3.cgi?map=metabolic>) (Yamada et al., 2011) to obtain an overview of complete metabolic pathways and biosynthesis of other secondary metabolites customized in thin red color. While up-regulated enzymes were customized in bold red color, down-regulated enzymes were customized in bold blue color in the respective figures.

Based on the pathway of glycolysis, pentose phosphate and TCA cycle from the BioCyc Database Collection (<https://biocyc.org>), all enzymes involved in each reaction step were subjected to manual check if they were present in translated open reading frames (ORFs) files annotated from NCBI and RAST. In detail, if one enzyme involved in a pathway was manually checked to be present in both files, its corresponding ORF was further imported into NCBI Conserved Domain Search (<https://www.ncbi.nlm.nih.gov/Structure/cdd/wrpsb.cgi>) and Smart BLAST ([https://blast.ncbi.nlm.nih.gov/smartblast/?LINK\\_LOC=BlastHomeLink](https://blast.ncbi.nlm.nih.gov/smartblast/?LINK_LOC=BlastHomeLink)) to manually

double check the functional analysis of this enzyme. In this way, the enzyme was eventually confirmed to be present based on the functional genome prediction. Also, the presence of enzymes involved in pyruvate metabolism, the arginine deiminase (ADI) pathway and biosynthesis pathway of amino acids were verified in the similar workflow except the source of reference schematic pathway was different. The pathway of pyruvate metabolism was according to Geißler (Geißler, 2016) and Quintans et al (García-Quintáns et al., 2008), while ADI pathway was based on Rimaux et al and Tonon et al (Rimaux et al., 2011; Tonon and Lonvaud-Funel, 2002). The biosynthesis pathway of amino acids was generated from KEGG mapper ([http://www.genome.jp/kegg/tool/map\\_pathway1.html](http://www.genome.jp/kegg/tool/map_pathway1.html)) by importing EC numbers involved in amino acids biosynthesis.

## **3.6 Proteomics**

### **3.6.1 Sample preparation for proteomic analysis**

1% (v/v) pre-cultured *L. hordei*, *L. nagelii* and *S. cerevisiae* were respectively inoculated into 40 ml WKM in triplicate as single-culture samples, while 1% (v/v) pre-cultured *L. hordei* and 1% *S. cerevisiae*, as well as 1% (v/v) pre-cultured *L. nagelii* and 1% *S. cerevisiae* were inoculated into 40 ml WKM in triplicate to prepare for co-cultivation samples. All samples were anaerobically cultured at 30 °C for 10 h. Afterwards, trichloroacetic acid (TCA; stock concentration of 100% w/v) was added to those samples to a final concentration of 6.25% w/v. Subsequently samples were stored on ice for 10 min. The bacterial pellets were collected by centrifugation (5000 rpm, 5 min) at 4°C, washed twice with acetone, reconstituted in lysis buffer [8 M urea, 5 mM EDTA di-

sodium salt, 100 mM  $\text{NH}_4\text{HCO}_3$ , and 1 mM dithiothreitol (DTT), pH 8.0] and mechanically disrupted with acid-washed glass beads (G8772, 425-600  $\mu\text{m}$ , Sigma, Germany). Total protein concentration of the lysate was determined using the Bradford method (Bio-Rad Protein Assay, Bio-Rad Laboratories GmbH, Munich, Germany). 100  $\mu\text{g}$  protein extract was used per sample for in-solution digestion. Proteins were reduced with 10 mM DTT at 30 °C for 30 min, and subsequently carbamidomethylated with 55 mM chloroacetamide in the dark at room temperature for 60 min. Subsequently proteins were digested by addition of 1  $\mu\text{g}$  trypsin (1:100 trypsin:protein) for 3 h at 37°C and another 1  $\mu\text{g}$  of trypsin overnight at 37 °C. Digested peptide samples were desalted according to the manufacturer's instructions by C18 solid phase extraction using Sep-Pak columns (Waters, WAT054960). Purified peptide samples were dried in a SpeedVac concentrator (Acid-Resistant CentriVap Vacuum Concentrator, Labconco) and resuspended in 2 % acetonitrile, 98 %  $\text{H}_2\text{O}$ , 0.1 % formic acid to a final concentration of 0.25  $\mu\text{g}/\mu\text{l}$  as determined by Nanodrop measurement.

### **3.6.2 Liquid chromatography and mass spectrometry**

Generated peptides were analyzed on a Dionex Ultimate 3000 nano LC system coupled to a Q-Exactive HF mass spectrometer (Thermo Scientific, Bremen, Germany). Peptides were delivered to a trap column (75  $\mu\text{m} \times 2$  cm, self-packed with Reprosil-Pur C18 ODS-35  $\mu\text{m}$  resin, Dr. Maisch, Ammerbuch, Germany) at a flow rate of 5  $\mu\text{l}/\text{min}$  in solvent A<sub>0</sub> (0.1% formic acid in water). Peptides were separated on an analytical column (75  $\mu\text{m} \times 40$  cm, self-packed with Reprosil-Gold C18, 3  $\mu\text{m}$  resin, Dr. Maisch, Ammerbuch, Germany) using a 120 min linear gradient from 4-32 % solvent B (0.1 % formic acid, 5 % DMSO in acetonitrile) and solvent A<sub>1</sub> (0.1 % formic acid, 5 % DMSO in water) at a flow

rate of 300 ml/min. The mass spectrometer was operated in data dependent mode, automatically switching between MS1 and MS2 spectra. MS1 spectra were acquired over a mass-to-charge ( $m/z$ ) range of 360-1300  $m/z$  at a resolution of 60,000 (at  $m/z$  200) using a maximum injection time of 50 ms and an AGC target value of  $3e6$ . Up to 20 peptide precursors were isolated (isolation window 1.7  $m/z$ , maximum injection time 25 ms, AGC value  $1e5$ ), fragmented by higher-energy collisional dissociation (HCD) using 25 % normalized collision energy (Aziz et al.) and analyzed at a resolution of 15,000 with a scan range from 200 to 2000  $m/z$ . Precursor ions that were singly-charged, unassigned or with charge states  $> 6+$  were excluded. The dynamic exclusion duration of fragmented precursor ions was 20 s.

### **3.6.3 Identification and quantification of peptides and proteins**

Identification and quantification of peptides and proteins were performed with MaxQuant (version 1.5.7.4) (Cox and Mann, 2008) by searching the MS2 data against all protein sequences obtained from UniProt - Reference proteome *S. cerevisiae* S288c (6,724 entries, downloaded 13.03.2017) and all protein sequences from *L. hordei* TMW 1.1822 (GenBank CP018176-CP018179), *L. nagelii* TMW 1.1827 (GenBank CP018180-CP018183) using the embedded search engine Andromeda (Cox et al., 2011). Carbamidomethylated cysteine was a fixed modification; oxidation of methionine, and N-terminal protein acetylation were variable modifications. Trypsin/P was specified as the proteolytic enzyme and up to 2 missed cleavage sites were allowed. Precursor and fragment ion tolerances were 10 ppm and 20 ppm, respectively. Label-free quantification (Cox et al., 2014) and data matching between consecutive analyses were enabled within MaxQuant. Search results were filtered for a minimum peptide length of 7 amino acids, 1%

peptide and protein false discovery rate (FDR) plus common contaminants and reverse identifications. MaxQuant output files (proteinGroups.txt) were further performed using Perseus (version 1.5.6.0) (Tyanova et al., 2016). Protein groups were filtered for entries “only identified by site”, reverse identifications and contaminants. Protein groups from each investigated species were moved to different data matrices. iBAQ intensities were  $\log_2$ -transformed and used for further statistical analysis. NCBI annotation, Psorb subcellular localization, SEED category (subcategory and subsystem) as previously annotated (cf. section 2.5.3 and 2.5.4) were added to the matrix through identifier matching. For the comparison between two groups, t-tests were performed.  $\log_2$  fold change  $\geq 2$  or  $\leq -2$  and  $-\log_{10}$  P-value  $\geq 2$  (p value  $\leq 0.05$ ) were considered to be significantly differentially expressed proteins of *L. hordei* TMW 1.1822 and *L. nagelii* TMW 1.1827 in response to the presence of *S. cerevisiae* TMW 3.221.

#### **4. RESULTS (PUBLICATIONS BASED)**

This thesis contains four manuscripts. Their publication status, the abstracts and the contributions of the authors are given in the following.

##### **4.1 Manuscript 1: *Lactobacillus hordei* dextrans induce *Saccharomyces cerevisiae* aggregation and network formation on hydrophilic surfaces**

Di Xu, Lea Fels, Daniel Wefers, Jürgen Behr, Frank Jakob, Rudi F. Vogel., 2018.

Published in International Journal of Biological Macromolecules. 115, 236–242.

<https://doi.org/10.1016/j.ijbiomac.2018.04.068>.

Water kefir generally consists of a multispecies community, namely lactic acid bacteria (LAB), acetic acid bacteria, and yeasts. Some LAB isolated from water kefir granules has been reported to be able to produce EPS, and the granules are supposed to mainly consist of dextrans produced by *Lactobacillus (L.) hilgardii*. However, the contributions of other microorganisms to the formation of granules, such as *L. hordei*, *L. nagelii*, *Leuconostoc (Lc.) citreum* and *Saccharomyces (S.) cerevisiae* which are also commonly isolated from water kefir granules, remains unknown. We developed a simplified model system which was comprised of hydrophilic slide to mimic the hydrophilic surface of a growing kefir granule. It was found out that all tested predominant LAB (*L. hordei*, *L. nagelii*, *Lc. citreum*) isolated from water kefir grains produced glucans, but solely those glucans isolated from the four different *L. hordei* strains induced yeast aggregation on the hydrophilic model system. Therefore, structural analysis of these glucans was performed via methylation, chromatographic analysis and asymmetric flow field-flow fractionation with respect to their linkage types and size distributions. This study showed that all glucans were investigated as dextrans, and had major implications for the interpretation that those of the four *L. hordei* strains were highly similar among each other regarding portions of linkage types and size distributions. Thus, our study suggested that the specific size and structural organization of the dextran produced by *L. hordei* was the main cause for inducing *S. cerevisiae* aggregation and network formation on hydrophilic surfaces and acted as crucial initiation for forming a growing water kefir granule.

Authors contributions: Di Xu designed the research project and experimental approach guided by Jürgen Behr and conducted the main experiments under the supervision of Frank Jakob and Rudi F. Vogel. Lea Fels carried out the experiments on the structural

analysis of EPS under the supervision of Daniel Wefers in a collaboration. Frank Jakob helped to establish the contact with Daniel Wefers from the Karlsruhe Institute of Technology, and assisted data analyses of asymmetric flow field-flow fractionation. Di Xu wrote the draft with the part from Lea Fels. Frank Jakob revised and submitted the manuscript. All authors reviewed and approved the final manuscript.





## *Lactobacillus hordei* dextrans induce *Saccharomyces cerevisiae* aggregation and network formation on hydrophilic surfaces

Di Xu<sup>a</sup>, Lea Fels<sup>b</sup>, Daniel Wefers<sup>b</sup>, Jürgen Behr<sup>a,c</sup>, Frank Jakob<sup>a,\*</sup>, Rudi F. Vogel<sup>a</sup>

<sup>a</sup> Lehrstuhl für Technische Mikrobiologie, Technische Universität München, Freising, Germany

<sup>b</sup> Karlsruhe Institute of Technology (KIT), Institute of Applied Biosciences, Karlsruhe, Germany

<sup>c</sup> Bavarian Center for Biomolecular Mass Spectrometry (BayBioMS), Freising, Germany

### ARTICLE INFO

#### Article history:

Received 18 January 2018

Received in revised form 11 April 2018

Accepted 12 April 2018

Available online 13 April 2018

#### Keywords:

Water kefir

*Lactobacillus hordei*

*Saccharomyces cerevisiae*

Network formation

Dextran

### ABSTRACT

Water kefir granules are supposed to mainly consist of dextrans produced by *Lactobacillus* (*L.*) *hilgardii*. Still, other microorganisms such as *L. hordei*, *L. nagelii*, *Leuconostoc* (*Lc.*) *citreum* and *Saccharomyces* (*S.*) *cerevisiae* are commonly isolated from water kefir granules, while their contribution to the granule formation remains unknown. We studied putative functions of these microbes in granule formation, upon development of a simplified model system containing hydrophilic object slides, which mimics the hydrophilic surface of a growing kefir granule. We found that all tested lactic acid bacteria produced glucans, while solely those isolated from the four different *L. hordei* strains induced yeast aggregation on the hydrophilic slides. Therefore, structural differences between these glucans were investigated with respect to their size distributions and their linkage types. Beyond the finding that all glucans were identified as dextrans, those of the four *L. hordei* strains were highly similar among each other regarding portions of linkage types and size distributions. Thus, our study suggests the specific size and structural organization of the dextran produced by *L. hordei* as the main cause for inducing *S. cerevisiae* aggregation and network formation on hydrophilic surfaces and thus as crucial initiation of the stepwise water kefir granule growth.

© 2018 Elsevier B.V. All rights reserved.

### 1. Introduction

Water kefir is a traditional fermented beverage made from sucrose, water, water kefir grains, and dried or fresh fruits. The microbiota isolated from water kefir grains has been described to be a stable symbiotic multispecies community, which generally consists of lactic acid bacteria (LAB), acetic acid bacteria (AAB), bifidobacteria and yeasts [1–4]. Common LAB isolated from kefir grains are (among others) *Leuconostoc* (*Lc.*) *mesenteroides*, *Lactobacillus* (*L.*) *hilgardii*, *L. hordei*, *L. casei*. Furthermore, yeasts of the genera *Saccharomyces*, *Hanseniaspora*, *Zygorulasporea* and *Candida* are commonly present in water kefir [2,4–7].

The key organisms involved in water kefir preparation are embedded in the kefir granules. The backbone of the kefir granule is made from a dextran matrix mainly produced by *L. hilgardii*, which is the basic layer for biofilm formation by the embedded microorganisms [5,7–9]. Dextran is produced by dextransucrases from sucrose and contains consecutive  $\alpha$ -1,6-linkages in its major chains, which usually make up >50% of the total linkages [10,11]. These glucans also contain side chains, which are mainly attached through  $\alpha$ -1,3-branched linkages and occasionally through  $\alpha$ -1,4- or  $\alpha$ -1,2-branched linkages. Gulitz et al. [2] and Stadie [12] showed that the majority of LAB strains (81%) from water kefir belonging to the

species of *L. hordei*, *L. nagelii*, *L. hilgardii*, *Lc. mesenteroides/citreum* were able to produce exopolysaccharides (EPS) from sucrose.

Since microbial interaction processes are important for the establishment of the typical kefir microbiota, metabolic interactions among kefir organisms have been explored in different studies. Stadie et al. [13] studied metabolic activity and symbiotic interactions of LAB (*L. hordei* and *L. nagelii*) and yeasts (*S. cerevisiae* and *Zygorulasporea florentina*) isolated from water kefir. Although these works described some of the microbial metabolic interactions in kefir fermentation, little is still known about how key microbes build up and adhere to the growing hydrophilic kefir granule. Consequently, any attempts to reconstitute the naturally formed kefir granules in single or co-cultivation experiments failed in the past. Therefore, we set up a simple model system made up of hydrophilic slides and investigated the possible adhesion of water kefir born *S. cerevisiae* upon co-cultivation with different glucan-producing, water kefir LAB and finally correlated the observed aggregation results with the produced glucan types.

### 2. Material and methods

#### 2.1. Strain and pre-culture medium

*L. hordei* TMW 1.1817, TMW 1.1821, TMW 1.1822, TMW 1.1907, *L. nagelii* TMW 1.1827, *Lc. citreum* TMW 2.1194, and *S. cerevisiae* TMW

\* Corresponding author.

E-mail address: [frank.jakob@wzw.tum.de](mailto:frank.jakob@wzw.tum.de) (F. Jakob).

3.221 isolated from water kefir were chosen for this experiment [2]. All LAB were pre-cultured anaerobically for 24 h at 30 °C in modified MRS medium described by Stolz et al. [14]. *S. cerevisiae* was pre-cultured anaerobically for 24 h at 30 °C in YPG medium made of peptone from casein (10 g/L), yeast extract (5 g/L), glucose (20 g/L).

## 2.2. EPS production activity test and isolation

Each LAB strain was spread onto sucrose-MRS agar plates (80 g/L sucrose, 10 g/L peptone, 2 g/L meat extract, 4 g/L yeast extract, 1 g/L tween 80, 2.5 g/L  $K_2HPO_4 \cdot 3H_2O$ , 2 g/L  $(NH_4)_2$ -citrate, 5 g/L Na-Acetate- $3H_2O$ , 0.2 g/L  $MgSO_4 \cdot 7H_2O$ , 0.038 g/L  $MnSO_4 \cdot H_2O$ , 15 g/L agar), which were incubated anaerobically at 30 °C for 48 h to observe macroscopic EPS production activity. For isolation of EPS from liquid cultures, 1% (v/v) of the respective pre-cultured LAB strain was inoculated into sucrose-MRS medium and incubated at 30 °C for 24 h. The fermentation broth was then centrifuged (8000g, 15 min) to collect the supernatant. The supernatant was precipitated with two sample volumes of ethanol for 24 h at 4 °C. Afterwards, the precipitate was recovered by centrifugation (10,000g, 15 min) and the supernatant was discarded. Remaining ethanol was vaporized for 1 h at 60 °C. Subsequently, precipitated EPS were redissolved in water and dialyzed in dialysis tubings (3500 Da MWCO; MEMBRA-CEL, Serva Electrophoresis GmbH, Germany) against 2 L water for 48 h at 4 °C with smooth stirring. Deionized water was changed at least five times. The dialyzed EPS solution was finally vacuum freeze dried (FreezeZone 2.5 Plus, Labconco, USA) at –80 °C [15]. Furthermore, these EPS were used for AF4-MALS-UV, HPAEC-PAD and methylation analysis.

## 2.3. Setting up a hydrophilic slide model mimicking physical contact in kefir granules

The slides (Fisherbrand™ Superfrost™ Excell™ Microscope Slides, Fisher Scientific GmbH, Germany), which have excellent uniform hydrophilic surface to adhere to bacterial cells, had been validated to set up our model to mimic the physical contact in the kefir granule in the easiest way according to Franklin et al. [16]. Firstly, the slides were sterilized with 70% ethanol and dried under the clean bench. 20 mL water kefir medium (WKM) [13] were filled into the petri dish (92 × 16 mm without cams, Sarstedt, Germany) and inoculated with 1% (v/v) pre-cultured *S. cerevisiae* and one strain each of the LAB as co-cultivation partner in triplicate. Single cultures were inoculated with 1% of pre-cultured strain, and served as controls. Sterilized hydrophilic slides were immersed into the petri dishes, which had been filled with WKM with the coated side of slides upwards. The hydrophilic slide models were incubated at 30 °C, 70 rpm for 2 d. Afterwards the slides were taken out with sterilized tweezers, and put into new petri dishes containing fresh WKM without any inoculation. These new petri dishes were then incubated for another 2 d at 30 °C, 70 rpm. After the second incubation, the slides were taken out, washed once gently with deionized water (ddH<sub>2</sub>O) and finally dried for 2 min. Microscopic images were observed and taken under Axiostar plus transmitted-light microscope with a coupled AxioCam digital camera (Zeiss, Germany) at the magnification of 400× in which the network formation of *S. cerevisiae* and LAB can be seen although LAB was 4–10 times smaller in diameter than yeast [17,18]. The microscopic imaging of *S. cerevisiae* in presence of *L. hordei* TMW 1.1822 are shown additionally under both 100× and 1000× magnification. For the isolated and added glucans of LAB strains upon cultivation with *S. cerevisiae* on the slide model, the lyophilized EPS were added into WKM at a concentration of 1.67 mg/mL, respectively. This EPS concentration was determined when *L. hordei* TMW 1.1822 was cultivated in the slide model after 24 h. The following slide experiment was performed as above. To check the possible role of sucrose and the concomitantly formed α-glucans for *S. cerevisiae* bio-film formation in presence of *L. hordei*, the sucrose in WKM was

replaced by equimolar amounts of glucose and fructose (42.1 g/L, respectively).

## 2.4. Structural analysis

The monosaccharide composition of the EPS was determined after a combination of methanolysis and TFA hydrolysis [19,20]. Briefly, the polysaccharides were methanolized with 1.25 M methanolic HCl for 16 h at 80 °C. After evaporation, the methyl-glycosides were hydrolyzed with 2 M TFA for 1 h at 121 °C. After removal of the acid, the monosaccharides were analyzed by high performance anion exchange chromatography with pulsed amperometric detection (HPAEC-PAD) as described previously [20].

Glycosidic linkages were determined by methylation analysis as described previously [20,21]. In brief, the polysaccharides were permethylated by using finely ground sodium hydroxide and methyl iodide. The methylated polysaccharides were extracted from the reaction mix by using dichloromethane. After drying, methylation was repeated once to ensure complete methylation. Subsequently, the polysaccharides were hydrolyzed with 2 M TFA for 90 min at 121 °C. After evaporation of the acid, the partially methylated monosaccharides were reduced by using sodium borodeuteride. Following acetylation with acetylhydride, the partially methylated alditol acetates (PMAAs) were identified by GC-MS (GC-2010 Plus, GCMS-QP2010) (Shimadzu, Kyoto, Japan) equipped with a DB5-MS column (30 m × 0.25 mm i.d., 0.25 μm film thickness, Agilent Technologies, CA). The following conditions were used: Initial column temperature, 140 °C, held for 2 min; ramped at 1 °C/min to 180 °C, held for 5 min; ramped at 10 °C/min to 300 °C, held for 5 min. The injection temperature was 250 °C and split injection with a split ratio of 30:1 was used. Helium was used as carrier gas at 40 cm/s. The transfer line temperature was 275 °C and electron impact spectra were recorded at 70 eV. The portions of the PMAAs were determined by using a GC-FID system (GC-2010 Plus, Shimadzu) equipped with a DB5-MS column (30 m × 0.25 mm i.d., 0.25 μm film thickness, Agilent Technologies, CA) and the same conditions as described for the GC-MS analyses. A reduced split ratio of 10:1 was used, the FID temperature was 240 °C, and nitrogen was used as a makeup gas. Molar response factors were used for semiquantitative determination of the PMAAs [22].

For chromatographic analysis of the enzymatically liberated oligosaccharides, the EPS were dissolved in bidistilled water (1 mg/mL) and *endo*-dextranase solution (from *Chaetomium erraticum*, EC 3.2.1.11, >100 KDU/g EPS) was added. Subsequently, the mixture was incubated at 30 °C for 24 h. The enzyme was inactivated by heating to 100 °C for 10 min and the liberated oligosaccharides were analyzed by HPAEC-PAD on an ICS-5000 system (Thermo Scientific Dionex, Sunnyvale, CA) equipped with a CarboPac PA200 column (250 mm × 3 mm i.d., 5.5 μm) (Thermo Scientific Dionex). A flow rate of 0.4 mL/min and a gradient composed of the following eluents was used at 25 °C: (A) bidistilled water, (B) 0.1 M sodium hydroxide, (C) 0.1 M sodium hydroxide + 0.5 M sodium acetate. Before every run, the column was washed with 100% C for 10 min and equilibrated with 90% A and 10% B for 20 min. 0–10 min, isocratic 90% A and 10% B. 10–20 min, from 90% A and 10% B linear to 100% B; 20–45 min, from 100% B linear to 80% B and 20% C; 45–55 min, from 80% B and 20% C linear to 100% C; 55–60 min, isocratic 100% C.

## 2.5. Molar mass and radius determination by AF4-MALS-UV

To analyze the size distributions of isolated EPS, asymmetric flow field-flow fractionation (AF4) (Wyatt Technology, Germany) coupled to multi-angle laser light scattering (MALS) (Dawn Heleos II, Wyatt Technology, Germany) and UV detection (UV) as quantitative detector (Dionex) was used as previously described [23,24]. Each lyophilized EPS was redissolved in ddH<sub>2</sub>O at the concentration of 0.2 mg/mL. 75 μL were automatically injected to the channel equipped with a 10 kDa

regenerated cellulose membrane (Superon GmbH, Germany) for the separation. 50 mM NaNO<sub>3</sub> (aq.) were used as eluent solution. Program settings were as follows: injection flow (0.2 mL/min), focus flow (1.5 mL/min) and cross flow (linear gradient from 3 mL/min to 0.1 mL/min within 10 min). Then the cross flow was kept at 0.1 mL/min for 15 min and finally reduced to 0 mL/min within 4 min. Finally, our data resulting from AF4-MALS-UV were computationally evaluated using the berry model, which works well for large molecules ( $M_w > 1 \times 10^6$  Da). For final molar mass determinations using ASTRA 6.1 software (Wyatt Technology, Germany), a refractive index increment (dn/dc) value of 0.1423 mL/g [25] for dextran was applied. Furthermore, the UV extinction coefficients of each isolated dextran at 400 nm were determined and calculated as described by Ua-Arak et al. [26].

### 3. Results

#### 3.1. Aggregation and network formation of *S. cerevisiae* in co-cultivation experiments and after supplementation of different isolated dextrans

LAB, yeast and polysaccharides are the main components of the gelatinous kefir grains, which provide the spot for cell-cell physical contact. Previous works demonstrated that *L. hordei*, *L. nagelii*, *Lc. citreum* are the predominant LAB in water kefir granules at our institute, while *S. cerevisiae* was one of the most dominant yeasts species [2,12]. Moreover, preliminary experiments revealed that *L. hilgardii* TMW 1.828, which is supposed to be the main producer of the water-kefir dextran, did not induce *S. cerevisiae* aggregation upon co-cultivation (data not shown). Therefore, 4 strains of *L. hordei* (TMW 1.1822, 1.1817, 1.1821, 1.1907), *L. nagelii* TMW 1.1827, *Lc. citreum* TMW 2.1194, and *S. cerevisiae* TMW 3.221 were selected for the following experiments. All test strains could adhere to the slides upon single cultivation (data not shown). This ensured that the simplified hydrophilic slide model system allowed LAB and *S. cerevisiae* to adhere and thus to possibly get in close physical contact. Afterwards, the 6 LAB strains were co-cultivated with *S. cerevisiae* in the slide model system, respectively. As depicted in Table 1 and exemplarily shown in Fig. 1, *L. hordei* TMW 1.1822 induced the aggregation and network formation of *S. cerevisiae* TMW 3.221. The 3 other strains of *L. hordei* also induced the aggregation of *S. cerevisiae* (Table 1, Fig. S2, Fig. S3A + B). In some cases, some *L. hordei* cells were attached to the yeast aggregates, while the networks were mainly composed of *S. cerevisiae* cells. The other tested LAB, namely *L. nagelii* TMW 1.1827 and *Lc. citreum* TMW 2.1194, did not induce any aggregation/network formation of *S. cerevisiae* TMW 3.221 (Fig. S3C + D). Moreover, additional co-cultivation experiments between the 4 *L. hordei* strains and *S. cerevisiae* using glucose and fructose instead of sucrose as carbon source, respectively, revealed, that *S. cerevisiae* was not able to form aggregates and networks on the hydrophilic surfaces (Fig. S4).

As specific glucans may therefore be causative for induction of *S. cerevisiae* aggregation and because all tested LAB have been previously shown to produce excess glucan from sucrose [12], we additionally isolated these glucans and added them to the model system in combination with *S. cerevisiae* alone. EPS isolated from the 4 strains of *L. hordei* induced the aggregation and network formation of *S. cerevisiae* (Fig. 2,

Figs. S5 + S6). On the contrary, the EPS isolated from *L. nagelii* TMW 1.1827 and *Lc. citreum* TMW 2.1194, as well as commercially available dextran ( $M_r \sim 6000$ , Merck, Germany) did not cause aggregation of *S. cerevisiae* (Fig. S5B). Remarkably, it was clearly observable that many more individual yeast cells were attached to the hydrophilic slides in form of aggregates/networks upon co-cultivation with *L. hordei* or addition of glucan from *L. hordei*, than in all other experiments (single-/co-cultivation with other LAB or addition of other glucans).

#### 3.2. Structural analysis of isolated glucans

To gain further insight into the identity of the isolated EPS, the structural characteristics such as the monosaccharides composition and the glycosidic linkages of the glucans were further investigated through HPAEC-PAD and methylation analysis. The monosaccharide composition of the EPS was analyzed by HPAEC-PAD after acid hydrolysis. The sole detection of glucose in all EPS confirmed the presence of glucans. To obtain information about the glycosidic linkages and to detect possible differences between the glucan samples, methylation analysis was performed. The results are shown in Table 2. Determination of the PMAA portions demonstrated that 1,6-linked glucose is predominant in all analyzed glucan samples. Most likely, terminal units mainly result from glucose residues attached to branched units of the 1,6-linked backbone, which is supported by the portions of the corresponding PMAAs. Varying portions of glycosidic linkages representing branching points were detected and in part allowed for a differentiation between the different glucans. For glucans from *L. nagelii* and all *L. hordei* strains, 1,3,6-linked glucose was detected in higher portions than 1,4,6- and 1,2,6-linked glucose. Therefore, position O3 is the most abundant branching position these polysaccharides. In contrast, 1,2,6-linked glucose was not detected in *Lc. citreum* glucan while 1,4,6- and 1,3,6-linked glucose residues were detected in comparably higher portions. The relative abundance of these two linkage types suggested highly branched dextrans, which are preferably branched at position O4, but also contain notable portions of branching at position O3. Therefore, *Lc. citreum* dextrans have a clearly different structural composition than dextrans produced by *L. nagelii* and all *L. hordei* strains, which also contained slightly higher portions of 1,3-linked glucose. However, methylation analysis did not allow for a clear differentiation between the *S. cerevisiae* aggregation inducing *L. hordei* dextrans and the *L. nagelii* dextran. Therefore, all dextrans were digested with *endo*-dextranase for a chromatographic analysis of the hydrolysis products. The digestion procedure results in the cleavage of the linear areas of the dextran backbone and the obtained hydrolysates are comprised of isomaltose and side chain containing oligosaccharides. Thus, an analysis of the liberated oligosaccharides potentially allows for the detection of different side chain patterns, which are not detectable by methylation analysis [9,27,28]. The oligosaccharides liberated by *endo*-dextranase were analyzed by HPAEC-PAD and the results are shown in Fig. 3. The chromatograms of the hydrolysates of *Lc. citreum* dextran clearly contained more peaks than the other hydrolysates. This confirms the structural differences between *Lc. citreum* dextran and dextrans produced by the other strains which were already observed by methylation analysis. Comparable chromatograms were obtained for dextrans produced by the four *L. hordei* strains. The hydrolysate of the *L. nagelii* dextran contained the same peaks than the hydrolysates from the *L. hordei* dextrans, but the peak eluting at ca. 32 min showed a clearly higher abundance than in the *L. hordei* dextrans. Thus structural elements represented by the different HPAEC-PAD peaks are of varying abundance. Although the exact release mechanism of the oligosaccharides is yet unknown, these data indicate that different side chain patterns may occur in the dextrans between *L. hordei* and *L. nagelii*. These differences in the structural organization may further influence the macromolecular organization of the polymers. Therefore, AF4-MALS-UV was applied to obtain further information about the dextrans.

**Table 1**  
Network formation of *S. cerevisiae* TMW 3.221 in presence of EPS-producing LAB isolated from water kefir and in presence of the isolated EPS from these bacteria.

Species	Strain	Network formation in presence of LAB	Network formation in presence of isolated EPS
<i>Lc. citreum</i>	TMW 2.1194	–	–
<i>L. hordei</i>	TMW 1.1822	+	+
<i>L. hordei</i>	TMW 1.1821	+	+
<i>L. hordei</i>	TMW 1.1817	+	+
<i>L. hordei</i>	TMW 1.1907	+	+
<i>L. nagelii</i>	TMW 1.1827	–	–

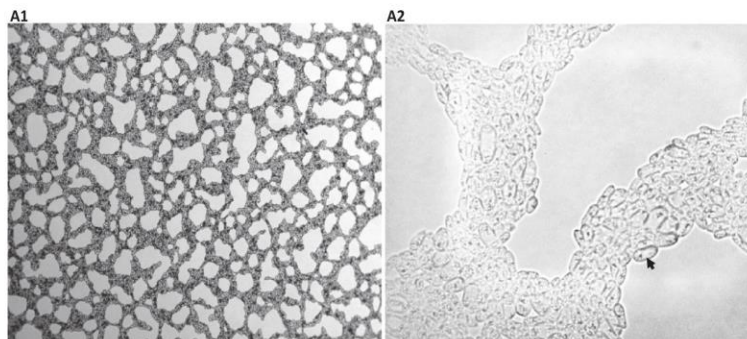


**Fig. 1.** Microscopic images of *S. cerevisiae* TMW 3.221 in presence of *L. hordei* TMW 1.1822 (A1 under 100 $\times$  magnification and A2 under 1000 $\times$  magnification), the arrow indicates a single cell of *S. cerevisiae* under 1000 $\times$  magnification.

### 3.3. Molar mass and radius determinations of isolated glucans

All 6 isolated dextrans were further characterized by AF4-MALS-UV regarding averaged molar masses ( $M_w$ ), averaged rms radii ( $R_w$ ) and the respective total molar mass and radii distributions. Clear similarities and distinctions between all dextran samples were already observed via comparison of the retention times and separation profiles of the separated dextrans. Fig. 4 A displays the LS signals at 90 $^\circ$ , where the shift of retention time can be easily seen from the peak maxima (about 16 min for *Lc. citreum* TMW 2.1194 dextran; about 21 min for *L. nagelii* TMW 1.1827 dextran). While the dextrans of *L. hordei* TMW 1.1822, 1.1817, 1.1821, 1.1907 eluted at consistent retention times of about 19 min. In Fig. 4 B + C, the respective cumulative molar mass and cumulative rms radius distributions are depicted. Table 3 summarizes the obtained averaged molar masses and rms radii as well as the respective polydispersity values of total dextran fractions. In accordance with the obtained retention times of the separated dextran molecules, the dextrans produced by *L. hordei* were highly similar regarding  $M_w$ ,  $R_w$  and size distributions among each other, but significantly differed in terms of these parameters from the other investigated dextrans. Moreover, the secondary structures of dextrans produced by *L. hordei* and *L. nagelii* were different in aqueous solutions, as the sphere model integrated in ASTRA 6.1 software could be exclusively applied for accurate evaluation of *L. nagelii* dextran ( $R^2 > 0.99$ ), while the dextrans produced by the 4 *L.*

*hordei* strains could be evaluated by the models sphere, random coil and rod (each  $R^2 > 0.99$ ). Therefore, the dextran particles of *L. hordei* seem to exhibit more “elongated” secondary structures than *L. nagelii* dextrans.

## 4. Discussion

The most dominant species isolated and identified from the water kefir source studied in this work were *L. hordei*, *L. nagelii*, *Lc. citreum*, and *S. cerevisiae* [2]. In order to get insight into their possible interactions in the complex granule system, they were investigated in a newly set-up hydrophilic slide model system. *S. cerevisiae* were co-cultivated with *L. hordei*, *L. nagelii*, *Lc. citreum* in petri dishes containing hydrophilic slides, respectively. The slides should mimic the hydrophilic surface of the growing kefir granules, which mainly consist of dextrans produced by *L. hilgardii* [6,7]. Our results at first indicated that aggregation and network formation of *S. cerevisiae* on these slides is induced in the presence of *L. hordei*, but not in the presence of *L. nagelii* or *Lc. citreum*. In milk kefir, it was found that bacterial surface proteins of *L. kefirifaciens* mediate the co-aggregation with *S. lipolytica* isolated from kefir grains [29]. Our study focusing on water kefir reveals for the first time, that *L. hordei* and most likely its specifically structured dextrans induce the aggregation and network formation of *S. cerevisiae* on hydrophilic surfaces in contrast to other water-kefir dextrans. The role and contribution of  $\alpha$ -glucans (such as dextrans) in/for biofilm formation by diverse  $\alpha$ -glucan-producing LAB species such as *Streptococcus mutans*, *Lc. mesenteroides* and *L. reuteri* has been reported in different works [30–33]. However, a dextran-mediated induction of biofilm formation by glucanucrase-deficient organisms such as yeasts has not been reported so far.

To get first insights into the molecular structure and differences of the tested dextrans, the EPS produced by the different organisms were further characterized by various analytical approaches. All investigated EPS contained >50% of 1,6-linked glucose, and lower percentages of

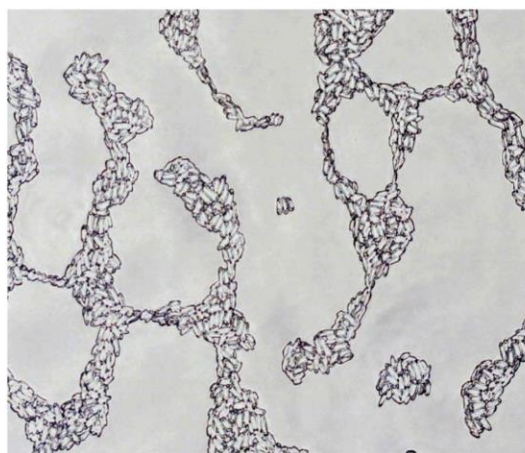


**Fig. 2.** Microscopic images of *S. cerevisiae* TMW 3.221 in presence of dextrans isolated from *L. hordei* TMW 1.1822.

**Table 2**  
Glycosidic linkages (mol%) of glucans produced by different LAB as determined by methylation analysis.

	<i>L. hordei</i> TMW 1.1822	<i>L. hordei</i> TMW 1.1817	<i>L. hordei</i> TMW 1.1821	<i>L. hordei</i> TMW 1.1907	<i>L. nagelii</i> TMW 1.1827	<i>Lc. citreum</i> TMW 2.1194
t-Glcp	7.8	6.7	6.2	5.4	6.4	25.3
1,3-Glcp	1.8	1.2	1.3	1.2	1.0	0.2
1,4-Glcp	0.3	0.2	0.2	0.1	0.3	0.4
1,6-Glcp	85.8	87.7	87.7	89.5	87.3	51.7
1,4,6-Glcp	0.6	0.8	0.9	0.4	0.6	13.7
1,2,6-Glcp	0.4	0.3	0.3	0.3	0.4	
1,3,6-Glcp	3.4	3.0	3.4	3.0	4.0	8.7

t = terminal, Glc = glucose, p = pyranose. Numbers indicate the substituted positions of a sugar unit.

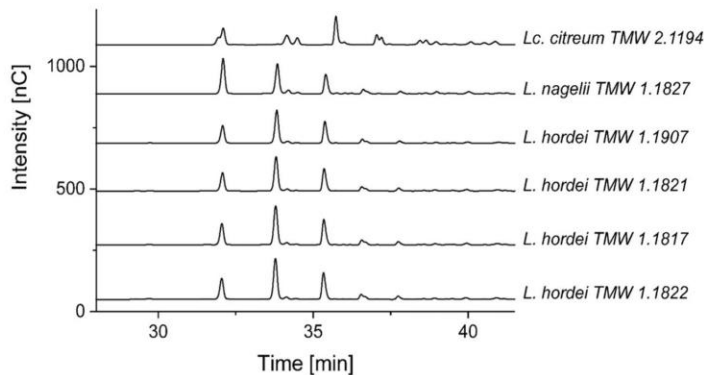


Fig. 3. HPAEC-PAD chromatograms of the *endo*-dextranase hydrolysates of dextrans derived from the different LAB.

1,3-, 1,4-, 1,2,6-, 1,4,6- or 1,3,6-linked glucose, which confirmed their identity as dextrans. Methylation analysis demonstrated that the dextrans produced by the *L. hordei* strains and by *L. nagelii* contained similar portions of glycosidic linkages, but had a different structural composition than the dextran from *Lc. citreum*. Furthermore, enzymatic fingerprinting by HPAEC-PAD and molar mass, radius and secondary structure comparisons allowed for a clear differentiation between the dextrans produced by the four *L. hordei* strains and the dextran produced by *L. nagelii*. Therefore, it can be concluded that the specific size, the structural organization and the possibly concomitant specific properties of the dextrans of *L. hordei* are decisive factors for yeast aggregation/adhesion. This hypothesis is supported by recent findings, that differing molecular weights/particle shapes/polydispersities within

one EPS type (same portions of same linkages) are mainly decisive for the functional properties of EPS [15,23,24,26]. However, it is currently not possible to clearly identify the mechanisms for *S. cerevisiae* aggregation and network formation in dependence of the specific dextrans produced by *L. hordei*, while *S. cerevisiae* strains are known to contain surface proteins leading to the formation of flocs, flors, biofilms or filaments (in some cases via binding of mannose polymers) [34].

The isolated dextrans produced by *L. hordei* and by the other tested LAB could theoretically contain small amounts of other molecules (<1%; [35]), which can contribute to *S. cerevisiae* aggregation, adhesion and network formation as well. Due to the used isolation procedure, such possible biofilm-inducing substances produced by *L. hordei* would be larger than 3500 Da (MWCO of used dialysis membranes).

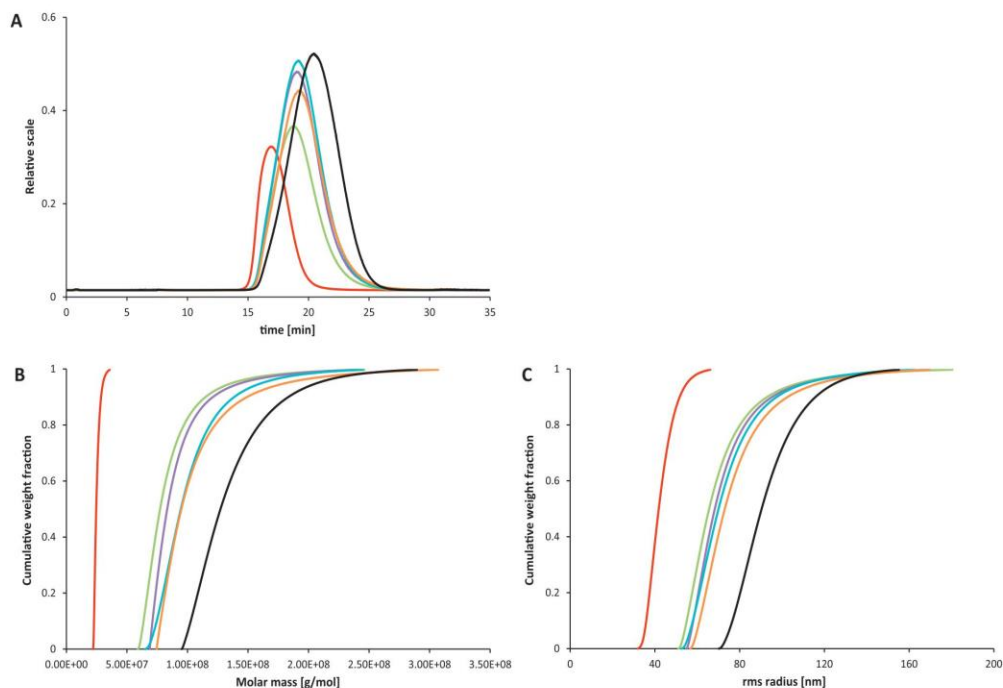


Fig. 4. Light scattering signals at 90° (A), cumulative molar mass ( $M_w$ , B) and rms radius ( $R_w$ , C) distributions of dextrans isolated from *Lc. citreum* TMW 2.1194 (red, left), *L. hordei* TMW 1.1822 (green), *L. hordei* TMW 1.1821 (purple), *L. hordei* TMW 1.1817 (blue), *L. hordei* TMW 1.1907 (yellow), *L. nagelii* TMW 1.1827 (black, right). Depicted LAB are shown from left to right in turn.

**Table 3**

List of molar mass, rms radius and polydispersity of EPS produced by LAB isolated from water kefir according to Model Berry.

Species	Strain	Molar mass		RMS radius		Polydispersity [Mw/Mn]
		Mw [ $\times 10^7$ g/mol]	Mn [ $\times 10^7$ g/mol]	Rw [nm]	Rn [nm]	
<i>Lc. citreum</i>	TMW 2.1194	2.531 $\pm$ 0.158%	2.509 $\pm$ 0.152%	43.5 $\pm$ 0.2%	42.9 $\pm$ 0.2%	1.009 $\pm$ 0.219%
<i>L. hordei</i>	TMW 1.1822	8.548 $\pm$ 0.367%	8.007 $\pm$ 0.271%	73.8 $\pm$ 0.1%	69.0 $\pm$ 0.1%	1.067 $\pm$ 0.456%
<i>L. hordei</i>	TMW 1.1821	9.178 $\pm$ 0.209%	8.685 $\pm$ 0.169%	76.1 $\pm$ 0.1%	71.8 $\pm$ 0.1%	1.057 $\pm$ 0.269%
<i>L. hordei</i>	TMW 1.1817	10.23 $\pm$ 0.355%	9.607 $\pm$ 0.297%	77.1 $\pm$ 0.2%	72.7 $\pm$ 0.2%	1.065 $\pm$ 0.463%
<i>L. hordei</i>	TMW 1.1907	10.70 $\pm$ 0.295%	9.903 $\pm$ 0.238%	80.9 $\pm$ 0.1%	75.8 $\pm$ 0.1%	1.080 $\pm$ 0.379%
<i>L. nagelii</i>	TMW 1.1827	13.69 $\pm$ 0.289%	12.99 $\pm$ 0.232%	95.2 $\pm$ 0.1%	91.7 $\pm$ 0.1%	1.053 $\pm$ 0.371%

Note: Mw = weight-average molar mass, Mn = number-average molar mass, Rw = weight-average mean square radius, Rn = number-average mean square radius.

The known mechanism for *S. cerevisiae* aggregation via  $\text{Ca}^{2+}$ -mediated, lectin-mannan binding [34] can therefore be excluded, as  $\text{Ca}^{2+}$  had been removed by dialysis in all tested dextran preparations. Moreover, *S. cerevisiae* adopts adhesiveness to diverse solid surfaces under nitrogen/glucose starvation [34]. As our aggregation/adhesion experiments with added dextrans from different LAB strains were performed under the same growth conditions, an effect of different starving conditions inducing altered yeast adhesion can be excluded as well. On the contrary, addition of the dextran preparation from *L. hordei* allowed significantly more *S. cerevisiae* cells to tightly adhere to the hydrophilic object slide in contrast to the dextran preparations produced by other water-kefir LAB (only few single cells adhered without network formation). Consequently, it is most likely that *S. cerevisiae* either got highly hydrophilic for enhanced adhesion (via binding of specific motifs in hydrophilic *L. hordei* dextrans or sudden induced production of any other hydrophilic surface structures) or got entrapped in form of sedimenting networks/aggregates on a glue-like film, which is exclusively formed in presence of *L. hordei* dextrans and *S. cerevisiae*.

We could recently show, that dextrans are the main components of the kefir granules [9], from which the organisms used in the present study had initially been isolated. The EPS isolated in the present work from different LAB species were composed of different dextrans. Thus, we suggest the specific size and structural organization of the dextran produced by *L. hordei* as the main cause for inducing *S. cerevisiae* aggregation and network formation on hydrophilic surfaces. Further experiments are on the way to clarify the exact mechanisms of this so far non-described, inducible aggregation and ordered network formation by water-kefir born *S. cerevisiae*. If the hydrophilic surface of the used object slides mimicked the growing kefir granule, our approach would nicely demonstrate how further water-kefir dextrans – apart from the main structure-forming dextran of the kefir granules produced by *L. hilgardii* – could contribute to the complex, stepwise kefir granule growth and, in this way, to multispecies biofilm formation.

### Acknowledgement

Part of this work was supported by the China Scholarship Council in grant no. 201306820010 and by the German Ministry of Economics and Technology (via AiF) and the Wifoe (Wissenschaftsförderung der Deutschen Brauwirtschaft e.V., Berlin) projects AiF 16454 N and AiF 19180 N. The authors are grateful to Felix Urvat and Andreas Becker for experimental support.

### Appendix A. Supplementary data

Supplementary data to this article can be found online at <https://doi.org/10.1016/j.ijbiomac.2018.04.068>.

### References

- [1] A. Irigoyen, I. Arana, M. Castiella, P. Torre, F. Ibanez, Microbiological, physicochemical, and sensory characteristics of kefir during storage, *Food Chem.* 90 (4) (2005) 613–620.

- [2] A. Gultiz, J. Stadie, M. Wenning, M.A. Ehrmann, R.F. Vogel, The microbial diversity of water kefir, *Int. J. Food Microbiol.* 151 (3) (2011) 284–288.
- [3] T. Vardjan, P.M. Lorbeg, I. Rogelj, A.C. Majhenič, Characterization and stability of lactobacilli and yeast microbiota in kefir grains, *J. Dairy Sci.* 96 (5) (2013) 2729–2736.
- [4] A.J. Marsh, O. O'Sullivan, C. Hill, R.P. Ross, P.D. Cotter, Sequence-based analysis of the microbial composition of water kefir from multiple sources, *FEMS Microbiol. Lett.* 348 (1) (2013) 79–85.
- [5] H. Neve, K. Heller, The microflora of water kefir: a glance by scanning electron microscopy, *Kieler Milchwirtschaftliche Forschungsberichte* 54 (4) (2002) 337–349.
- [6] M. Pidoux, Microscopic and chemical studies of a gelling polysaccharide from *Lactobacillus hilgardii*, *Carbohydr. Polym.* 13 (1990) 351–362.
- [7] F.W. Waldherr, V.M. Doll, D. Meißner, R.F. Vogel, Identification and characterization of a glucan-producing enzyme from *Lactobacillus hilgardii* TMW 1.828 involved in granule formation of water kefir, *Food Microbiol.* 27 (5) (2010) 672–678.
- [8] M. Horisberger, Structure of the dextran of the Tibi grain, *Carbohydr. Res.* 10 (1969) 379–385.
- [9] L. Fels, F. Jakob, R.F. Vogel, D. Wefers, Structural characterization of the exopolysaccharides from water kefir, *Carbohydr. Polym.* 189 (2018) 296–303.
- [10] M. Naessens, A. Cerdobbel, W. Soetaert, E.J. Vandamme, *Leuconostoc* dextranucrase and dextran: production, properties and applications, *J. Chem. Technol. Biotechnol.* 80 (8) (2005) 845–860.
- [11] J.M.R. Tingirikari, D. Kothari, A. Goyal, Superior prebiotic and physicochemical properties of novel dextran from *Weissella cibaria* JAG8 for potential food applications, *Food Funct.* 5 (9) (2014) 2324–2330.
- [12] J. Stadie, Metabolic Activity and Symbiotic Interaction of Bacteria and Yeasts in Water Kefir, Technische Universität München, 2013.
- [13] J. Stadie, A. Gultiz, M.A. Ehrmann, R.F. Vogel, Metabolic activity and symbiotic interactions of lactic acid bacteria and yeasts isolated from water kefir, *Food Microbiol.* 35 (2) (2013) 92–98.
- [14] P. Stolz, R.F. Vogel, W.P. Hammes, Utilization of electron acceptors by lactobacilli isolated from sourdough, *Z. Lebensm. Unters. Forsch.* 201 (4) (1995) 402–410.
- [15] T. Ua-Arak, F. Jakob, R.F. Vogel, Characterization of growth and exopolysaccharide production of selected acetic acid bacteria in buckwheat sourdoughs, *Int. J. Food Microbiol.* 239 (2016) 103–112.
- [16] R.B. Franklin, A.H. Campbell, C.B. Higgins, M.K. Barker, B.L. Brown, Enumerating bacterial cells on bioadhesive coated slides, *J. Microbiol. Methods* 87 (2) (2011) 154–160.
- [17] A. Kokkiosa, C. Fasseas, E. Eliopoulos, G. Kalantzopoulos, Cell size of various lactic acid bacteria as determined by scanning electron microscope and image analysis, *Lait* 78 (5) (1998) 491–500.
- [18] D. Yelin, Y. Silberberg, Laser scanning third-harmonic-generation microscopy in biology, *Opt. Express* 5 (8) (1999) 169–175.
- [19] G.A. De Ruyter, H.A. Schols, A.G.J. Voragen, F.M. Rombouts, Carbohydrate analysis of water-soluble uronic acid-containing polysaccharides with high-performance anion-exchange chromatography using methanolysis combined with TFA hydrolysis is superior to four other methods, *Anal. Biochem.* 207 (1) (1992) 176–185.
- [20] D. Wefers, M. Bunzel, Characterization of dietary fiber polysaccharides from dehulled, common buckwheat (*Fagopyrum esculentum*) seeds, *Cereal Chem.* 92 (6) (2015) 598–603.
- [21] F.M. Nunes, A. Reis, A.M.S. Silva, M.R.M. Domingues, M.A. Coimbra, Rhamnoarabinosyl and rhamnoarabinoarabinosyl side chains as structural features of coffee arabinoxylans, *Phytochemistry* 69 (7) (2008) 1573–1585.
- [22] D.P. Sweet, R.H. Shapiro, P. Albersheim, Quantitative-analysis by various GLC response-factor theories for partially methylated and partially ethylated alditol acetates, *Carbohydr. Res.* 40 (2) (1975) 217–225.
- [23] F. Jakob, A. Pfaff, R. Novoa-Carballal, H. Rübsum, T. Becker, R.F. Vogel, Structural analysis of fructans produced by acetic acid bacteria reveals a relation to hydrocolloid function, *Carbohydr. Polym.* 92 (2) (2013) 1234–1242.
- [24] T. Ua-Arak, F. Jakob, R.F. Vogel, Fermentation pH modulates the size distributions and functional properties of *Gluconobacter albidus* TMW 2.1191 Levan, *Front. Microbiol.* 8 (2017) 807.
- [25] P. Vladimir, P.T. Yuryev, Eric Bertoff, Achievements in understanding of structure and functionality, *Starch* (2006) 149.
- [26] T. Ua-Arak, F. Jakob, R.F. Vogel, Influence of Levan-producing acetic acid bacteria on buckwheat-sourdough breads, *Food Microbiol.* 65 (2017) 95–104.
- [27] K. Katina, N.H. Maina, R. Juvonen, L. Flander, L. Johansson, L. Virkki, M. Tenkanen, A. Laitila, In situ production and analysis of *Weissella confusa* dextran in wheat sourdough, *Food Microbiol.* 26 (7) (2009) 734–743.

- [28] Y. Xu, R. Coda, Q. Shi, P. Tuomainen, K. Katina, M. Tenkanen, Exopolysaccharides production during the fermentation of soybean and fava bean flours by *Leuconostoc mesenteroides* DSM 20343, *J. Agric. Food Chem.* 65 (13) (2017) 2805–2815.
- [29] M.A. Golowczyc, P. Mobili, G.L. Garrote, M. de Los Angeles Serradell, A.G. Abraham, G.L. De Antoni, Interaction between *Lactobacillus kefir* and *Saccharomyces lipolytica* isolated from kefir grains: evidence for lectin-like activity of bacterial surface proteins, *J. Dairy Res.* 76 (1) (2009) 111–116.
- [30] T.D. Leathers, K.M. Bischoff, Biofilm formation by strains of *Leuconostoc citreum* and *L. mesenteroides*, *Biotechnol. Lett.* 33 (3) (2011) 517–523.
- [31] T.D. Leathers, G.L. Côté, Biofilm formation by exopolysaccharide mutants of *Leuconostoc mesenteroides* strain NRRL B-1355, *Appl. Microbiol. Biotechnol.* 78 (6) (2008) 1025–1031.
- [32] J. Walter, C. Schwab, D.M. Loach, M.G. Gänzle, G.W. Tannock, Glucosyltransferase A (GtA) and inulosucrase (Inu) of *Lactobacillus reuteri* TMW1. 106 contribute to cell aggregation, in vitro biofilm formation, and colonization of the mouse gastrointestinal tract, *Microbiology* 154 (1) (2008) 72–80.
- [33] M. Zhu, D. Ajdić, Y. Liu, D. Lynch, J. Merritt, J.A. Banas, Role of the *Streptococcus mutans* *irvA* gene in GbpC-independent, dextran-dependent aggregation and biofilm formation, *Appl. Environ. Microbiol.* 75 (22) (2009) 7037–7043.
- [34] S. Bruckner, H.U. Mosch, Choosing the right lifestyle: adhesion and development in *Saccharomyces cerevisiae*, *FEMS Microbiol. Rev.* 36 (1) (2012) 25–58.
- [35] S. Notararigo, M. Náchter-Vázquez, I. Ibarburu, M.L. Werning, P.F. de Palencia, M.T. Dueñas, R. Aznar, P. López, A. Prieto, Comparative analysis of production and purification of homo- and hetero-polysaccharides produced by lactic acid bacteria, *Carbohydr. Polym.* 93 (1) (2013) 57–64.

## **4.2 Manuscript 2: Lifestyle of *Lactobacillus hordei* isolated from water kefir based on genomic, proteomic and physiological characterization**

Di Xu<sup>#</sup>, Julia Bechtner<sup>#</sup>, Jürgen Behr, Lara Eisenbach, Andreas J. Geißler, Rudi F. Vogel., 2019. Published in International Journal of Food Microbiology. 290, 141-149.

<https://doi.org/10.1016/j.ijfoodmicro.2018.10.004>.

#joint first authorship

Water kefir is a traditional fermented beverage, which is generally fermented by lactic acid bacteria (LAB), acetic acid bacteria and yeasts. Homemade water kefir is usually fermented for 2-3 days and its materials for making water kefir are sucrose, water, kefir granules, dried or fresh fruits (e.g. figs). *Lactobacillus (L.) hordei* is one of the predominant LAB species isolated from water kefir granules. Since it faced abundant sucrose *versus* innutrition of amino- and fatty acids in water kefir, the lifestyle of *L. hordei* was indicated and constructed through label-free quantitative proteomic analysis combined with genomic analysis and physiological characterization. The whole-genome sequence of *L. hordei* TMW 1.1822 revealed one chromosome plus three plasmids with the length of 2.42 Mbp in the range of some other lactobacilli. The number of coding sequences was predicted to be 2461. Further, 1474 proteins were identified via proteomic analysis upon growth on water kefir medium. So, there are increasing concerns regarding metabolic activity traceability.

Metabolic prediction of *L. hordei* TMW 1.1822 based on both annotated genes and quantified proteins revealed the presence of all enzymes, which were required for the glycolytic Embden-Meyerhof (EMP) and phosphoketolase (PK) pathways. Also, genes



encoding all enzymes involved in citrate, pyruvate and mannitol metabolism were present. Further, it was confirmed that *L. hordei* was prototrophic for 11 amino acids and auxotrophic for 6 amino acids according to the putative amino acids biosynthesis pathways and growth determination with amino acid deficiency. The peptide transport and arginine deiminase systems contributed to acid tolerance, and fatty acid synthesis were further predicted to enable the lifestyle of *L. hordei* in water kefir: abundant sucrose was consumed directly via parallel EMP and PK pathways and was also extracellularly converted to dextran and fructose by a glucansucrase, leaving fructose as additional carbon source. Essential amino acids (in the form of peptides) and citrate was acquired from fruits. In the lack of FabB, unsaturated fatty acids were likely synthesized by alternative enzymes. Formation of acetoin and diacetyl as well as arginine conversion reactions enabled acidification limitation. Thus, first insight was provided as a basis for understanding how other members of the water kefir consortium (yeasts, acetic acid bacteria) facilitate or support the growth of *L. hordei*.

Authors contributions: Di Xu planned the research project guided by Jürgen Behr and Rudi F. Vogel. The genomic and proteomic sample preparations were accomplished by Di Xu. The genomic sequence data obtained from GATC were assembled with the help of Lara Eisenbach. The proteomic samples were analyzed with the aid of Jürgen Behr from the Bavarian Center for Biomolecular Mass Spectrometry. The proteomic data were evaluated by Di Xu with the suggestions from Andreas J. Geißler. Di Xu wrote the manuscript draft. Julia Bechtner optimized the schemes of sucrose and pyruvate metabolism, conducted BADGE analysis and introduced respective parts into the manuscript. All authors reviewed and approved the final manuscript.



Contents lists available at ScienceDirect

## International Journal of Food Microbiology

journal homepage: [www.elsevier.com/locate/ijfoodmicro](http://www.elsevier.com/locate/ijfoodmicro)Lifestyle of *Lactobacillus hordei* isolated from water kefir based on genomic, proteomic and physiological characterizationDi Xu<sup>a,1</sup>, Julia Bechtner<sup>a,1</sup>, Jürgen Behr<sup>a,b,2</sup>, Lara Eisenbach<sup>a</sup>, Andreas J. Geißler<sup>a</sup>, Rudi F. Vogel<sup>a,\*</sup><sup>a</sup> Lehrstuhl für Technische Mikrobiologie, Technische Universität München, Freising, Germany<sup>b</sup> Bavarian Center for Biomolecular Mass Spectrometry (BayBioMS), Freising, Germany

## ARTICLE INFO

## Keywords:

*Lactobacillus hordei*  
Functional genome prediction  
Proteomic analysis  
Lifestyle  
Metabolism

## ABSTRACT

Water kefir is a traditional fermented beverage made from sucrose, water, kefir granules, dried or fresh fruits. In our water kefir granules, *Lactobacillus (L.) hordei* is one of the predominant lactic acid bacteria (LAB) species of this presumed symbiotic consortium. It faces abundant sucrose versus limitation of amino- and fatty acids in an acidic environment. Sequencing of the genome of *L. hordei* TMW 1.1822 revealed one chromosome plus three plasmids. The size of the chromosome was 2.42 Mbp with a GC content of 35% GC and 2461 predicted coding sequences. Furthermore, we identified 1474 proteins upon growth on water kefir medium. Metabolic prediction revealed all enzymes required for the glycolytic Embden-Meyerhof (EMP) and phosphoketolase (PKP) pathways. Genes encoding all enzymes involved in citrate, pyruvate and mannitol metabolism are present.

Moreover, it was confirmed that *L. hordei* is prototrophic for 11 amino acids and auxotrophic for 6 amino acids when combining putative biosynthesis pathways for amino acids with physiological characterization. Still, for glycine, serine and methionine no sure auxotype could be determined. The OppABCDF peptide transport system is complete, and 13 genes encoding peptidases are present. The arginine deiminase system, was predicted to be complete except for carbamate kinase, thus enabling neutralization reactions via ammonium formation but no additional energy generation. Taken together our findings enable prediction of the *L. hordei* lifestyle in water kefir: Abundant sucrose is consumed directly via parallel EMP and PK pathways and is also extracellularly converted to dextran and fructose by a glucansucrase, leaving fructose as additional carbon source. Essential amino acids (in the form of peptides) and citrate are acquired from fruits. In the lack of FabB unsaturated fatty acids are synthesized by predicted alternative enzymes. Formation of acetoin and diacetyl as well as arginine conversion reactions enable acidification limitation. Other members of the water kefir consortium (yeasts, acetic acid bacteria) likely facilitate or support growth of *L. hordei* by delivering gluconate, mannitol, amino- and fatty acids and vitamins.

## 1. Introduction

Water kefir is a traditional fermented beverage made from sucrose, water, kefir grains, and dried or fresh fruits (e.g. figs). The microbiota isolated from kefir grains comprise a stable presumably symbiotic multispecies consortium, which generally consists of lactic acid bacteria (LAB), acetic acid bacteria and yeasts (Gulitz et al., 2011; Irigoyen et al., 2005; Marsh et al., 2013; Vardjan et al., 2013). Strains of *L. hordei* are among the most commonly isolated LAB from kefir grains (Gulitz et al., 2011; Hsieh et al., 2012; Laureys and De Vuyst, 2017). Under a biochemical perspective, LAB are classified as homofermentative and heterofermentative based on their main products from carbohydrate

fermentation. In general, homofermentative LAB including *L. hordei* convert carbohydrates mainly into lactic acid through the Embden-Meyerhof pathway (EMP), whereas heterofermentative LAB produce acetic acid, ethanol and carbon dioxide apart from lactic acid using the phosphoketolase pathway (PKP) (Årsköld et al., 2008; Kandler, 1983; Kleerebezem et al., 2003; Kleerebezem and Hugenholtz, 2003). However, along the species description *L. hordei* (isolated from barley (*Hordeum vulgare*)) is unable to ferment pentoses, but ferments a variety of hexoses and disaccharides, including sucrose and also mannitol to produce acids (Rouse et al., 2008). Therefore, the role of the PKP should be different from using pentoses in this organism.

Information on the metabolism of LAB from the water kefir

\* Corresponding author.

E-mail address: [rudi.vogel@wzw.tum.de](mailto:rudi.vogel@wzw.tum.de) (R.F. Vogel).<sup>1</sup> Joint first authorship for equal contribution.<sup>2</sup> Current address: Leibniz-Institut für Lebensmittel-Systembiologie an der Technischen Universität München, Freising, Germany.<https://doi.org/10.1016/j.ijfoodmicro.2018.10.004>

Received 22 May 2018; Received in revised form 10 September 2018; Accepted 3 October 2018

Available online 09 October 2018

0168-1605/ © 2018 Elsevier B.V. All rights reserved.

consortium is restricted to a few studies. As sucrose is the main carbon source, the organisms either directly take it up and metabolize it intracellularly, or it is metabolized via extracellular or cell-bound bacterial glycosyltransferases producing glucans or fructans and leaving fructose or glucose as “secondary” carbon sources, respectively (Gulitz et al., 2011). Looking at the overall conversion reactions of the consortium it was found that a mixture of lactic and acetic acid as well as ethanol and glycerol are formed as can be expected from the composition of the microbial consortium of LAB, yeasts and acetic acid bacteria. In addition, mannitol formation has been observed (Laureys and De Vuyst, 2014). This suggests the use of fructose not only as carbon source but also as electron acceptor by some members of the consortium. Also, the consortium produces volatile compounds with sensory attributes including isoamyl acetate, isoamyl alcohol, ethyl acetate, 2-methyl-1-propanol, ethyl octanoate, ethyl decanoate, ethyl hexanoate (Laureys and De Vuyst, 2014). From this study, the specific contribution of groups or species remains speculative. In a more detailed study employing single isolates and mixtures, thereof the metabolic interaction of *L. nagelii* and *L. hordei* with *Zygorhizula* (*Z. florentina*) was examined (Stadie et al., 2013). This study suggests that *Z. florentina* appreciates the pH decrease caused by lactic acid fermentation, while a trophic interaction between *L. hordei* and this yeast is constituted by the release of amino acids and vitamin B<sub>6</sub>. Co-cultivation of *L. nagelii* with *Z. florentina* apparently induced the release of arginine by the yeast, which was found to be essential for the growth of *L. nagelii*.

Despite the research on water kefir and its microbiome, the formation of the kefir granule is not yet understood. Previous research suggested *L. hilgardii* to be the main producer of the kefir granule polysaccharide (Fels et al., 2018; Pidoux, 1988; Waldherr et al., 2010). Still, it remains unclear, how other bacteria and yeasts become embedded into this polysaccharide network. In this context, recent results showed, that different *L. hordei* strains produce extracellular polysaccharides from sucrose, capable of inducing yeasts to form aggregates, which has not been observed for other lactic acid bacteria (Xu et al., 2018). This renders *L. hordei* as an interesting target for further investigations on its lifestyle and contribution to the formation of the water kefir consortium and granule.

Apart from the findings reported in the species description of *L. hordei* strains isolated from barley (Rouse et al., 2008), glycolytic pathways and pyruvate metabolism of *L. hordei* from water kefir as well as amino acid biosynthesis and conversion reactions are widely unexplored. Here, an isolate of *L. hordei* from water kefir was whole-genome sequenced for the first time and the putative metabolic pathways were reconstructed. Specific metabolic traits were also investigated in physiological tests. Together with a comprehensive proteomic analysis of cells growing in water kefir medium a basis is provided for understanding how *L. hordei* adapts to the water kefir environment and potentially interacts with other microbiota in water kefir.

## 2. Material and methods

### 2.1. Strain culture and DNA isolation

*L. hordei* TMW 1.1822, isolated from water kefir by Gulitz et al. (Gulitz et al., 2011), was spread directly on mMRS agar plates described by Stolz et al. (Stolz et al., 1995), from a  $-80^{\circ}\text{C}$  stock of our strain collection and incubated anaerobically at  $30^{\circ}\text{C}$  for 2 d. A single colony was transferred into 15 mL liquid mMRS medium and cultured anaerobically at  $30^{\circ}\text{C}$  for 20 h. Isolation of high molecular weight DNA was performed using the Genomic-tip 100/G kit (Qiagen, Venlo, Netherlands) according to the manufacturer. The isolation protocol was modified on the lysis time of proteinase K overnight. Quality and quantity of isolated DNA was checked by NanoDrop (Thermo Fisher Scientific) and agarose gel electrophoresis.

### 2.2. Sequencing strategy, assembly and annotation

About 15  $\mu\text{g}$  of the isolated genomic DNA of *L. hordei* TMW 1.1822 at the concentration of 560 ng/ $\mu\text{L}$  was sent to and sequenced by GATC Biotech (Konstanz, Germany) via PacBio Single Molecule Real Time (SMRT) sequencing as described previously (Eid et al., 2009; Geißler et al., 2016a; McCarthy, 2010). Raw data were assembled according to SMRT Analysis (Version 2.2.0.p2), the hierarchical genome assembly process (HGAP) (Chin et al., 2013) and manual curation described by PacBio (<https://github.com/PacificBiosciences/Bioinformatics-Training/wiki/Finishing-Bacterial-Genomes>). Upon assembly of chromosome and all plasmids separately, these contigs were circularized using minimus2 (AMOS, <http://amos.sourceforge.net>) to generate the whole genome. Finally, the complete whole genome sequence was submitted to NCBI GenBank. The genome was further annotated by the NCBI Prokaryotic Genome Annotation Pipeline ([https://www.ncbi.nlm.nih.gov/genome/annotation\\_prok/](https://www.ncbi.nlm.nih.gov/genome/annotation_prok/)) and RAST, which is a SEED-based prokaryotic genome annotation service using default settings (Aziz et al., 2008; Overbeek et al., 2013).

### 2.3. Chromatographic analysis of sugars and organic acids, determination of auxotrophic and prototrophic amino acids

Consumption and production of sugars and organic acids of *L. hordei* grown in chemically defined medium (CDM, pH 6.5) after 24 h were quantified by a Dionex UltiMate 3000 HPLC system (Dionex, Idstein, Germany) with Rezex ROA-Organic Acid H<sup>+</sup> column (Phenomenex, Aschaffenburg, Germany) and RI-101 detector (Shodex, München, Germany) as described by Geissler et al. (Geißler et al., 2016b). The composition of CDM is listed in Table S1. The supernatants of each fermented sample were collected by centrifugation (14,000g, 10 min) and then treated with protein precipitation before injecting into HPLC system. Protein precipitation was carried out as follows. 1 mL of each sample in triplicate were added with 50  $\mu\text{L}$  70% perchloric acid (v/v) and vortex for mixing. After 24 h, standing at  $4^{\circ}\text{C}$ , the mixture was centrifuged (14,000g, 10 min) again to collect the supernatant. The supernatant was diluted if necessary, filtered by 0.2  $\mu\text{m}$  regenerated cellulose membrane (Phenomenex) and ready for chromatographic analysis. Analytes were separated at a constant flow rate of 0.7 mL/min with column temperature of  $85^{\circ}\text{C}$  for 30 min. Sulfuric acid (Rotipuran, Roth, Karlsruhe, Germany) solution with a concentration of 5 mM was served as mobile phase.

The growth of *L. hordei* TMW 1.1822 was tested in full CDM in comparison to incomplete CDM, in which one amino acid was respectively omitted to reveal the auxotrophic or prototrophic for amino acids by Stadie et al. (Stadie, 2013). If *L. hordei* could grow, or could not grow when one amino acid was omitted, then *L. hordei* was considered as prototrophic or auxotrophic for this amino acid, respectively.

### 2.4. Genomic statistical analyses and visualization

A genomic atlas was generated using Artemis and DNA plotter (<http://www.sanger.ac.uk/science/tools/artemis/>) (Carver et al., 2008) by importing the whole genome GenBank file. Subcellular localization of proteins was predicted utilizing the tool PSORTb (Version 3.0.2, <http://www.psort.org/psortb/>) (Gardy et al., 2004; Yu et al., 2010). Functional analysis was accomplished using SEED categorization based on RAST and SEED subsystem analysis (Subsystem and FIGfams Technology) (Aziz et al., 2008; Overbeek et al., 2013). The SEED subsystem analysis enables the assignment of predicted genes to a category, subcategory and subsystem. All the annotated EC and KO numbers, which were extracted from RAST fasta files (Table S2), could be directly imported into iPath 3.0 (<https://pathways.embl.de/ipath3.cgi?map=metabolic>) (Yamada et al., 2011) to obtain an overview of complete metabolic pathways and biosynthesis of other secondary metabolites customized in red color.

Based on the pathway of glycolysis, pentose phosphate and TCA cycle from the BioCyc Database Collection (<https://biocyc.org/>), all enzymes involved in each reaction step were subjected to manual check if they were present in translated open reading frames (ORFs) files annotated from NCBI and RAST. In detail, if one enzyme involved in a pathway was manually checked to be present in both files, its corresponding ORF was imported into NCBI Conserved Domain Search (<https://www.ncbi.nlm.nih.gov/Structure/cdd/wrpsb.cgi>) and Smart BLAST ([https://blast.ncbi.nlm.nih.gov/Smartblast/?LINK\\_LOC=BlastHomeLink](https://blast.ncbi.nlm.nih.gov/Smartblast/?LINK_LOC=BlastHomeLink)) to manually double check the function of this enzyme. In this way, the enzyme was eventually confirmed to be present based on the functional genome prediction.

The presence of enzymes involved in pyruvate metabolism, the arginine deiminase (ADI) pathway and biosynthesis pathway of amino acids were verified in the similar workflow except the source of reference schematic pathway was different. The pathway of pyruvate metabolism was according to Geißler (Geißler, 2016) and Quintans et al. (Quintans et al., 2008), while ADI pathway based on Rimaux et al. and Tonon et al. (Rimaux et al., 2011; Tonon and Lonvaud-Funel, 2002), biosynthesis pathway of amino acids referred to KEGG mapper (<http://www.genome.jp/kegg/pathway.html>). The figure of the biosynthesis pathway of amino acids was generated using KEGG PATHWAY mapping tool ([http://www.genome.jp/kegg/tool/map\\_pathway1.html](http://www.genome.jp/kegg/tool/map_pathway1.html)) by importing EC numbers only involved in amino acids biosynthesis (Table S2).

The whole genome sequence of *L. hordei* DSM 19519 (Accession no. AZDX01000000), originally isolated from barley (Sun et al., 2015) was downloaded from NCBI (<https://www.ncbi.nlm.nih.gov/>). Genomic differences to *L. hordei* TMW 1.1822 were identified by whole genome comparison using Blast Diagnostic Gene findEr (BADGE) (Behr et al., 2016) under default settings.

### 2.5. Sample preparation for proteomic analysis, liquid chromatography and mass spectrometry

1% (v/v) pre-cultured *L. hordei* were inoculated into 40 mL WKM in triplicate and cultured anaerobically at 30 °C for 10 h. Afterwards, trichloroacetic (TCA) was added to those samples to a final concentration of 6.25% w/v (stock concentration TCA 100% w/v). Subsequently samples were stored on ice for 10 min. The bacterial pellets were collected by centrifugation (5000 rpm, 5 min) at 4 °C, washed twice with acetone, reconstituted in lysis buffer (8 M urea, 5 mM EDTA di-sodium salt, 100 mM (NH<sub>4</sub>)<sub>2</sub>CO<sub>3</sub>, 1 mM Dithiothreitol (DDT), pH 8.0) and mechanically disrupted with acid-washed glass beads (G8772, 425–600 µm, Sigma, Germany). Total protein concentration of the lysate was determined using the Bradford method (Bio-Rad Protein Assay, Bio-Rad Laboratories GmbH, Munich, Germany). 100 µg protein extract was used per sample for in-solution digestion. Proteins were reduced with 10 mM DTT at 30 °C for 30 min, and subsequently carbamidomethylated with 55 mM chloroacetamide in the dark at room temperature for 60 min. Subsequently proteins were digested by addition of 1 µg trypsin (1:100 trypsin:protein) for 3 h at 37 °C and another 1 µg of trypsin overnight at 37 °C. Digested peptide samples were desalted according to the manufacturer's instructions by C18 solid phase extraction using Sep-Pak columns (Waters, WAT054960). Purified peptide samples were dried in a SpeedVac and resuspended in 2% acetonitrile, 98% H<sub>2</sub>O, 0.1% formic acid to a final concentration of 0.25 µg/µl as determined by Nanodrop measurement.

Generated peptides were analyzed on a Dionex Ultimate 3000 nano LC system coupled to a Q-Exactive HF mass spectrometer (Thermo Scientific, Bremen, Germany). Peptides were delivered to a trap column (75 µm × 2 cm, self-packed with Reprosil-Pur C18 ODS-3 5 µm resin, Dr. Maisch, Ammerbuch, Germany) at a flow rate of 5 µL/min in solvent A<sub>0</sub> (0.1% formic acid in water). Peptides were separated on an analytical column (75 µm × 40 cm, self-packed with Reprosil-Gold C18, 3 µm resin, Dr. Maisch, Ammerbuch, Germany) using a 120 min linear

gradient from 4 to 32% solvent B (0.1% formic acid, 5% DMSO in acetonitrile) and solvent A<sub>1</sub> (0.1% formic acid, 5% DMSO in water) at a flow rate of 300 mL/min. The mass spectrometer was operated in data dependent mode, automatically switching between MS1 and MS2 spectra. MS1 spectra were acquired over a mass-to-charge (*m/z*) range of 360–1300 *m/z* at a resolution of 60,000 (at *m/z* 200) using a maximum injection time of 50 ms and an AGC target value of 3e6. Up to 20 peptide precursors were isolated (isolation window 1.7 *m/z*, maximum injection time 25 ms, AGC value 1e5), fragmented by higher-energy collisional dissociation (HCD) using 25% normalized collision energy (NCE) and analyzed at a resolution of 15,000 with a scan range from 200 to 2000 *m/z*. Precursor ions that were singly-charged, unassigned or with charge states > 6+ were excluded. The dynamic exclusion duration of fragmented precursor ions was 20 s.

### 2.6. Peptide and protein identification and quantification

Peptide and protein identification plus quantification were performed with MaxQuant (version 1.5.7.4) (Cox and Mann, 2008) by searching the MS2 data against all protein sequences from *L. hordei* (cf. Section 3.1, GenBank CP018176 - CP018179) using the embedded search engine Andromeda (Cox et al., 2011). Carbamidomethylated cysteine was a fixed modification; oxidation of methionine, and N-terminal protein acetylation were variable modifications. Trypsin/P was specified as the proteolytic enzyme and up to 2 missed cleavage sites were allowed. Precursor and fragment ion tolerances were 10 ppm and 20 ppm, respectively. Label-free quantification (Cox et al., 2014) and data matching between consecutive analyses were enabled within MaxQuant. Search results were filtered for a minimum peptide length of 7 amino acids, 1% peptide and protein false discovery rate (FDR) plus common contaminants and reverse identifications. MaxQuant output files (proteinGroups.txt) were further performed using Perseus (version 1.5.6.0) (Tyanova et al., 2016). NCBI annotation, Psortb subcellular localization, SEED category (subcategory and subsystem) as previously annotated (cf. Sections 2.2 and 2.4) were added to the matrix through matching rows by Protein IDs and Locus.

## 3. Results and discussions

### 3.1. General genomic features and prediction of metabolic pathways

*L. hordei* is a predominant and stable fermentation species isolated from water kefir (Gulitz et al., 2011). The complete genome of *L. hordei* TMW 1.1822 in this study was sequenced by PacBio RS II SMRT to get insight into its niche adaptation to the water kefir system and provide the basis for consecutive analyses. It was submitted to GenBank designated as BioSample SAMN06052353, which was part of the BioProject PRJNA343197. Referred to as accession numbers CP018176 to CP018179, the four resulting contigs were identified as one chromosome plus three plasmids. Consisting of 2.42 Mbp in size, the chromosome was found to fit in the typical range of some other lactobacilli (Vogel et al., 2011), and exhibits a GC content of 35%. The 3 plasmids exhibited a GC content of 37.37%, 39.27%, 40.12%. Plasmid sizes ranged from 38, 056 bp, 60, 901 bp to 68, 542 bp, resulting in an overall genome size of 2.59 Mbp. The number of coding sequences (CDS) according to NCBI were 2461 and the coding density is 86.27%, which is visualized as a circular genome in Fig. 1. There were 105 pseudogenes, 61 tRNA and 6 rRNA found randomly distributed in the chromosome. The GC skew graph observed in circular chromosome was clarifying the shift point, which was reported, correlated with the loci of *ori* and *ter* (Frank and Lobry, 1999). The genome of *L. hordei* TMW 1.1822 isolated from water kefir is the second whole genome sequence besides *L. hordei* DSM 19519, which was isolated from malted barley in 2015 (Sun et al., 2015). The availability of the genome sequence provided the basis for consecutive proteomic analysis, with the objective to derive the basic metabolism and lifestyle of *L. hordei* in water kefir. An

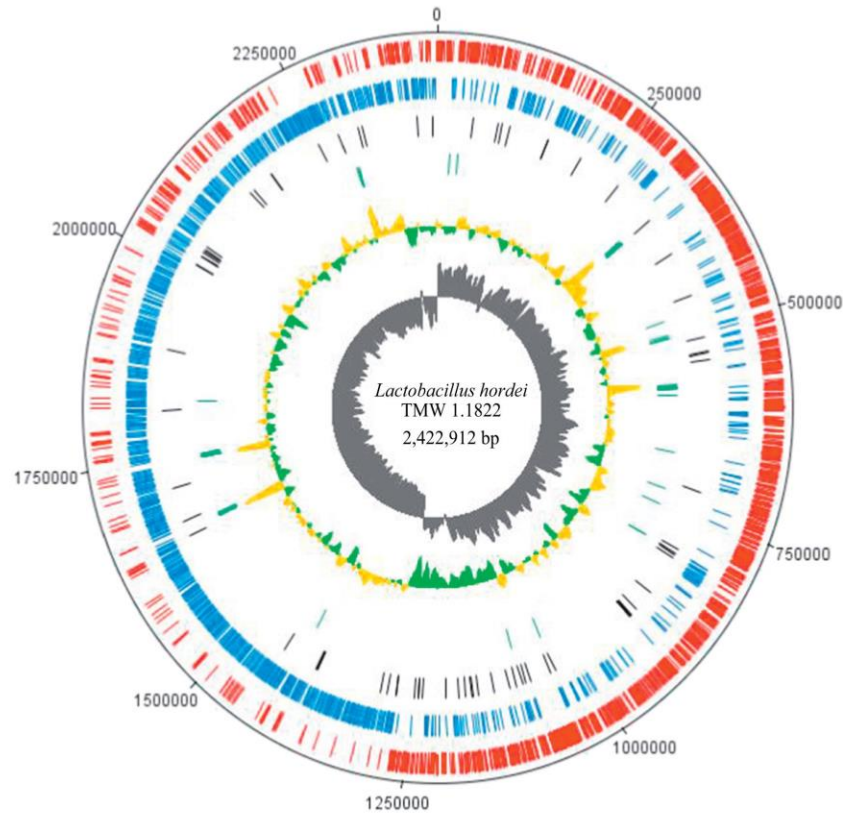


**Fig. 1.** Genomic atlas of *L. hordei* TMW 1.1822. From the outer circle to inner circle are as below. Forward CDS (red), Reverse CDS (blue), Pseudogenes on both strands (black), tRNA and rRNA (dark green), %GC plot (green, low GC spike and yellow, high GC spike), GC skew  $[(G - C) / (G + C)]$  (grey). (For interpretation of the references to color in this figure legend, the reader is referred to the web version of this article.)

overview of the metabolic pathways was generated as a basis for subsequent, detailed analyses (shown in Fig. S1).

### 3.2. Proteomic analysis

A total of 1474 proteins were identified in triplicate proteomic analyses from *L. hordei* growing in water kefir medium, representing nearly 60% of the genes predicted from the genome. The in silico predicted and identified proteins were thoroughly annotated in terms of subcellular localization and SEED category prediction. Fig. 2A shows the absolute number of respective proteins in cytoplasmic, cytoplasmic membrane, cell wall, extracellular space and unknown location in the table below and their proportions with respect to the total number of proteins (above the histogram) by the bar chart. As shown in Fig. 2B, most abundant proteins were assigned to protein metabolism (16%) and carbohydrates (11%), followed by amino acids and derivatives (10%) and cell wall and capsule (9%). Taken together, it was in agreement with the fact that LAB express a relatively simple, limited in metabolism and generally need nutrient-rich environments where carbohydrates, amino acid sources and other nutrients are abundant. Since water kefir medium is characterized by rich sucrose supply at the concentration of 80 g/L and is limited in the supply of amino acids and lipids, we focused our analysis on respective metabolic and biosynthetic functions to depict the lifestyle of *L. hordei* in water kefir.

### 3.3. Sugar transport and central carbohydrate metabolism

An overview on the key reactions involved in sucrose metabolism of *L. hordei* is provided in Fig. 3. Generally, sucrose can either be taken up and metabolized or converted by a glycosyltransferase (glucansucrase) into a glucan and fructose, which is subsequently metabolized. The structure and ecological function of *L. hordei* glucan have been previously characterized (Xu et al., 2018). It has been demonstrated that a specific glucan structure is produced, which induces network formation of *Saccharomyces cerevisiae* sharing the water kefir consortium and thus ensures close proximity of this yeast. A total of 10 PTS sugar transport systems were predicted from the genome, which catalyze the phosphorylation of incoming sugar and transport them into the cell. According to the annotation, these PTS should enable for the transport of sucrose, glucose, fructose, mannose, sorbose, mannitol,  $\beta$ -glucoside, cellobiose, galactitol and galactosamine. These PTS deliver phosphorylated sugar derivatives, which feed the central carbon metabolism. Analysis of the annotated whole genome of *L. hordei* confirmed the presence of the genes encoding all enzymes required for the EMP and PKP pathways. Detailed information on these enzymes is given in Table S3, which includes locus tags of NCBI and IDs of RAST. The proteins encoded in those genes were also identified as being expressed when *L. hordei* was grown in WKM after 10 h. Thus, *L. hordei* TMW 1.1822 could be considered as facultatively homofermentative with regard to the discrimination of LAB into three physiological groups: (i) the facultatively homofermentative LAB, possessing both EMP and PKP, but

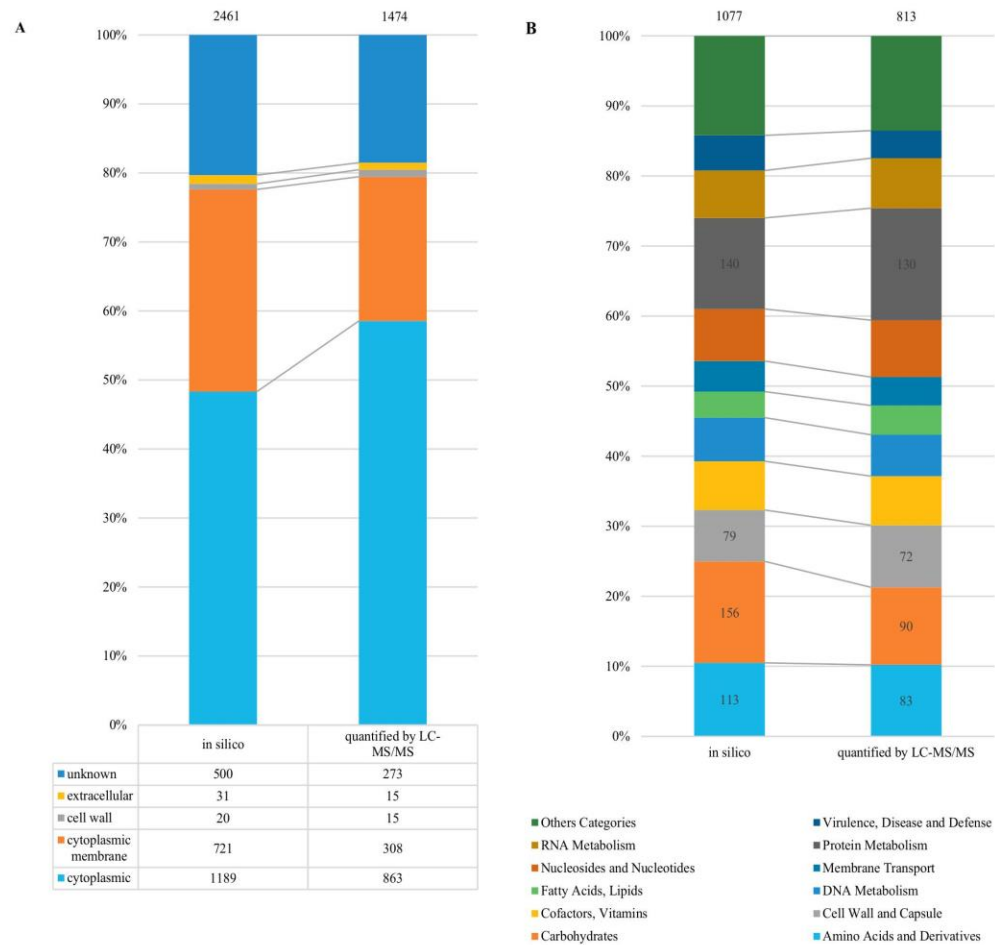


**Fig. 2.** Subcellular localization of proteins (in silico, identified by LC-MS/MS) which were predicted by PsortB (A). The proportion of proteins assigned to each respective subcellular compartment and the group “unknown” with respect to the total number of proteins is shown by the bar chart. The table below shows the respective absolute numbers, and the number above is the total number of proteins. SEED categories of proteins (in silico, identified by LC-MS/MS) which were predicted by SEED (B). The proportion of proteins assigned to each respective categories of metabolism and the group “other categories” which is the sum of several small categories with respect to the total number of proteins is shown by the bar chart. Above each column is the total number of predicted SEED categories.

preferably degrading glucose via EMP and potentially use the PKP for the degradation of pentoses such as *L. plantarum* WCFS1, *Lactococcus lactis* (Kleerebezem et al., 2003; Kleerebezem and Hugenholtz, 2003), (ii) the obligately homofermentative LAB, lacking both glucose-6-phosphate dehydrogenase and phosphogluconate dehydrogenase (*Thermobacterium*), and (iii) the heterofermentative LAB, lacking fructose-bisphosphate aldolase (*Betabacterium*) (Ljungh and Wadström, 2009) or 6-phosphofructokinase (Cibrario et al., 2016). The expression of the PKP in *L. hordei* could enable production but also utilization of gluconate. The gluconate may simply be an intermediate of the PKP but could also result from the metabolism of acetic acid bacteria in this water-kefir consortium, and thus gluconate utilization appears to be a decisive trait reflecting adaptation to live in the water kefir consortium. Phosphoketolase as key enzyme of PKP can catalyze xylulose-5-phosphate into acetylphosphate (acetyl-P) and glyceraldehyde-3-phosphate (GAP). On one hand, acetyl-P could be converted into ethanol or (preferably) acetate enabling additional ATP generation in the acetate kinase reaction. This reaction depends on the presence and utilization of external electron acceptors, which would be needed to enable

maintenance of the redox balance. In fact, fructose is generated by the activity of the glycosyltransferase, which produces a glucan from sucrose. However, *L. hordei* does not possess a known homolog for mannitol dehydrogenase. Still, mannitol could be generated by other members of the consortium, e.g. *S. cerevisiae*, which is held in proximity by the glucan-induced network formation (Xu et al., 2018), and serve as a substrate for *L. hordei*. Indeed, a predicted PTS system for mannitol transport and phosphorylation as well as mannitol-P-5 dehydrogenase delivering fructose-6-phosphate are expressed, which enable the growth on mannitol even as sole carbon source upon entering the EMP. Indeed, *L. hordei* can grow with mannitol and also gluconate as sole carbon sources, which matches the prediction from the genome.

Furthermore, *L. hordei* produced 19.8 mM lactic acid and 6.1 mM acetic acid, while no ethanol was detected by HPLC after 24 h fermentation (Fig. 4). In the presence of EMP and PKP pathways *L. hordei* could have two alternatives for acetate formation. Acetate could result from the PKP as an alternative to ethanol, or via pyruvate decarboxylase from pyruvate stemming from either EMP or PKP. With a lactate/acetate ratio of 3.2 *L. hordei* cannot be considered an obligate



extracellular glycosyltransferases found in the genome. Also, transporters involved in fructose import were less represented than in *L. hordei* TMW 1.1822 from water kefir. These findings provide evidence for the adaptation of *L. hordei* TMW 1.1822 to the sucrose-rich water kefir environment as a stable part of the water kefir consortium.

### 3.4. Citrate and pyruvate metabolism, TCA cycle

Since water kefir contains lemon slices, metabolic conversion of citrate is a common trait of associated lactobacilli (Hugenholtz, 1993). Therefore, the putative functional genome of *L. hordei* was searched for the presence of genes involved in citrate uptake and metabolism.

Besides undirected transfer of citrate into the cytoplasm at low pH, the organism should be capable of directed import via a citrate/sodium symporter, which was also detected upon proteomic analysis. Also found in genome and proteome of *L. hordei*, the enzymes citrate lyase and oxaloacetate decarboxylase contribute to pyruvate generation by conversion of the imported citrate, requiring no  $\text{NAD}^+$  recycling upon acetate formation. Completing these results, also the presence and expression in the proteome of the citrate lyase transcriptional regulator (*citI*) was confirmed, which was reported as a citrate activated switch, allowing the cell to optimize generation of metabolic energy (Martin et al., 2005). Thus, the pyruvate pool is filled from both the glycolytic pathway and citrate metabolism. Depicted in Fig. 5, further genomic and proteomic analysis revealed the presence of enzymes involved in different strategies for downstream pyruvate conversion. *L. hordei* should not only be capable of ATP generation upon acetate formation by an acetate kinase, but also of maintenance of redox balance by L/D-lactate (No. 11, shown in Table S3) and ethanol release. Since ethanol was not detectable by HPLC analysis, other strategies for  $\text{NAD}^+$  recycling appeared to be more favorable, also including transformation of pyruvate to diacetyl, acetoin and 2,3-butanediol. Catalyzing the reaction of pyruvate to  $\alpha$ -acetylacetyl, acetylacetyl synthase represents the key enzyme in the synthesis of these compounds. Once synthesized,  $\alpha$ -acetylacetyl is unstable and is either non-enzymatically decarboxylated to diacetyl or converted to acetoin by  $\alpha$ -acetylacetyl decarboxylase. Eventually, a diacetyl/acetoin reductase transforms diacetyl to acetoin, which is subsequently converted to 2,3-butanediol upon simultaneous  $\text{NAD}^+$  recycling. Since *L. hordei* was found to express all relevant enzymes in its proteome for the synthesis of these  $\text{C}_4$  compounds, it may also contribute to the sensory characteristics of water kefir.

Further genomic analysis revealed the lack of citrate synthase, 2-oxoglutarate dehydrogenase, succinyl-CoA synthetase, succinate dehydrogenase, malate dehydrogenase and malate oxidoreductase, impeding the organism from running a complete TCA cycle. This was

confirmed by proteomic analysis and is consistent with other LAB, including *Lactococcus lactis* IL1403 and *L. plantarum* WCFS1 (Bolotin et al., 2001; Kleerebezem et al., 2003; Kleerebezem and Hugenholtz, 2003), which are the most extensively studied LAB in food fermentation.

### 3.5. Proteolytic system, amino acids biosynthesis, metabolism and transport

Many LAB, namely those adapted to environments lacking intrinsic protease activity (e.g. milk in contrast to meat or plant-derived environments) are equipped with a protein-degradation machinery, which enables the ability to obtain peptides and amino acids from proteins (Lopez-Kleine and Monnet, 2011). However, our in silico analyses of the genome of *L. hordei* isolated from water kefir did not reveal homologs to a protease (*prt*) gene. Still, it encoded and expressed on proteome level the complete uptake system for peptides, which originate from the fruits in the water kefir directly or via the proteolytic activity of plant enzymes or other microbes of the consortium. There were OppABCDF consisting of an oligopeptide-binding protein (OppA), two integral membrane proteins (OppB and OppC), and two nucleotide-binding proteins (OppD and OppF) which transport di-, tripeptides, and oligopeptides (Detmers et al., 1998; Tynkkynen et al., 1993). Upon uptake, these peptides can be degraded by a variety of peptidases (Christensen et al., 1999; Kunji et al., 1996). The *L. hordei* genome contains 13 genes encoding peptidases such as aminopeptidases, oligo-/di-/tri-peptidases, endopeptidases and uncharacterized peptidases listed in Table S4. The predicted peptidases of *L. hordei* were shown to be more closely related to those of *L. sanfranciscensis* TMW 1.1304 and *L. plantarum* WCFS1, but more distant to intestinal *L. johnsonii* NCC 533, which were shown to have > 25 peptidases (Kleerebezem et al., 2003; Pridmore et al., 2004; Vogel et al., 2011). Possibly this reflects their relation to plant proteins versus milk proteins.

The analysis of the *L. hordei* genome revealed biosynthesis pathways for 12 amino acids and incomplete pathways for 8 amino acids (shown in Fig. S2). Therefore, prototrophy was predicted of *L. hordei* for 12 amino acids and auxotrophy for 8 amino acids (Table S5). This result was not further proven by identified proteins, because there were only 83 proteins identified by LC-MS/MS compared to 113 proteins predicted in silico involved in amino acids and derivatives (Fig. 2B). Due to the absence of branched-chain amino acid aminotransferase, biosynthesis pathways of branched-chain amino acids (leucine, isoleucine and valine) were incomplete. The biosynthesis pathways of phenylalanine, tryptophan and tyrosine were incomplete either, due to the absence of 3-deoxy-7-phosphoheptulonate synthase and other enzymes. Auxotrophy for serine and glycine was predicted from the absence of

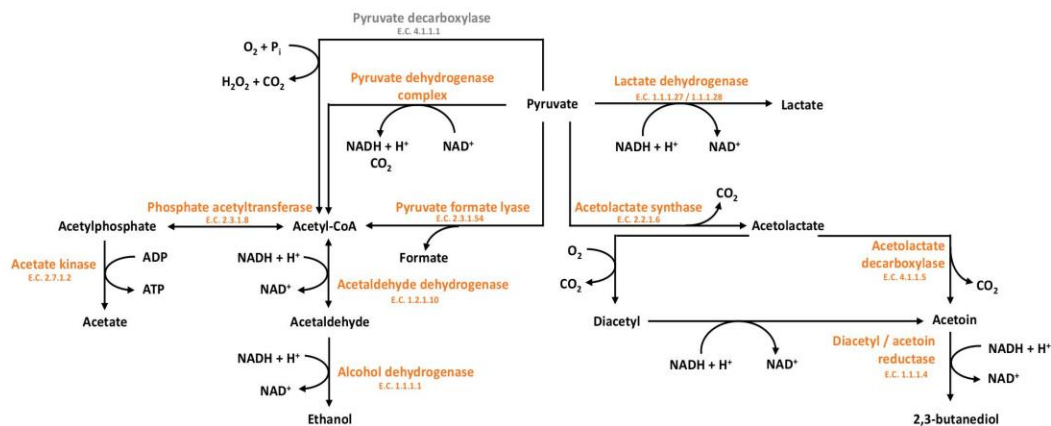


Fig. 5. Pyruvate metabolism of *L. hordei* TMW 1.1822.



phosphoserine phosphatase and other enzymes (see Table S5 for details). What is more, auxotrophy for serine, glycine, leucine, isoleucine and valine is consistent with the presence of serine/alanine/glycine transporter (CycA) and the branched-chain amino acid transporter (AzlC). It suggests the capability to uptake these amino acids directly from the secretion of other symbiotic microbes such as yeast or the degradation of peptides from fruits or yeast. A gene encoding a putative arginine transporter was predicted to be present, which could import any arginine produced by members of the consortium.

In addition, the growth of *L. hordei* was examined in incomplete CDM compared to full CDM to reveal amino acids auxotrophies. The results were almost identical with biosynthesis pathways of amino acids predicted from the genome, but different in the deductive auxotype of glycine, serine and methionine (Table S5). For instance, *L. hordei* was considered as auxotroph for serine from genomic prediction, but inferred to be prototroph with respect to serine upon physiological characterization. This suggests an alternative pathway for the biosynthesis of serine or a mistake in genome sequencing or annotation. Hence, it was confirmed that *L. hordei* was surely prototrophic for 11 amino acids and auxotrophic for 6 amino acids when combining genomic prediction with physiological analysis. For comparison, the genome of *L. plantarum* WCFS1 predicts prototrophy for 17 amino acids except for leucine, isoleucine and valine (Kleerebezem et al., 2003). In contrast, *L. sanfranciscensis* TMW 1.1304 is predicted to be auxotrophic for 12 amino acids (Vogel et al., 2011), and *L. acidophilus* NCFM for 14 amino acids (Altermann et al., 2005). So the capability of de novo synthesis of amino acids of *L. hordei* is intermediate, which suggests that in the water kefir there are still enough amino acids available from (dried) fruit or symbionts to enable prominent *L. hordei* growth.

### 3.6. Acid tolerance via arginine deiminase system

Degradation of arginine via the arginine deiminase (ADI) system is widely distributed in LAB genera such as *Lactobacillus*, *Lactococcus*, *Leuconostoc* and *Weissella*. Functionally, it enables enhanced acid tolerance and energy provision (Fernández and Zúñiga, 2006; Rimaux et al., 2011; Tonon and Lonvaud-Funel, 2002). The ADI system comprises three reactions catalyzed by arginine deiminase (ADI), ornithine transcarbamoylase (OTC), carbamate kinase (CK) and a transmembrane arginine/ornithine antiporter, catalyzing the exchange between extracellular arginine and intracellular ornithine. According to genomic and proteomic analysis no CK could be found in *L. hordei*. Therefore, ADI can convert arginine to citrulline and ammonia, resulting in the alkalization of the cytoplasm and protection against an acidic external pH (Cotter and Hill, 2003). Secondly, citrulline could be converted by OTC into carbamoyl phosphate (carbamoyl-P), which is essential for de novo pyrimidine biosynthesis (Kilstrup et al., 2005). Nevertheless, carbamoyl-P cannot be converted in the lack of CK, which generates additional ATP in other organisms harboring the full ADI pathway. This does not appear to be a disadvantage/not necessary in a high energy containing environment as water kefir. The fate of carbamoyl-P therefore remains unclear. *L. hordei* did not encode all the enzymes involved in alternative systems, which are corresponding to acid tolerance such as the agmatine deiminase (AGDI) system and glutamate decarboxylase (GAD) system. To date, few LAB producing putrescine by AGDI system had been detected, such as *L. brevis*, *L. sakei* (Griswold et al., 2004; Lucas et al., 2007). The GAD system, which catalyzes the decarboxylation of L-glutamate to  $\gamma$ -aminobutyric acid (GABA), had been studied in *L. paracasei* NFRI 7415, *L. plantarum* DSM 19463 (Di Cagno et al., 2010; Komatsuzaki et al., 2008) and related to their acid tolerance. Therefore, above neutralization via ammonia from the partial arginine conversion, acidification appears mainly limited by the switch from lactic and acetic acid to butanediol formation.

### 3.7. Fatty acid biosynthesis

In addition to the limited availability of amino acids, *L. hordei* suffers from limits of fatty acids in the water kefir. On first glance, it appears that *L. hordei* should not be able to synthesize any unsaturated fatty acids by itself in the absence of *fabB*. However, it grew to high cell densities in water kefir medium without any fatty acids added. An answer to these conflicting results may be from in the study of Wang and Cronan (Wang and Cronan, 2004). These authors demonstrate that FabF from *Enterococcus faecalis* can functionally replace FabB in *E. coli*. Furthermore *E. faecalis* FabZ can replace *E. coli* FabA functions, despite different sequence alignments. They conclude that bacterial fatty acid biosynthetic pathways cannot be deduced solely by sequence comparisons. While this may be true also for other predictions from genomics, it is clear from growth experiments that in such alternative functions of bifunctional enzymes must exist for the biosynthesis of unsaturated fatty acids enabling growth of *L. hordei* under strict limitation of external fatty acids. In the lack of *fabB* and other sequence homologs annotated for functions introducing double bonds in fatty acids this gap is likely closed by the present functional homologs residing in FabA and FabZ, which may replace respective functions of the missing FabB and FabF in *L. hordei* (Table S6).

### 4. Conclusions

The putative functional genome and protein identification of *L. hordei* TMW 1.1822 revealed adaptation to the water kefir environment and suggests links to other members of the consortia, which likely reside in mutualistic (related to compounds) but also environmental (related to pH and redox maintenance) relationships. This way, it can handle sucrose in various effective ways including EMP, PKP and glucanase reactions, use gluconate and mannitol as additional carbon sources and for redox maintenance and limit acid stress by formation of butanediol instead of lactate or ammonia formation upon arginine conversion. The limits in amino- and fatty acids are handled by the uptake of peptides, synthesis of essential amino acids and use of alternative enzyme functions for the biosynthesis of unsaturated fatty acids. This work also shows, that genomic analysis greatly wins upon its support by proteomics and targeted physiological testing for traits in question from prediction.

Supplementary data to this article can be found online at <https://doi.org/10.1016/j.ijfoodmicro.2018.10.004>.

### Acknowledgement

Part of work was supported by the China Scholarship Council in grant no. 201306820010, and the German Ministry of Economics and Technology (via AiF) and the WIFö (Wissenschaftsförderung der Deutschen Brauwirtschaft e.V., Berlin) in project AiF 19180 N.

### References

- Altermann, E., Russell, W.M., Azcarate-Peril, M.A., Barrangou, R., Buck, B.L., McAuliffe, O., Souther, N., Dobson, A., Duong, T., Callanan, M., 2005. Complete genome sequence of the probiotic lactic acid bacterium *Lactobacillus acidophilus* NCFM. Proc. Natl. Acad. Sci. U. S. A. 102, 3906–3912.
- Årsköld, E., Lohmeier-Vogel, E., Cao, R., Roos, S., Rådström, P., van Niel, E.W., 2008. Phosphoketolase pathway dominates in *Lactobacillus reuteri* ATCC 55730 containing dual pathways for glycolysis. J. Bacteriol. 190, 206–212.
- Aziz, R.K., Bartels, D., Best, A.A., DeJongh, M., Disz, T., Edwards, R.A., Formsma, K., Gerdes, S., Glass, E.M., Kubal, M., 2008. The RAST Server: rapid annotations using subsystems technology. BMC Genomics 9, 75.
- Behr, J., Geissler, A.J., Schmid, J., Zehe, A., Vogel, R.F., 2016. The identification of novel diagnostic marker genes for the detection of beer spoiling *Pediococcus damnosus* strains using the BIast Diagnostic Gene finder. PLoS One 11, e0152747.
- Bolotin, A., Wincker, P., Mauger, S., Jaillon, O., Malarme, K., Weissenbach, J., Ehrlich, S.D., Sorokin, A., 2001. The complete genome sequence of the lactic acid bacterium *Lactococcus lactis* ssp. *lactis* IL1403. Genome Res. 11, 731–753.
- Carver, T., Thomson, N., Bleasby, A., Berriman, M., Parkhill, J., 2008. DNAPlotter: circular and linear interactive genome visualization. Bioinformatics 25, 119–120.

- Chin, C.-S., Alexander, D.H., Marks, P., Klammer, A.A., Drake, J., Heiner, C., Clum, A., Copeland, A., Huddleston, J., Eichler, E.E., 2013. Nonhybrid, finished microbial genome assemblies from long-read SMRT sequencing data. *Nat. Methods* 10, 563.
- Christensen, J.E., Dudley, E.G., Pederson, J.A., Steele, J.L., 1999. Peptidases and amino acid catabolism in lactic acid bacteria. *Antonie Van Leeuwenhoek* 76, 217–246.
- Cibrario, A., Peanne, C., Lailheugue, M., Campbell-Sills, H., Dols-Lafargue, M., 2016. Carbohydrate metabolism in *Oenococcus oeni*: a genomic insight. *BMC Genomics* 17, 984.
- Cotter, P.D., Hill, C., 2003. Surviving the acid test: responses of gram-positive bacteria to low pH. *Microbiol. Mol. Biol. Rev.* 67, 429–453.
- Cox, J., Mann, M., 2008. MaxQuant enables high peptide identification rates, individualized p/bb-range mass accuracies and proteome-wide protein quantification. *Nat. Biotechnol.* 26, 1367.
- Cox, J., Neuhauser, N., Michalski, A., Scheltema, R.A., Olsen, J.V., Mann, M., 2011. Andromeda: a peptide search engine integrated into the MaxQuant environment. *J. Proteome Res.* 10, 1794–1805.
- Cox, J., Hein, M.Y., Lubner, C.A., Paron, I., Nagaraj, N., Mann, M., 2014. Accurate proteome-wide label-free quantification by delayed normalization and maximal peptide ratio extraction, termed MaxLFQ. *Mol. Cell. Proteomics* 13, 2513–2526.
- Detmers, F.J., Kunji, E.R., Lanfermeijer, F.C., Poolman, B., Konings, W.N., 1998. Kinetics and specificity of peptide uptake by the oligopeptide transport system of *Lactococcus lactis*. *Biochemistry* 37, 16671–16679.
- Di Cagno, R., Mazzacane, F., Rizzello, C.G., De Angelis, M., Giuliani, G., Meloni, M., De Servi, B., Gobetti, M., 2010. Synthesis of  $\gamma$ -aminobutyric acid (GABA) by *Lactobacillus plantarum* DSM19463: functional grape must beverage and dermatological applications. *Appl. Microbiol. Biotechnol.* 86, 731–741.
- Eid, J., Fehr, A., Gray, J., Luong, K., Lyle, J., Otto, G., Peluso, P., Rank, D., Baybayan, P., Bettman, B., 2009. Real-time DNA sequencing from single polymerase molecules. *Science* 323, 133–138.
- Fels, L., Jakob, F., Vogel, R.F., Wefers, D., 2018. Structural characterization of the exopolysaccharides from water kefir. *Carbohydr. Polym.* 189, 296–303.
- Fernández, M., Zúñiga, M., 2006. Amino acid catabolic pathways of lactic acid bacteria. *Crit. Rev. Microbiol.* 32, 155–183.
- Frank, A., Lobry, J., 1999. Asymmetric substitution patterns: a review of possible underlying mutational or selective mechanisms. *Gene* 238, 65–77.
- Gardy, J.L., Laird, M.R., Chen, F., Rey, S., Walsh, C., Ester, M., Brinkman, F.S., 2004. PSORTb v. 2.0: expanded prediction of bacterial protein subcellular localization and insights gained from comparative proteome analysis. *Bioinformatics* 21, 617–623.
- Geißler, A., 2016. Lifestyle of Beer Spoiling Lactic Acid Bacteria. Technische Universität München.
- Geißler, A.J., Behr, J., Vogel, R.F., 2016a. Multiple genome sequences of the important beer-spoiling species *Lactobacillus backii*. *Genome Announc.* 4 (e00826-00816).
- Geißler, A.J., Behr, J., von Kamp, K., Vogel, R.F., 2016b. Metabolic strategies of beer spoilage lactic acid bacteria in beer. *Int. J. Food Microbiol.* 216, 60–68.
- Griswold, A.R., Chen, Y.-Y.M., Burne, R.A., 2004. Analysis of an agmatine deiminase gene cluster in *Streptococcus mutans* UA159. *J. Bacteriol.* 186, 1902–1904.
- Gulitz, A., Stadie, J., Wenning, M., Ehrmann, M.A., Vogel, R.F., 2011. The microbial diversity of water kefir. *Int. J. Food Microbiol.* 151, 284–288.
- Hsieh, H.-H., Wang, S.-Y., Chen, T.-L., Huang, Y.-L., Chen, M.-J., 2012. Effects of cow's and goat's milk as fermentation media on the microbial ecology of sugary kefir grains. *Int. J. Food Microbiol.* 157, 73–81.
- Hugenholtz, J., 1993. Citrate metabolism in lactic acid bacteria. *FEMS Microbiol. Rev.* 12, 165–178.
- Irigoyen, A., Arana, I., Castiella, M., Torre, P., Ibanez, F., 2005. Microbiological, physicochemical, and sensory characteristics of kefir during storage. *Food Chem.* 90, 613–620.
- Kandler, O., 1983. Carbohydrate metabolism in lactic acid bacteria. *Antonie Van Leeuwenhoek* 49, 209–224.
- Kilstrup, M., Hammer, K., Ruhdal Jensen, P., Martinussen, J., 2005. Nucleotide metabolism and its control in lactic acid bacteria. *FEMS Microbiol. Rev.* 29, 555–590.
- Kleerebezem, M., Hugenholtz, J., 2003. Metabolic pathway engineering in lactic acid bacteria. *Curr. Opin. Biotechnol.* 14, 232–237.
- Kleerebezem, M., Boekhorst, J., van Kranenburg, R., Molenaar, D., Kuipers, O.P., Leer, R., Turchini, R., Peters, S.A., Sandbrink, H.M., Fiers, M.W., 2003. Complete genome sequence of *Lactobacillus plantarum* WCFS1. *Proc. Natl. Acad. Sci.* 100, 1990–1995.
- Komatsuzaki, N., Nakamura, T., Kimura, T., Shima, J., 2008. Characterization of glutamate decarboxylase from a high  $\gamma$ -aminobutyric acid (GABA)-producer, *Lactobacillus paracasei*. *Biosci. Biotechnol. Biochem.* 72, 278–285.
- Kunji, E.R., Mierau, I., Hagting, A., Poolman, B., Konings, W.N., 1996. The proteolytic systems of lactic acid bacteria. *Antonie Van Leeuwenhoek* 70, 187–221.
- Laureys, D., De Vuyst, L., 2014. Microbial species diversity, community dynamics, and metabolic kinetics of water kefir fermentation. *Appl. Environ. Microbiol.* 80, 2564–2572.
- Laureys, D., De Vuyst, L., 2017. The water kefir grain inoculum determines the characteristics of the resulting water kefir fermentation process. *J. Appl. Microbiol.* 122, 719–732.
- Ljungh, Å., Wadström, T., 2009. *Lactobacillus* Molecular Biology: From Genomics to Probiotics. Horizon Scientific Press.
- Lopez-Kleine, L., Monnet, V., 2011. Lactic acid bacteria | proteolytic systems. *Encyclopedia of Dairy Sciences* 101, 49–55.
- Lucas, P.M., Blancato, V.S., Claisse, O., Magni, C., Lolkema, J.S., Lonvaud-Funel, A., 2007. Agmatine deiminase pathway genes in *Lactobacillus brevis* are linked to the tyrosine decarboxylation operon in a putative acid resistance locus. *Microbiology* 153, 2221–2230.
- Marsh, A.J., O'Sullivan, O., Hill, C., Ross, R.P., Cotter, P.D., 2013. Sequence-based analysis of the microbial composition of water kefir from multiple sources. *FEMS Microbiol. Lett.* 348, 79–85.
- Martin, M.G., Magni, C., De Mendoza, D., López, P., 2005. Cit, a transcription factor involved in regulation of citrate metabolism in lactic acid bacteria. *J. Bacteriol.* 187, 5146–5155.
- McCarthy, A., 2010. Third generation DNA sequencing: pacific biosciences' single molecule real time technology. *Chem. Biol.* 17, 675–676.
- Overbeek, R., Olson, R., Pusch, G.D., Olsen, G.J., Davis, J.J., Disz, T., Edwards, R.A., Gerdes, S., Parrello, B., Shukla, M., 2013. The SEED and the Rapid Annotation of microbial genomes using Subsystems Technology (RAST). *Nucleic Acids Res.* 42, D206–D214.
- Pidoux, M., 1988. The microbial flora of sugary kefir grain (the gingerbeer plant): biosynthesis of the grain from *Lactobacillus hilgardii* producing a polysaccharide gel. *Food Microbiol.* 5, 223–238.
- Pridmore, R.D., Berger, B., Desiere, F., Vilanova, D., Barretto, C., Pittet, A.C., Zwahlen, M.C., Rouvet, M., Altermann, E., Barrangou, R., 2004. The genome sequence of the probiotic intestinal bacterium *Lactobacillus johnsonii* NCC 533. *Proc. Natl. Acad. Sci. U. S. A.* 101, 2512–2517.
- Quintans, N.G., Blancato, V., Repizo, G., Magni, C., López, P., 2008. Citrate metabolism and aroma compound production in lactic acid bacteria. *Mol. Aspects Lactic Acid Bacteria Tradit. New Appl* 65–88.
- Rimaux, T., Vrancken, G., Pothakos, V., Maes, D., De Vuyst, L., Leroy, F., 2011. The kinetics of the arginine deiminase pathway in the meat starter culture *Lactobacillus sakei* CTC 494 are pH-dependent. *Food Microbiol.* 28, 597–604.
- Rouse, S., Canchaya, C., van Sinderen, D., 2008. *Lactobacillus hordei* sp. nov., a bacteriocinogenic strain isolated from malted barley. *Int. J. Syst. Evol. Microbiol.* 58, 2013–2017.
- Stadie, J., 2013. Metabolic Activity and Symbiotic Interaction of Bacteria and Yeasts in Water Kefir. Technische Universität München.
- Stadie, J., Gulitz, A., Ehrmann, M.A., Vogel, R.F., 2013. Metabolic activity and symbiotic interactions of lactic acid bacteria and yeasts isolated from water kefir. *Food Microbiol.* 35, 92–98.
- Stolz, P., Vogel, R.F., Hammes, W.P., 1995. Utilization of electron acceptors by lactobacilli isolated from sourdough. *Z. Lebensm. Unters. Forsch.* 201, 402–410.
- Sun, Z., Harris, H.M., McCann, A., Guo, C., Argimon, S., Zhang, W., Yang, X., Jeffery, I.B., Cooney, J.C., Kagawa, T.F., Liu, W., Song, Y., Salvetti, E., Wrobel, A., Rasinkangas, P., Parkhill, J., Rea, M.C., O'Sullivan, O., Ritari, J., Douillard, F.P., Paul Ross, R., Yang, R., Briner, A.E., Felis, G.E., de Vos, W.M., Barrangou, R., Klaenhammer, T.R., Caufield, P.W., Cui, Y., Zhang, H., O'Toole, P.W., 2015. Expanding the biotechnology potential of lactobacilli through comparative genomics of 213 strains and associated genera. *Nat. Commun.* 6, 8322.
- Tonon, T., Lonvaud-Funel, A., 2002. Arginine metabolism by wine lactobacilli isolated from wine. *Food Microbiol.* 19, 451–461.
- Tyanova, S., Temu, T., Sinitcyn, P., Carlson, A., Hein, M.Y., Geiger, T., Mann, M., Cox, J., 2016. The Perseus computational platform for comprehensive analysis of (prote) omics data. *Nat. Methods* 13, 731.
- Tynkkynen, S., Buist, G., Kunji, E., Kok, J., Poolman, B., Venema, G., Haandrikman, A., 1993. Genetic and biochemical characterization of the oligopeptide transport system of *Lactococcus lactis*. *J. Bacteriol.* 175, 7523–7532.
- Vardjan, T., Lorbeg, P.M., Rogelj, I., Majhenič, A.Č., 2013. Characterization and stability of lactobacilli and yeast microbiota in kefir grains. *J. Dairy Sci.* 96, 2729–2736.
- Vogel, R.F., Pavlovic, M., Ehrmann, M.A., Wiewer, A., Liesegang, H., Offschanska, S., Voget, S., Angelov, A., Böcker, G., Lieb, W., 2011. Genomic analysis reveals *Lactobacillus sanfranciscensis* as stable element in traditional sourdoughs. *Microb. Cell Factories*. BioMed Central 56.
- Waldherr, F.W., Doll, V.M., Meißner, D., Vogel, R.F., 2010. Identification and characterization of a glucan-producing enzyme from *Lactobacillus hilgardii* TMW 1.828 involved in granule formation of water kefir. *Food Microbiol.* 27, 672–678.
- Wang, H., Cronan, J.E., 2004. Functional replacement of the FabA and FabB proteins of *Escherichia coli* fatty acid synthesis by *Enterococcus faecalis* FabZ and FabF homologues. *J. Biol. Chem.* 279, 34489–34495.
- Xu, D., Fels, L., Wefers, D., Behr, J., Jakob, F., Vogel, R.F., 2018. *Lactobacillus hordei* dextrans induce *Saccharomyces cerevisiae* aggregation and network formation on hydrophilic surfaces. *Int. J. Biol. Macromol.* 115, 236–242.
- Yamada, T., Letunic, I., Okuda, S., Kanehisa, M., Bork, P., 2011. iPath2.0: interactive pathway explorer. *Nucleic Acids Res.* 39, W412–W415.
- Yu, N.Y., Wagner, J.R., Laird, M.R., Mellé, G., Rey, S., Lo, R., Dao, P., Sahinalp, S.C., Ester, M., Foster, L.J., 2010. PSORTb 3.0: improved protein subcellular localization prediction with refined localization subcategories and predictive capabilities for all prokaryotes. *Bioinformatics* 26, 1608–1615.

### **4.3 Manuscript 3: Label-free quantitative proteomic analysis reveals the lifestyle of *Lactobacillus hordei* in presence of *Sacchromyces cerevisiae***

Di Xu, Jürgen Behr, Andreas J. Geißler, Julia Bechtner, Christina Ludwig, Rudi F. Vogel., 2019. International Journal of Food Microbiology. Accepted.

*Lactobacillus (L.) hordei* and *Sacchromyces (S.) cerevisiae* are as predominant and stable lactic acid bacteria and yeasts, respectively, isolated from water kefir consortia. In this study, we investigated the response of co-cultivated *L. hordei* TMW 1.1822 in the presence of *S. cerevisiae* TMW 3.221 as compared with single-cultivated *L. hordei*, by label-free proteomic analysis. In total, 233 proteins of *L. hordei* were significantly differentially expressed in the presence of *S. cerevisiae*. Those differentially expressed proteins were mainly distributed in sugar transport, carbohydrate metabolism, peptide transport systems, peptidases, and amino acid biosynthesis and metabolism. The data suggested that *L. hordei* responded to the presence of *S. cerevisiae* with adjustment of intracellular redox reactions controlled of proteins, which were part of Rex regulons proteins involved in the glycolytic pathway and energy fermentation. The concomitant high production of NADH, H<sup>+</sup> should enable the preferential production of butanediol instead of acetate or lactate, which resulted in the limitation of acidification. Also, the arginine deiminase system in *L. hordei* was significantly up-regulated, which further alleviated acid stress and concomitantly protected *S. cerevisiae* against an acidic environment, which *L. hordei* generated in single culture. Moreover, it suggested that the presence of *S. cerevisiae* in the nitrogen and fatty acids limited environment of the water kefir facilitated and improved the growth of *L. hordei* by delivering gluconate, fructose, amino acids, fatty acids or substrates for their biosynthesis. Up-regulation of the

OppABCDF peptide transport and enzymes involved in amino acid metabolism in *L. hordei* indicated enhanced peptide uptake, as well as the feeding of glutamate, glutamine, histidine, methionine, arginine, tryptophan, and proline from *S. cerevisiae*.

Authors contributions: Di Xu was responsible for planning the research project under the supervision of Jürgen Behr and Rudi F. Vogel. Di Xu prepared the proteomic samples and conducted the other experiments. The proteomic samples were analyzed with the aid of Christina Ludwig from the at Bavarian Center for Biomolecular Mass Spectrometry. Further, Di Xu analyzed the data with the help of Jürgen Behr and Andreas J. Geißler, and wrote the manuscript draft. Julia Bechtner and Rudi F. Vogel helped in finalizing and proofreading of the manuscript. All authors reviewed and approved the final manuscript.

**Label-free quantitative proteomic analysis reveals the lifestyle of *Lactobacillus hordei* in the presence of *Sacchromyces cerevisiae***

Di Xu<sup>1</sup>, Jürgen Behr<sup>1,2,3</sup>, Andreas J. Geißler<sup>1</sup>, Julia Bechtner<sup>1</sup>, Christina Ludwig<sup>2</sup>, Rudi F. Vogel<sup>1\*</sup>

1. Lehrstuhl für Technische Mikrobiologie, Technische Universität München, Freising, Germany
2. Bavarian Center for Biomolecular Mass Spectrometry (BayBioMS), Freising, Germany
3. Current address: Leibniz-Institut für Lebensmittel-Systembiologie an der Technischen Universität München, Freising, Germany

**\* corresponding author:** Rudi F. Vogel

[rudi.vogel@wzw.tum.de](mailto:rudi.vogel@wzw.tum.de)

## Abstract

Water kefir is a fermented beverage, which is traditionally prepared from sucrose, kefir grains, dried or fresh fruits, and water. *L. hordei* and *S. cerevisiae* are isolated as predominant and stable species of lactic acid bacteria and yeasts, respectively. In this study we demonstrate that label free quantitative proteomics is useful to study microbial interaction along the response of co-cultivated *L. hordei* TMW 1.1822 in the presence of *S. cerevisiae* TMW 3.221 as compared with their single cultures in a water kefir model. It is shown and *L. hordei* responds to *S. cerevisiae* in many respects revealing a mutualistic relationship. The data suggest that *L. hordei* responds to the presence of *S. cerevisiae* with adjustment of intracellular redox reactions controlled of proteins, which are part of Rex regulons and proteins involved in the glycolytic pathway and energy fermentation. An NADH, H<sup>+</sup>-driven metabolic switch to preferential production of butanediol instead of acetate or lactate, and up-regulation of arginine deiminase, alleviated acid stress and concomitantly protected *S. cerevisiae* against an acidic environment, which *L. hordei* generated in single culture. Moreover, the data suggest that the presence of *S. cerevisiae* in the nitrogen and fatty acids limited environment of the water kefir facilitated and improved the growth of *L. hordei* by delivering gluconate, fructose, amino acids, fatty acids or substrates for their biosynthesis. Up-regulation of the OppABCDF peptide transport and enzymes involved in amino acid metabolism indicates enhanced peptide uptake, as well as cross-feeding of *L. hordei* by glutamine, glutamate, histidine, tryptophan, methionine, proline, tryptophan delivered by *S. cerevisiae*.

**Keywords:** *Lactobacillus hordei*, *Saccharomyces cerevisiae*, label-free quantitative proteomic, lifestyle, water kefir

## 1. Introduction

Water kefir is a fermented beverage, which is traditionally prepared from sucrose, kefir grains, dried or fresh fruits, and water. After one or two days' fermentation, it results in an acidic and lightly alcoholic drink. It is reported that the microbial consortium isolated from water kefir grains generally consists of lactic acid bacteria (LAB), yeast, acetic acid bacteria (AAB) and bifidobacteria (Gulitz et al., 2011; Laureys and De Vuyst, 2014; Marsh et al., 2013). The most predominant genus isolated by Gulitz et al (Gulitz et al., 2011) in water kefir was *Lactobacillus*, with abundant *Lactobacillus (L.) hordei* followed by *L. nagelii*, *Leuconostoc mesenteroides* and *L. casei* while the predominant yeast were respectively *Saccharomyces (S.) cerevisiae*, *Zygorulaspora (Z.) florentina*, *Dekkera bruxellensis* etc (Gulitz et al., 2011; Laureys and De Vuyst, 2014).

To date, there are rare studies exploring microbial consortium and their interaction in water kefir, so the specific contribution of groups or species such as LAB, AAB, yeast remains speculative. Stadie et al (Stadie et al., 2013) delineate the metabolic interaction between LAB (*L. hordei* and *L. nagelii*) and yeasts (*S. cerevisiae* and *Z. florentina*) isolated from water kefir as mutualism based on the significant increase of cell yield. It was inferred that the growth of *L. hordei* TMW 1.1822 may be improved by the disposed nutrients produced by both yeast, such as release of several auxotrophic amino acids (isoleucine, leucine, methionine, phenylalanine, tryptophan, tyrosine and valine) and vitamin B6 (Stadie et al., 2013). This study also suggests that *Z. florentina* appreciates the

pH decrease caused by lactobacilli, whereas *S. cerevisiae* did not. Furthermore, arginine is released by *Z. florentina* due to the co-cultivation of *L. nagelii* and *Z. florentina*, which may support the growth of *L. nagelii*. Lactic acid and ethanol were found to be the main metabolites of water kefir consortium of LAB, yeasts and AAB (Laureys and De Vuyst, 2014). In addition, glycerol, acetic acid and mannitol formation has been observed in low concentrations (Laureys and De Vuyst, 2014).

Although metabolic exchanges are ubiquitous in microbial communities, detecting metabolite cross-feedings constituting mutualism between species is difficult due to their intrinsically dynamic nature and the complexity of communities (Ponomarova and Patil, 2015). Also, such metabolites provided by an organism are immediately consumed by another one living in close proximity. Functional genomics approaches enable identification of metabolic pathways involved in adaptation of an organism to its specific habitat and also the presence of possible competitive or supportive metabolite formation (Durham et al., 2015; Maligoy et al., 2008; Ponomarova et al., 2017). Still, proteomic studies based on functional genomics have not yet widely been applied to study the adaptation or interaction of LAB and yeasts in a food consortium. An example for a respective transcriptome analysis is provided for the comparison of single and mixed cultivation of *Lactococcus lactis* IL-1403 in the absence or presence of *S. cerevisiae* CEN-PK905, respectively. A total of 158 genes was identified along determination of mRNA levels, which were significantly modified in their expression (particularly pyrimidine metabolism) (Maligoy et al., 2008). Another finding about the specific contribution of yeast (*S. cerevisiae* S90) to symbiotic LAB (*Lactococcus lactis* subsp. *lactis* IL1403 and *L. plantarum* WCFS1) through nitrogen overflow in grape juice was



studied using mass spectrometry based on their genome-scale metabolic models (Ponomarova et al., 2017). It suggested that *S. cerevisiae* benefits *Lactococcus lactis* by secreting glutamine and threonine, and benefits *L. plantarum* by secreting glutamine, threonine, phenylalanine, tryptophan and serine. In addition, cross-feeding of 2-oxoglutarate to *L. plantarum* was also observed as predicted by metabolic modeling (Ponomarova et al., 2017). Still the knowledge of metabolic exchange between groups or species especially cellular regulation is limited to few communities with small number of exchanged metabolites. We used label-free quantitative proteomic analysis, whole-genome sequencing and reconstructed putative metabolic pathways to describe the lifestyle of *L. hordei* TMW 1.1822 in water kefir (Xu et al., 2019). It was demonstrated that abundant sucrose is consumed directly via parallel EMP and PK pathways and is also extracellularly converted to dextran and fructose by a glucansucrase, leaving fructose as additional carbon source. Essential amino acids (in the form of peptides) and citrate are acquired from fruits. In the lack of FabB unsaturated fatty acids are synthesized by predicted alternative enzymes. Formation of acetoin and diacetyl as well as arginine conversion reactions enable acidification limitation. We postulated that other members of the water kefir consortium (yeasts, acetic acid bacteria) likely facilitate or support growth of *L. hordei* by delivering gluconate, mannitol, amino- and fatty acids and vitamins. Based on these findings we explored the response of *L. hordei* to the presence of *S. cerevisiae* TMW 3.221 in this environment.

## **2. Material and methods**

### **2.1. Strain culture and growth determination**

*L. hordei* TMW 1.1822 and *S. cerevisiae* TMW 3.221 isolated from water kefir by Gulitz et al (Gulitz et al., 2011) were used to set up this co-cultivation experiment. Briefly, *L. hordei* TMW 1.1822 was pre-cultured anaerobically overnight at 30 °C in modified MRS (mMRS) medium (Stolz et al., 1995) as described previously (Xu et al., 2019), while *S. cerevisiae* from a -80°C stock was spread on YPG (Xu et al., 2018) agar plates and cultivated aerobically for 24 h at 30 °C, and a single colony was transferred into 10 ml YPG medium and pre-cultured anaerobically at 30 °C under the same growth condition as *L. hordei*. Then 1 % (v/v) pre-cultured *L. hordei*, *S. cerevisiae* were separately inoculated into 40 ml water kefir medium (WKM) (Stadie et al., 2013) in replicate as single-cultivated samples, while 1 % pre-cultured *L. hordei* and 1 % *S. cerevisiae* were simultaneously inoculated into 40 ml WKM as co-cultivated samples. 100 µl aliquots were respectively taken out from each samples for plate counting at the fermentation time point of 0 h, 2 h, 4 h, 5 h, 6 h, 7 h, 8 h, 12 h, 24 h, 48 h. Single-cultivated *L. hordei* samples were plated in mMRS agar plates, and single-cultivated *S. cerevisiae* samples were plated in YPG agar plates. Meanwhile co-cultivated *L. hordei* and *S. cerevisiae* samples were plated in mMRS agar plates with added cycloheximide (final concentration at 0.1 g/l) to inhibit the growth of yeast for counting *L. hordei* cells, and also plated in YPG agar plates with added chloramphenicol (final concentration at 0.1 g/l) to inhibit the growth of bacteria for counting *S. cerevisiae* cells.

## **2.2. Sample preparation for proteomic analysis, liquid chromatography and mass spectrometry**

1 % (v/v) pre-cultured *L. hordei*, *S. cerevisiae* were separately inoculated into 40 ml WKM in triplicate and cultured anaerobically at 30 °C for 10 h to prepare single-culture

samples, while 1 % *L. hordei* and 1 % *S. cerevisiae* were simultaneously inoculated into 40 ml WKM in triplicate and cultured in the same growth condition to prepare co-cultivation samples. As previously described (Xu et al., 2019), trichloroacetic (TCA) were added to those single-culture and co-cultivation samples to a final concentration of 6.25 % (w/v). Subsequently samples were stored on ice for 10 min. The bacterial pellets were collected by centrifugation (5000 rpm, 5 min) at 4 °C, washed twice with acetone, reconstituted in lysis buffer and mechanically disrupted with glass beads (G8772, 425-600 µm, Sigma, Germany). Total protein concentration of the lysate was determined using the Bradford method (Bio-Rad Protein Assay, Bio-Rad Laboratories GmbH, Munich, Germany). 100 µg protein extract was used per sample for in-solution digestion. Proteins were reduced with 10 mM DTT at 30 °C for 30 min, and subsequently carbamidomethylated with 55 mM chloroacetamide in the dark for 60 min. Subsequently proteins were digested by addition of trypsin overnight at 37 °C. Digested peptide samples were desalted according to the manufacturer's instructions by C18 solid phase extraction using Sep-Pak columns (Waters, WAT054960). Purified peptide samples were dried in a SpeedVac and resuspended in 2 % acetonitrile, 98 % H<sub>2</sub>O, 0.1 % formic acid to a final concentration of 0.25 µg/µl.

Generated peptides were analyzed on a Dionex Ultimate 3000 nano LC system coupled to an Q-Exactive HF mass spectrometer (Thermo Scientific, Bremen, Germany). Peptides were delivered to a trap column (75 µm × 2 cm, self-packed with Reprosil-Pur C18 ODS-3 5 µm resin, Dr. Maisch, Ammerbuch) at a flow rate of 5 µl/min in solvent A<sub>0</sub> (0.1% formic acid in water). Peptides were separated on an analytical column (75 µm × 40 cm, self-packed with Reprosil-Gold C18, 3 µm resin, Dr. Maisch, Ammerbuch) using a 120

min linear gradient from 4-32 % solvent B (0.1 % formic acid, 5 % DMSO in acetonitrile) and solvent A<sub>1</sub> (0.1 % formic acid, 5 % DMSO in water) at a flow rate of 300 nl/min. The mass spectrometer was operated in data dependent mode, automatically switching between MS1 and MS2 spectra. MS1 spectra were acquired over a mass-to-charge (m/z) range of 360-1300 m/z using a maximum injection time of 50 ms and an AGC target value of 3e6. Up to 20 peptide precursors were isolated (isolation window 1.7 m/z, maximum injection time 25 ms, AGC value 1e5), fragmented by higher-energy collisional dissociation (HCD) using 25 % normalized collision energy (NCE) and analyzed at a resolution of 15,000 with a scan range from 200 to 2000 m/z. Precursor ions that were singly-charged, unassigned or with charge states > 6+ were excluded.

### **2.3. Peptide and protein identification and quantification, statistical analysis**

Peptide and protein identification plus quantification were performed with MaxQuant (version 1.5.7.4) by searching the MS2 data against all protein sequences obtained from UniProt - Reference proteome *S. cerevisiae* S288c (6,724 entries, downloaded 13.03.2017) and all protein sequences from *L. hordei* using the embedded search engine Andromeda (Cox et al., 2011) as previously described (Xu et al., 2019). MaxQuant output files (proteinGroups.txt) were further analysed using Perseus (version 1.5.6.0) (Tyanova et al., 2016). Protein groups were filtered for entries “only identified by site”, reverse identifications and contaminants. Protein groups from each investigated species were moved to different data matrices. iBAQ intensities were log<sub>2</sub>-transformed and used for further statistical analysis. NCBI annotation, PSORTb subcellular localization, SEED category (subcategory and subsystem) as previously annotated (Xu et al., 2019) were added to the matrix through identifier matching. For the comparison between two

groups, t-tests were performed. Log<sub>2</sub> fold change  $\geq 2$  or  $\leq -2$  and  $-\text{Log}_{10}$  P-value  $\geq 2$  (p value  $\leq 0.05$ ) were considered to be significantly differentially expressed proteins of *L. hordei* TMW 1.1822 in response to co-cultivation with *S. cerevisiae* TMW 3.221.

#### **2.4. Chromatographic analysis of amino acids, pH measurement**

1 % pre-cultured *L. hordei* TMW 1.1822 and *S. cerevisiae* TMW 3.221 were separately inoculated into chemically defined medium (CDM, pH 6.5) (Xu et al., 2019) in triplicate. After 24 h cultivation at 30 °C, 1 ml *L. hordei*, *S. cerevisiae* cultures and CDM were respectively mixed with 50  $\mu\text{l}$  of 70 % (v/v) perchloric acid (Sigma-Aldrich, St. Louis, USA) standing overnight at 4 °C for protein precipitation. After centrifugation (12000 rpm, 10 min), the supernatant was collected and diluted 1:5 in 0.1 M HCl. Samples were filtered through Phenex<sup>TM</sup> Nylon Filter Membrane (0.2  $\mu\text{m}$ , Phenomenex, Germany). Amino acids were analyzed on a Dionex Ultimate 3000 HPLC system (Dionex, Idstein, Germany) using a Gemini C18 column (Phenomenex, Aschaffenburg, Germany) with UV detection at 338 and 269 nm. Before separation, samples were performed to pre-column derivatisation with o-phthalaldehyde-3-mercaptopropionic acid (OPA) and 9-fluorenylmethyl chloroformate (FMOC) following Bartóak et al (Bartóak et al., 1994). A gradient was as described by Schurr et al (Schurr et al., 2013) with a flow rate of 0.8 ml/min. Quantification was executed employing calibration adjustment by external HPLC grade standards and the Chromeleon software version 6.80 (Dionex, Idstein, Germany). After 72 h fermentation, single-cultivated *L. hordei* TMW 1.1822, single-cultivated *S. cerevisiae* TMW 3.221, co-cultivated *L. hordei* and *S. cerevisiae* samples in triplicate were respectively performed pH measurement (761 pH-meter Calimatic, Knick, Germany).

## 2.5. Statistical analysis

All the annotated EC and KO numbers, which were extracted from RAST fasta files were performed into iPath 3.0 (<http://pathways.embl.de/index.html>) (Yamada et al., 2011) to obtain an overview of complete metabolic pathways and biosynthesis of other secondary metabolites customized in thin red color as previously described (Xu et al., 2019). While up-regulated enzymes were customized in bold red color, down-regulated enzymes were customized in bold blue color. Other data visualization and analysis (cell counts, subcellular localization, SEED categories, amino acid consumption and pH values) were done with Microsoft Excel (Microsoft, Redmond, USA).

## 3. Results and Discussion

### 3.1. Growth characteristics of *L. hordei* in the presence of *S. cerevisiae*

To investigate interaction of *L. hordei* and *S. cerevisiae* in the water kefir system, the viable cell counts were determined in co-cultivation between *L. hordei* TMW 1.1822 and *S. cerevisiae* TMW 3.221 compared with those of their respective single cultures. The cell yield of *L. hordei* TMW 1.1822 increased from  $8.08 \pm 0.013 \log_{10}$  CFU/ml in single culture to  $8.30 \pm 0.046 \log_{10}$  CFU/ml in co-cultivation with *S. cerevisiae* after 8 h fermentation, and increased from  $8.29 \pm 0.105 \log_{10}$  CFU/ml in single culture to  $8.54 \pm 0.019 \log_{10}$  CFU/ml in co-cultivation after 12 h fermentation (Fig. 1). Cells grew exponentially until 12 h of fermentation to subsequently enter the stationary phase as indicated by no further OD increase. For comparative proteomic analysis a sampling time point was chosen at the late exponential phase, i.e. at 10 h fermentation time. This ensured a high amount of proteins from a metabolically active status. The viable count of

*L. hordei* was insignificantly affected in the presence of *S. cerevisiae* after 24 h, but declined upon co-cultivation as compared to that one in single culture after 48h. The cell number of *S. cerevisiae* was merely unaffected in the presence of *L. hordei* from 0 h to 24 h, and slightly decreased upon co-cultivation after 48 h (Fig. S2).

### **3.2. General features of differential proteomics**

Only three proteins of *S. cerevisiae* were quantified to be significantly differentially expressed in the presence of *L. hordei*, namely inhibitory regulator protein BUD2/CLA2 (3.4 log<sub>2</sub> fold change), probable electron transfer flavoprotein-ubiquinone oxidoreductase (3.8 log<sub>2</sub> fold change) and glutamate decarboxylase (4.2 log<sub>2</sub> fold change). This is consistent with the finding that growth of *S. cerevisiae* was hardly affected upon co-cultivation with *L. hordei* (Fig. S2). In contrast, the growth of *L. hordei* was significantly enhanced in the presence of *S. cerevisiae*, and the impact on the *L. hordei* proteome was significant upon co-cultivation. Consequently the proteomic analysis was focused on any differential proteomic pattern of *L. hordei* resulting from such co-cultivation, to possibly provide predictions for the causes of this growth stimulation.

The proteomic analysis enabled quantification of 1474 proteins out of 2461 proteins predicted from the genome of *L. hordei*. Among these 131 proteins were significantly up-regulated, 102 proteins were significantly down-regulated and 1241 proteins were unregulated in the presence of *S. cerevisiae* (Fig. 2). Most DE proteins were localized in cytoplasmic and cytoplasmic membrane except those categorized for unknown subcellular localization. Furthermore, as shown in Fig. 3, up-regulated proteins of *L. hordei* in the presence of *S. cerevisiae* were abundant in the SEED categories of amino

acids and derivatives (21 out of 83), carbohydrates (9 out of 90) and nucleosides and nucleotides (24 out of 80), cell wall and capsule (5 out of 72). A summary of the DE proteins were provided in Fig. S1.

Taken together these up/down-regulated proteins of *L. hordei* involved in carbohydrate and energy metabolism, amino acid metabolism and biosynthesis enabled predictions on the change of the *L. hordei* lifestyle in the nutritionally poor water kefir medium in response to the presence of *S. cerevisiae*.

### **3.3. Sugar transport, central carbohydrate metabolism**

The previous overview on sucrose metabolism of *L. hordei* revealed that sucrose can either be transformed into a glucan and fructose by a glycosyltransferase (glucansucrase), or transported into the cell by PTS sugar transport systems and subsequently metabolized through glycolysis (Xu et al., 2019). Whereas the glucansucrase of *L. hordei*, which was characterized as dextransucrase (Xu et al., 2018), was not significantly regulated in the presence of *S. cerevisiae*, the PTS mannose/fructose/sorbose family was significantly up-regulated (shown in Fig. S3). This suggested that in addition to fructose, resulting from the dextransucrase reaction, resulted from yeast invertase splitting of sucrose into glucose and fructose. While the yeast preferentially consumed glucose, (some) additional fructose was available for *L. hordei*, which readily took it up by various PTS, which were annotated as fructose transporters. Depending on the type of PTS, *L. hordei* gained more fructose-6-phosphate or fructose-1-phosphate, which was subsequently metabolized via glycolysis (see Fig. S4) enabling faster growth.



As it was reported previously, both analysis of putative functional genome and quantified proteome of *L. hordei* characterized it as a facultative homofermentative LAB (Xu et al., 2019). There were no significantly DE enzymes of *L. hordei* involved in the Embden-Meyerhof pathway (EMP) based on comparative proteomic analysis, when *L. hordei* was co-cultivated with *S. cerevisiae* after 10 h fermentation. Nevertheless, glucose-6-phosphate dehydrogenase (G6PDD, No. 12 in Table 1 and Fig. S4) involved in the phosphoketolase pathway (PKP) and pentose phosphate pathway (PPP) was significantly up-regulated, leading to high production of 6-phosphogluconolactone and reductive power (NADPH). This supports the previous interpretation that *L. hordei* not only possess PKP but also indeed employs the PKP to adapt to changing environmental conditions. Furthermore, this could be interpreted to that the yeast induced a different redox potential in the water kefir system and delivered additional electron acceptors (fructose). As a result, *L. hordei* switched from EMP to PKP producing gluconate. Fructose could act as electron acceptor and be reduced to mannitol. Also, in the full consortium harboring also *Gluconobacter* spp. *L. hordei* was likely offered additional exogenous gluconate resulting from their fructosyltransferases and subsequent oxidative metabolism of remaining glucose.

On the other hand, *L. hordei* UCC125, UCC126, UCC127, UCC128 isolated from barley have been reported as homofermentative since they are capable of producing acid from glucose, fructose, maltose, sucrose, mannose, mannitol, cellobiose but not from pentose, arabinose, galactose, sorbitol et al (Rouse et al., 2008). In the lack of respective genomic data of *L. hordei* UCC125, UCC126, UCC127, UCC128, one cannot define whether similar metabolic switches could occur in isolates from that barley. But *L. hordei* DSM

19519 also isolated from barley (Sun et al., 2015), had no sucrose specific PTS and extracellular glycosyltransferases and less transporters involved in fructose import found in the genome compared to *L. hordei* TMW 1.1822 as mentioned previously (Xu et al., 2019). So *L. hordei* likely expresses specific lifestyles in the different food systems and responds to the presence of other consortium members.

### **3.4. Pyruvate and citrate metabolism**

Beyond the indicated switch from EMP to PKP more redox related metabolic reactions were affected upon co-cultivation of *L. hordei* with *S. cerevisiae*. Such reactions are generally regulated by the redox-sensing repressor Rex. Initially described in *S. coelicolor*, Rex regulated metabolism of Gram-positive bacteria in response to the cellular NADH/NAD<sup>+</sup> levels. The core conserved part of the Rex regulons as a set of 22 genes and operons were preceded by candidate Rex-binding sites in 11 taxonomic groups of bacteria (Ravcheev et al., 2012). Although the Rex proteins of *L. hordei* were not significantly DE in the presence of *S. cerevisiae*, Rex apparently sensed a change in the cellular NAD/NADH ratio and induced DE of enzymes in reconstructed Rex regulons (Bitoun et al., 2012; Ravcheev et al., 2012; Zhang et al., 2014), which were involved in pyruvate metabolism. As shown in Fig. 5, these included bifunctional acetaldehyde/alcohol dehydrogenase (ADHE, No. 19/20), pyruvate formate lyase (PFL, No. 25), and acetoin reductase (AR, No. 28). ADHE involved in PKP and pyruvate metabolism was significantly down-regulated in the presence of *S. cerevisiae*, reducing the utilization of NADH, H<sup>+</sup> and production of ethanol. In the presence of ethanol, which is mainly produced by the yeast in alcoholic water kefir (Beshkova et al., 2003), *S. cerevisiae* limits production of ethanol by *L. hordei* in the water kefir consortium.

Furthermore, three enzymes (citrate lyase, PFL, AR) involved in pyruvate metabolism were highly abundant in *L. hordei* when co-cultivated with *S. cerevisiae* (shown in Table 1 and Fig. 4). The up-regulated citrate lyase (*citEF*) promoted the production of acetate and oxaloacetate converted from citrate. In addition, triphosphoribosyl-dephospho-CoA synthase (*citG*), which could activate citrate lyase from the apo to the holo enzyme, was significantly up-regulated, while citrate lyase transcriptional regulator (*citI*) was significantly down-regulated. Taken together, this suggested that citrate present in the water kefir was readily consumed by *L. hordei* preferentially in the presence of *S. cerevisiae* and can be used as carbon source and electron acceptor. Over-expressed PFL enabled an electron acceptor reaction and generates a high amount of NADH, H<sup>+</sup>, which was available for the also over-expressed AR to produce 2,3- butanediol instead of producing ethanol. This re-direction of pyruvate metabolism in the presence of citrate was consistent with the results that high diacetyl production from *L. helveticus* MP12 and *Lactococcus lactis* subsp. *lactis* C15 isolated from (milk) kefir grains were recorded (Beshkova et al., 2003). Accordingly, the acidification of co-cultivated *L. hordei* and *S. cerevisiae* became limited through the switch from lactic and acetic acid to butanediol formation. Taken together, this group of regulated enzymes of *L. hordei* in the presence of *S. cerevisiae* was associated with maintenance of redox homeostasis targeted at optimization of energy generation and reduction of ethanol and acid stress.

### **3.5. Peptide transport systems, peptidases, amino acids biosynthesis and metabolism**

Periplasmic oligopeptide - binding protein A (OppA, TC 3.A.1.5.1) and oligopeptide transport system permease protein B (OppB) of the peptide transport system (OppABCDF) were 2.5 log<sub>2</sub>fold and 2.2 log<sub>2</sub>fold up-regulated, respectively. As

demonstrated for *Lactococcus lactis* the Opp system is over expressed upon peptide limitation, and repressed in their abundance (Guédon et al., 2001). This suggests that the competition for the limited nitrogen source in this environment increases in the presence of *S. cerevisiae*. Once uptaken, peptides were degraded by a variety of peptidases (Christensen et al., 1999; Kunji et al., 1996). *L. hordei* was predicted to have 13 genes encoding peptidases (Xu et al., 2019). Among them, alpha-aspartyl dipeptidase E (*pepE*) was up-regulated (2.7 log<sub>2</sub> fold change) catalyzing the hydrolysis of dipeptides Asp-|-Xaa. It did not act on peptides with N-terminal Glu, Asn or Gln, nor did it cleave isoaspartyl peptides. While aminopeptidase S (*pepS*) belonging to the peptidase M29 family was down-regulated (-1.9 log<sub>2</sub> fold change), which decreased the ability of displaying broad substrate specificity towards peptides containing leucine, valine, phenylalanine, tyrosine.

The predictive analysis of the complete genome of *L. hordei* combined with physiological results revealed that *L. hordei* is prototrophic for 11 amino acids and auxotrophic for 6 amino acids (Xu et al., 2019). In total, 16 identified and quantified enzymes of *L. hordei* involved in the biosynthesis of histidine, tryptophan, methionine, arginine, glutamate, glutamine, proline were up-regulated in the presence of *S. cerevisiae*, while only 2 enzymes involved in the biosynthesis of aromatic amino acids (tryptophan, tyrosine, phenylalanine) and serine were down-regulated (listed in Table 2, visualized in Fig. S5). However, from the KEGG *in silico* metabolic pathways, the direction of a respective metabolic reaction often remains ambiguous. Still, together with metabolic data on the amino acids consumption/formation of *L. hordei* and *S. cerevisiae* this can be solved for some of the predicted cases. For example, as shown in Fig. 5, about 68.6 % of glutamine (4.82 mM) in CDM was consumed by *L. hordei* after 24 h. In contrast, 6.15

mM glutamine was produced by *S. cerevisiae* after 24 h compared to initial concentration in CDM. This suggested that *L. hordei*, even though it is prototrophic for glutamine, takes advantage of glutamine provided by *S. cerevisiae* via the up-regulated glutamate synthase (6.4 log<sub>2</sub> fold change) and possibly used this reaction for anaplerotic sequences in transamination reactions in biosynthetic pathways of other amino acids. Ponomarova et al (Ponomarova et al., 2017) also predicted that glutamate/glutamine are secreted by *S. cerevisiae* and consumed by *Lactococcus lactis* and *L. plantarum*. In a targeted LC-MS/MS approach they quantified the amounts of secreted amino acids in yeast-conditioned medium and further suggested cross-feeding of phenylalanine and proline (in concentration below the limit of exact quantification) from the yeast to *L. plantarum*. However, in our case, except glutamine, other amino acids were not produced but partly consumed by *S. cerevisiae* after 24 h fermentation in CDM. Therefore, we were unable to prove the real-time metabolic exchange (release/uptake) between LAB and yeast based on physiological results. Still, the label-free quantitative comparative proteomic analysis enabled investigation of real-time, dynamic, and integrated metabolic exchange and molecular response between microbial communities in fermented foods along DE. The up-regulated enzymes involved in amino acid metabolism or catabolism suggested that *S. cerevisiae* secreted glutamine, glutamate, arginine, histidine, tryptophan, methionine and proline, which were subsequently assimilated by *L. hordei* for its enhanced growth in this symbiotic water kefir environment.

### **3.6. Acid tolerance by ADI pathway**

Arginine catabolism via arginine deiminase (ADI) system, which is widely distributed in LAB is considered an important characteristic conferring acid tolerance, was identified

and quantified in *L. hordei* (Xu et al., 2019). In the lack of carbamate kinase, this partial operon cannot deliver additional ATP. As shown in Fig. 6A, ADI (5.5 log<sub>2</sub> fold change), ornithine transcarbamoylase (OTC, 6.9 log<sub>2</sub> fold change) of *L. hordei* were significantly up-regulated leading to high production of ammonia in the presence of *S. cerevisiae*. This was also demonstrated by pH determination of single-cultivated and co-cultivated *L. hordei* and *S. cerevisiae* after 72h fermentation (Fig. 6B). The pH value of co-cultivated *L. hordei* and *S. cerevisiae* increased to around 3.49 from 3.28 determined with single-cultivated *L. hordei*. Partial arginine conversion contributed to maintenance of intracellular pH in *L. hordei*, and alleviated acid stress of *S. cerevisiae*. In conclusion, *S. cerevisiae* provides arginine for *L. hordei*, whose conversion is beneficial for both partners.

### **3.7. Fatty acid biosynthesis**

Although *L. hordei* should not be able to synthesize any unsaturated fatty acids by itself in the absence of FabB, alternative functional enzymes for the biosynthesis of unsaturated fatty acids must exist, which enabled growth under strict limits of fatty acids in water kefir. This should likely be FabF (Xu et al., 2019). In the presence of *S. cerevisiae* the significant up-regulation of acetyl-CoA carboxylase (EC 6.3.4.14, 2.4 log<sub>2</sub> fold change) and biotin carboxylase (2.1 log<sub>2</sub> fold change) of *L. hordei* was observed, which are involved in providing the malonyl-CoA substrate for the biosynthesis fatty acids.

### **Conclusions**

While this study is limited to the response of *L. hordei* to *S. cerevisiae* in co-culture of a water kefir model, it demonstrates the potential of label-free quantitative proteomics to study microbial

interaction within consortia and provides first insight into interactions of water kefir inhabitants. The predicted functional genome and protein regulations of *L. hordei* TMW 1.1822 in the presence of *S. cerevisiae* TMW 3.221 revealed the adaptation and link to *S. cerevisiae* in this water kefir environment. This way, the PKP using gluconate as additional carbon source and simultaneous generation of NADPH for redox maintenance was up-regulated. The neutralization of the cytoplasm protected *S. cerevisiae* in this water kefir consortium against an acidic external pH via over-expressed formation of butanediol instead of lactate or acetate and over-expressed ammonia production upon the partial arginine conversion. Furthermore, many regulated enzymes belong to regulons of Rex related to redox homeostasis. The strict limits of amino acids in water kefir medium were attenuated by the uptake of peptides or amino acids such as glutamine from *S. cerevisiae*, and biosynthesis of some essential amino acids by *L. hordei*, as indicated by up-regulation of related enzymes. This differential proteomic analysis provides a powerful tool to understand modulations in the lifestyle of bacteria in the presence of other microbes sharing the environment or under different environmental stimuli.

### **Acknowledgement**

Part of this work was supported by the China Scholarship Council in grant no.201306820010 and the WiFö (Wissenschaftsförderung der Deutschen Brauwirtschaft e.V., Berlin) in project AiF 19180 N.

### **References**

Bartóak, T., Szalai, G., Lőrincz, Z., Bőurcsök, G., Sági, F., 1994. High-speed RP-HPLC/FL analysis of amino acids after automated two-step derivatization with o-

- phthaldialdehyde/3-mercaptopropionic acid and 9-fluorenylmethyl chloroformate. J. Liq. Chromatogr. R. T. 17, 4391-4403.
- Behr, J., Israel, L., Gänzle, M.G., Vogel, R.F., 2007. Proteomic approach for characterization of hop-inducible proteins in *Lactobacillus brevis*. Appl. Environ. Microbiol. 73, 3300-3306.
- Beshkova, D., Simova, E., Frengova, G., Simov, Z., Dimitrov, Z.P., 2003. Production of volatile aroma compounds by kefir starter cultures. Int. Dairy J. 13, 529-535.
- Bitoun, J.P., Liao, S., Yao, X., Xie, G.G., Wen, Z.T., 2012. The redox-sensing regulator Rex modulates central carbon metabolism, stress tolerance response and biofilm formation by *Streptococcus mutans*. PloS One 7, e44766.
- Christensen, J.E., Dudley, E.G., Pederson, J.A., Steele, J.L., 1999. Peptidases and amino acid catabolism in lactic acid bacteria. Antonie Van Leeuwenhoek 76, 217-246.
- Cox, J., Neuhauser, N., Michalski, A., Scheltema, R.A., Olsen, J.V., Mann, M., 2011. Andromeda: a peptide search engine integrated into the MaxQuant environment. J. Proteome Res. 10, 1794-1805.
- Durham, B.P., Sharma, S., Luo, H., Smith, C.B., Amin, S.A., Bender, S.J., Dearth, S.P., Van Mooy, B.A., Campagna, S.R., Kujawinski, E.B., 2015b. Cryptic carbon and sulfur cycling between surface ocean plankton. PNAS 112, 453-457.
- Guédon, E., Renault, P., Ehrlich, S.D., Delorme, C., 2001. Transcriptional pattern of genes coding for the proteolytic system of *Lactococcus lactis* and evidence for coordinated regulation of key enzymes by peptide supply. J. Bacteriol. 183, 3614-3622.
- Gulitz, A., Stadie, J., Wenning, M., Ehrmann, M.A., Vogel, R.F., 2011. The microbial diversity of water kefir. Int. J. Food Microbiol. 151, 284-288.



- Kunji, E.R., Mierau, I., Hagting, A., Poolman, B., Konings, W.N., 1996. The proteolytic systems of lactic acid bacteria. *Antonie Van Leeuwenhoek* 70, 187-221.
- Laureys, D., De Vuyst, L., 2014. Microbial species diversity, community dynamics, and metabolite kinetics of water kefir fermentation. *Appl. Environ. Microbiol.*, 03978-03913.
- Maeda, K., Nagata, H., Ojima, M., Amano, A., 2014. Proteomic and transcriptional analysis of interaction between oral microbiota *Porphyromonas gingivalis* and *Streptococcus oralis*. *J. Proteome Res.* 14, 82-94.
- Maligoy, M., Mercade, M., Cocaign-Bousquet, M., Loubiere, P., 2008. Transcriptome analysis of *Lactococcus lactis* in coculture with *Saccharomyces cerevisiae*. *Appl. Environ. Microbiol.* 74, 485-494.
- Marsh, A.J., O'Sullivan, O., Hill, C., Ross, R.P., Cotter, P.D., 2013. Sequence-based analysis of the microbial composition of water kefir from multiple sources. *FEMS Microbiol. Lett.* 348, 79-85.
- Ponomarova, O., Gabrielli, N., Sévin, D.C., Mülleder, M., Zirngibl, K., Bulyha, K., Andrejev, S., Kafkia, E., Typas, A., Sauer, U., 2017. Yeast creates a niche for symbiotic lactic acid bacteria through nitrogen overflow. *Cell Systems* 5, 345-357.
- Ponomarova, O., Patil, K.R., 2015. Metabolic interactions in microbial communities: untangling the Gordian knot. *Curr. Opin. Microbiol.* 27, 37-44.
- Ravcheev, D.A., Li, X., Latif, H., Zengler, K., Leyn, S.A., Korostelev, Y.D., Kazakov, A.E., Novichkov, P.S., Osterman, A.L., Rodionov, D.A., 2012. Transcriptional regulation of central carbon and energy metabolism in bacteria by redox-responsive repressor Rex. *J. Bacteriol.* 194, 1145-1157.

- Rouse, S., Canchaya, C., van Sinderen, D., 2008. *Lactobacillus hordei* sp. nov., a bacteriocinogenic strain isolated from malted barley. *Int. J. Syst. Evol. Microbiol.* 58, 2013-2017.
- Schurr, B.C., Behr, J., Vogel, R.F., 2013. Role of the GAD system in hop tolerance of *Lactobacillus brevis*. *Eur. Food Res. Technol.* 237, 199-207.
- Siragusa, S., De Angelis, M., Calasso, M., Campanella, D., Minervini, F., Di Cagno, R., Gobbetti, M., 2014. Fermentation and proteome profiles of *Lactobacillus plantarum* strains during growth under food-like conditions. *J. Proteomics* 96, 366-380.
- Stadie, J., Gulitz, A., Ehrmann, M.A., Vogel, R.F., 2013. Metabolic activity and symbiotic interactions of lactic acid bacteria and yeasts isolated from water kefir. *Food Microbiol.* 35, 92-98.
- Stolz, P., Vogel, R.F., Hammes, W.P., 1995. Utilization of electron acceptors by lactobacilli isolated from sourdough. *Z. Lebensm. Unters. Forsch.* 201, 402-410.
- Sun, Z., Harris, H.M., McCann, A., Guo, C., Argimón, S., Zhang, W., Yang, X., Jeffery, I.B., Cooney, J.C., Kagawa, T.F., 2015. Expanding the biotechnology potential of lactobacilli through comparative genomics of 213 strains and associated genera. *Nat. Commun.* 6, 8322.
- Tyanova, S., Temu, T., Sinitcyn, P., Carlson, A., Hein, M.Y., Geiger, T., Mann, M., Cox, J., 2016. The Perseus computational platform for comprehensive analysis of (prote) omics data. *Nat. Methods* 13, 731.
- Xu, D., Bechtner, J., Behr, J., Eisenbach, L., Geißler, A.J., Vogel, R.F., 2019. Lifestyle of *Lactobacillus hordei* isolated from water kefir based on genomic, proteomic and physiological characterization. *Int. J. Food Microbiol.* 290, 141-149.

- Xu, D., Fels, L., Wefers, D., Behr, J., Jakob, F., Vogel, R.F., 2018. *Lactobacillus hordei* dextrans induce *Saccharomyces cerevisiae* aggregation and network formation on hydrophilic surfaces. *Int. J. Biol. Macromol.* 115, 236-242.
- Yamada, T., Letunic, I., Okuda, S., Kanehisa, M., Bork, P., 2011. iPath2. 0: interactive pathway explorer. *Nucleic Acids Res.* 39, W412-W415.
- Zhang, L., Nie, X., Ravcheev, D.A., Rodionov, D.A., Sheng, J., Gu, Y., Yang, S., Jiang, W., Yang, C., 2014. Redox-responsive repressor Rex modulates alcohol production and oxidative stress tolerance in *Clostridium acetobutylicum*. *J. Bacteriol.*, JB. 02037-02014.

Table 1. Significantly differentially expressed proteins in *L. hordei* TMW 1.1822 in response to co-cultivation with *S. cerevisiae* TMW 3.221 involved in carbohydrate metabolism (PKP, pentose phosphate pathway, pyruvate metabolism).

Number	Enzyme	EC number	Log <sub>2</sub> fold change (co-cultivation vs single culture)	-Log(P-value)
Up-regulated				
12	Glucose-6-phosphate dehydrogenase	EC 1.1.1.49	4.2	5.7
21	Citrate lyase	EC 4.1.3.6	4.8	6.7
25	Pyruvate formate lyase	EC 2.3.1.54	2.7	3.1
28	Acetoin reductase	EC 1.1.1.4	4.7	3.3
Down-regulated				
19/20	Bifunctional acetaldehyde/ alcohol dehydrogenase	EC 1.2.1.10/ EC 1.1.1.1	-1.9	2.9

Table 2. Significantly differentially expressed proteins in *L. hordei* TMW 1.1822 in response to co-cultivation with *S. cerevisiae* TMW 3.221 involved in amino acids biosynthesis.

Number	Enzyme	EC number	Log <sub>2</sub> fold change (co-cultivation vs single culture)	-Log (P-value)	SEED subcategory
Up-regulated					
1	ATP phosphoribosyltransferase	EC 2.4.2.17	3.0	3.8	
2	Imidazole glycerol phosphate synthase cyclase	EC 4.1.3.-	3.6	4.8	Histidine biosynthesis
3	Histidinol-phosphate aminotransferase	EC 2.6.1.9	3.5	3.3	
4	Histidinol dehydrogenase	EC 1.1.1.23	1.8	5.0	
5	Tryptophan synthase	EC 4.2.1.20	3.6	5.4	Tryptophan synthesis
6	S-ribosylhomocysteine lyase	EC 4.4.1.21	2.1	3.1	
7	Cystathionine beta-lyase	EC 4.4.1.8	3.5	2.0	Methionine biosynthesis
8	O-succinylhomoserine sulphydrylase	EC 2.5.1.48	2.1	4.2	
9	5-methyltetrahydropteroyltri -glutamate-homocysteine S-methyltransferase	EC 2.1.1.14	3.3	3.0	
10	Glutamate synthase	EC 1.4.1.13	6.4	2.8	Glutamate, arginine biosynthesis
11	Glutamine synthetase	EC 6.3.1.2	2.2	4.6	Glutamine, arginine biosynthesis
12	Acetylmethionine aminotransferase	EC 2.6.1.11	7.9	5.4	
13	Ornithine carbamoyltransferase	EC 2.1.3.3	6.9	5.6	Arginine biosynthesis
14	Argininosuccinate synthase	EC 6.3.4.5	4.5	7.2	
15	Argininosuccinate lyase	EC 4.3.2.1	3.3	4.9	
16	Ornithine cyclodeaminase	EC 4.3.1.12	2.6	5.8	Proline biosynthesis
Down-regulated					
17	Chorismate synthase	EC 4.2.3.5	-1.5	4.0	Aromatic amino acid biosynthesis
18	D-3-phosphoglycerate dehydrogenase	EC 1.1.1.95	-1.7	2.8	Serine biosynthesis

## Figure Captions

Fig. 1. Cell counts of *L. hordei* TMW 1.1822 in single culture (●) and co-cultivation with *S. cerevisiae* TMW 3.221 (▲).

Fig. 2. Subcellular localization of proteins (in silico, quantified by LC-MS/MS, unregulated, differentially expressed, up-regulated in co-cultivation, down-regulated in co-cultivation) which were predicted by PSORTb. The proportion of proteins assigned to each respective subcellular compartment and the group “unknown” with respect to the total number of proteins is shown by the bar chart. The table below shows the respective absolute numbers. A bias can be obviously seen for the proportion of cytoplasmic and cytoplasmic membrane proteins. Asterisk content was cited from Xu et al (Xu et al., 2019).

Fig. 3. SEED categories of proteins (in silico, quantified by LC-MS/MS, unregulated, differentially expressed, up-regulated in co-cultivation, down-regulated in co-cultivation) which were predicted by SEED. The proportion of proteins assigned to each respective categories of metabolism and the group “other categories”, which is the sum of several small categories with respect to the total number of proteins is shown by the bar chart. The ratio on the top of each column is the number of predicted SEED categories accounts for the number of all coding DNA sequence (CDS). Asterisk content was cited from Xu et al (Xu et al., 2019).

Fig. 4. Predicted outline of pyruvate metabolism of *L. hordei* TMW 1.1822 in the presence of *S. cerevisiae* TMW 3.221. The enzymes colored in red represent up-regulated,

in blue represent down-regulated enzymes or proteins according to proteomic data, while enzymes colored in yellow are both annotated by genomic and quantified by proteomic, enzymes colored in grey are neither present in genome nor proteome.

Fig. 5. Consumption of amino acids of *L. hordei* TMW 1.1822 and *S. cerevisiae* TMW 3.221 isolated from water kefir grown in CDM after 24 h. Black histogram represented CDM, slash histogram represented *L. hordei*, grey histogram represented *S. cerevisiae*.

Fig. 6. Predicted outline of ADI pathway of *L. hordei* TMW 1.1822 in the presence of *S. cerevisiae* TMW 3.221 (A). ADI, OTC colored in red showed up-regulation. pH value of single-cultivated and co-cultivated *L. hordei* and *S. cerevisiae* after 72h fermentation in WKM (B). Black histogram represented pH of co-cultivated *L. hordei* and *S. cerevisiae*, slash histogram represented single-cultivated *L. hordei*, grey histogram represented single-cultivated *S. cerevisiae*.

### **Supplementary Figure Captions**

Fig. S1. Overview on predicted enzymatic activities of *L. hordei* TMW 1.1822 in the complete metabolic and other pathways in the presence of *S. cerevisiae* TMW 3.221 according to genomic annotation data presented in iPath 3.0. The nodes colored in bold red represent up-regulated, in bold blue represent down-regulated enzymes or proteins according to proteomic data, while nodes colored in thin red represent all the rest enzymes or proteins.

Fig. S2. Growth of *S. cerevisiae* TMW 3.221 in the presence and absence of *L. hordei* TMW 1.1822 in WKM. *S. cerevisiae* in single culture (solid line), in co-cultivation with *L. hordei* (dashed line).

Fig. S3. Overview on the key reactions involved in sucrose metabolism of *L. hordei* TMW 1.1822 in the presence of *S. cerevisiae* TMW 3.221.

Fig. S4. Predicted PKP (A) and pentose phosphate pathway (B) of *L. hordei* TMW 1.1822 in the presence of *S. cerevisiae* TMW 3.221. The marked number of involved enzymes colored in red represented up-regulated proteins while blue represented down-regulated proteins.

Fig. S5. Predicted regulated pathway of amino acid biosynthesis of *L. hordei* TMW 1.1822 in the presence of *S. cerevisiae* TMW 3.221. Red lines with arrows indicated up-regulated enzymes, while blue lines indicated down-regulated enzymes according to proteomic prediction. The figure was obtained from the KEGG PATHWAY mapping tool.



Fig. 1

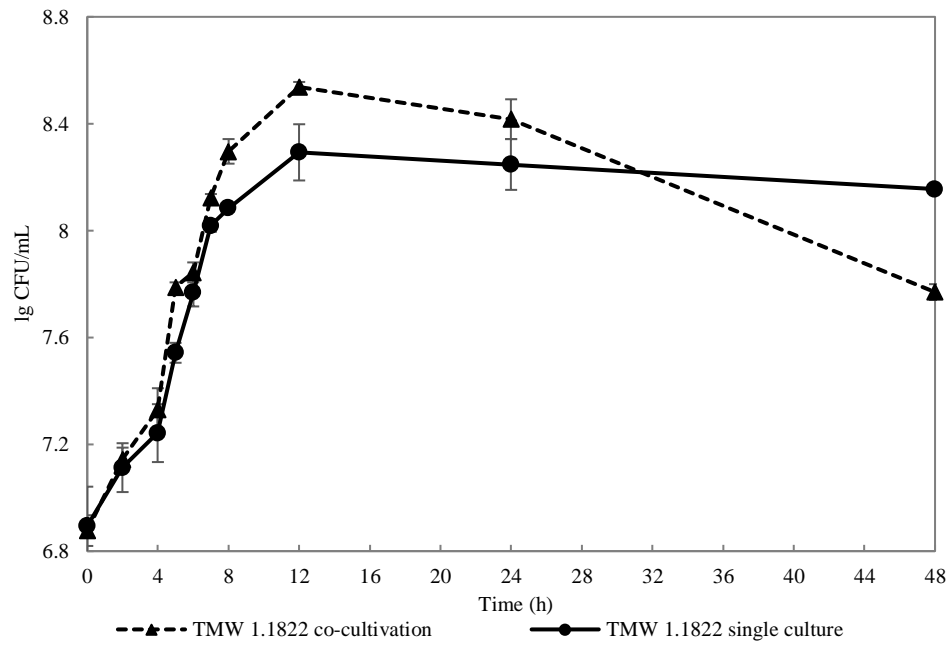


Fig. 2

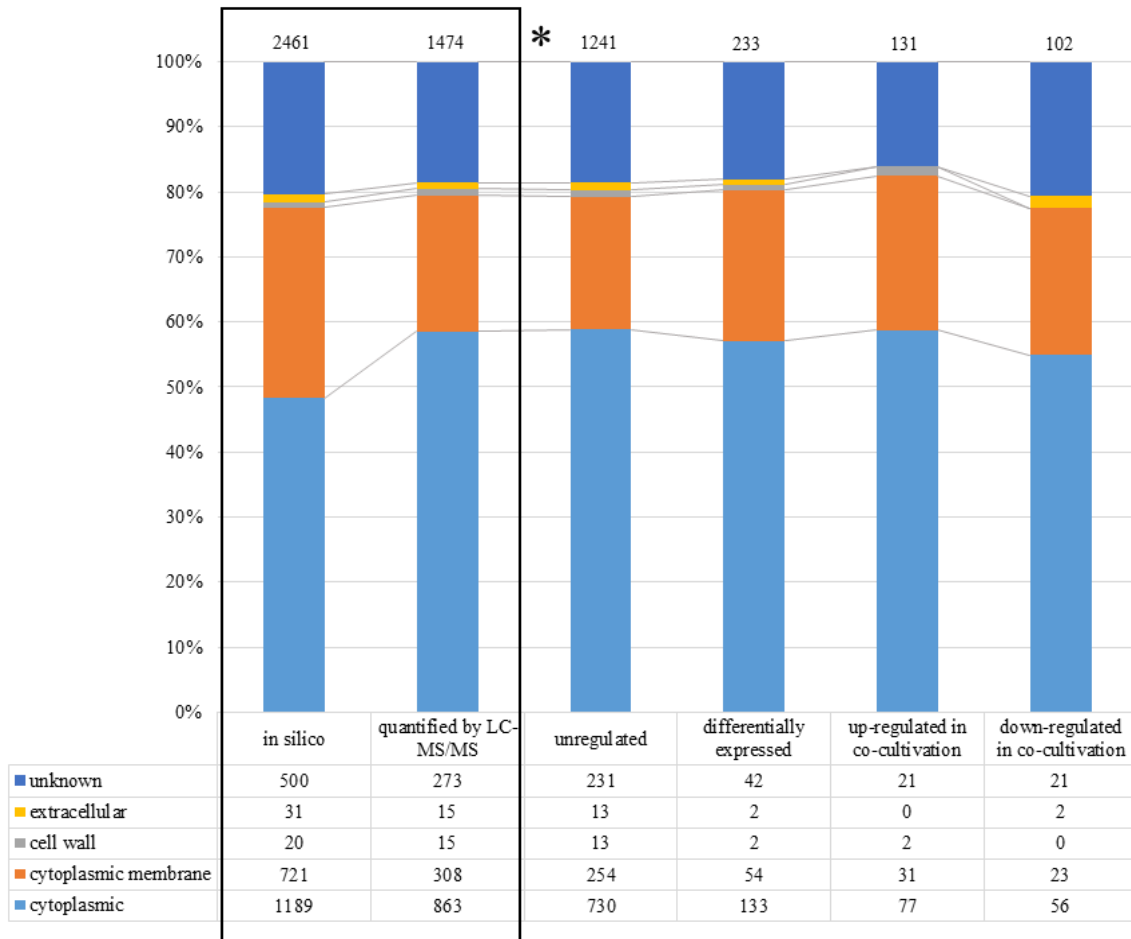


Fig. 3

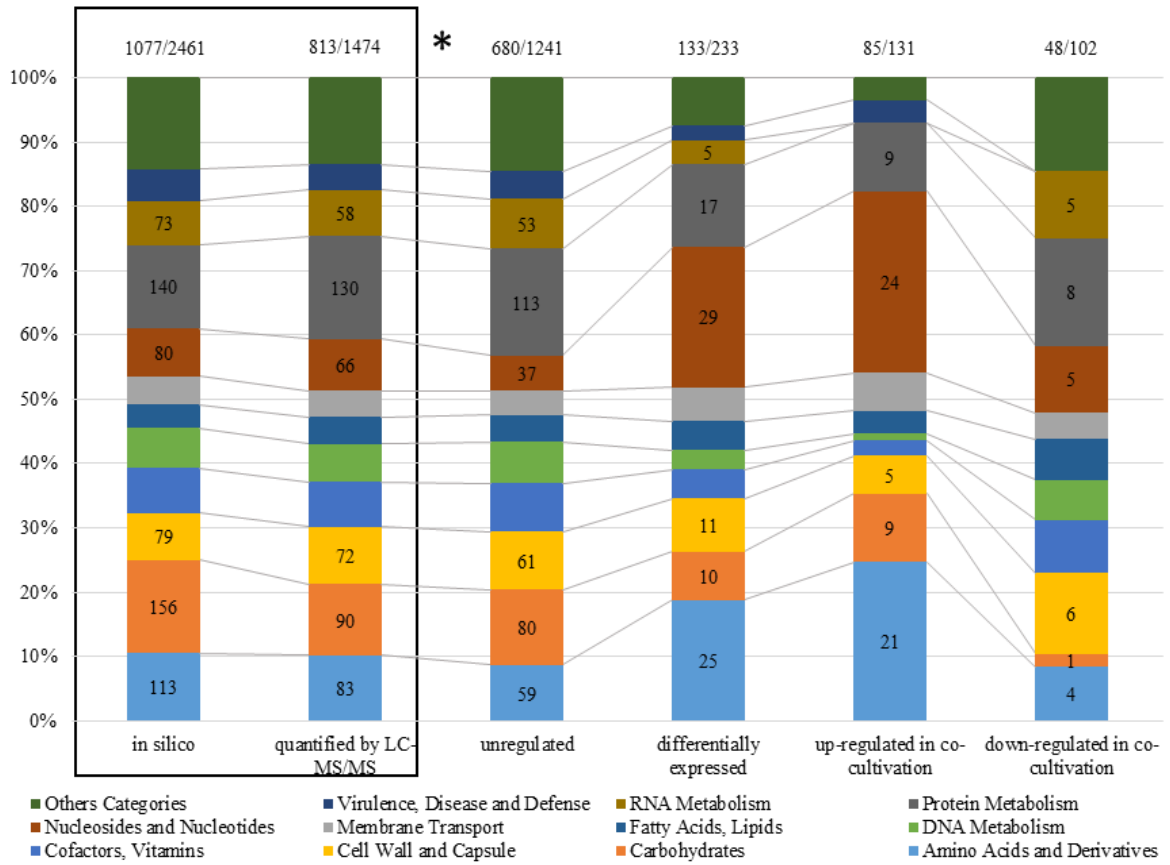


Fig. 4

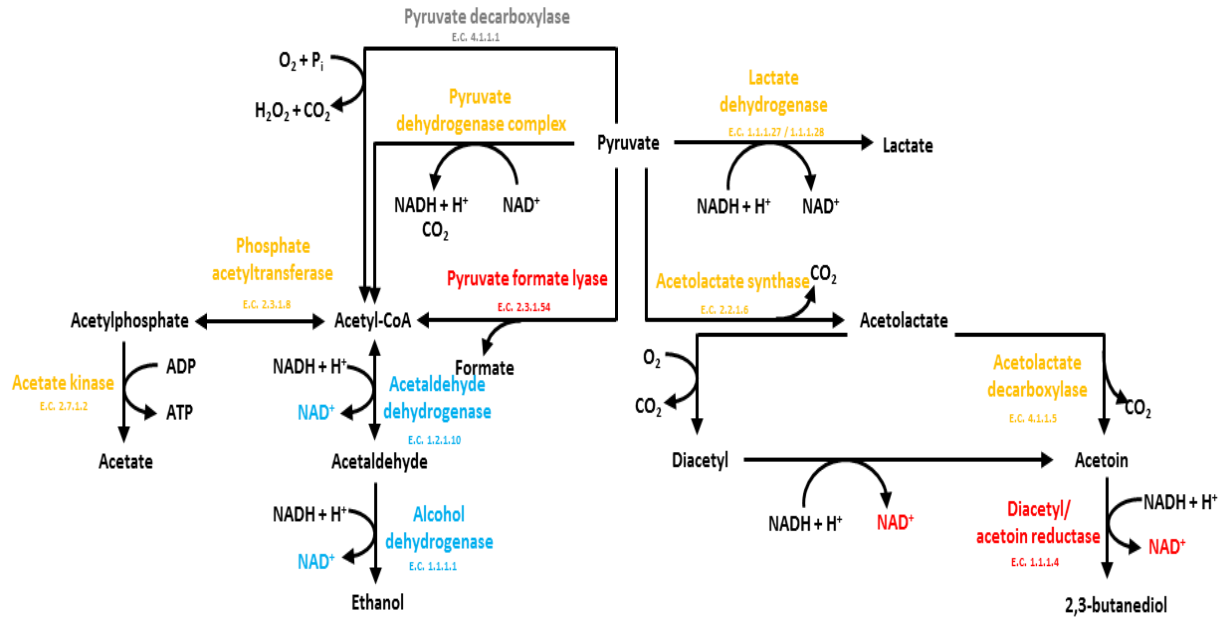


Fig. 5

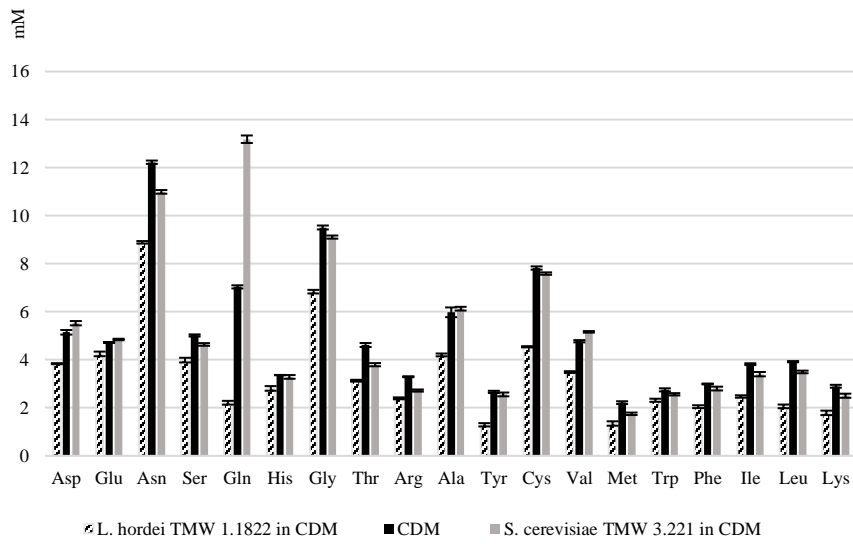


Fig. 6

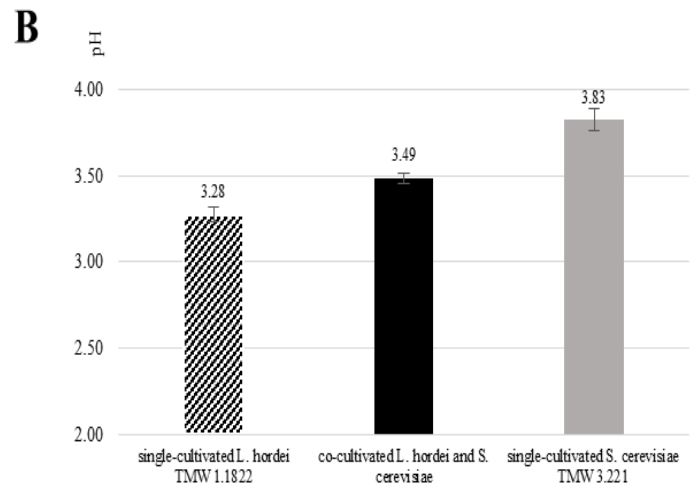
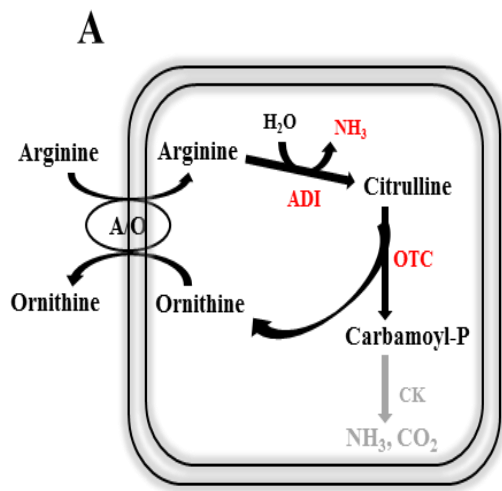


Fig. S1

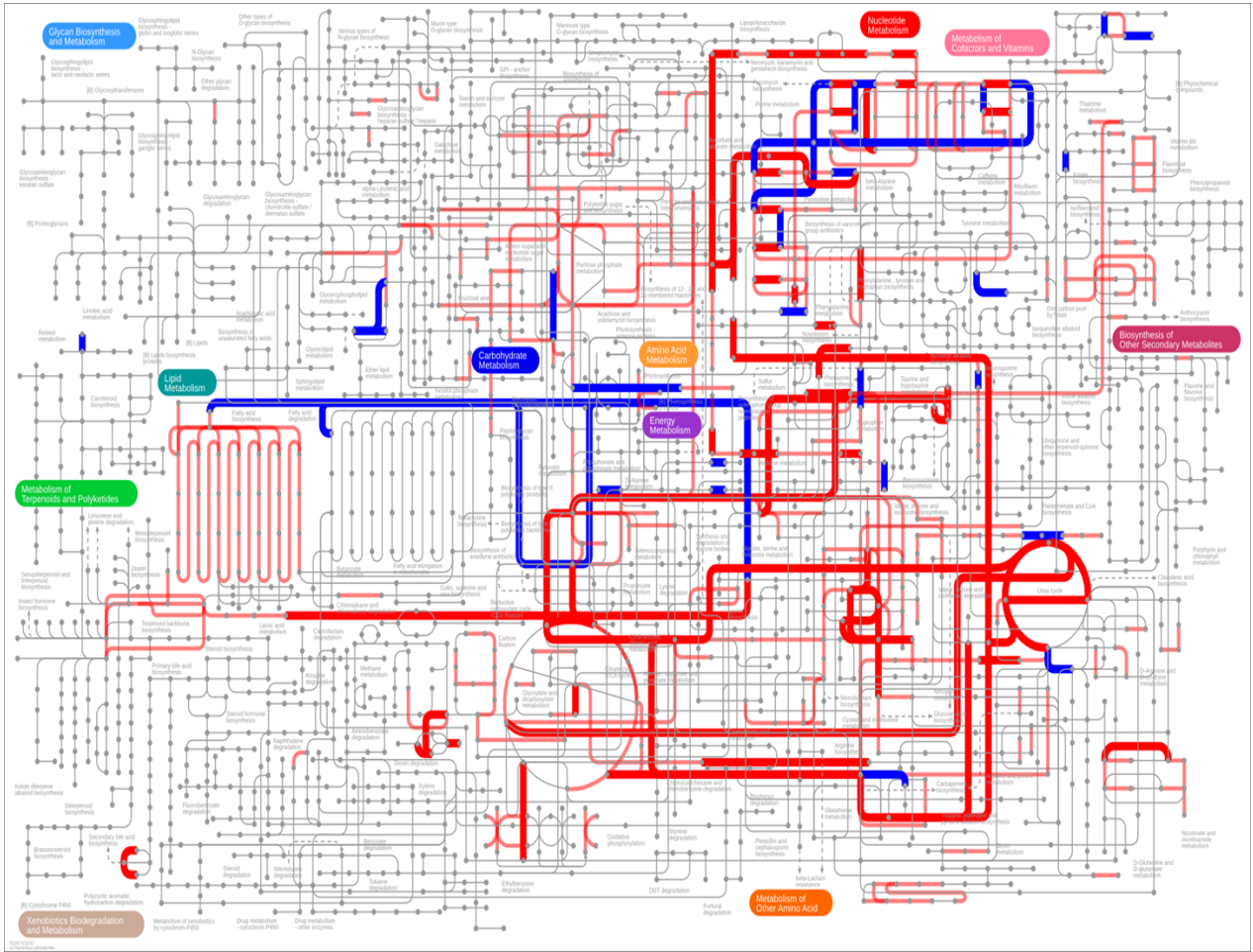


Fig. S2

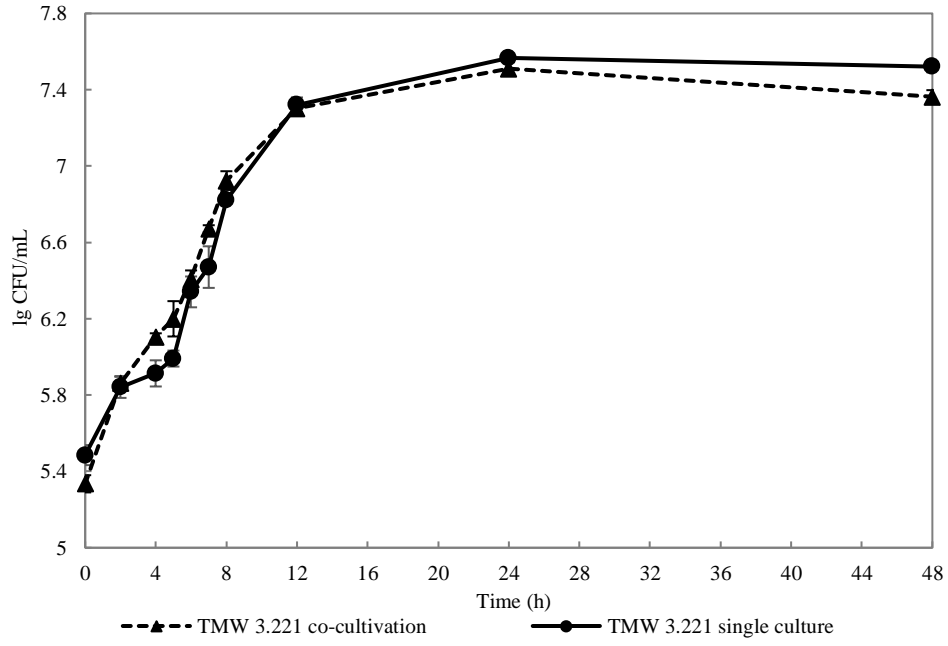




Fig. S3

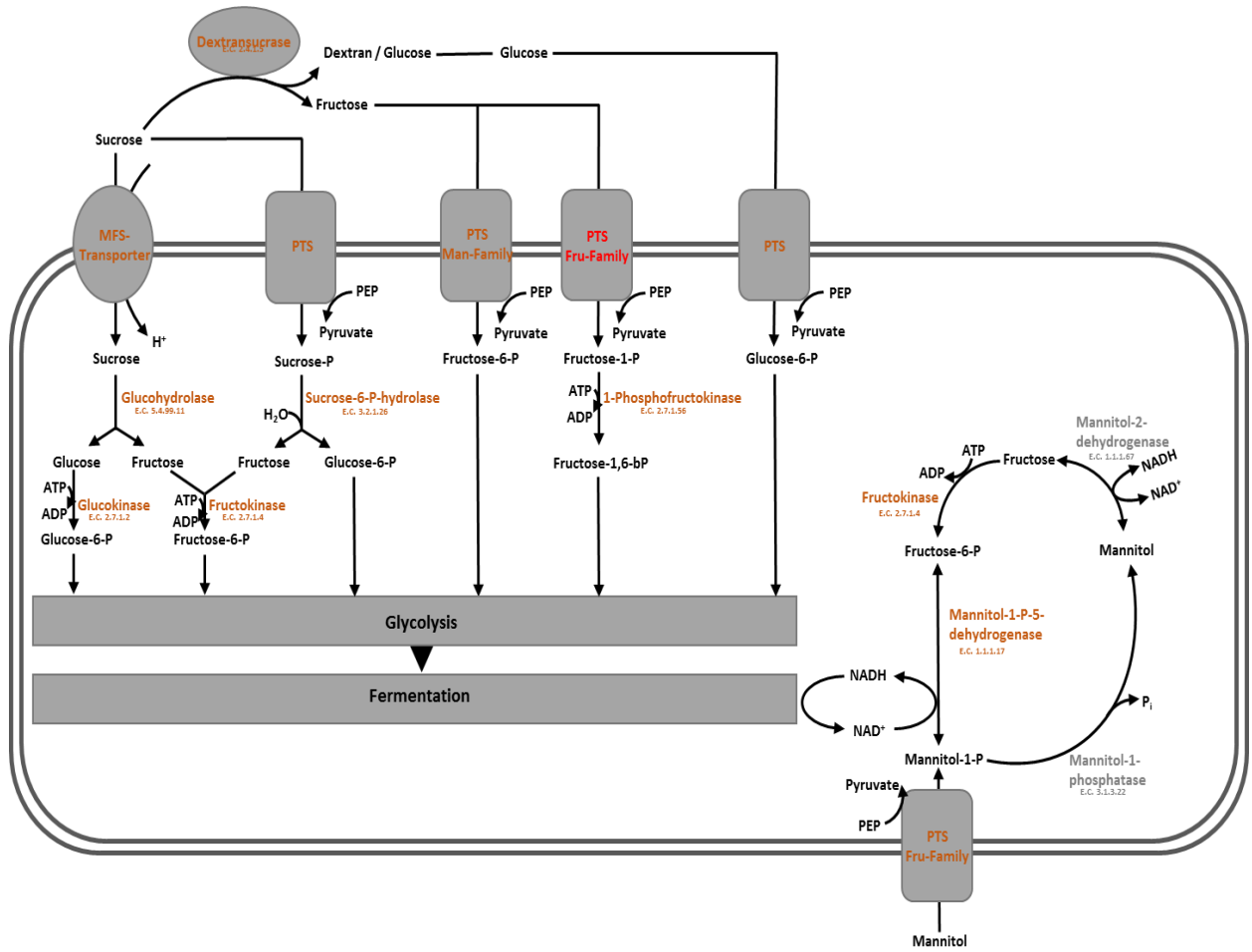


Fig. S4

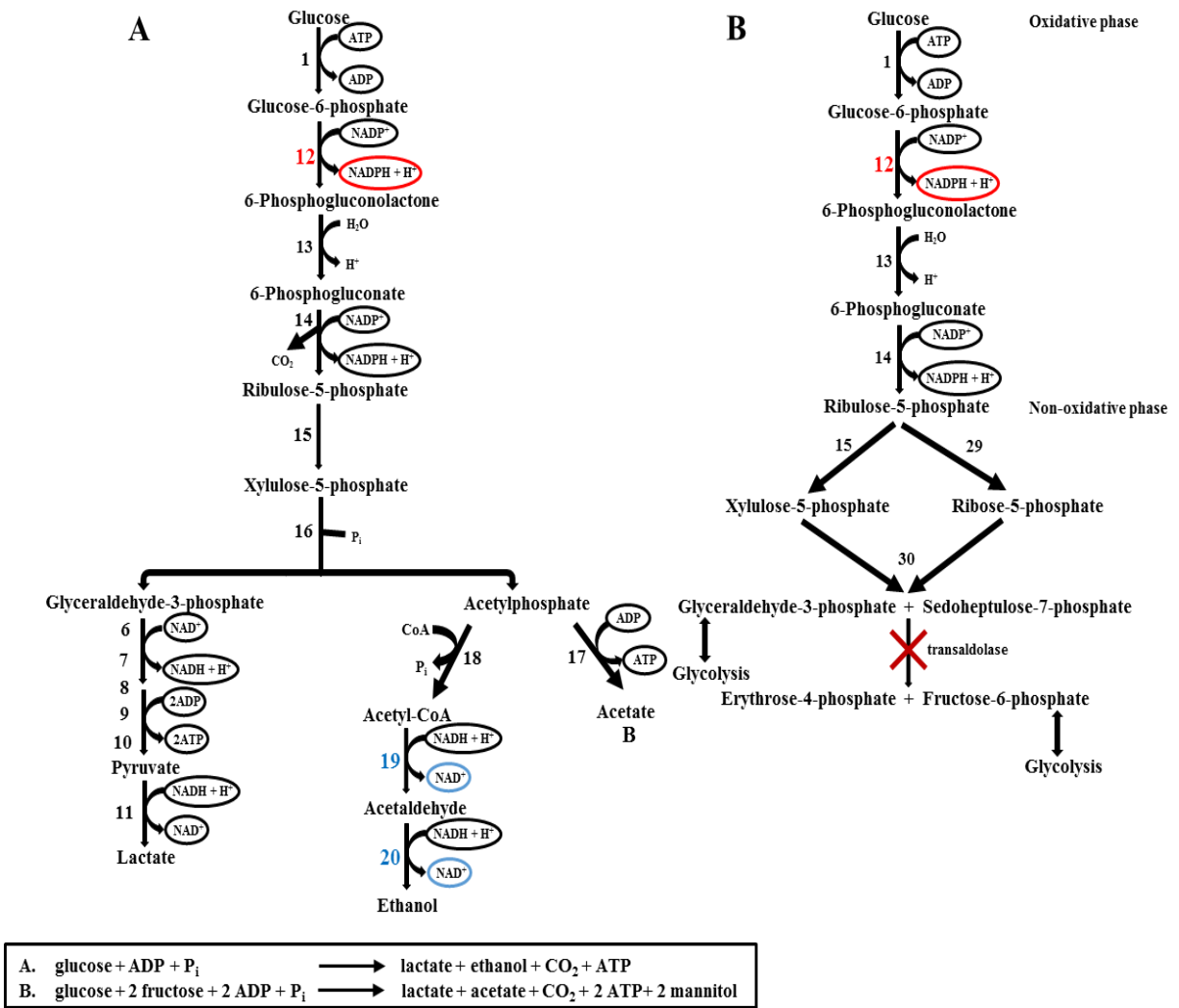
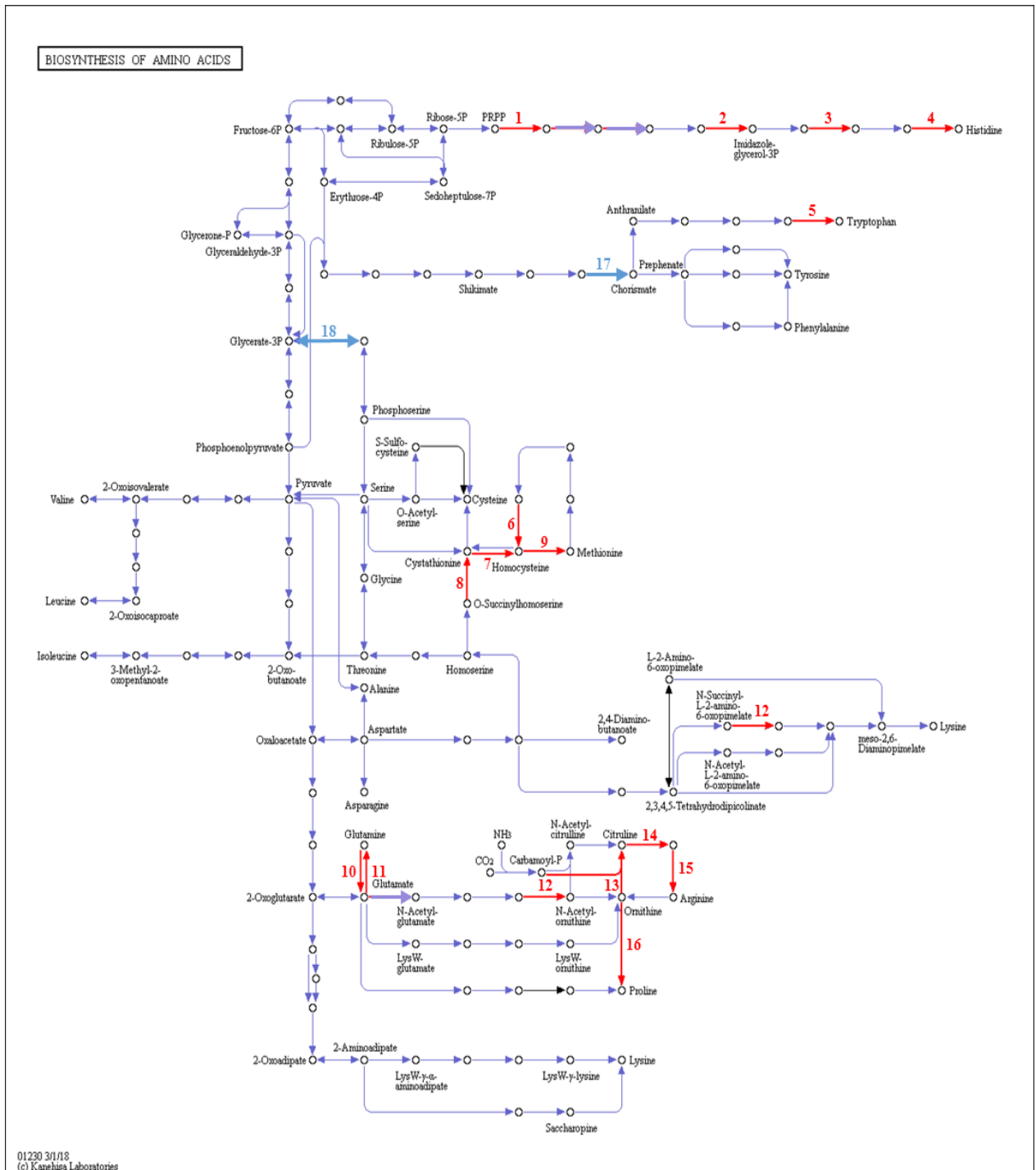


Fig. S5



#### **4.4 Manuscript 4: Comparative proteomic analysis of *Lactobacillus nagelii* and *Lactobacillus hordei* in the presence of *Saccharomyces cerevisiae* isolated from water kefir**

Julia Bechtner<sup>#</sup>, Di Xu<sup>#</sup>, Jürgen Behr, Rudi F. Vogel., 2019. *Frontiers in Microbiology*.  
Under review.

# joint first authorship

Water kefir is a slightly alcoholic and traditionally fermented beverage, which is prepared from sucrose, water, kefir grains, and dried or fresh fruits (e.g. figs). *Lactobacillus* (*L.*) *hordei*, *L. nagelii* and *Saccharomyces* (*S.*) *cerevisiae* are predominant and stable lactic acid bacteria and yeasts, respectively, isolated from water kefir consortia. The growth of *L. nagelii* and *L. hordei* was improved in the presence of *S. cerevisiae*. Quantitative comparative proteomics in this work enabled the investigation of interactions between LAB and yeast, and the prediction of real-time metabolic exchange in water kefir or other food fermentation consortia. It revealed 73 differentially expressed (DE) in *L. nagelii* TMW 1.1827 as compared to 233 DE proteins in *L. hordei* TMW 1.1822, respectively, in the presence of *S. cerevisiae*. The changes in the carbohydrate metabolism of *L. nagelii* revealed that, *L. hordei* and *L. nagelii* displayed antidromic strategies to maintain NAD<sup>+</sup>/NADH homeostasis after the metabolic switch induced by *S. cerevisiae*. Furthermore, nine up-regulated enzymes involved in amino acid biosynthesis or catabolism indicated that *S. cerevisiae* released glutamine, histidine, methionine and arginine, which were subsequently used by *L. nagelii* to ensure its survival in the water kefir consortia. While *L. hordei* reacted with an enhanced utilization of citrate in co-culture with *S. cerevisiae*, *L. nagelii* profited from riboflavin, most likely secreted by the

yeast. So far, aggregation promotion factors, i.e. formation of a specific glucan and bifunctional enzymes were only detected in *L. hordei*, which also appeared to react more distinct to the presence of *S. cerevisiae* than *L. nagelii*.

Authors contributions: Di Xu was responsible for planning the research project under the supervision of Jürgen Behr and Rudi F. Vogel and conducting the experiments. The prepared proteomic samples were analyzed with the aid of Christina Ludwig from the Bavarian Center for Biomolecular Mass Spectrometry. Di Xu analyzed the data with the help of Jürgen Behr, and wrote the manuscript draft. Julia Bechtner evaluated some more metabolic traits, and conducted BADGE analysis. Then Julia Bechtner added more contents and revised the whole manuscript as co-author. Rudi F. Vogel helped in finalizing and proofreading of the manuscript. All authors reviewed and approved the final manuscript.

**Comparative proteomic analysis of *Lactobacillus nagelii* and *Lactobacillus hordei* in  
the presence of *Saccharomyces cerevisiae* isolated from water kefir**

Julia Bechtner<sup>1#</sup>, Di Xu<sup>1#</sup>, Jürgen Behr<sup>1,2,3</sup>, Rudi F. Vogel<sup>1\*</sup>

# joint first authorship for equal contribution

1. Lehrstuhl für Technische Mikrobiologie, Technische Universität München, Freising,  
Germany
2. Bavarian Center for Biomolecular Mass Spectrometry (BayBioMS), Freising,  
Germany
3. Current address: Leibniz-Institut für Lebensmittel-Systembiologie an der  
Technischen Universität München, Freising, Germany

**\* corresponding author:** Rudi F. Vogel

rudivogel@wzw.tum.de

## Abstract

Water kefir is a slightly alcoholic and traditionally fermented beverage, which is prepared from sucrose, water, kefir grains, and dried or fresh fruits (e.g. figs). *Lactobacillus* (*L.*) *hordei*, *L. nagelii* and *Saccharomyces* (*S.*) *cerevisiae* are predominant and stable lactic acid bacteria and yeasts, respectively, isolated from water kefir consortia. The growth of *L. nagelii* and *L. hordei* are improved in the presence of *S. cerevisiae*. In this work we demonstrate that Quantitative comparative proteomics enables the investigation of interactions between LAB and yeast to predict real-time metabolic exchange in water kefir or other food fermentation consortia. It revealed 73 differentially expressed (DE) in *L. nagelii* TMW 1.1827 as compared to 233 proteins in *L. hordei* TMW 1.1822, respectively, in the presence of *S. cerevisiae*. The changes in the carbohydrate metabolism of *L. nagelii* revealed that, *L. hordei* and *L. nagelii* display antidromic strategies to maintain NAD<sup>+</sup>/NADH homeostasis after the metabolic switch induced by *S. cerevisiae*. Furthermore, the DE enzymes involved in amino acid biosynthesis or catabolism predict that *S. cerevisiae* releases glutamine, histidine, methionine and arginine, which are subsequently used by *L. nagelii* to ensure its survival in the water kefir consortium. While *L. hordei* reacts with an enhanced utilization of citrate in co-culture with *S. cerevisiae*, *L. nagelii* profits from riboflavin, most likely secreted by the yeast. So far, aggregation promotion factors, i.e. formation of a specific glucan and bifunctional enzymes were only detected in *L. hordei*, which also appears to react more distinct to the presence of *S. cerevisiae* than *L. nagelii*.

**Keywords:** *Lactobacillus nagelii*, *Lactobacillus hordei*, functional genome prediction, proteomic analysis, metabolism

## 1. Introduction

Water kefir is a slightly alcoholic, traditionally fermented beverage, which is prepared from sucrose, water, kefir grains, and dried or fresh fruits (e.g. figs). Water kefirs, originating from definitely different sources, exhibit different species diversities. Still, the basic consortium, which mainly consists of lactic acid bacteria (LAB), acetic acid bacteria (AAB) and yeasts (Ward, 1891; Neve and Heller, 2002; Gulitz et al., 2011; Marsh et al., 2013; Laureys and De Vuyst, 2014) appears to be stable. *L. hordei*, *L. nagelii* and *S. cerevisiae* are dominant LAB and yeast species, respectively, isolated from water kefir grains (Gulitz et al., 2011; Stadie et al., 2013; Laureys and De Vuyst, 2014).

In contrast to milk kefir, there is only very limited research on water kefir. Most of the available studies focused on its species diversity (Ward, 1891; Pidoux, 1989; Neve and Heller, 2002; Gulitz et al., 2011; Marsh et al., 2013; Laureys and De Vuyst, 2014; Martínez - Torres et al., 2017), or on the chemical and structural composition of the water kefir grains (Horisberger, 1969; Pidoux et al., 1988; Pidoux et al., 1990; Waldherr et al., 2010; Fels et al., 2018; Xu et al., 2018). To date, several attempts have been made to understand the interactions of the microorganisms in water kefir. For instance, Stadie et al (Stadie et al., 2013) studied the metabolic interaction between LAB (*L. hordei* and *L. nagelii*) and yeasts (*S. cerevisiae* and *Zygotriulasporea florentina*) isolated from water kefir and inferred, that the growth of *L. hordei* TMW 1.1822 should be improved by nutrients produced by both yeasts, such as several amino acids (isoleucine, leucine, methionine, phenylalanine, tryptophan, tyrosine and valine) and vitamin B6.

Another study explored the metabolite dynamics in a water kefir fermentation. The major



metabolites produced were ethanol and lactic acid during 192 h of fermentation. Glycerol, acetic acid, and mannitol were produced in low concentrations. The prevailing volatile aroma compounds were ethyl acetate, isoamyl acetate, ethyl hexanoate, ethyl octanoate, and ethyl decanoate after 72 h (Laureys and De Vuyst, 2014). Further, the water kefir was supplied with dried figs, apricots and raisins, respectively, as different nutrient sources delivering various concentrations. Also, the influence of oxygen has been investigated. It was concluded, that raisins led to low nutrient concentrations in the water kefir formulation, which favored the growth of *L. hilgardii* and *Dekkera bruxellensis*. In contrast, figs supplied the water kefir with high nutrient concentrations, which favored the growth of *L. nagelii* and *S. cerevisiae*. The presence of oxygen allowed the proliferation of AAB, resulting in high concentrations of acetic acid (Laureys et al., 2018). In addition, three main metabolic products were evaluated from the carbon flux from sucrose during 192 h of fermentation (Martínez - Torres et al., 2017). After 24 h, lactic and acetic acid have been postulated to be initially produced by *L. hilgardii* and subsequently produced by *Acetobacter* spp, mainly *A. tropicalis*. Ethanol was almost entirely oxidized to acetic acid, which could be further dissimilated by *Acetobacter* species.

However, these studies only determined total metabolite concentrations produced by the microorganisms during fermentation, but they did not reveal, how LAB, AAB and yeasts benefit from or affect each other through dynamic metabolite exchanges. In order to address this interaction we used differential label-free quantitative proteomic analysis, based on whole-sequenced genomes of *L. nagelii* TMW 1.1827 and *L. hordei* TMW 1.1822 to predict metabolic pathways (Xu et al., 2019a). The comparison of the

proteomes in single and co-culture should furthermore reveal the changes in the lifestyles of *L. nagelii* and *L. hordei* in the presence of *S. cerevisiae*.

## **2. Material and methods**

### **2.1. Strain culture, whole-genome sequencing and cell counts**

*L. hordei* TMW 1.1822, *L. nagelii* TMW 1.1827 isolated from water kefir by Gulitz et al. (Gulitz et al., 2011) were single-cultured anaerobically at 30 °C in modified MRS (mMRS) medium (Stolz et al., 1995). Genomic DNA was isolated, as described previously (Xu et al., 2019a), and sent to GATC Biotech (Konstanz, Germany) for PacBio SingleMolecule RealTime sequencing. The whole genome sequences were annotated by the NCBI Prokaryotic Genome Annotation Pipeline and RAST, which is a SEED-based prokaryotic genome annotation service using default settings (Aziz et al., 2008; Overbeek et al., 2013), as described previously (Xu et al., 2019a), and their key features were summarized in Table S1.

*S. cerevisiae* TMW 3.221 was pre-cultured in YPG medium (Xu et al., 2019b). Single-cultivated *S. cerevisiae*, *L. nagelii* and co-cultivated *L. nagelii* TMW 1.1827 and *S. cerevisiae* TMW 3.221 were prepared in water kefir medium (WKM) (Stadie et al., 2013). Cell counts were assessed by plating serial dilutions of co-cultivated *L. nagelii* and *S. cerevisiae* on mMRS agar plates, supplemented with cycloheximide and YPG agar plates, supplemented with chloromycetin, respectively. In the same way, single-cultivated *L. nagelii* was plated on mMRS agar plates and single-cultivated *S. cerevisiae* on YPG agar plates, as described in (Xu et al., 2019b).

## 2.2. Chromatographic analysis of amino acids, sugars and organic acids

1 % pre-cultured *L. nagelii* TMW 1.1827 and *S. cerevisiae* TMW 3.221 were separately inoculated into chemically defined medium (CDM) in triplicate, as described previously (Xu et al., 2019a). After 24 h of cultivation at 30 °C, 1 ml of each culture and 1 ml of CDM as a control were mixed with 50 µl of 70% (v/v) perchloric acid (Sigma-Aldrich, St. Louis, USA) and subsequently incubated overnight at 4 °C for protein precipitation. After centrifugation (12000 rpm, 10 min), the supernatant was collected and filtered by 0.2 µm Phenex™ Regenerated Cellulose Membrane (Phenomenex, Aschaffenburg, Germany) for the detection of amino acids and organic acids as below. Amino acids were analyzed on a Dionex Ultimate 3000 HPLC system (Dionex, Idstein, Germany) using a Gemini C18 column (Phenomenex, Aschaffenburg, Germany) with UV detection at 338 and 269 nm. Quantification was executed employing calibration adjustment by external HPLC grade standards and the Chromeleon software version 6.80 (Dionex, Idstein, Germany).

Consumption and production of sugars and organic acids of *L. nagelii* and *S. cerevisiae* grown in CDM for 24 h were quantified by a Dionex UltiMate 3000 HPLC system (Dionex, Idstein, Germany) with Rezex ROA-Organic Acid H<sup>+</sup> column (Phenomenex, Aschaffenburg, Germany) and RI-101 detector (Shodex, München, Germany), as described previously (Xu et al., 2019a). For sugar analysis, 500 µl of each sample were mixed with 250 µl of a 10 % (w/v) ZnSO<sub>4</sub>\*7H<sub>2</sub>O solution and afterwards added with 250 µl 0.5 M NaOH. After incubation for 20 min at 25° C, the supernatant was obtained by centrifugation and filtered as described above. Analytes were separated at a constant flow rate of 0.7 ml/min with a column temperature of 85 °C for 30 min. Sulfuric acid

(Rotipuran, Roth, Karlsruhe, Germany) solution with a concentration of 5 mM served as mobile phase.

### **2.3. Proteomic sample preparation and label-free quantitative proteomic analysis**

Co-cultivated *L. nagelii* and *S. cerevisiae*, as well as single-cultured *L. nagelii* and *S. cerevisiae* were incubated anaerobically in WKM at 30 °C for 10 h in triplicate and prepared for proteomic analysis, as previously described (Xu et al., 2019a). First of all, these samples were treated with trichloroacetic acid (TCA), centrifuged (5000 rpm, 5 min) at 4°C, washed with acetone and reconstituted in lysis buffer (8 M urea, 5 mM EDTA disodium salt, 100 mM (NH)<sub>4</sub>HCO<sub>3</sub>, 1 mM dithiothreitol (DDT)). Subsequently, the cells were mechanically disrupted with acid-washed glass beads (G8772, 425-600 µm, Sigma, Germany). Proteins were reduced with 10 mM DTT at 30 °C for 30 min, and subsequently carbamidomethylated with 55 mM chloroacetamide in the dark for 60 min. Finally, proteins were digested by trypsin and desalted by C18 solid phase extraction using Sep-Pak columns (Waters, WAT054960). Purified peptide samples were dried in a SpeedVac concentrator (Acid-Resistant CentriVap Vacuum Concentrator, Labconco) and resuspended in an aqueous solution containing 2 % acetonitrile and 0.1 % formic acid to a final concentration of 0.25 µg/µl.

Generated peptides were analyzed on a Dionex Ultimate 3000 nano LC system, coupled to a Q-Exactive HF mass spectrometer (Thermo Scientific, Bremen, Germany), as described previously (Xu et al., 2019b). Peptides were delivered to a trap column (75 µm × 2 cm, self-packed with Reprosil-Pur C18 ODS-3 5 µm resin, Dr. Maisch, Ammerbuch, Germany) at a flow rate of 5 µl/min in solvent A<sub>0</sub> (0.1 % formic acid in water). Peptides

were separated on an analytical column (75  $\mu\text{m}$   $\times$  40 cm, self-packed with Reprosil-Gold C18, 3  $\mu\text{m}$  resin, Dr. Maisch, Ammerbuch, Germany), using a 120 min linear gradient from 4-32 % solvent B (0.1% formic acid, 5% DMSO in acetonitrile) and solvent A<sub>1</sub> (0.1 % formic acid, 5 % DMSO in water) at a flow rate of 300 nl/min. The mass spectrometer was operated in data dependent mode, automatically switching between MS1 and MS2 spectra. MS1 spectra were acquired over a mass-to-charge ( $m/z$ ) range of 360-1300  $m/z$  at a resolution of 60,000 (at  $m/z$  200) using a maximum injection time of 50 ms and an AGC target value of 3e6. Up to 20 peptide precursors were isolated (isolation window 1.7  $m/z$ , maximum injection time 25 ms, AGC value 1e5), fragmented by higher-energy collisional dissociation (HCD), using 25 % normalized collision energy (Letort et al.) and analyzed at a resolution of 15,000 with a scan range from 200 to 2000  $m/z$ .

Peptide and protein identification plus quantification were performed with MaxQuant (version 1.5.7.4) by searching the MS2 data against all protein sequences obtained from UniProt - Reference proteome *S. cerevisiae* S288c (6,724 entries, downloaded 13.03.2017) and all protein sequences from *L. nagelii* TMW 1.1827 (cf. section 3.1, GenBank CP018176 - CP018179), using the embedded search engine Andromeda (Cox et al., 2011), as previously described (Xu et al., 2019a). Carbamidomethylated cysteine was a fixed modification. Oxidation of methionine, and N-terminal protein acetylation were variable modifications. Precursor and fragment ion tolerances were 10 ppm and 20 ppm, respectively. Label-free quantification and data matching between consecutive analyses were enabled within MaxQuant. Search results were filtered for a minimum peptide length of 7 amino acids, 1 % peptide and protein false discovery rate (FDR) plus common contaminants and reverse identifications. MaxQuant output files were further

analyzed using Perseus (version 1.5.6.0) (Tyanova et al., 2016). iBAQ intensities were log<sub>2</sub>-transformed for further statistical analysis. NCBI annotation, PSORTb subcellular localization, SEED category (subcategory and subsystem) as previously annotated (cf. section 2.1) were added to the matrix through identifier matching. For the comparison between two groups, t-tests were performed. Log<sub>2</sub> fold change  $\geq 2$  or  $\leq -2$  and  $-\text{Log}_{10} P\text{-value} \geq 2$  (p value  $\leq 0.05$ ) were considered to be significantly differentially expressed proteins of *L. nagelii* TMW 1.1827 in the presence of *S. cerevisiae* TMW 3.221.

#### **2.4. Statistical analysis and visualization**

A genomic atlas of *L. nagelii* TMW 1.1827 was generated using Artemis and DNA plotter (<http://www.sanger.ac.uk/science/tools/artemis>) (Carver et al., 2008) as described previously (Xu et al., 2019a). Subcellular localization of proteins was predicted, using the tool PSORTb (Version 3.0.2, <http://www.psort.org/psortb/>) (Gardy et al., 2004; Yu et al., 2010). All the annotated EC numbers from RAST were imported into iPath 3.0 (<https://pathways.embl.de/ipath3.cgi?map=metabolic>) (Yamada et al., 2011) for generating an overview of complete metabolic pathways and biosynthesis of other secondary metabolites.

The sucrose metabolism, pyruvate metabolism and amino acid biosynthesis pathways of *L. nagelii* TMW 1.1827 were constructed based on the self-constructed overview on the key reactions involved in sucrose metabolism, pyruvate metabolism and amino acid biosynthesis pathways of *L. hordei* TMW 1.1822 as described previously (Xu et al., 2019a). Enzymes involved in each reaction step were manually checked, whether they were present in translated open reading frames (ORFs) annotated from both, NCBI and

RAST. The figure of the biosynthesis pathways of amino acids and riboflavin was generated using the KEGG PATHWAY mapping tool ([http://www.genome.jp/kegg/tool/map\\_pathway1.html](http://www.genome.jp/kegg/tool/map_pathway1.html)) by importing EC numbers only involved in amino acid biosynthesis and riboflavin metabolism.

Genomic differences between *L. nagelii* TMW 1.1827 and *L. hordei* TMW 1.1822 were identified using Blast Diagnostic Gene findEr (BADGE) (Behr et al., 2016) under modified settings. The “min\_DMG\_occurance” was set to 0.00000000000001. The “megablast\_perc\_identity\_cut” value was set to 90, while both, the “megablast\_within\_groub\_qscov” and the “megablast\_between\_group\_qscov” value was set to 0.90. The dc\_mode was enabled. Additionally, BADGE was run on protein level using default protein-level options. The BADGE output was divided in pan and core genome. The genome comparison was graphically visualized by the BLAST Ring Image Generator (BRIG) (Alikhan et al., 2011) using the annotated and translated ORFs of the pan genome as reference. Furthermore, the genomic differences between *L. nagelii* TMW 1.1827 and *L. nagelii* DSM 13675 were identified by BADGE using default settings.

### **3. Results and Discussion**

#### **3.1. Comparative genomic features and growth characteristics of *L. nagelii* in presence of *S. cerevisiae***

*L. hordei*, *L. nagelii* and *S. cerevisiae* are predominant and stable LAB and yeast isolated from water kefir (Gulitz et al., 2011). The whole-genome sequence of *L. nagelii* TMW 1.1827 was submitted to GenBank designated as BioSample SAMN06052354, referred to

as accession numbers CP018180 to CP018183. The genomic size of *L. nagelii* TMW 1.1827 is 2.41 Mbp, which is almost the same size as *L. hordei* TMW 1.1822 (2.42 Mbp) (Xu et al., 2019a), and exhibits a GC content of 36.68 % (shown in Table 1). Although the genomic size was similar, *L. nagelii* TMW 1.1827 exhibits a total number of 2391 coding sequences (CDS), including all three plasmids, while *L. hordei* TMW 1.1822 features 70 more CDS (shown in Table 1 and visualized in Fig. S1). So far, the only published whole genome sequences of *L. hordei* and *L. nagelii* strains result from a comparative genomics project together with 211 other lactic acid bacteria strains (Sun et al., 2015). Here, both strains, *L. hordei* DSM 19519 isolated from malted barley and *L. nagelii* DSM 13675 isolated from wine, were associated to different environments than water kefir and therefore face different conditions. Those differences in the adaptation to distinct environmental conditions were also displayed in the genomes. For *L. hordei* the differences between the type strain isolated from barley and the water kefir born strain TMW 1.1822 reside in sucrose metabolism (Xu et al., 2019a). Also for the two *L. nagelii* strains from wine and water kefir the differences could mainly be referred to genes related to carbohydrate metabolism, also suggesting an adaption to the sugar-rich water kefir environment of *L. nagelii* TMW 1.1827.

In this work, the whole genome sequences of *L. hordei* TMW 1.1822 and *L. nagelii* TMW 1.1827 were compared to each other using BADGE. As visualized in figure 1, the core genome of both microorganisms included 1380 CDS, which displays 56.0 % of the whole genome of *L. hordei* TMW 1.1822 and 57.7 % of the whole genome of *L. nagelii* TMW 1.1827. The main components of the core genome were found in the SEED categories of protein, carbohydrate and amino acid metabolism. The accessory genome of



*L. hordei* TMW 1.1822 as compared to that one of *L. nagelii* TMW 1.1827 was dominated by additional genes for carbohydrate and amino acid metabolism, and cell wall biosynthesis. Corresponding results were found for *L. nagelii* TMW 1.1827, except for the SEED category of cell wall formation, which was substituted by CDS involved in DNA metabolism (shown in Fig. 2). Since both microorganisms are associated to water kefir, representing an environment rich in sugar, it was not surprising, that *L. nagelii* TMW 1.1827 and *L. hordei* TMW 1.1822 mainly adapted to it by additional genes coding for carbohydrate metabolism.

The cell yield of single cultivated *L. nagelii* TMW 1.1827 was increased upon co-cultivation with *S. cerevisiae* after 8 and 12 h of fermentation (Fig. 3). As observed previously for *L. hordei*, the cfu of *L. nagelii* TMW 1.1827 were significantly higher in the presence of *S. cerevisiae* after 24 h. Furthermore, it declined slower in co-cultivated *L. nagelii* as compared to single-cultivated *L. nagelii* until 24 h. On the other hand, the cfu of *S. cerevisiae* were reduced upon co-cultivation with *L. nagelii* (Fig. S2), while it was only little affected upon co-cultivation with *L. hordei* as compared to its single-cultivation (Xu et al., 2019b). This indicates, that *L. nagelii* TMW 1.1827 affects the growth of *S. cerevisiae* much more than *L. hordei* TMW 1.1822. To get insights into the reasons of these phenomena, prediction of dynamic metabolite exchanges were explored by proteomics in this study.

### **3.2. General proteomic analysis and overview of predicted complete metabolic activities**

As shown in Fig. 4, 1243 proteins of *L. nagelii* TMW 1.1827 were identified and quantified by proteomic analysis, comprising about 52 % of the genes annotated by whole genome analysis. A comprehensive overview of the complete metabolic pathways and significantly differentially expressed (DE) proteins of *L. nagelii* in the presence of *S. cerevisiae* is provided in Fig. S3. Compared to the results obtained for *L. hordei* TMW 1.1822 (Xu et al., 2019b), *L. nagelii* expressed less proteins significantly different, when co-cultivated with the yeast. As shown in Fig. 5, there were only 73 DE proteins in *L. nagelii* regulated in the presence of *S. cerevisiae*, while there were 233 DE proteins found in *L. hordei* under the same conditions. Those up/down-regulated proteins of *L. nagelii* were most abundant in the SEED categories “amino acids and derivatives” (9 out of 69), “carbohydrates” (5 out of 93) “nucleosides and nucleotides” (4 out of 61) and “cofactors, vitamins” (7 out of 54) (shown in Fig. 5). In summary, it was shown, that the proteome and connected metabolism of *L. nagelii* was less influenced in the presence of *S. cerevisiae* than the metabolism of *L. hordei*.

### **3.3. Comparative sugar transport and carbohydrate metabolism**

The overview on the key reactions involved in sucrose metabolism of *L. nagelii* is provided in figure 6. Like *L. hordei* (Xu et al., 2019a), also *L. nagelii* encoded and expressed an MFS-transporter specific for sucrose uptake. As previously demonstrated, *L. nagelii* also produces a glucan from sucrose by an extracellular glucansucrase (Xu et al., 2018), like it was shown for *L. hordei* (Xu et al., 2019a). Still, only the dextran of *L. hordei* induced aggregation of *S. cerevisiae* (Xu et al., 2018). The residual fructose can then be transported into the cell by a fructose specific PTS and simultaneous phosphorylation. Once inside the cell, the phosphorylated fructose can directly enter the

glycolytic pathway. All PTS, namely for sucrose, glucose, fructose, mannose, sorbose and mannitol uptake, were identified by proteomic analysis, as it was demonstrated for *L. hordei*. In contrast, the PTS specific for  $\beta$ -glucoside and cellobiose transport were not found in the proteome of *L. nagelii*. While PTS belonging to the mannose-fructose-sorbose family were significantly up-regulated in *L. hordei* (Xu et al., 2019b), no PTS were differentially expressed in *L. nagelii*. Whole genome sequence analysis of *L. nagelii* TMW 1.1827 confirmed the presence of the genes encoding all enzymes required for the EMP and PKP pathways as it was demonstrated for *L. hordei* TMW 1.1822 (Locus tags and IDs given in Table S2). Thus, *L. nagelii* TMW 1.1827 has also been considered as facultative heterofermentative, such as *L. plantarum* WCFS1 and *Lactococcus lactis* (Kleerebezem et al., 2003; Kleerebezem and Hugenholtz, 2003). This is contrary to the fact that *L. hordei* DSM 19519 and *L. nagelii* DSM 13675 were inferred as obligate homofermentative microorganisms according to their phenotype (Sun et al., 2015). Unlike obligately heterofermentative *L. hilgardii*, which produces high acetate concentrations and high ratios of acetate to lactic acid during water kefir fermentation (Laureys et al., 2018), *L. nagelii* TMW 1.1827 produced 40.1 mM lactate and 6.9 mM acetate after 24 h of fermentation in CDM (Fig. S4). This corroborates a homofermentative metabolism, in which energy generation via EMP and recycling of  $\text{NAD}^+$  by reducing pyruvate to lactate is favored. The small amount of acetate may reside from pyruvate by either generating formate via pyruvate formate lyase or by  $\text{NADH}$  and  $\text{CO}_2$  generation via pyruvate dehydrogenase complex. Subsequently, the resulting acetyl-CoA may be metabolized to acetate. However, the latter option requires subsequent  $\text{NAD}^+$  recycling.

In the presence of *S. cerevisiae*, the 3-phosphoglycerate mutase of *L. nagelii* TMW 1.1827 was significantly down-regulated. As postulated previously, the expression of this enzyme is linked to the concentration of its substrate 3-phosphoglycerate (Smeianov et al., 2007). This indicates, that intermediates of early glycolytic steps may be used for other metabolic reactions or hexoses may rather enter PKP or PPP than EMP, resulting in less production of 3-phosphoglycerate. At the same time, the alcohol dehydrogenase of *L. nagelii* was significantly up-regulated in the presence of *S. cerevisiae* (shown in Fig. 7 and Table S3). Yielding less ATP, but more reductive power, this metabolic switch to ethanol production may be important to keep the PKP running. As discussed previously (Xu et al., 2019a), *L. hordei* TMW 1.1822 is capable of transporting and phosphorylating mannitol, possibly delivered by *S. cerevisiae*, inside the cell by a specific PTS and subsequent oxidation to fructose-6-P via mannitol-1-P-5-dehydrogenase. Equally, *L. nagelii* TMW 1.1827 was found to be equipped with those enzymes, also giving evidence for the enhanced ethanol production as a recycling mechanism for the NADH, which is generated upon mannitol oxidation. Since fructose-6-P must not be phosphorylated prior to entering the EMP or PKP, there is less need for ATP generation upon acetate formation.

In contrast to *L. nagelii*, the expression of EMP specific enzymes of *L. hordei* TMW 1.1822 was not influenced by *S. cerevisiae*. However, the expression of glucose-6-phosphate dehydrogenase, which is part of the PKP and PPP, was significantly up-regulated (Xu et al., 2019b). As discussed previously, this metabolic switch from EMP to PKP/PPP may also help both microorganisms to utilize gluconate, which appears to be a decisive trait in the water kefir environment (Xu et al., 2019a). Looking at the metabolic

phenotype of other abundant LAB species in water kefir, these results are in line with the findings of Laureys et al., who described the species *Lactobacillus casei*, which is also facultative heterofermentative, as the most dominant one during their water kefir grain growth (Laureys et al., 2018).

Furthermore,  $\alpha$ -acetolactate decarboxylase (shown in Fig. 7, Table S3) was significantly down-regulated in *L. nagelii*, blocking the direct decarboxylation of acetolactate to acetoin. Under aerobic conditions, acetolactate spontaneously decomposes into diacetyl enabling regeneration of 2 molecules of  $\text{NAD}^+$  upon reduction to 2,3-butanediol via diacetyl/ acetoin reductase. Since oxygen is probably limited for *L. nagelii* due to the subsidence of the water kefir granules, this pathway for  $\text{NAD}^+$  regeneration may be completely disabled in the water kefir environment. In contrast, *L. hordei* reacts to the presence of *S. cerevisiae* by down-regulation of alcohol dehydrogenase and up-regulation of diacetyl/ acetoin reductase and  $\alpha$ -acetolactate decarboxylase, yielding 2,3-butanediol and  $\text{NAD}^+$  (Xu et al., 2019b). In summary, *L. hordei* TMW 1.1822 and *L. nagelii* TMW 1.1827 displayed totally antidromic strategies to maintain  $\text{NAD}^+/\text{NADH}$  homeostasis after the metabolic switch induced by *S. cerevisiae*.

As it was already described for *L. hordei*, both, genomic and proteomic analyses revealed an incomplete TCA cycle in *L. nagelii*. In the case of *L. nagelii*, aconitate hydratase (EC 4.2.1.3), which catalyses the stereo-specific isomerization of citrate to isocitrate via cis-aconitate, and isocitrate dehydrogenase (EC 1.1.1.42), which catalyzes the oxidative decarboxylation of isocitrate, producing 2-oxoglutarate and  $\text{CO}_2$ , were significantly up-regulated (4.5  $\log_2$ fold change, 2.0  $\log_2$ fold change). Despite its incompleteness, the TCA

cycle is an important supplier for compounds involved in other metabolic reactions and thus, isocitrate and 2-oxoglutarate may be useful for amino acid metabolism in *L. nagelii*.

Water kefir is a challenging environment for its inhabitants regarding low nutrient concentrations except for the excess sugar. Since lemon slices are added, it is not surprising that microorganisms in water kefir use citrate as a nutrient. Like *L. hordei* TMW 1.1822, also *L. nagelii* is capable of directed citrate import using malate permease. Once inside the cell, citrate is converted by citrate lyase segregating one molecule of acetate. The resulting oxaloacetate may then be decarboxylated via oxaloacetate decarboxylase yielding pyruvate or is further used for amino acid biosynthesis. Unlike in *L. hordei*, those enzymes were not DE in *L. nagelii* as a result of co-cultivation with *S. cerevisiae*. As *L. hordei* appears to be positively influenced in its metabolism of citrate as an additional carbon source, this may help to explain, why *L. hordei* is more abundant in the water kefir consortium than *L. nagelii* (Gulitz et al., 2011).

#### **3.4. Amino acids biosynthesis, metabolism and transport**

Like in *L. hordei* TMW 1.1822, the *in silico* analysis of the genome and proteome of *L. nagelii* TMW 1.1827 did not reveal any known homologs of a cell wall proteinase (Prt). Like *L. hordei*, also *L. nagelii* encodes the complete oligopeptide transport system OppABCDF (Tynkkynen et al., 1993; Detmers et al., 1998). Except from OppB, all genes of both annotated OppABCDF clusters were found to be present in the proteome of *L. nagelii*. Despite lacking an expressed OppB, the growth of *L. nagelii* was not impaired. This phenomenon was already described for other bacteria (Nepomuceno et al., 2007) indicating, that the function of OppB may be compensable by other trans-membrane

proteins. In the presence of the yeast, the remaining proteins were widely un-regulated with the exception of OppF, which was significantly down-regulated in one cluster. Since OppF is responsible for coupling the energy of ATP hydrolysis with the import of oligopeptides, *L. nagelii* may reduce energy consumption caused by oligopeptide uptake. In contrast, *L. hordei* upregulated its OppABCDF system and a set of peptidases, suggesting that *L. hordei* benefits from peptides provided by the yeast (Xu et al., 2019b). Since water kefir provides very limited resources of proteins and free amino acids, mainly originating from dried fruits and the yeast, these findings may also explain the fact, that the growth of *L. hordei* is stimulated in co-culture.

Nonetheless, from genomic annotation, *L. nagelii* encodes several amino acid permeases and transporters. In the presence of *S. cerevisiae*, two of those permeases were significantly up-regulated, suggesting that the yeast induces amino acid uptake in *L. nagelii*. However, it was not possible to specify from sequence comparison, which amino acids were ingested by *L. nagelii*. Still, this may be solved by a closer look at amino acid synthesis pathways and auxotrophies. The genomic analysis of *L. nagelii* TMW 1.1827 revealed the prototrophy for 13 amino acids and auxotrophy for 7 amino acids (Table 2). This result also applied to *L. hordei*, except for 3-deoxy-7-phosphoheptulonate synthase, which is additionally missing in *L. hordei*. Therefore, only *L. nagelii* is capable of producing tyrosine. According to the quantitative proteomic analysis, 9 enzymes of *L. nagelii* involved in histidine, methionine, glutamate and arginine biosynthesis pathways were all significantly up-regulated in the presence of *S. cerevisiae* (shown in Fig. 8 and Table 3). Except for acetylglutamate kinase, those up-regulated enzymes of *L. nagelii* were also among 16 over-expressed enzymes of *L. hordei* (Xu et al., 2019b). Since those

biosynthesis pathways can also be used for amino acid catabolism, water kefir microorganisms may profit from amino acids secreted by the yeast, creating a symbiotic consortium. However, from *in silico* analysis, the direction of a respective metabolic pathway remains speculative. Still, together with physiological data on amino acid consumption and secretion of *L. nagelii* and *S. cerevisiae*, this can be solved for at least some of the predicted cases.

As shown most prominently in Fig. 9, *S. cerevisiae* secreted glutamine in high amounts, whereas *L. nagelii* consumed the amino acid at high levels via an up-regulated amino acid permease involved in glutamine uptake. This suggests, that *L. nagelii*, even though it is capable of producing glutamine by itself, profits from the glutamine provided by the yeast via the up-regulated glutamate synthase, as it was also described for *L. hordei* (Xu et al., 2019b). Since glutamine plays an important role in anaplerotic sequences of transamination reactions in the biosynthesis of other amino acids, and also as a nitrogen carrier for the production of amino sugars and nucleotides, the uptake of this amino acid may be crucial to persist in the water kefir environment. In contrast to *L. hordei*, *L. nagelii* was predicted to produce glutamate by itself via the up-regulated glutamate synthase using glutamine and 2-oxoglutarate, which probably results from the incomplete TCA cycle. This was consistent with an un-regulated glutamine synthetase in the presence of *S. cerevisiae*, while this enzyme was significantly up-regulated in *L. hordei*. As already described for *Lactobacillus crispatus* ST1, this enzyme might exhibit additional functions, if displayed on the bacterial surface, which enable physical coherence of the water kefir consortium under stressful conditions (Kainulainen et al., 2012). As a result, the yeast aggregation promotion of *L. hordei* by its functional dextran



(Xu et al., 2018) may be even enhanced by over expression of this enzyme. Furthermore, among all amino acids, the production of glutamate is of primary importance in the assimilation of nitrogen, representing a donor for amino groups in the synthesis of other amino acids (Bernard and Habash, 2009; Dincturk et al., 2011).

Other amino acids were not produced, but partly consumed by the yeast after 24 h of fermentation in CDM. Therefore, it was not possible to determine real-time metabolic exchange (release/uptake) between *L. nagelii* and *S. cerevisiae* based on physiological data. Still, the label-free quantitative proteomic analysis enabled the investigation of the dynamic metabolic exchanges between microbial communities in water kefir. The DE enzymes involved in amino acid biosynthesis or catabolism predict that *S. cerevisiae* releases glutamine, histidine, methionine and arginine, which are subsequently used by *L. nagelii* to ensure its survival in the water kefir consortium.

### **3.5. Acid tolerance by ADI pathway**

Functionally, the ADI pathway enables enhanced acid tolerance and energy provision in a variety of LAB genera such as *Lactobacillus*, *Lactococcus*, *Leuconostoc* and *Weissella* (Tonon and Lonvaud-Funel, 2002; Fernández and Zúñiga, 2006; Rimaux et al., 2011). The system involves the three enzymes arginine deiminase (ADI), ornithine transcarbamoylase (OTC), carbamate kinase (CK) and a transmembrane arginine/ornithine antiporter, which exchanges extracellular arginine against intracellular ornithine. While ADI and OTC were present in both, the genome and proteome of *L. nagelii* TMW 1.1827, CK and the arginine/ornithine antiporter were only detectable in the genome. Since, *L. hordei* TMW 1.1822 lacks CK in its putative functional genome,

both microorganisms are not able to convert carbamoyl-P to generate additional ATP in co-culture (Xu et al., 2019a). In the energy rich environment of water kefir, this does not appear to be a disadvantage. Therefore, the fate of carbamoyl-P remains unclear. However, only OTC was significantly up-regulated in *L. nagelii* in co-culture with *S. cerevisiae*. This reaction may occur in both directions yielding citrulline or ornithine and carbamoyl-phosphate. In contrast, all present enzymes of *L. hordei* were up-regulated in co-culture with the yeast. Although the fate of carbamoyl-phosphate and other incidental compounds remains unclear, *L. hordei* likely produces ammonia upon arginine hydrolysis to protect itself from pH stress by alkalization of its cytoplasm and proximal environment. Consequently, it should reduce the acid stress for the yeast. As it was shown for *L. hordei*, also *L. nagelii* did not encode any complete alternative acid tolerance systems, e.g. the agmatine deiminase (AGDI) system or the glutamate decarboxylase (GAD) system. Except for neutralization upon ammonia formation via the ADI system, acidification appears limited by the switch from lactic and acetic acid production to ethanol formation, when *L. nagelii* and *S. cerevisiae* were co-cultivated.

### **3.6. Fatty acid biosynthesis and riboflavin metabolism**

Another limit in the water kefir environment is the limited availability of fatty acids. As discussed previously, *L. hordei* lacks *fabB* and may therefore be unable to synthesize any unsaturated fatty acids by itself (Xu et al., 2019b). Also *L. nagelii* TMW 1.1827 appears to be deficient in *fabB* and, additionally, in *fabA*. As demonstrated by Wang and Cronan (Wang and Cronan, 2004), FabF can functionally replace FabB, while FabZ adopts the function of FabA. Due to low sequence homologies, those enzymatic bi-functionalities are not predictable by genome analysis. Since both microorganisms grew to high cell

densities in water kefir medium without any external fatty acids, those findings might also indicate the existence of other functional homologs for FabB and FabA in *L. hordei* and *L. nagelii*. Co-cultivation with *S. cerevisiae* does not alter the expression of any proteins involved in the fatty acid metabolism in both LAB (Table S4). This indicates, that the beneficial effects of *S. cerevisiae* do not reside in a bilateral supply with unsaturated fatty acids.

Moreover, there was a group of enzymes of *L. nagelii*, which showed decreased expression in response to the co-cultivation with *S. cerevisiae*, which are involved in the biosynthesis of riboflavin (as shown in Fig. S5). Riboflavin synthase (EC 2.5.1.9), 6,7-dimethyl-8-ribityllumazine synthase (EC 2.5.1.78), 5-amino-6-(5-phosphoribosylamin) uracil reductase (EC 1.1.1.193), GTP cyclohydrolase II (EC 3.5.4.25) and 3,4-dihydroxy-2-butanone 4-phosphate synthase (EC 4.1.99.12) were down-regulated in a range from -3.2 to -4.0 log<sub>2</sub> fold. Those enzymes connect the purine metabolism and pentose phosphate pathway to synthesize riboflavin. This may be an evidence for the cross-feeding of riboflavin from *S. cerevisiae* to *L. nagelii*, supporting its growth and leading to a stable water kefir consortium.

## **Conclusions**

The label-free quantitative approach represents a powerful tool for the identification and quantification of proteins to study the bacteria-yeast interaction of microorganisms involved in food fermentation processes (Behr et al., 2007; Siragusa et al., 2014; Maeda et al., 2015). The predicted functional genome and the differentially expressed proteins in the presence of *S. cerevisiae* TMW 3.221 depicted the adaption of *L. nagelii* TMW

1.1827 to the water kefir consortium and environment, although protein regulations were less distinct than in *L. hordei* TMW 1.1822 (Xu et al., 2019). Both microorganisms are highly efficient in degrading sucrose by an extracellular glucansucrase and subsequent fructose uptake, which may then enter EMP, PKP or mannitol metabolism. As already described for *L. hordei*, also *L. nagelii* appears to favor PKP over EMP, indicating a metabolic switch induced by an altered redox potential in the presence of *S. cerevisiae*. While *L. nagelii* remained widely un-affected in its citrate metabolism, the yeast stimulated *L. hordei* to use citrate as additional carbon source and therefore, promoting its growth.

Both LAB profit from glutamine secreted by the yeast, whereas *L. hordei* also takes advantage of the provided glutamate. While *L. hordei* up-regulated all of its enzymes involved in the reduction of acid stress via ADI pathway, *L. nagelii* only altered the expression of OTC. It was obvious, that both microorganisms reduced external acid stress by switching from lactate and acetate production to butanediol formation in the case of *L. hordei* and ethanol production in the case of *L. nagelii*.

At first glance, the fatty acid metabolism of both microorganisms appears to be impaired by the lack of one or more genes coding for key fatty acid biosynthesis enzymes. As it was already reported for other bacteria (Wang and Cronan, 2004), it is likely, that the functional role of those enzymes may be undertaken by other enzymes of the fatty acid biosynthesis gene cluster. This would explain, why both, *L. hordei* and *L. nagelii*, grew to high cell densities while facing an environment insufficient in unsaturated fatty acids. While *S. cerevisiae* TMW 3.221 modulated the protein expression of *L. hordei* TMW

1.1822 mainly in its carbohydrate metabolism, *L. nagelii* TMW 1.1827 seems to profit from secreted riboflavin. With respect to the establishment of a consortium maintaining physical proximity of lactobacilli and yeasts *L. hordei* appears to have a more prominent role as compared to *L. nagelii* as a result of its unique dextran causing yeast aggregation and proteins involved in adhesion functions

### **Acknowledgement**

Part of work was supported by the China Scholarship Council in grant no.201306820010, and the German Ministry of Economics and Technology (via AiF) and the WiFö (Wissenschaftsförderung der Deutschen Brauwirtschaft e.V., Berlin) in project AiF 19180 N.

### **References**

- Alikhan, N.F., Petty, N.K., Zakour, N.L.B., and Beatson, S.A. (2011). BLAST ring image generator (BRIG): simple prokaryote genome comparisons. *BMC Genomics* 12, 402. doi:10.1186/1471-2164-12-402.
- Aziz, R.K., Bartels, D., Best, A.A., Dejongh, M., Disz, T., Edwards, R.A., Formsma, K., Gerdes, S., Glass, E.M., and Kubal, M. (2008). The RAST server: rapid annotations using subsystems technology. *BMC Genomics* 9, 75. doi:10.1186/1471-2164-9-75.
- Behr, J., Geissler, A.J., Schmid, J., Zehe, A., and Vogel, R.F. (2016). The identification of novel diagnostic marker genes for the detection of beer spoiling *Pediococcus damnosus* strains using the BIAst diagnostic gene findEr. *PloS One* 11, e0152747. doi:10.1371/journal.pone.0152747.

- Behr, J., Israel, L., Ganzle, M.G., and Vogel, R.F. (2007). Proteomic approach for characterization of hop-inducible proteins in *Lactobacillus brevis*. *Appl Environ Microbiol* 73, 3300-3306. doi:10.1128/AEM.00124-07.
- Bernard, S.M., and Habash, D.Z. (2009). The importance of cytosolic glutamine synthetase in nitrogen assimilation and recycling. *New Phytologist* 182, 608-620. doi:10.1111/j.1469-8137.2009.02823.x
- Carver, T., Thomson, N., Bleasby, A., Berriman, M., and Parkhill, J. (2008). DNAPlotter: circular and linear interactive genome visualization. *Bioinformatics* 25, 119-120. doi:10.1093/bioinformatics/btn578.
- Cox, J., Neuhauser, N., Michalski, A., Scheltema, R.A., Olsen, J.V., and Mann, M. (2011). Andromeda: a peptide search engine integrated into the MaxQuant environment. *J Proteome Res* 10, 1794-1805. doi:10.1021/pr101065j.
- Detmers, F.J.M., Kunji, E.R.S., Lanfermeijer, F.C., Poolman, B., and Konings, W.N. (1998). Kinetics and specificity of peptide uptake by the oligopeptide transport system of *Lactococcus lactis*. *Biochemistry* 37, 16671-16679. doi:10.1021/bi981712t.
- Dincturk, H.B., Cunin, R., and Akce, H. (2011). Expression and functional analysis of glutamate synthase small subunit-like proteins from archaeon *Pyrococcus horikoshii*. *Microbiol Res* 166, 294-303. doi:10.1016/j.micres.2010.03.006.
- Fels, L., Jakob, F., Vogel, R.F., and Wefers, D. (2018). Structural characterization of the exopolysaccharides from water kefir. *Carbohydr Polym* 189, 296-303. doi:10.1016/j.carbpol.2018.02.037.
- Fernández, M., and Zúñiga, M. (2006). Amino acid catabolic pathways of lactic acid bacteria. *Crit Rev Microbiol* 32, 155-183. doi:10.1080/10408410600880643.

- Gardy, J.L., Laird, M.R., Chen, F., Rey, S., Walsh, C.J., Ester, M., and Brinkman, F.S.L. (2004). PSORTb v. 2.0: expanded prediction of bacterial protein subcellular localization and insights gained from comparative proteome analysis. *Bioinformatics* 21, 617-623. doi:10.1093/bioinformatics/bti057.
- Gulitz, A., Stadie, J., Wenning, M., Ehrmann, M.A., and Vogel, R.F. (2011). The microbial diversity of water kefir. *Int J Food Microbiol* 151, 284-288. doi:10.1016/j.ijfoodmicro.2011.09.016.
- Horisberger, M. (1969). Structure of the dextran of the tibi grain. *Carbohydr Res* 10, 379-385. doi:10.1016/S0008-6215(00)80897-6.
- Kainulainen, V., Loimaranta, V., Pekkala, A., Edelman, S., Antikainen, J., Kylväjä, R., Laaksonen, M., Laakkonen, L., Finne, J., and Korhonen, T.K. (2012). Glutamine synthetase and glucose-6-phosphate isomerase are adhesive moonlighting proteins of *Lactobacillus crispatus* released by cathelicidin LL-37. *J Bacteriol*, 06704-06711. doi:10.1128/JB.06704-11.
- Kleerebezem, M., Boekhorst, J., Van Kranenburg, R., Molenaar, D., Kuipers, O.P., Leer, R., Turchini, R., Peters, S.A., Sandbrink, H.M., and Fiers, M.W.E.J. (2003). Complete genome sequence of *Lactobacillus plantarum* WCFS1. *PNAS* 100, 1990-1995. doi:10.1073/pnas.0337704100.
- Kleerebezem, M., and Hugenholtz, J. (2003). Metabolic pathway engineering in lactic acid bacteria. *Curr Opin Biotechnol* 14, 232-237. doi:10.1016/S0958-1669(03)00033-8.
- Laureys, D., Aerts, M., Vandamme, P., and De Vuyst, L. (2018). Oxygen and diverse nutrients influence the water kefir fermentation process. *Food Microbiol* 73, 351-361. doi:10.1016/j.fm.2018.02.007.

- Laureys, D., and De Vuyst, L. (2014). Microbial species diversity, community dynamics, and metabolite kinetics of water kefir fermentation. *Appl Environ Microbiol*, 03978-03913. doi:10.1128/AEM.03978-13.
- Letort, C., Nardi, M., Garault, P., Monnet, V., and Juillard, V. (2002). Casein utilization by *Streptococcus thermophilus* results in a diauxic growth in milk. *Appl Environ Microbiol* 68, 3162-3165. doi:10.1128/AEM.68.6.3162-3165.2002.
- Maeda, K., Nagata, H., Ojima, M., and Amano, A. (2015). Proteomic and transcriptional analysis of interaction between oral microbiota *Porphyromonas gingivalis* and *Streptococcus oralis*. *J Proteome Res* 14, 82-94. doi:10.1021/pr500848e.
- Marsh, A.J., O'sullivan, O., Hill, C., Ross, R.P., and Cotter, P.D. (2013). Sequence-based analysis of the microbial composition of water kefir from multiple sources. *FEMS Microbiol Lett* 348, 79-85. doi:10.1111/1574-6968.12248.
- Martínez - Torres, A., Gutiérrez - Ambrocio, S., Heredia - Del - Orbe, P., Villa - Tanaca, L., and Hernández - Rodríguez, C. (2017). Inferring the role of microorganisms in water kefir fermentations. *Int J Food Sci Technol* 52, 559-571. doi:10.1111/ijfs.13312.
- Nepomuceno, R., Tavares, M., Lemos, J., Griswold, A., Ribeiro, J., Balan, A., Guimaraes, K., Cai, S., Burne, R., and Ferreira, L. (2007). The oligopeptide (*opp*) gene cluster of *Streptococcus mutans*: identification, prevalence, and characterization. *Oral Microbiol Immunol* 22, 277-284. doi:10.1111/j.1399-302X.2007.00368.x
- Neve, H., and Heller, K.J. (2002). The microflora of water kefir: a glance by scanning electron microscopy. *Kiel Milchwirtsch Forschungsber* 54, 337-349.
- Overbeek, R., Olson, R., Pusch, G.D., Olsen, G.J., Davis, J.J., Disz, T., Edwards, R.A., Gerdes, S., Parrello, B., and Shukla, M. (2013). The SEED and the rapid annotation



of microbial genomes using subsystems technology (RAST). *Nucleic Acids Res* 42, D206-D214. doi:10.1093/nar/gkt1226.

- Pidoux, M. (1989). The microbial flora of sugary kefir grain (the gingerbeer plant): biosynthesis of the grain from *Lactobacillus hilgardii* producing a polysaccharide gel. *MIRCEN Journal of Applied Microbiology and Biotechnology* 5, 223-238. doi:10.1007/BF01741847.
- Pidoux, M., Brillouet, J.M., and Quemener, B. (1988). Characterization of the polysaccharides from a *Lactobacillus brevis* and from sugary kefir grains. *Biotechnol Lett* 10, 415-420. doi:10.1007/BF01087442.
- Pidoux, M., De Ruiter, G.A., Brooker, B.E., Colquhoun, I.J., and Morris, V.J. (1990). Microscopic and chemical studies of a gelling polysaccharide from *Lactobacillus hilgardii*. *Carbohydr Polym* 13, 351-362. doi:10.1016/0144-8617(90)90035-Q.
- Rimaux, T., Vrancken, G., Pothakos, V., Maes, D., De Vuyst, L., and Leroy, F. (2011). The kinetics of the arginine deiminase pathway in the meat starter culture *Lactobacillus sakei* CTC 494 are pH-dependent. *Food Microbiol* 28, 597-604. doi:10.1016/j.fm.2010.11.016.
- Siragusa, S., De Angelis, M., Calasso, M., Campanella, D., Minervini, F., Di Cagno, R., and Gobbetti, M. (2014). Fermentation and proteome profiles of *Lactobacillus plantarum* strains during growth under food-like conditions. *J Proteomics* 96, 366-380. doi:10.1016/j.jprot.2013.11.003.
- Smeianov, V.V., Wechter, P., Broadbent, J.R., Hughes, J.E., Rodríguez, B.T., Christensen, T.K., Ardö, Y., and Steele, J.L. (2007). Comparative high-density microarray analysis of gene expression during growth of *Lactobacillus helveticus* in

- milk versus rich culture medium. *Appl Environ Microbiol* 73, 2661-2672.  
doi:10.1128/AEM.00005-07.
- Stadie, J., Gulitz, A., Ehrmann, M.A., and Vogel, R.F. (2013). Metabolic activity and symbiotic interactions of lactic acid bacteria and yeasts isolated from water kefir. *Food Microbiol* 35, 92-98. doi:10.1016/j.fm.2013.03.009.
- Stolz, P., Vogel, R.F., and Hammes, W.P. (1995). Utilization of electron acceptors by lactobacilli isolated from sourdough. *Z Lebensm Unters Forsch* 201, 402-410.  
doi:10.1007/BF01193208.
- Sun, Z., Harris, H.M.B., Mccann, A., Guo, C., Argimón, S., Zhang, W., Yang, X., Jeffery, I.B., Cooney, J.C., and Kagawa, T.F. (2015). Expanding the biotechnology potential of lactobacilli through comparative genomics of 213 strains and associated genera. *Nat Commun* 6, 8322. doi:10.1038/ncomms9322.
- Tonon, T., and Lonvaud-Funel, A. (2002). Arginine metabolism by wine *Lactobacilli* isolated from wine. *Food Microbiol* 19, 451-461. doi:10.1006/fmic.2002.0502.
- Tyanova, S., Temu, T., Sinitcyn, P., Carlson, A., Hein, M.Y., Geiger, T., Mann, M., and Cox, J. (2016). The Perseus computational platform for comprehensive analysis of (prote) omics data. *Nat Methods* 13, 731. doi:10.1038/NMETH.3901.
- Tynkkynen, S., Buist, G., Kunji, E., Kok, J., Poolman, B., Venema, G., and Haandrikman, A. (1993). Genetic and biochemical characterization of the oligopeptide transport system of *Lactococcus lactis*. *J Bacteriol* 175, 7523-7532.  
doi:10.1128/jb.175.23.7523-7532.1993.
- Waldherr, F.W., Doll, V.M., Meißner, D., and Vogel, R.F. (2010). Identification and characterization of a glucan-producing enzyme from *Lactobacillus hilgardii* TMW

- 1.828 involved in granule formation of water kefir. *Food Microbiol* 27, 672-678.  
doi:10.1016/j.fm.2010.03.013.
- Wang, H., and Cronan, J.E. (2004). Functional replacement of the FabA and FabB proteins of *Escherichia coli* fatty acid synthesis by *Enterococcus faecalis* FabZ and FabF homologues. *J Biol Chem* 279, 34489-34495. doi:10.1074/jbc.
- Ward, H.M. (1891). The 'ginger-beer plant,' and the organisms composing it: a contribution to the study of fermentation-yeasts and bacteria. *Proceedings of the Royal Society of London* 50, 261-265.
- Xu, D., Bechtner, J., Behr, J., Eisenbach, L., Geißler, A.J., and Vogel, R.F. (2019a). Lifestyle of *Lactobacillus hordei* isolated from water kefir based on genomic, proteomic and physiological characterization. *Int J Food Microbiol* 290, 141-149. doi:10.1016/j.ijfoodmicro.2018.10.004.
- Xu, D., Behr, J., Geißler, A.J., Bechtner, J., Ludwig, C., and Vogel, R.F. (2019b). Label-free quantitative proteomic analysis reveals the lifestyle of *Lactobacillus hordei* in the presence of *Saccharomyces cerevisiae*. *Int J Food Microbiol* Resubmitted.
- Xu, D., Fels, L., Wefers, D., Behr, J., Jakob, F., and Vogel, R.F. (2018). *Lactobacillus hordei* dextrans induce *Saccharomyces cerevisiae* aggregation and network formation on hydrophilic surfaces. *Int J Biol Macromol* 115, 236-242. doi:10.1016/j.ijbiomac.2018.04.068.
- Yamada, T., Letunic, I., Okuda, S., Kanehisa, M., and Bork, P. (2011). iPath2. 0: interactive pathway explorer. *Nucleic Acids Res* 39, W412-W415. doi:10.1093/nar/gkr313.
- Yu, N.Y., Wagner, J.R., Laird, M.R., Melli, G., Rey, S., Lo, R., Dao, P., Sahinalp, S.C., Ester, M., and Foster, L.J. (2010). PSORTb 3.0: improved protein subcellular

localization prediction with refined localization subcategories and predictive capabilities for all prokaryotes. *Bioinformatics* 26, 1608-1615.

doi:10.1093/bioinformatics/btq249.

Table 1. Comparative genomic features of *L. nagelii* TMW 1.1827 with *L. hordei* TMW 1.1822

	Genome length(Mbp)	GC content	Number of features	Total number of coding sequences plus plasmids	Total feature length(Mbp)	Coding density(%)
<i>L. nagelii</i> TMW 1.1827	2.41	36.68	2232	2461	2.10	87.18
<i>L. hordei</i> TMW 1.1822	2.42	35	2268	2391	2.09	86.27

Table 2. List of the auxotrophies of *L. nagelii* TMW 1.1827

Name of amino acid	Biosynthesis based on genome	Absent enzyme of biosynthesis of amino acid pathway	EC number
Alanine	P	None	
Arginine	P	None	
Asparagine	P	None	
Aspartic Acid	P	None	
Cysteine	P	None	
Glutamic Acid	P	None	
Glutamine	P	None	
Glycine	A	Phosphoserine phosphatase	EC 3.1.3.3
		Threonine aldolase	EC 4.1.2.48
Serine	A	Phosphoserine phosphatase	EC 3.1.3.3
Histidine	P	None	
Leucine	A	Ketol-acid reductoisomerase	EC 1.1.1.86
		Dihydroxy-acid dehydratase	EC 4.2.1.9
Isoleucine	A	Citramalate synthase	EC 2.3.1.182
		Ketol-acid reductoisomerase	EC 1.1.1.86
		Dihydroxy-acid dehydratase	EC 4.2.1.9
Valine	A	Ketol-acid reductoisomerase	EC 1.1.1.86
		Dihydroxy-acid dehydratase	EC 4.2.1.9
Lysine	P	None	
Methionine	P	None	
Proline	P	None	
Phenylalanine	A	Prephenate dehydratase	EC 4.2.1.51
		Aromatic-amino-acid transaminase	EC 2.6.1.57
Tryptophan	A	Anthranilate phosphoribosyltransferase	EC 2.4.2.18
		Anthranilate synthase	EC 4.1.3.27
		Indole-3-glycerol phosphate synthase	EC 4.1.1.48
		Phosphoribosylanthranilate isomerase	EC 5.3.1.24
Tyrosine	P	None	
Threonine	P	None	

Note: P represented prototrophic for amino acids, while A represented auxotrophic for amino acids.

Table 3. Significantly differentially expressed proteins in *L. nagelii* TMW 1.1827 in response to *S. cerevisiae* TMW 3.221 involved in amino acids biosynthesis.

Number	Enzyme	EC number	Log <sub>2</sub> fold change (co-cultivation vs single culture)	-Log (P-value)	SEED subcategory
Up-regulated					
1	Imidazoleglycerol-phosphate dehydratase	EC 4.2.1.19	4.6	3.5	
2	Histidinol-phosphate aminotransferase	EC 2.6.1.9	4.4	3.8	Histidine biosynthesis
3	Histidinol dehydrogenase	EC 1.1.1.23	5.3	4.5	
4	5-methyltetrahydropteroyltriglutamate -homocysteine methyltransferase	EC 2.1.1.14	3.8	3.7	Methionine biosynthesis
5	Glutamate synthase	EC 1.4.1.13	4.1	2.5	Glutamate, arginine biosynthesis
6	Acetylglutamate kinase	EC 2.7.2.8	3.0	1.7	
7	Acetylnornithine aminotransferase	EC 2.6.1.11	8.7	3.3	Arginine biosynthesis
8	Ornithine carbamoyltransferase	EC 2.1.3.3	7.5	2.9	
9	Argininosuccinate synthase	EC 6.3.4.5	3.3	3.6	

Table S1. Significantly differentially expressed proteins in *L. nagelii* TMW 1.1827 in response to co-cultivation with *S. cerevisiae* TMW 3.221 involved in carbohydrate metabolism (PKP, pentose phosphate pathway, pyruvate metabolism).

Number	Enzyme	EC number	Log <sub>2</sub> fold change (co-cultivation vs single culture)	-Log(P-value)
Up-regulated				
20	Alcohol dehydrogenase	EC 1.1.1.1	3.5	3.4
Down-regulated				
27	$\alpha$ -acetolactate decarboxylase	EC 4.1.1.5	-2.2	2.6



Table S2. List of annotated enzymes by NCBI and RAST involved in carbohydrate metabolism (glycolysis, pentose phosphate pathway, pyruvate metabolism and TCA cycle).

Number	Enzyme	EC number	Locus tag from NCBI	RAST-ID
1	Glucokinase	EC 2.7.1.2	BSQ50_07330	peg_1459
2	Glucose-6-phosphate isomerase	EC 5.3.1.9	BSQ50_08580	peg_1678
3	6-phosphofructokinase	EC 2.7.1.11	BSQ50_06330	peg_1260
4	Fructose-bisphosphate aldolase	EC 4.1.2.13	BSQ50_04840 BSQ50_07790	peg_956 peg_1552
5	Triose-phosphate isomerase	EC 5.3.1.1	BSQ50_02645	peg_510
6	Glyceraldehyde 3-phosphate dehydrogenase	EC 1.2.1.12	BSQ50_02635	peg_508
7	Phosphoglycerate kinase	EC 2.7.2.3	BSQ50_02640	peg_509
8	Phosphoglycerate mutase	EC 5.4.2.1	BSQ50_02110 BSQ50_09155	peg_403 peg_1797
9	Enolase	EC 4.2.1.11	BSQ50_02650 BSQ50_05885	peg_511 peg_1168
10	Pyruvate kinase	EC 2.7.1.40	BSQ50_06325	peg_1259
11	(L/D) Lactate dehydrogenase	EC 1.1.1.27/28	BSQ50_01780 BSQ50_01955 BSQ50_05430 BSQ50_06640 BSQ50_08630	peg_342 peg_379 peg_1074 peg_1321 peg_1688
12	Glucose-6-phosphate dehydrogenase	EC 1.1.1.49	BSQ50_02990	peg_579
13	6-phosphogluconolactonase	EC 3.1.1.31	BSQ50_02805	peg_542
14	Phosphogluconate dehydrogenase	EC 1.1.1.44	BSQ50_06855 BSQ50_10385	peg_1363 peg_2045
15	Ribulose-phosphate 3-epimerase	EC 5.1.3.1	BSQ50_04865 BSQ50_07245	peg_961 peg_1441
16	Phosphoketolase	EC 4.1.2.9	BSQ50_09315	peg_1830
17	Acetate kinase	EC 2.7.2.1	BSQ50_01685 BSQ50_04570 BSQ50_07705 BSQ50_08365 BSQ50_09355	peg_325 peg_901 peg_1535 peg_1633 peg_1838

18	Phosphate acetyltransferase	EC 2.3.1.8	BSQ50_02695	peg_520
19	Acetaldehyde dehydrogenase	EC 1.2.1.10	BSQ50_04565	peg_900
20	Alcohol dehydrogenase	EC 1.1.1.1	BSQ50_00575 BSQ50_04565 BSQ50_05330 BSQ50_09365 BSQ50_09675 BSQ50_09870	peg_116 peg_900 peg_1053 peg_1840 peg_1902 peg_1943
21	Citrate lyase	EC 4.1.3.6	BSQ50_03225 BSQ50_03230	peg_625 peg_626
22	Oxaloacetate decarboxylase	EC 4.1.1.3	BSQ50_03205	peg_621
23	Pyruvate oxidase	EC 1.2.3.3	BSQ50_00690 BSQ50_08185	peg_141 peg_1616
24	Pyruvate dehydrogenase	EC 1.2.4.1	BSQ50_00245 BSQ50_00250	peg_49 peg_50
25	Pyruvate formate lyase	EC 2.3.1.54	BSQ50_04390 BSQ50_09420	peg_863 peg_1851
26	Acetolactate synthase	EC 2.2.1.6	BSQ50_00550 BSQ50_01140	peg_112 peg_231
27	$\alpha$ -acetolactate decarboxylase	EC 4.1.1.5	BSQ50_10370	peg_2042
28	Acetoin reductase	EC 1.1.1.4	BSQ50_05200	peg_1026
29	Ribose-5-phosphate isomerase	EC 5.3.1.6	BSQ50_02120 BSQ50_04870 BSQ50_08850 BSQ50_09890	peg_405 peg_962 peg_1732 peg_1947
30	Transketolase	EC 2.2.1.1	BSQ50_03545	peg_688

---

Table S3. List of enzymes involved in fatty acid biosynthesis.

Number	Enzyme	EC number	Locus tag from NCBI	RAST-ID	Proteome
1	Acetyl-CoA carboxylase	EC 6.4.1.2	BSQ50_02960	peg_573	+
			BSQ50_02970	peg_575	+
			BSQ50_02975	peg_576	+
			BSQ50_02980	peg_577	+
2	Beta-hydroxyacyl-acyl-carrier-protein dehydratase (FabZ)	EC 4.2.1.59	BSQ50_02965	peg_574	+
3	3-oxoacyl-acyl-carrier-protein synthase II (FabF)	EC 2.3.1.179	BSQ50_02955	peg_572	-
4	Malonyl CoA-acyl carrier protein transacylase (FabD)	EC 2.3.1.39	BSQ50_02945	peg_570	+
5	3-oxoacyl-acyl-carrier protein reductase (FabG)	EC 1.1.1.100	BSQ50_00780	peg_159	+
			BSQ50_02855	peg_552	+
			BSQ50_02950	peg_571	+
6	3-oxoacyl-acyl-carrier-protein synthase III (FabH/FabY)	EC 2.3.1.180	BSQ50_02090	peg_399	+
			BSQ50_02935	peg_568	+
7	Enoyl-acyl-carrier-protein reductase (FabI/FabK/ FabV)	EC 1.3.1.9	BSQ50_02985	peg_578	+

Note: “+” presents that this enzyme annotated by genome is also identified in proteome, “-” presents that this enzyme annotated by genome is not identified in proteome.

## Figure Captions

Fig. 1. Whole genome comparison was visualized by BRIG (Alikhan et al., 2011). CDS of the pan genome was used as reference and the genomes of both microorganisms were aligned to this reference. As a result, the structures of the genomes and the pan genome did not reflect the physical structure of the chromosomes or plasmids. The core genome was approximately half of the pan genome and was detected from the beginning until about 1300 kbp. Strain specific genes were displayed in the range of approximately 1300 kbp until the end.

Fig. 2. Annotated SEED categories of proteins, divided in the core and accessory genomes of *L. hordei* TMW 1.1822 and *L. nagelii* TMW 1.1827, which was done by BADGE analysis. The proportion of proteins assigned to each SEED category with respect to the total number of proteins is shown in the bar chart.

Fig. 3. Cell counts of *L. nagelii* TMW 1.1827 in single culture (●) and co-cultivation with *S. cerevisiae* TMW 3.221 (▲).

Fig. 4. Subcellular localization of proteins (in silico, quantified by LC-MS/MS, unregulated, differentially expressed, up-regulated in co-cultivation, down-regulated in co-cultivation), which were predicted by PSORTb. The proportion of proteins assigned to each respective subcellular compartment and the group “unknown” with respect to the total number of proteins is shown by the bar chart. The table below shows the respective absolute numbers.

Fig. 5. SEED categories of proteins (in silico, quantified by LC-MS/MS, unregulated, differentially expressed, up-regulated in co-cultivation, down-regulated in co-cultivation) which were predicted by SEED. The proportion of proteins assigned to each respective category of metabolism and the group “other categories” which is the sum of several small categories with respect to the total number of proteins is shown by the bar chart. The ratio on the top of each column is the number of predicted SEED categories accounts for the number of all coding DNA sequence (CDS).

Fig. 6. Modified overview on the key reactions involved in sucrose metabolism (Xu et al., 2019a) of *L. nagelii* TMW 1.1827 in the presence of *S. cerevisiae* TMW 3.221: the enzyme colored in blue was annotated by genomics but not quantified by proteomics, the enzymes colored in orange were both annotated by genomics and quantified by proteomics, the enzymes colored in grey were neither annotated by genomics nor quantified by proteomics.

Fig. 7. Modified predicted outline of pyruvate metabolism (Xu et al., 2019a) of *L. nagelii* TMW 1.1827 in presence of *S. cerevisiae* TMW 3.221. The enzymes colored in red represented the up-regulated ones, while blue represented down-regulated proteins. Un-regulated proteins are indicated in green and proteins, neither annotated in the genome or proteome are colored in grey.

Fig. 8. Biosynthesis of amino acids of *L. nagelii* TMW 1.1827 (A) and *L. nagelii* TMW 1.1827 in presence of *S. cerevisiae* TMW 3.221 (B). In figure A, the red arrowed lines

show the presence of enzymes annotated from genome. In figure B, the red arrowed lines indicate up-regulated proteins.

Fig. 9. Consumption of amino acids of *L. nagelii* TMW 1.1827 and *S. cerevisiae* TMW 3.221 isolated from water kefir grown in CDM after 24 h. Black histogram represents CDM, slash histogram represents *L. nagelii*, grey histogram represents *S. cerevisiae*.

### Supplementary Figure Captions

Fig. S1. Genomic atlas of *L. nagelii* TMW 1.1827. Forward CDS (red), Reverse CDS (blue), Pseudogenes on both strands (black), tRNA and rRNA (dark green), % GC plot (yellow, high GC spike and green, low GC spike), GC skew  $[(G-C)/(G+C)]$  (grey).

Fig. S2. Cell counts of *S. cerevisiae* TMW 3.221 in single culture (●) and in co-cultivation with *L. nagelii* TMW 1.1827 (▲).

Fig. S3. Overview of enzymatic activity of *L. nagelii* TMW 1.1827 in the complete metabolic and other pathways in presence of *S. cerevisiae* TMW 3.221: the nodes colored in bold red represent up-regulated, in bold blue represent down-regulated enzymes or proteins according to proteomic data, while nodes colored in thin red represent all the rest enzymes or proteins according to genomic annotation data presented in iPath 3.0.

Fig. S4. Consumption and production of sugar (A) and organic acids (B) of *L. nagelii* TMW 1.1827 and *S. cerevisiae* TMW 3.221 grown in CDM after 24 h of fermentation. Black histogram represents CDM as negative control, slash histogram represents

detectable consumption of CDM after incubation with *L. nagelii*, and mosaic histogram represents detectable consumption of CDM after incubation with *S. cerevisiae*.

Fig. S5. Overview of riboflavin metabolism of *L. nagelii* TMW 1.1827 generated in KEGG mapper. The EC numbers colored in red show up-regulated enzymes of *L. nagelii* in the presence of *S. cerevisiae*.

Fig. 1

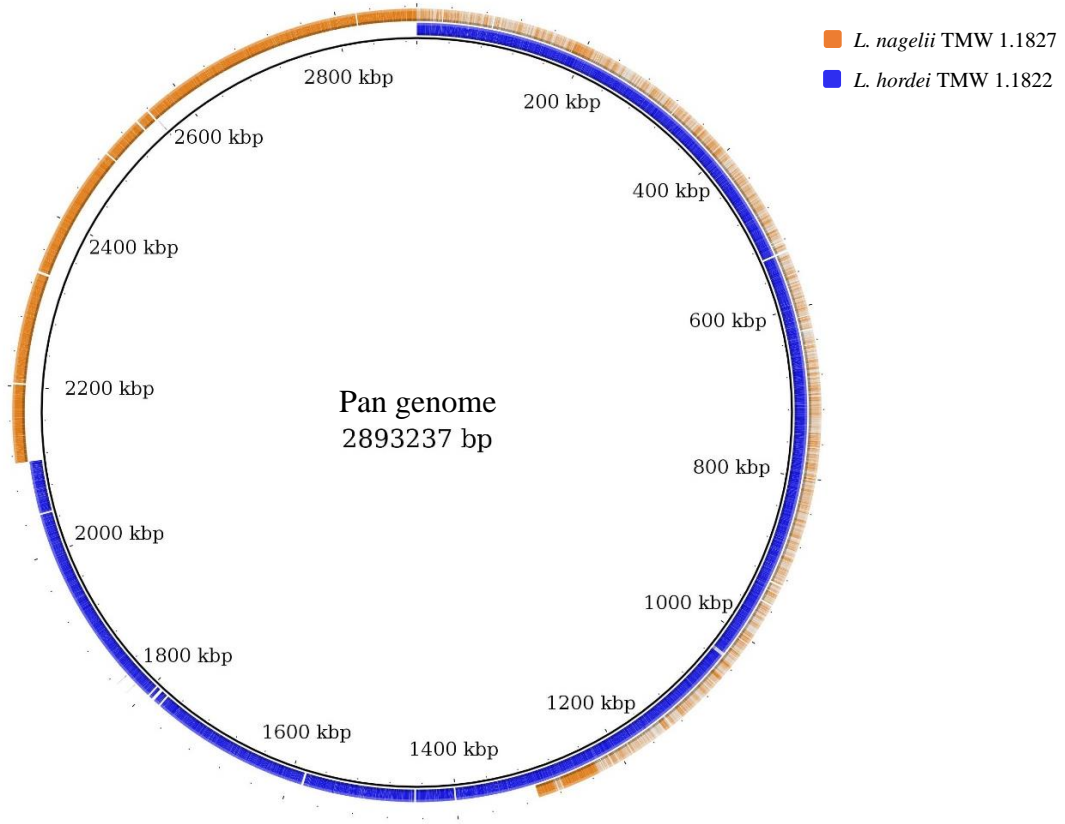




Fig. 2

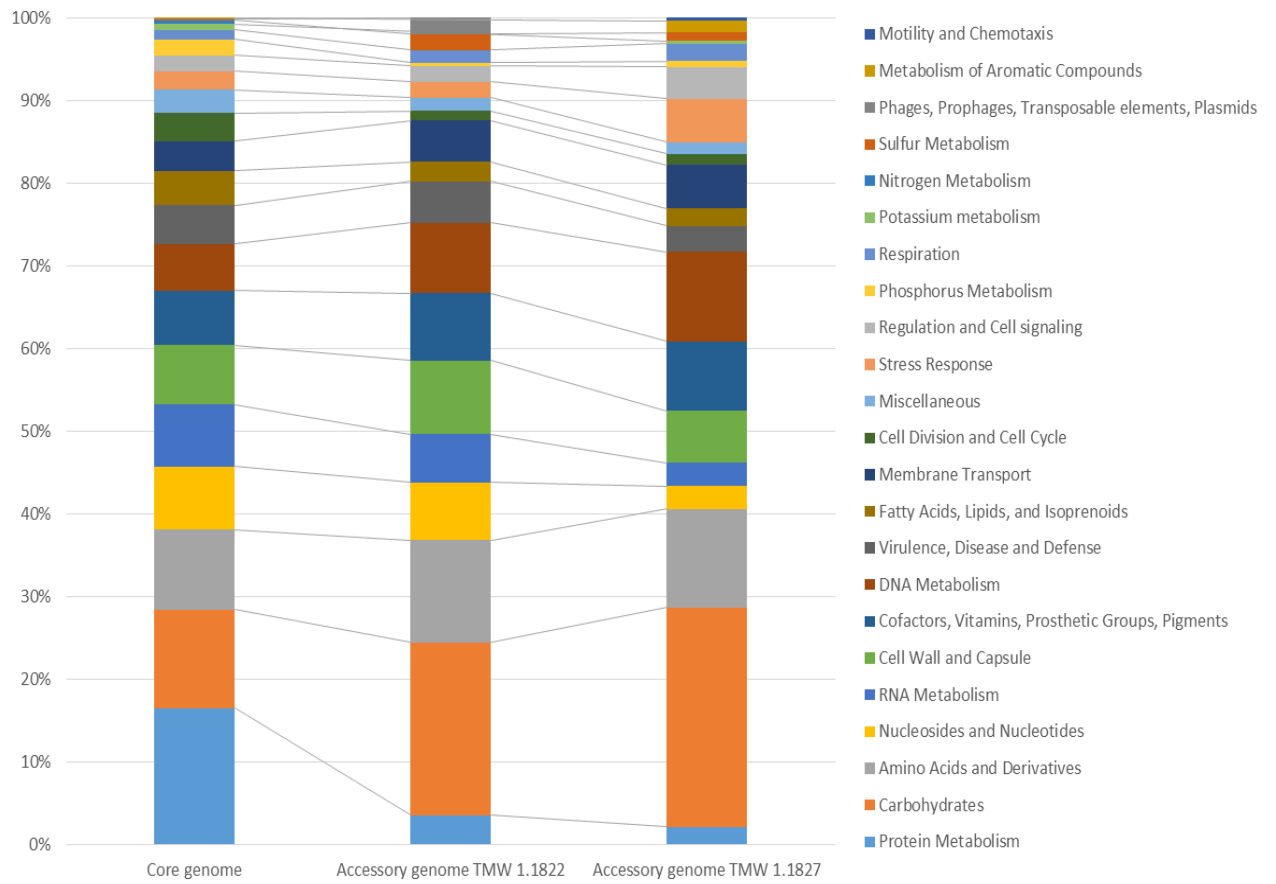


Fig. 3

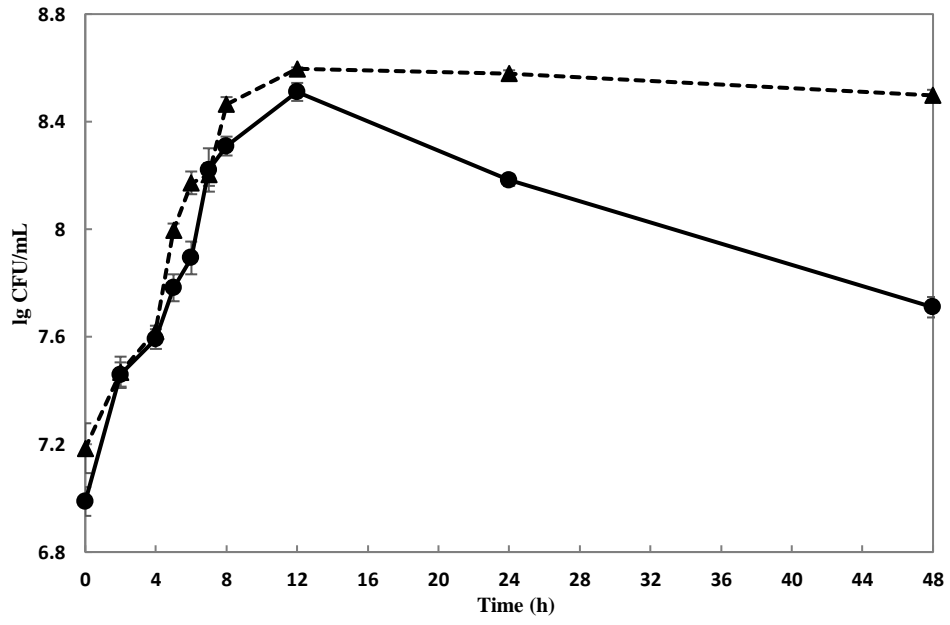


Fig. 4

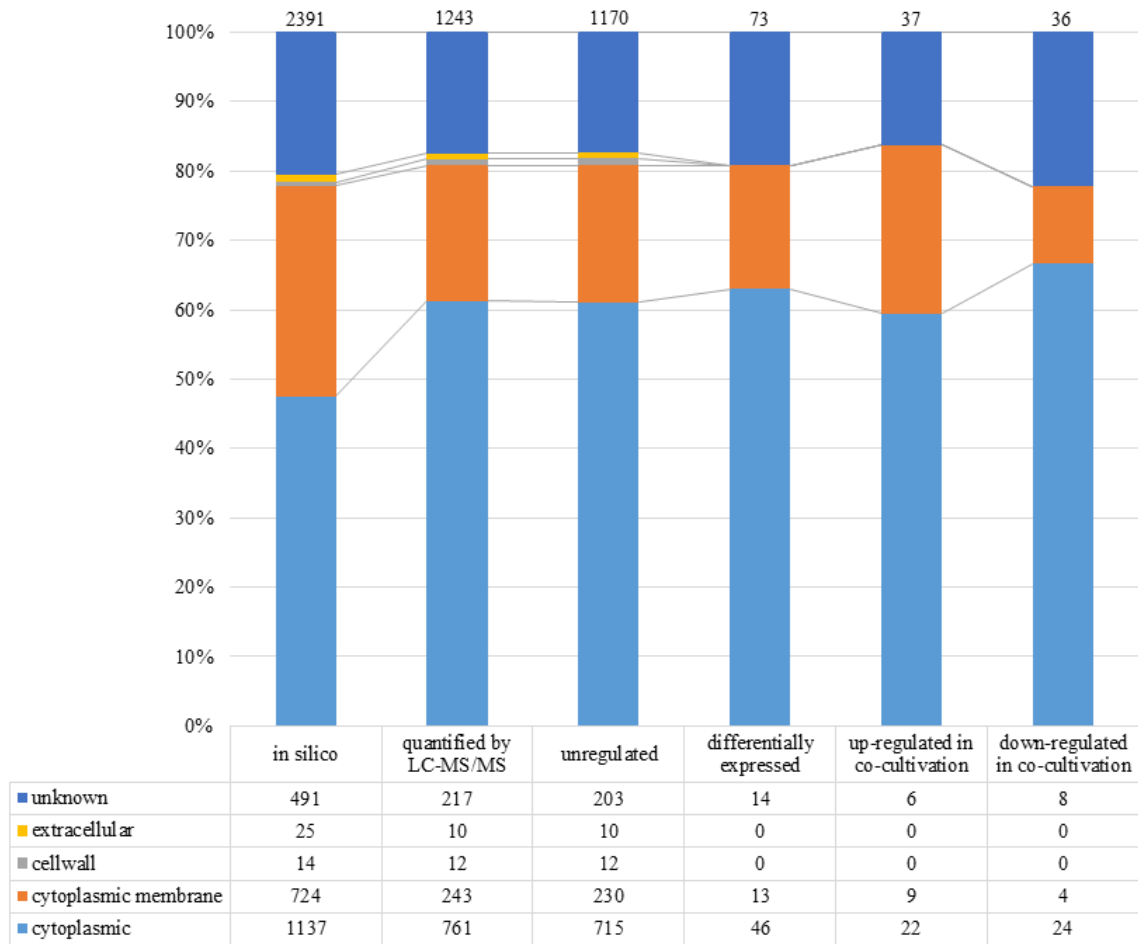


Fig. 5

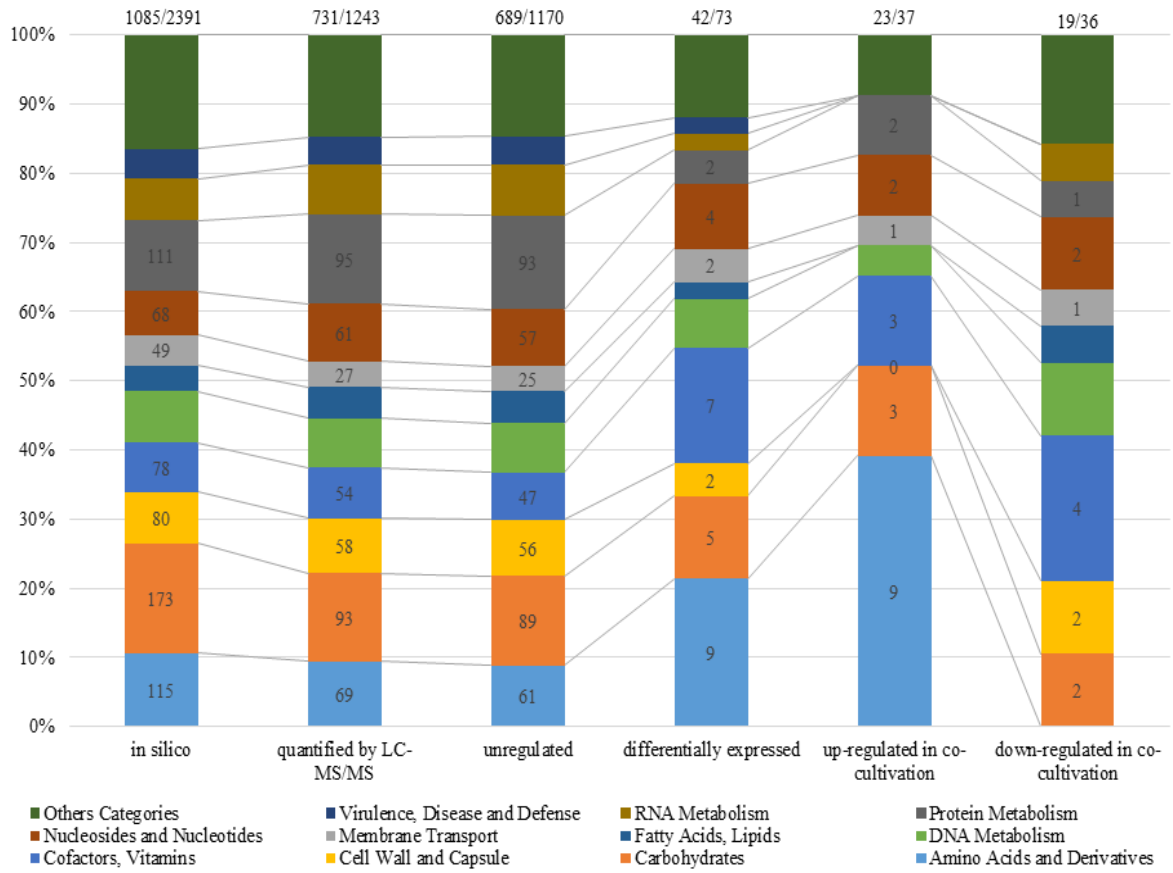


Fig. 6

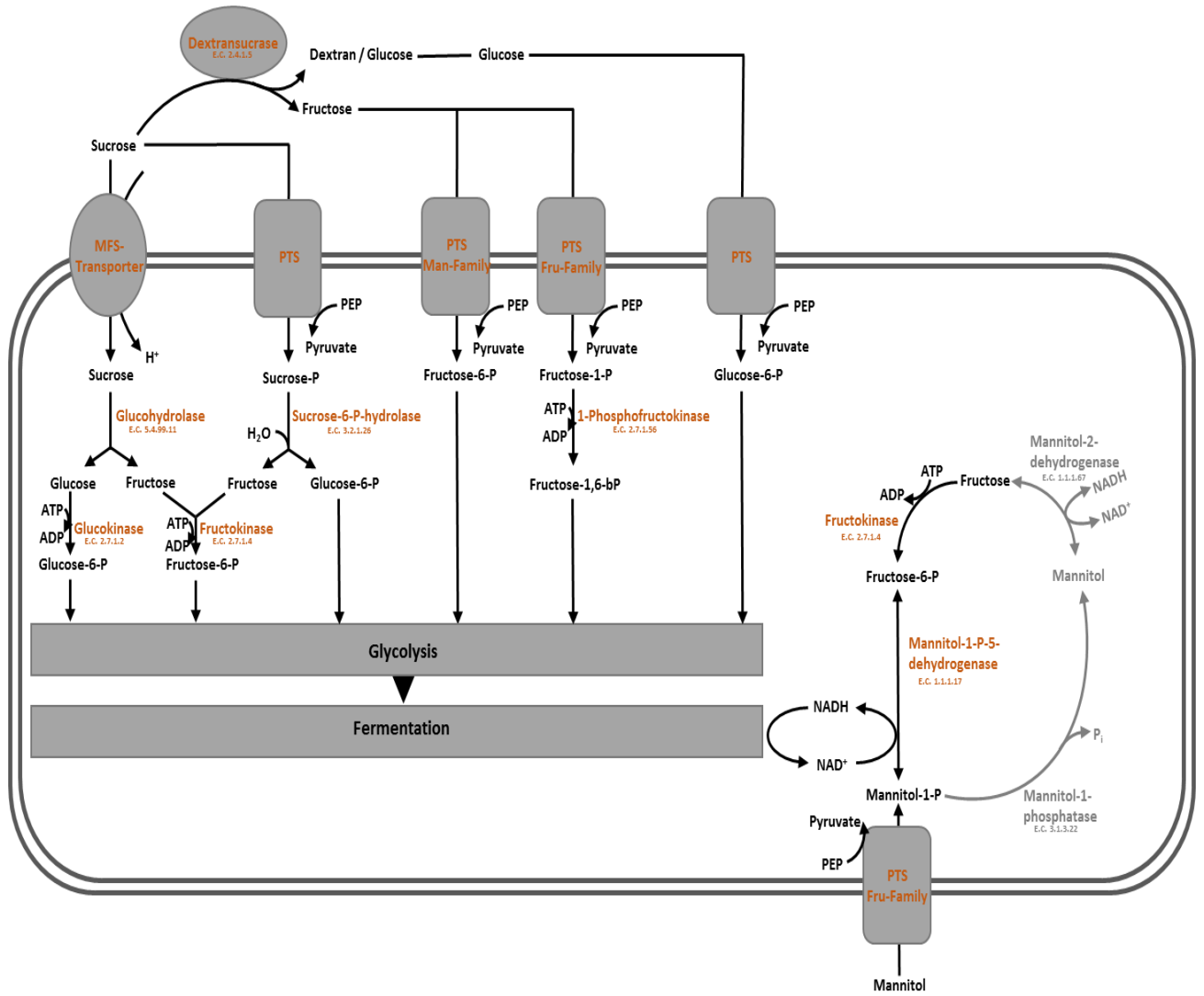
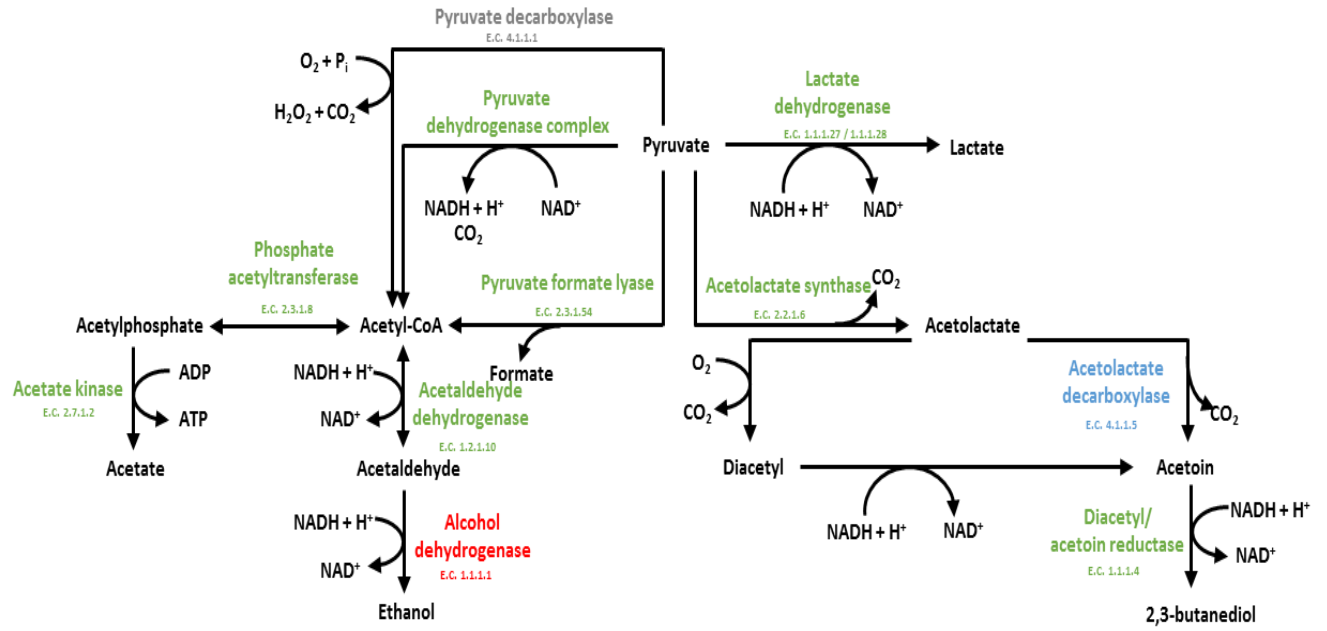
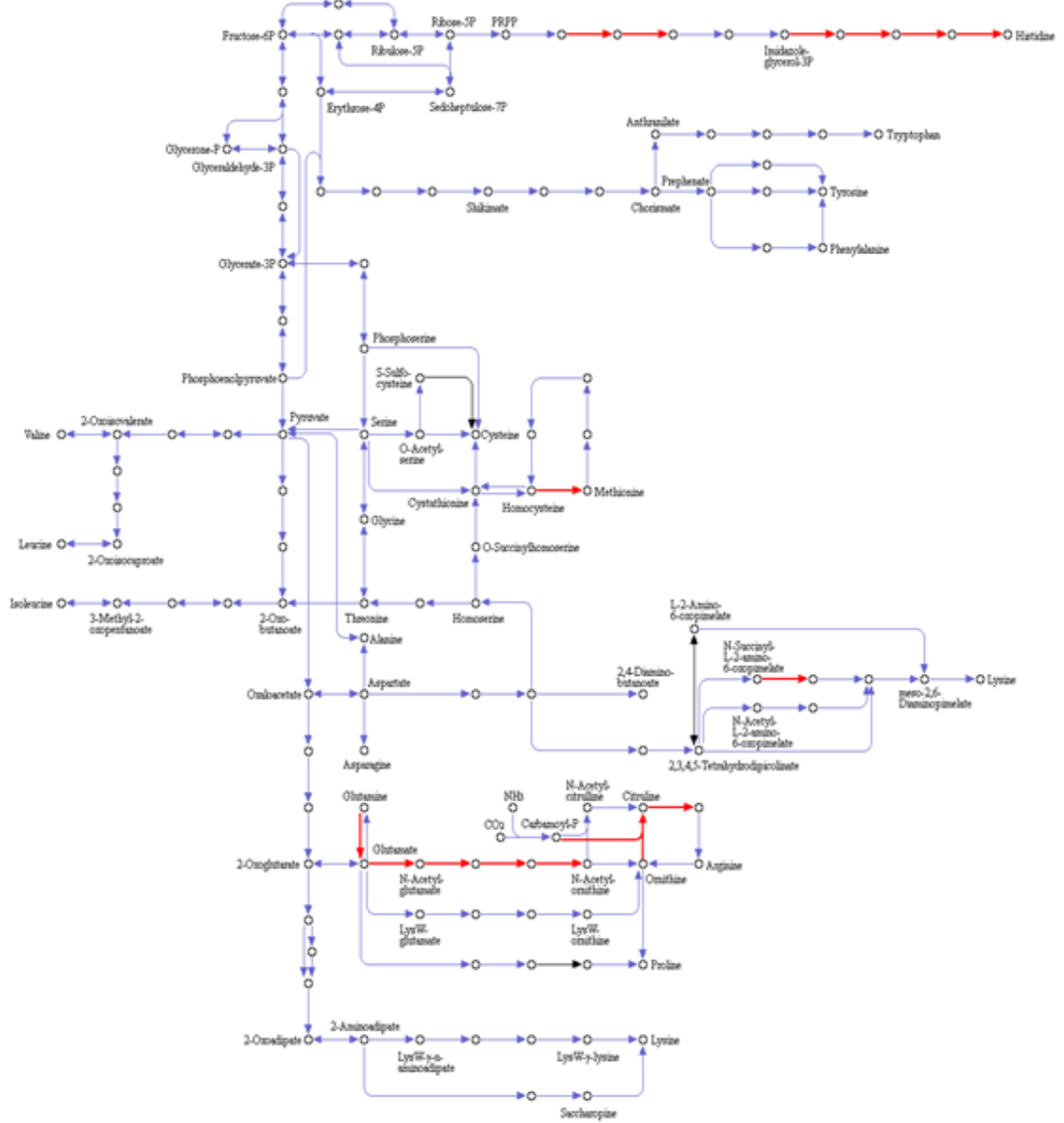


Fig. 7





BIOSYNTHESIS OF AMINO ACIDS



0120 3/18  
© Karelson Laboratories



Fig. 9

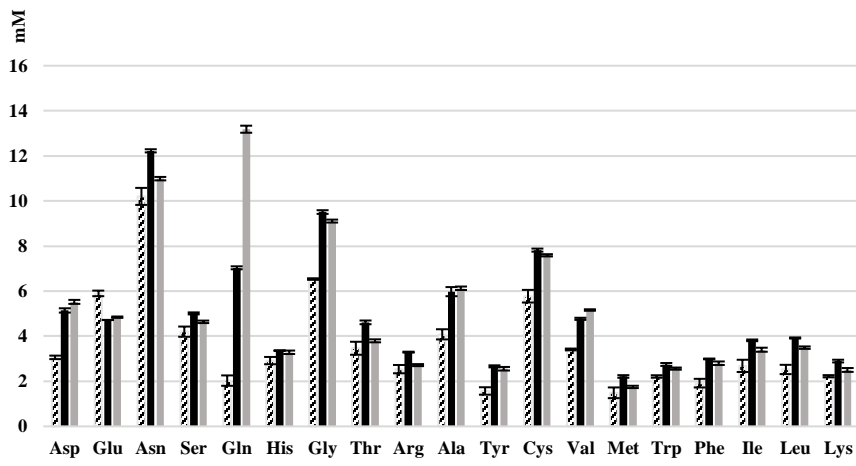


Fig. S1

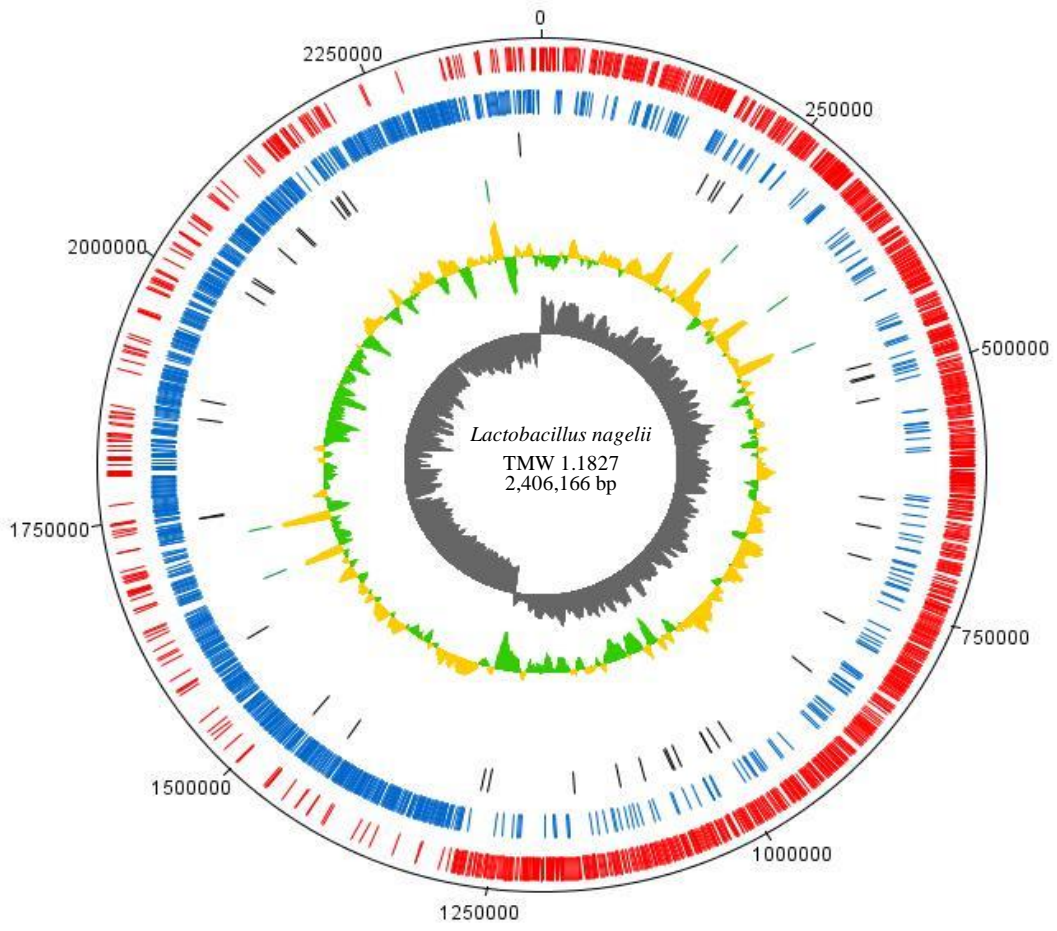


Fig. S2

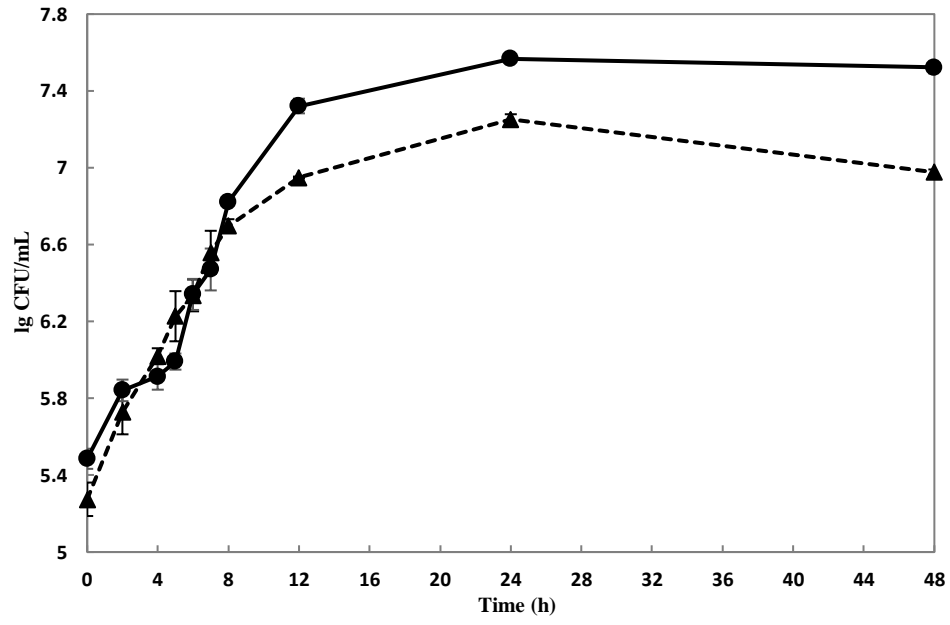


Fig. S3

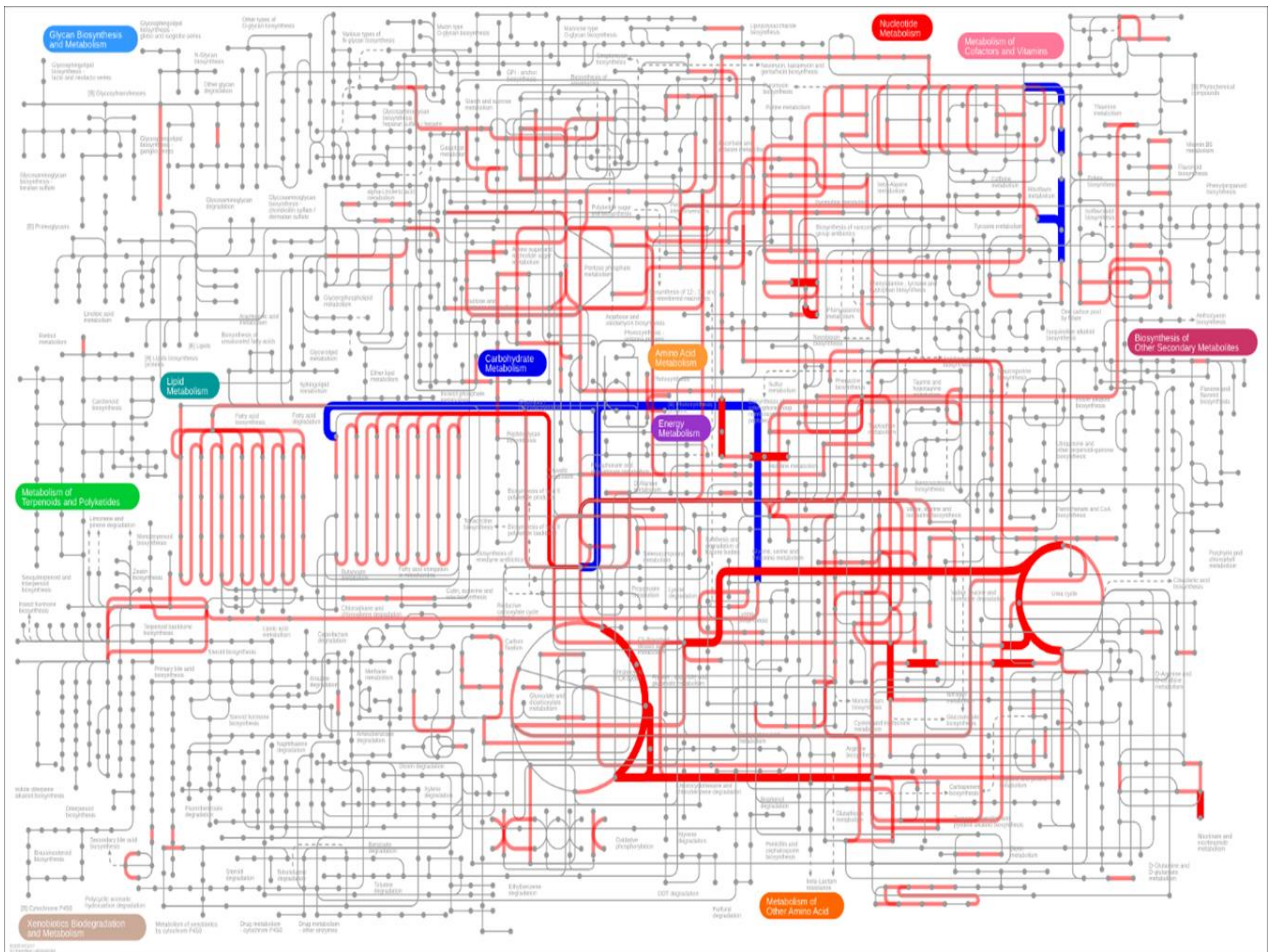


Fig. S4

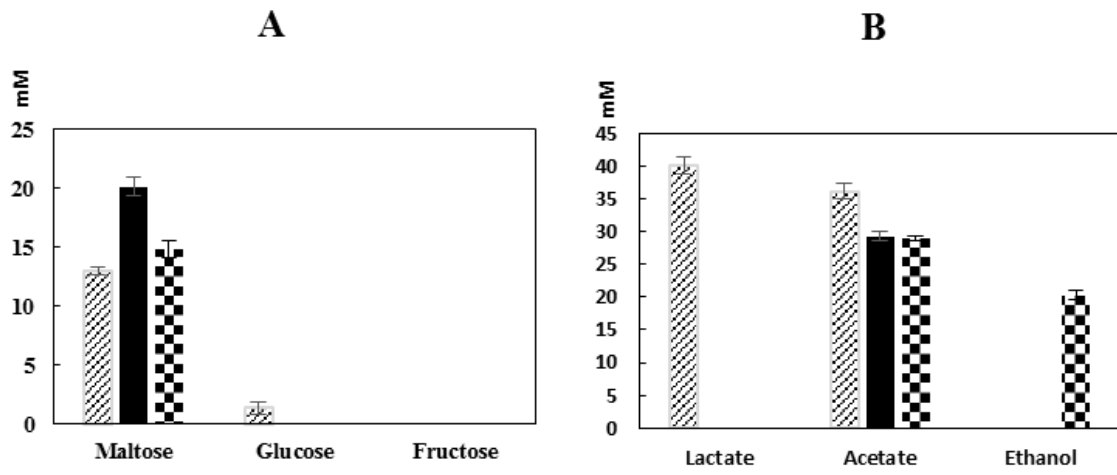
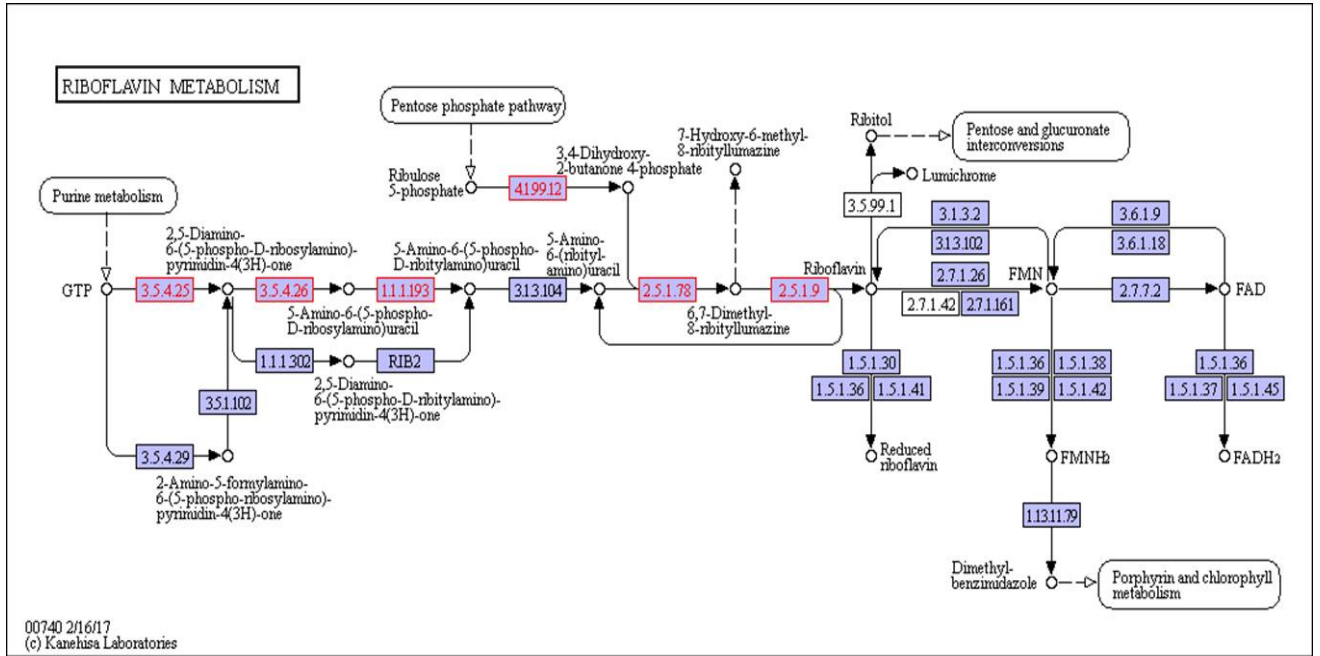


Fig. S5



## 5. MAIN FINDINGS

Before the general discussion of this thesis, I will briefly outline the primary results and findings from the manuscripts in the following theses:

- *L. hordei* TMW 1.1822 and *L. nagelii* TMW 1.1827 directly take abundant sucrose up by a PTS sucrose transporter and/or an MFS transporter, and metabolize it intracellularly via EMP and/or PKP pathways. Alternatively, sucrose is also extracellularly converted to glucans and fructose by a glucansucrase.
- Both lactobacilli favour PKP over EMP pathway in the presence of *S. cerevisiae*. *S. cerevisiae* delivers gluconate and fructose to *L. hordei*, while *S. cerevisiae* delivers vitamins to *L. nagelii*.
- *L. hordei* and *L. nagelii* display antidromic strategies to maintain NAD<sup>+</sup>/NADH homeostasis after the metabolic switch induced by *S. cerevisiae*.
- *L. hordei* and *L. nagelii* profit from amino acids secreted by the yeast, creating a niche-specific consortium. Besides, *L. hordei* also benefits from peptides provided by the yeast and protects yeast or other microorganisms from acid stress by alkalization of its cytoplasm and proximal environment.
- The beneficial effects of *S. cerevisiae* do not reside in a supply with unsaturated fatty acids to both lactobacilli in water kefir consortia.

- Specific exopolysaccharides, which are produced by *L. hordei*, promote the network formation of *S. cerevisiae*. Exopolysaccharide formation plays a major role in the physical interaction and establishment of space proximity of lactobacilli and yeasts.

## 6. DISCUSSION

### 6.1 Sugar transport and metabolism

Abundant sucrose was the main carbohydrate supplied in water kefir medium. It had been demonstrated that both *L. hordei* TMW 1.1822 and *L. nagelii* TMW 1.1827 upon growth in water kefir medium can directly take it up by PTS sucrose transporter and/or MFS transporter, and metabolize it intracellularly via EMP and/or PKP pathways (Manuscript 2 Section 3.3 and Manuscript 4 Section 3.3). Alternatively, sucrose was metabolized via glucansucrase, which resulted in the production of glucans, and leaving fructose as “secondary” carbon source. The residual fructose was transported into the cell by a fructose specific PTS and simultaneous phosphorylation. Once inside the cell, the phosphorylated fructose can directly enter the glycolytic pathway. Our isolates of *L. hordei* TMW 1.1822 and *L. nagelii* TMW 1.1827 from water kefir in this work revealed the expression of all enzymes involved in the EMP/PKP pathways via label-free quantitative proteomic analysis based on whole-genome sequence. Thus, they were inferred as facultatively heterofermentative microorganisms, like *L. plantarum* WCFS1 and *Lactococcus lactis* (Kleerebezem et al., 2003; Kleerebezem and Hugenholtz, 2003). However, four isolates (UCC125, UCC126, UCC127, and UCC128) from malted barley, which were identified to be *L. hordei* strains, were reported as homofermentative since



they were unable to ferment pentoses, but able to ferment a variety of hexoses and disaccharides including sucrose and mannitol (Rouse et al., 2008). And *L. hordei* UCC128 was shown identical to *L. hordei* DSM 19519, which was whole-genome sequenced (accession no. AZDX01000000) (Sun et al., 2015). *L. hordei* DSM 19519 isolated from barley and *L. nagelii* DSM 13675 isolated from wine, were also described as obligately homofermentative microorganisms (Sun et al., 2015). *L. hordei* DSM 19519 offered a different spectrum of carbohydrate substrates, namely starch (maltose) or arabino-xylans. In contrast to the water kefir isolate, there were no sucrose specific PTS and extracellular glycosyltransferases; and transporters involved in fructose import were less presented.

In the presence of *S. cerevisiae*, the 3-phosphoglycerate mutase, which was linked to the concentration of its substrate 3-phosphoglycerate (Smeianov et al., 2007), was significantly down-regulated in *L. nagelii* TMW 1.1827. This indicates, that intermediates of early glycolytic steps may be used for other metabolic reactions or hexoses may rather enter PKP or PPP than EMP, resulting in less production of 3-phosphoglycerate. In contrast to *L. nagelii*, the expression of EMP specific enzymes of *L. hordei* TMW 1.1822 was not influenced by *S. cerevisiae*. However, the expression of glucose-6-phosphate dehydrogenase, which is part of the PKP and PPP, was significantly up-regulated in *L. hordei*. This metabolic switch from EMP to PKP/PPP also helped both microorganisms to utilize gluconate, which was likely offered from *Gluconobacter* spp. (Matsushita et al., 2003; Qazi et al., 1991) harboring in water kefir consortium. Thus, it appeared to be a decisive trait in the water kefir environment. Both microorganisms appeared to favor PKP over EMP, indicating a metabolic switch induced by an altered

redox potential in the presence of *S. cerevisiae*. In addition, the glucansucrases of *L. hordei* and *L. nagelii* characterized as dextransucrases (Manuscript 1 Section 3.2) were not significantly regulated in the presence of *S. cerevisiae*, but the PTS mannose/fructose/sorbose family of *L. hordei* was significantly up-regulated. It suggested that additional fructose was provided to *L. hordei*, which was resulted from yeast invertase splitting of sucrose into glucose and fructose, and/or resulted from the dextransucrase reaction.

## **6.2 Pyruvate and citrate metabolism**

*In silico* analysis indicated that the pyruvate pool of *L. hordei* TMW 1.1822 and *L. nagelii* TMW 1.1827 could be filled from both the complete glycolytic pathway and citrate metabolism (Manuscript 2 Section 3.3 and Manuscript 4 Section 3.3). Further, genomic and proteomic analysis upon *L. hordei* and *L. nagelii* revealed the presence of all enzymes involved in the downstream of pyruvate conversion (Manuscript 2 Section 3.4 and Manuscript 4 Section 3.3). Beyond the indicated switch from EMP to PKP, more redox related metabolic reactions were affected upon the co-cultivation with *S. cerevisiae*. Initially described in *S. coelicolor*, such reactions were generally regulated by the redox-sensing repressor Rex in response to the change of cellular NADH/NAD<sup>+</sup> levels. A set of conserved core of 22 Rex-regulated genes from 11 taxonomic groups of bacteria were identified which were mainly implicated in energy metabolism and central carbohydrate metabolism (Ravcheev et al., 2012).

Although the Rex proteins of *L. hordei* and *L. nagelii* were not significantly regulated in the presence of *S. cerevisiae*, Rex apparently sensed a change in the cellular NADH/NAD<sup>+</sup> ratio and induced differentially expressed enzymes, which were Rex regulons involved in pyruvate metabolism. Bifunctional acetaldehyde/alcohol dehydrogenase of *L. hordei* was significantly down-regulated in the presence of *S. cerevisiae*, reducing the utilization of NADH and H<sup>+</sup> as well as the production of ethanol. In the presence of ethanol, which is mainly produced by the yeast in alcoholic water kefir (Beshkova et al., 2003), *S. cerevisiae* limited the production of ethanol by *L. hordei* in water kefir consortium. In contrast, alcohol dehydrogenase of *L. nagelii* was oppositely up-regulated. In the presence of *S. cerevisiae*,  $\alpha$ -acetolactate decarboxylase was significantly down-regulated in *L. nagelii*, blocking the direct decarboxylation of acetolactate to acetoin. Instead, under aerobic conditions, acetolactate spontaneously decomposed into diacetyl enabling regeneration of two molecules of NAD<sup>+</sup> upon reduction to 2,3-butanediol via diacetyl/ acetoin reductase. However, in the presence of *S. cerevisiae*, acetoin reductase was highly abundant in *L. hordei* generating a high amount of 2, 3-butanediol (Manuscript 3 Section 3.3). This re-direction of pyruvate metabolism in the presence of citrate was consistent with the results that high diacetyl production from *Lb. helveticus* MP12 and *Lc. lactis* subsp. *lactis* C15 isolated from (milk) kefir grains were recorded (Beshkova et al., 2003). On the other hand, the preferential production of butanediol in *L. hordei* and the preferential production of ethanol in *L. nagelii* instead of acetate or lactate, resulted in the limitation of acidification for the survival of yeast in water kefir environment. In summary, *L. hordei* TMW 1.1822 and *L. nagelii* TMW 1.1827 displayed antidromic strategies to maintain NAD<sup>+</sup>/NADH homeostasis after the metabolic switch induced by *S. cerevisiae*.

Like *L. hordei*, genomic and proteomic analysis revealed an incomplete TCA cycle in *L. nagelii*. But in the presence of *S. cerevisiae*, aconitate hydratase in *L. nagelii*, which catalyses the stereo-specific isomerization of citrate to isocitrate via cis-aconitate, and isocitrate dehydrogenase in *L. nagelii*, which catalyzed the oxidative decarboxylation of isocitrate producing 2-oxoglutarate and CO<sub>2</sub>, were significantly up-regulated. Despite its incompleteness, the TCA cycle was an important supplier for compounds involved in other metabolic reactions. Thus, isocitrate and 2-oxoglutarate were useful for amino acid metabolism in *L. nagelii*. Since lemon slices were normally added to water kefir fermentation, this was consistent with the result that microorganisms in water kefir were capable of directed citrate import using malate permease. Once inside the cell, citrate was converted by citrate lyase segregating one molecule of acetate and one molecule of oxaloacetate. The resulting oxaloacetate may then be decarboxylated via oxaloacetate decarboxylase yielding pyruvate or was used for amino acid biosynthesis. Further, citrate lyase and triphosphoribosyl-dephospho-CoA synthase were significantly up-regulated in *L. hordei* when co-cultivated with *S. cerevisiae*, while citrate lyase transcriptional regulator was significantly down-regulated (Manuscript 3 Section 3.3). It indicated that citrate was preferentially consumed by *L. hordei* in the presence of *S. cerevisiae*. Unlike in *L. hordei*, those enzymes were not differentially expressed in *L. nagelii* when it was co-cultivated with *S. cerevisiae*. As *L. hordei* appeared to be positively influenced in its metabolism of citrate as an additional carbon source, this may help to explain, why *L. hordei* is more abundant in the respective water kefir consortium than *L. nagelii*.

### **6.3 Peptide transport systems and peptidases, amino acids biosynthesis and metabolism**

Many LAB residing in milk products such as yoghurt, cheeses or milk kefir are equipped with a protein-degradation machinery, which enables peptide uptake and amino acids from proteins (Lopez-Kleine and Monnet, 2011; Simova et al., 2006). However, the *in silico* analyses of the genomes of *L. hordei* TMW 1.1822 and *L. nagelii* TMW 1.1827 isolated from water kefir did not reveal homologs to a cell wall protease (*prt*) gene. Still, they encoded the complete oligopeptide transport system (OppABCDF) and a large number of intracellular peptidases (Manuscript 3 Section 3.4 and Manuscript 4 Section 3.4). Except from OppB, all genes of annotated OppABCDF clusters were found to be present in the proteome of *L. nagelii*. Despite lacking an expressed OppB, the growth of *L. nagelii* was not impaired. This phenomenon was already described for other bacteria indicating, that the function of OppB may be compensable by other trans-membrane proteins (Nepomuceno et al., 2007). In the presence of the yeast, the remaining proteins were widely un-regulated with the exception of OppF, which was significantly down-regulated in *L. nagelii*. Since OppF is responsible for coupling the energy of ATP hydrolysis with the import of oligopeptides, *L. nagelii* may reduce energy consumption caused by oligopeptide uptake. On the contrary, *L. hordei* upregulated its OppABCDF system and one peptidase, suggesting that *L. hordei* benefited from peptides provided by the yeast. Since water kefir provided limited resources of proteins and free amino acids, mainly originating from dried fruits and the yeast, these findings may also explain the fact, that the growth of *L. hordei* was stimulated in co-cultivation.

Nonetheless, from genomic annotation, *L. nagelii* encoded several amino acid permeases and transporters. In the presence of *S. cerevisiae*, two of those permeases were significantly up-regulated, suggesting that the yeast induces amino acid uptake in *L. nagelii*. However, it was not possible to specify from sequence comparison, which amino acids were ingested by *L. nagelii*. Still, this may be solved by a closer look at amino acid synthesis pathways and auxotrophies. The genomic analysis of *L. nagelii* TMW 1.1827 revealed the prototrophy for 13 amino acids and auxotrophy for 7 amino acids (Manuscript 4 Section 3.4). This result also applied to *L. hordei*, except for 3-deoxy-7-phosphoheptulonate synthase, which was additionally missed in *L. hordei*. Therefore, only *L. nagelii* was capable of producing tyrosine. In other studies, the genome of *L. plantarum* WCFS1 predicted prototrophy for 17 amino acids (Kleerebezem et al., 2003), the genome of *L. sanfranciscensis* TMW 1.1304 predicted auxotrophy for 12 amino acids (Vogel et al., 2011), and the genome of *L. acidophilus* NCFM predicted auxotrophy for 14 amino acids (Altermann et al., 2005). Therefore, the capability of *de novo* synthesis of amino acids of *L. hordei* and *L. nagelii* was intermediate. According to the quantitative proteomic analysis, nine enzymes of *L. nagelii* involved in histidine, methionine, glutamate and arginine biosynthesis pathways were significantly up-regulated in the presence of *S. cerevisiae*. Except for acetylglutamate kinase, those up-regulated enzymes of *L. nagelii* were also among 16 over-expressed enzymes of *L. hordei* (Manuscript 4 Section 3.4). Since those biosynthesis pathways can also be used for amino acid catabolism, water kefir microorganisms may profit from amino acids secreted by the yeast, creating a symbiotic consortium. However, from *in silico* analysis, the direction of a respective metabolic pathway remained speculative. Still, together with physiological

data on amino acid consumption and secretion of *L. nagelii* and *S. cerevisiae*, this can be solved for at least some of the predicted cases.

*S. cerevisiae* secreted glutamine in high amounts, whereas *L. nagelii* consumed the amino acid at high levels via an up-regulated amino acid permease involved in glutamine uptake. This suggested, that *L. nagelii*, even though it was capable of producing glutamine by itself, profited from the glutamine provided by the yeast via the up-regulated glutamate synthase, as it was also described for *L. hordei* (Manuscript 4 Section 3.4). Since glutamine played an important role in anaplerotic sequences of transamination reactions in the biosynthesis of other amino acids, and also as a nitrogen carrier for the production of amino sugars and nucleotides, the uptake of glutamine was crucial to persist in the water kefir environment. In contrast to *L. hordei*, *L. nagelii* was predicted to produce glutamate by itself via the up-regulated glutamate synthase using glutamine and 2-oxoglutarate, which probably resulted from the incomplete TCA cycle. This was consistent with an un-regulated glutamine synthetase in the presence of *S. cerevisiae*, while this enzyme was significantly up-regulated in *L. hordei*. It has been demonstrated that glutamine synthetase played a very important role for the growth of *Lactococcus lactis* NCDO763 in milk by proteomic signature via two-dimensional gels (Gitton et al., 2005). As described for *Lactobacillus crispatus* ST1, this enzyme might exhibit additional adhesive function (Kainulainen et al., 2012). If glutamine synthetase was displayed on the bacterial surface, it may enable physical coherence of the water kefir consortium under stressful conditions. As a result, the yeast aggregation promotion of *L. hordei* by its functional dextran (Manuscript 1 Section 3.3) may be even enhanced by over-expression of this enzyme. Furthermore, among all amino acids, the production of

glutamate was of primary importance in the assimilation of nitrogen, representing a donor for amino groups in the synthesis of other amino acids (Bernard and Habash, 2009; Dincturk et al., 2011). Other amino acids were not produced, but partly consumed by the yeast. Therefore, it was not possible to determine real-time metabolic exchange (release/uptake) between LAB and *S. cerevisiae* based on physiological data. Still, the label-free quantitative proteomic analysis enabled the investigation of the dynamic metabolic exchanges between microbial communities in water kefir. The up-regulated enzymes involved in amino acid biosynthesis or catabolism predicted that *S. cerevisiae* released glutamine, histidine, methionine and arginine, which were subsequently used by *L. nagelii* to ensure its survival in the water kefir consortium. Also, it was suggested that the nutrient flux of glutamine, glutamate, histidine, methionine, arginine, tryptophan and proline from yeast to *L. hordei* occurred. There was another study about the specific contribution of *S. cerevisiae* S90 to *Lactococcus lactis* IL1403 and *L. plantarum* WCFS1 through nitrogen overflow in grape juice (Ponomarova et al., 2017). It has been predicted that *S. cerevisiae* benefited *Lactococcus lactis* by providing glutamine and threonine, and it benefited *L. plantarum* by providing glutamine, threonine, phenylalanine, tryptophan and serine. In summary, *L. hordei* and *L. nagelii* displayed the capability to uptake these amino acids secreted by the yeast, creating a niche-specific environment. Thus, it was also postulated that amino acids were the major agents for yeast-LAB interaction in water kefir.

#### **6.4 Acid tolerance by ADI pathway**

The degradation of arginine via the arginine deiminase (ADI) pathway was widely distributed in LAB genera, such as *Lactobacillus*, *Lactococcus*, *Leuconostoc* and



*Weissella*, resulting in additional ATP and acid tolerance (Arena et al., 2002; Fernández and Zúñiga, 2006; Rimaux et al., 2011; Tonon and Lonvaud-Funel, 2002). The ADI system comprised three reactions catalyzed by arginine deiminase (ADI), ornithine transcarbamoylase (OTC), and carbamate kinase (CK). While ADI and OTC were present in both, the genome and proteome of *L. nagelii* TMW 1.1827, CK was only detectable in the genome (Manuscript 4 Section 3.5). Since, *L. hordei* TMW 1.1822 lacked CK in its putative functional genome, both microorganisms were not able to convert carbamoyl-P to generate additional ATP in co-cultivation. Therefore, both of them lacked the ability to generate additional ATP, and the fate of carbamoyl-P remains unclear. However, in the energy rich environment of water kefir, it did not appear to influence the conversion of arginine into ammonia by ADI. This was verified by over-expressed ADI and OTC in *L. hordei*, and over-expressed OTC in *L. nagelii* in the presence of *S. cerevisiae*. The notion was also demonstrated by the increased pH value of co-cultivated *L. hordei* and *S. cerevisiae* compared with single-cultivated *L. hordei*. *L. hordei* likely produced ammonia to protect yeast or other microorganisms from acid stress by alkalization of its cytoplasm and proximal environment.

## **6.5 Fatty acid biosynthesis and riboflavin metabolism**

Although *L. hordei* and *L. nagelii* suffered from the limited availability of fatty acids in the water kefir, *L. hordei* seemed not be able to synthesize any unsaturated fatty acids in the absence of FabB, and *L. nagelii* appeared to be in the absence of FabA and FabB either (Manuscript 2 Section 3.7 and Manuscript 4 Section 3.6). However, as demonstrated in *Enterococcus (E.) faecalis* (Wang and Cronan, 2004), *E. faecalis* FabF

protein can functionally replace *E. coli* FabB protein and *E. faecalis* FabZ protein can adopt the function of *E. coli* FabA protein. Another study also reported that expression of *Lactococcus lactis* FabF can functionally replace both FabB and FabA in *E. coli* (Morgan-Kiss and Cronan, 2008). Despite those enzymatic bi-functionalities were not predictable by genome analysis, both microorganisms grew to high cell densities in water kefir medium without any external fatty acids. Therefore, this finding indicated the existence of other functional homologs for FabB and FabA in *L. hordei* and *L. nagelii*. Co-cultivation with *S. cerevisiae* did not alter the expression of any proteins involved in fatty acid metabolism in both LAB. It indicated, that the beneficial effects of *S. cerevisiae* did not reside in a bilateral supply with unsaturated fatty acids.

Moreover, there was a group of enzymes of *L. nagelii*, which showed decreased expression in response to the co-cultivation with *S. cerevisiae*, which were involved in riboflavin metabolism (Manuscript 4 Section 3.6). Those enzymes connected the purine metabolism and pentose phosphate pathway to synthesize riboflavin. This may be an evidence for the feeding of riboflavin from *S. cerevisiae* to *L. nagelii*, supporting its growth and leading to a stable water kefir consortium.

## **6.6 The role of *L. hordei* dextrans for granule formation**

Our results at first glance indicated that aggregation and network formation of *S. cerevisiae* on hydrophilic slide model system was induced in the presence of *L. hordei*, but not induced in the presence of *L. nagelii* or *Lc. citreum* (Manuscript 1 Section 3.1). Since the role of glucans (such as dextrans) in biofilm formation has been widely

reported by glucan-producing LAB species from different sources such as *Lc. mesenteroides* NRRL B-21414, *L. reuteri* TMW1.106 and *Streptococcus mutans* UA159 (Leathers and Côté, 2008; Walter et al., 2008; Zhu et al., 2009), isolated EPS from *L. hordei*, *L. nagelii* and *Lc. citreum* were further investigated in this slide model system. However, isolated EPS from *L. hordei* was solely found to induce the aggregation and network formation of *S. cerevisiae*. Although all isolated EPS from *L. hordei*, *L. nagelii* and *Lc. citreum* had been characterized to be dextrans, they varied at the percentages of 1,3-, 1,4-, 1,2,6-, 1,4,6- or 1,3,6-linked glucose and the molecular weight. Currently, the mechanism of *S. cerevisiae* aggregation and network formation cannot be clearly clarified, but specific dextrans of *L. hordei* were proven to be decisive factors for *S. cerevisiae* aggregation/adhesion. It was most likely that *S. cerevisiae* either became highly hydrophilic for enhanced adhesion via binding of specific motifs in hydrophilic *L. hordei* dextrans or sudden induction of any other hydrophilic surface structures, or got entrapped in the form of networks on a glue-like film which was formed in the presence of *L. hordei*. Previous studies showed that the backbone of the water kefir granule was primarily made of dextrans produced by *L. hilgardii* (Horisberger, 1969; Neve and Heller, 2002; Pidoux et al., 1990; Waldherr et al., 2010). Thus, our study suggested that the specific size and structural organization of the dextrans produced by *L. hordei* acted as the main cause for inducing *S. cerevisiae* aggregation and network formation and thus as crucial initiation of the stepwise water kefir granule growth.

## LIST OF PUBLICATIONS DERIVED FROM THIS WORK

### Peer-reviewed Journals

**Di Xu**, Lea Fels, Daniel Wefers, Jürgen Behr, Frank Jakob, Rudi F. Vogel., 2018. *Lactobacillus hordei* dextrans induce *Saccharomyces cerevisiae* aggregation and network formation on hydrophilic surfaces. International Journal of Biological Macromolecules 115, 236–242.

**Di Xu**<sup>#</sup>, Julia Bechtner<sup>#</sup>, Jürgen Behr, Lara Eisenbach, Andreas J. Geißler, Rudi F. Vogel., 2019. Lifestyle of *Lactobacillus hordei* isolated from water kefir based on genomic, proteomic and physiological characterization. International Journal of Food Microbiology 290, 141–149.

**Di Xu**, Jürgen Behr, Andreas J. Geißler, Christina Ludwig, Rudi F. Vogel., 2019. Label-free quantitative proteomic analysis reveals the lifestyle of *Lactobacillus hordei* in presence of *Sacchromyces cerevisiae*. International Journal of Food Microbiology. Accepted.

Julia Bechtner<sup>#</sup>, **Di Xu**<sup>#</sup>, Jürgen Behr, Rudi F. Vogel., 2019. Comparative proteomic analysis of *Lactobacillus nagelii* and *Lactobacillus hordei* in the presence of *Saccharomyces cerevisiae* isolated from water kefir. Frontiers in Microbiology. Under review.

#joint first authorship


### **Poster presentation**

Food Microbiology, 19 - 22 July 2016, Dublin, Ireland. **Di Xu**, Jürgen Behr, Rudi F. Vogel., Physical interaction between *Lactobacillus hordei* and *Saccharomyces cerevisiae* isolated from water kefir - towards a reconstruction of complex ecosystems.

### **Oral presentation (speaker is underlined)**

Welfers, D., Frauenhofer, M., Brandt, J. U., **Xu, D.**, Jakob, F., Vogel, R. F., Bunzel, M., 2017. Strukturelle Eigenschaften verschiedener Lebensmittelrelevanter bakterieller Exopolysaccharide. Symposium der Gesellschaft Deutscher Lebensmitteltechnologen „Hydrokolloide VIII“, Gerlingen.

## CURRICULUM VITAE

Name	Xu Di	Geschlecht	weiblich	
Geburtsdatum	5.Dez.1988	Geburtsort	Nanchang, China	
Staatsangehörigkeit	Chinesisch	Familienstand	ledig	
E-mail	ncuskxudi@163.com			
Anschrift	Am Mitterfeld 1, 85354, Freising, Germany			
<b>Bildungsstand</b>				
09.2006-07.2010	Nanchang Universität	Bachelor der Lebensmittelwissenschaft		
09.2010-07.2013	Nanchang Universität	Master der Mikrobiologie		
10.2013-2019	Technische Universität München	Doktorandin der Technische Mikrobiologie		
<b>Sonstiges Erfahrungen</b>				
07.2016	FoodMicro 2016 conference, poster	Dublin, Ireland		
08.2017	1st Munich Metabolomics Meeting	Freising, Germany		

## REFERENCES

- Altermann, E., Russell, W.M., Azcarate-Peril, M.A., Barrangou, R., Buck, B.L., McAuliffe, O., Souther, N., Dobson, A., Duong, T., Callanan, M., 2005. Complete genome sequence of the probiotic lactic acid bacterium *Lactobacillus acidophilus* NCFM. PNAS 102, 3906-3912.
- Altschul, S.F., Gish, W., Miller, W., Myers, E.W., Lipman, D.J., 1990. Basic local alignment search tool. J Mol Biol. 215, 403-410.
- Arena, M.E., de Nadra, M.a.C.M., Muñoz, R., 2002. The arginine deiminase pathway in the wine lactic acid bacterium *Lactobacillus hilgardii* X<sub>1</sub>B: structural and functional study of the *arcABC* genes. Gene 301, 61-66.
- Aziz, R.K., Bartels, D., Best, A.A., DeJongh, M., Disz, T., Edwards, R.A., Formsma, K., Gerdes, S., Glass, E.M., Kubal, M., 2008. The RAST Server: rapid annotations using subsystems technology. BMC Genomics 9, 75.
- Bartóak, T., Szalai, G., Lőrincz, Z., Böuresök, G., Sági, F., 1994. High-speed RP-HPLC/FL analysis of amino acids after automated two-step derivatization with o-phthaldialdehyde/3-mercaptopropionic acid and 9-fluorenylmethyl chloroformate. J Liq Chromatogr R T 17, 4391-4403.
- Bechtner, J., Xu, D., Behr, J., Vogel, R.F., 2019. Comparative proteomic analysis of *Lactobacillus nagelii* and *Lactobacillus hordei* in the presence of *Saccharomyces cerevisiae* isolated from water kefir. Front Microbiol. Under review.
- Bernard, S.M., Habash, D.Z., 2009. The importance of cytosolic glutamine synthetase in nitrogen assimilation and recycling. New Phytologist 182, 608-620.
- Beshkova, D., Simova, E., Frengova, G., Simov, Z., Dimitrov, Z.P., 2003. Production of volatile aroma compounds by kefir starter cultures. Int Dairy J. 13, 529-535.

- Camacho, C., Coulouris, G., Avagyan, V., Ma, N., Papadopoulos, J., Bealer, K., Madden, T.L., 2009. BLAST+: architecture and applications. *BMC Bioinformatics* 10, 421.
- Carver, T., Thomson, N., Bleasby, A., Berriman, M., Parkhill, J., 2008. DNAPlotter: circular and linear interactive genome visualization. *Bioinformatics* 25, 119-120.
- Chin, C.-S., Alexander, D.H., Marks, P., Klammer, A.A., Drake, J., Heiner, C., Clum, A., Copeland, A., Huddleston, J., Eichler, E.E., 2013. Nonhybrid, finished microbial genome assemblies from long-read SMRT sequencing data. *Nat Methods* 10, 563.
- Cox, J., Hein, M.Y., Lubner, C.A., Paron, I., Nagaraj, N., Mann, M., 2014. MaxLFQ allows accurate proteome-wide label-free quantification by delayed normalization and maximal peptide ratio extraction. *Mol Cell Proteomics*, mcp. M113. 031591.
- Cox, J., Mann, M., 2008. MaxQuant enables high peptide identification rates, individualized ppb-range mass accuracies and proteome-wide protein quantification. *Nat Biotechnol.* 26, 1367.
- Cox, J., Neuhauser, N., Michalski, A., Scheltema, R.A., Olsen, J.V., Mann, M., 2011. Andromeda: a peptide search engine integrated into the MaxQuant environment. *J Proteome Res* 10, 1794-1805.
- Davidović, S.Z., Miljković, M.G., Antonović, D.G., Rajilić-Stojanović, M.D., Dimitrijević-Branković, S.I., 2015. Water kefir grain as a source of potent dextran producing lactic acid bacteria. *Hem Ind.* 69, 595-604.
- De Ruiter, G.A., Schols, H.A., Voragen, A.G., Rombouts, F.M., 1992. Carbohydrate analysis of water-soluble uronic acid-containing polysaccharides with high-performance anion-exchange chromatography using methanolysis combined with TFA hydrolysis is superior to four other methods. *Anal Biochem* 207, 176-185.



- Dincturk, H.B., Cunin, R., Akce, H., 2011. Expression and functional analysis of glutamate synthase small subunit-like proteins from archaeon *Pyrococcus horikoshii*. *Microbiol Res* 166, 294-303.
- Eid, J., Fehr, A., Gray, J., Luong, K., Lyle, J., Otto, G., Peluso, P., Rank, D., Baybayan, P., Bettman, B., 2008. Real-time DNA sequencing from single polymerase molecules. *Science* 323, 133-138.
- Fels, L., Jakob, F., Vogel, R.F., Wefers, D., 2018. Structural characterization of the exopolysaccharides from water kefir. *Carbohydr Polym* 189, 296-303.
- Fernández, M., Zúñiga, M., 2006. Amino acid catabolic pathways of lactic acid bacteria. *Crit Rev Microbiol* 32, 155-183.
- Galli, A., Fiori, E., Franzetti, L., Pagani, M., Ottogalli, G., 1995. Microbiological and chemical-composition of sugar kefir grains. *Ann Microbiol Enzimol.* 45, 85-95.
- García-Quintáns, N., Blancato, V.S., Repizo, G.D., Magni, C., López, P., 2008. Citrate metabolism and aroma compound production in lactic acid bacteria. *Molecular Aspects of Lactic Acid Bacteria for Traditional and New Applications* 3, 65-88.
- Gardy, J.L., Laird, M.R., Chen, F., Rey, S., Walsh, C., Ester, M., Brinkman, F.S., 2004. PSORTb v. 2.0: expanded prediction of bacterial protein subcellular localization and insights gained from comparative proteome analysis. *Bioinformatics* 21, 617-623.
- Geißler, A., 2016. Lifestyle of beer spoiling lactic acid bacteria. Doctoral Thesis, Technische Universität München.
- Gitton, C., Meyrand, M., Wang, J., Caron, C., Trubuil, A., Guillot, A., Mistou, M.-Y., 2005. Proteomic signature of *Lactococcus lactis* NCDO763 cultivated in milk. *Appl Environ Microbiol.* 71, 7152-7163.

- Gulitz, A., Stadie, J., Ehrmann, M., Ludwig, W., Vogel, R., 2013. Comparative phylobiomic analysis of the bacterial community of water kefir by 16S rRNA gene amplicon sequencing and ARDRA analysis. *J Appl Microbiol.* 114, 1082-1091.
- Gulitz, A., Stadie, J., Wenning, M., Ehrmann, M.A., Vogel, R.F., 2011. The microbial diversity of water kefir. *Int J Food Microbiol.* 151, 284-288.
- Horisberger, M., 1969. Structure of the dextran of the Tibi grain. *Carbohydr Res* 10, 379-385.
- Jakob, F., Pfaff, A., Novoa-Carballal, R., Rübsam, H., Becker, T., Vogel, R.F., 2013. Structural analysis of fructans produced by acetic acid bacteria reveals a relation to hydrocolloid function. *Carbohydr Polym* 92, 1234-1242.
- Jay, J.M., 1992. History of microorganisms in food, *Modern Food Microbiology*. Springer, pp. 3-10.
- Kainulainen, V., Loimaranta, V., Pekkala, A., Edelman, S., Antikainen, J., Kylväjä, R., Laaksonen, M., Laakkonen, L., Finne, J., Korhonen, T.K., 2012. Glutamine synthetase and glucose-6-phosphate isomerase are adhesive moonlighting proteins of *Lactobacillus crispatus* released by cathelicidin LL-37. *J Bacteriol.*, 06704-06711.
- Kebler, L.F., 1921. California bees. *J Am Pharm Assoc* 10, 939-943.
- Kleerebezem, M., Boekhorst, J., van Kranenburg, R., Molenaar, D., Kuipers, O.P., Leer, R., Turchini, R., Peters, S.A., Sandbrink, H.M., Fiers, M.W., 2003. Complete genome sequence of *Lactobacillus plantarum* WCFS1. *PNAS* 100, 1990-1995.
- Kleerebezem, M., Hugenholtz, J., 2003. Metabolic pathway engineering in lactic acid bacteria. *Curr Opin Biotechnol.* 14, 232-237.

- Kokkinosa, A., Fasseas, C., Eliopoulos, E., Kalantzopoulos, G., 1998. Cell size of various lactic acid bacteria as determined by scanning electron microscope and image analysis. *Le Lait* 78, 491-500.
- Krumsiek, J., Arnold, R., Rattei, T., 2007. Gepard: a rapid and sensitive tool for creating dotplots on genome scale. *Bioinformatics* 23, 1026-1028.
- Laureys, D., Aerts, M., Vandamme, P., De Vuyst, L., 2018. Oxygen and diverse nutrients influence the water kefir fermentation process. *Food microbiology* 73, 351-361.
- Laureys, D., Cnockaert, M., De Vuyst, L., Vandamme, P., 2016. *Bifidobacterium aquikefiri* sp. nov., isolated from water kefir. *Int J Syst Evol Microbiol.* 66, 1281-1286.
- Laureys, D., De Vuyst, L., 2014. Microbial species diversity, community dynamics, and metabolite kinetics of water kefir fermentation. *Appl Environ Microbiol.*, 03978-03913.
- Leathers, T.D., Côté, G.L., 2008. Biofilm formation by exopolysaccharide mutants of *Leuconostoc mesenteroides* strain NRRL B-1355. *Appl Microbiol Biotechnol.* 78, 1025-1031.
- Leroi, F., Pidoux, M., 1993. Detection of interactions between yeasts and lactic acid bacteria isolated from sugary kefir grains. *J Appl Bacteriol.* 74, 48-53.
- Lopez-Kleine, L., Monnet, V., 2011. Lactic acid bacteria| proteolytic systems, *Encyclopedia of Dairy Sciences*, pp. 49-55.
- Lutz, M., 1899. Recherches biologiques sur la constitution du Tibi *Bull Soc Mycol France* 15, 68-72.

- Marsh, A.J., O'Sullivan, O., Hill, C., Ross, R.P., Cotter, P.D., 2013. Sequence-based analysis of the microbial composition of water kefir from multiple sources. *FEMS Microbiol Lett* 348, 79-85.
- Martínez - Torres, A., Gutiérrez - Ambrocio, S., Heredia - del - Orbe, P., Villa - Tanaca, L., Hernández - Rodríguez, C., 2017. Inferring the role of microorganisms in water kefir fermentations. *Int J Food Sci Technol* 52, 559-571.
- Matsushita, K., Fujii, Y., Ano, Y., Toyama, H., Shinjoh, M., Tomiyama, N., Miyazaki, T., Sugisawa, T., Hoshino, T., Adachi, O., 2003. 5-Keto-d-gluconate production is catalyzed by a quinoprotein glycerol dehydrogenase, major polyol dehydrogenase, in *Gluconobacter* species. *Appl Environ Microbiol* 69, 1959-1966.
- McCarthy, A., 2010. Third generation DNA sequencing: pacific biosciences' single molecule real time technology. *Chem Biol* 17, 675-676.
- Morgan-Kiss, R.M., Cronan, J.E., 2008. The *Lactococcus lactis* FabF fatty acid synthetic enzyme can functionally replace both the FabB and FabF proteins of *Escherichia coli* and the FabH protein of *Lactococcus lactis*. *Arch Microbiol* 190, 427-437.
- Naessens, M., Cerdobbel, A., Soetaert, W., Vandamme, E.J., 2005. *Leuconostoc* dextransucrase and dextran: production, properties and applications. *J Chem Technol Biotechnol* 80, 845-860.
- Nepomuceno, R., Tavares, M., Lemos, J., Griswold, A., Ribeiro, J., Balan, A., Guimaraes, K., Cai, S., Burne, R., Ferreira, L., 2007. The oligopeptide (*opp*) gene cluster of *Streptococcus mutans*: identification, prevalence, and characterization. *Oral Microbiol Immunol* 22, 277-284.
- Neve, H., Heller, K., 2002. The microflora of water kefir: a glance by scanning electron microscopy. *Kiel Milchwirtsch Forschungsber* 54, 337-349.

- Nunes, F.M., Reis, A., Silva, A.M., Domingues, M.R.M., Coimbra, M.A., 2008. Rhamnoarabinosyl and rhamnoarabinoarabinosyl side chains as structural features of coffee arabinogalactans. *Phytochemistry* 69, 1573-1585.
- Overbeek, R., Olson, R., Pusch, G.D., Olsen, G.J., Davis, J.J., Disz, T., Edwards, R.A., Gerdes, S., Parrello, B., Shukla, M., 2013. The SEED and the rapid annotation of microbial genomes using subsystems technology (RAST). *Nucleic Acids Res* 42, D206-D214.
- Pidoux, M., 1989. The microbial flora of sugary kefir grain (the gingerbeer plant): biosynthesis of the grain from *Lactobacillus hilgardii* producing a polysaccharide gel. *MIRCEN Journal of Applied Microbiology and Biotechnology* 5, 223-238.
- Pidoux, M., De Ruiter, G., Brooker, B., Colquhoun, I., Morris, V., 1990. Microscopic and chemical studies of a gelling polysaccharide from *Lactobacillus hilgardii*. *Carbohydr Polym* 13, 351-362.
- Ponomarova, O., Gabrielli, N., Sévin, D.C., Mülleder, M., Zirngibl, K., Bulyha, K., Andrejev, S., Kafkia, E., Typas, A., Sauer, U., 2017. Yeast creates a niche for symbiotic lactic acid bacteria through nitrogen overflow. *Cell systems* 5, 345-357.
- Qazi, G., Parshad, R., Verma, V., Chopra, C., Buse, R., Träger, M., Onken, U., 1991. Diketo-gluconate fermentation by *Gluconobacter oxydans*. *Enzyme Microb Technol* 13, 504-507.
- Ravcheev, D.A., Li, X., Latif, H., Zengler, K., Leyn, S.A., Korostelev, Y.D., Kazakov, A.E., Novichkov, P.S., Osterman, A.L., Rodionov, D.A., 2012. Transcriptional regulation of central carbon and energy metabolism in bacteria by redox-responsive repressor Rex. *J Bacteriol* 194, 1145-1157.

- Rimaux, T., Vrancken, G., Pothakos, V., Maes, D., De Vuyst, L., Leroy, F., 2011. The kinetics of the arginine deiminase pathway in the meat starter culture *Lactobacillus sakei* CTC 494 are pH-dependent. *Food Microbiol* 28, 597-604.
- Rouse, S., Canchaya, C., van Sinderen, D., 2008. *Lactobacillus hordei* sp. nov., a bacteriocinogenic strain isolated from malted barley. *Int J Syst Evol Microbiol* 58, 2013-2017.
- Schurr, B.C., Behr, J., Vogel, R.F., 2013. Role of the GAD system in hop tolerance of *Lactobacillus brevis*. *Eur Food Res Technol* 237, 199-207.
- Simova, E., Simov, Z., Beshkova, D., Frengova, G., Dimitrov, Z., Spasov, Z., 2006. Amino acid profiles of lactic acid bacteria, isolated from kefir grains and kefir starter made from them. *Int J Food Microbiol* 107, 112-123.
- Smeianov, V.V., Wechter, P., Broadbent, J.R., Hughes, J.E., Rodríguez, B.T., Christensen, T.K., Ardö, Y., Steele, J.L., 2007. Comparative high-density microarray analysis of gene expression during growth of *Lactobacillus helveticus* in milk versus rich culture medium. *Appl Environ Microbiol* 73, 2661-2672.
- Stadie, J., Gulitz, A., Ehrmann, M.A., Vogel, R.F., 2013. Metabolic activity and symbiotic interactions of lactic acid bacteria and yeasts isolated from water kefir. *Food Microbiol* 35, 92-98.
- Stolz, P., Vogel, R.F., Hammes, W.P., 1995. Utilization of electron acceptors by lactobacilli isolated from sourdough. *Z Lebensm Unters Forsch* 201, 402-410.
- Sun, Z., Harris, H.M., McCann, A., Guo, C., Argimón, S., Zhang, W., Yang, X., Jeffery, I.B., Cooney, J.C., Kagawa, T.F., 2015. Expanding the biotechnology potential of lactobacilli through comparative genomics of 213 strains and associated genera. *Nat Commun* 6, 8322.

- Sweet, D.P., Shapiro, R.H., Albersheim, P., 1975. Quantitative analysis by various GLC response-factor theories for partially methylated and partially ethylated alditol acetates. *Carbohydr Res* 40, 217-225.
- Tingirikari, J.M.R., Kothari, D., Goyal, A., 2014. Superior prebiotic and physicochemical properties of novel dextran from *Weissella cibaria* JAG8 for potential food applications. *Food Funct* 5, 2324-2330.
- Tonon, T., Lonvaud-Funel, A., 2002. Arginine metabolism by wine *Lactobacilli* isolated from wine. *Food Microbiol* 19, 451-461.
- Tyanova, S., Temu, T., Sinitcyn, P., Carlson, A., Hein, M.Y., Geiger, T., Mann, M., Cox, J., 2016. The Perseus computational platform for comprehensive analysis of (prote) omics data. *Nat Methods* 13, 731.
- Ua-Arak, T., Jakob, F., Vogel, R.F., 2017. Fermentation pH modulates the size distributions and functional properties of *Gluconobacter albidus* TMW 2.1191 levan. *Front Microbiol* 8, 807.
- Vogel, R.F., Pavlovic, M., Ehrmann, M.A., Wiezer, A., Liesegang, H., Offschanka, S., Voget, S., Angelov, A., Böcker, G., Liebl, W., 2011. Genomic analysis reveals *Lactobacillus sanfranciscensis* as stable element in traditional sourdoughs, *Microb Cell Fact.* BioMed Central, p. S6.
- Waldherr, F.W., Doll, V.M., Meißner, D., Vogel, R.F., 2010. Identification and characterization of a glucan-producing enzyme from *Lactobacillus hilgardii* TMW 1.828 involved in granule formation of water kefir. *Food Microbiol* 27, 672-678.
- Walter, J., Schwab, C., Loach, D.M., Gänzle, M.G., Tannock, G.W., 2008. Glucosyltransferase A (GtfA) and inulosucrase (Inu) of *Lactobacillus reuteri*

- TMW1. 106 contribute to cell aggregation, *in vitro* biofilm formation, and colonization of the mouse gastrointestinal tract. *Microbiology* 154, 72-80.
- Wang, H., Cronan, J.E., 2004. Functional replacement of the FabA and FabB proteins of *Escherichia coli* fatty acid synthesis by *Enterococcus faecalis* FabZ and FabF homologues. *J Biol Chem* 279, 34489-34495.
- Ward, H.M., 1891. The 'ginger-beer plant', and the organisms composing it: a contribution to the study of fermentation-yeasts and bacteria. *Proceedings of the Royal Society of London* 50, 261-265.
- Wefers, D., Bunzel, M., 2015. Characterization of dietary fiber polysaccharides from dehulled common buckwheat (*Fagopyrum esculentum*) seeds. *Cereal Chem* 92, 598-603.
- Xu, D., Bechtner, J., Behr, J., Eisenbach, L., Geißler, A.J., Vogel, R.F., 2019. Lifestyle of *Lactobacillus hordei* isolated from water kefir based on genomic, proteomic and physiological characterization. *Int. J. Food Microbiol* 290, 141-149.
- Xu, D., Behr, J., Geißler, A.J., Ludwig, C., Vogel, R.F., 2019. Label-free quantitative proteomic analysis reveals the lifestyle of *Lactobacillus hordei* in the presence of *Saccharomyces cerevisiae*. *Int J Food Microbiol*. Accepted.
- Xu, D., Fels, L., Wefers, D., Behr, J., Jakob, F., Vogel, R.F., 2018. *Lactobacillus hordei* dextrans induce *Saccharomyces cerevisiae* aggregation and network formation on hydrophilic surfaces. *Int J Biol Macromol* 115, 236-242.
- Yamada, T., Letunic, I., Okuda, S., Kanehisa, M., Bork, P., 2011. iPath2. 0: interactive pathway explorer. *Nucleic Acids Res* 39, W412-W415.
- Yelin, D., Silberberg, Y., 1999. Laser scanning third-harmonic-generation microscopy in biology. *Opt Express* 5, 169-175.



- Yu, N.Y., Wagner, J.R., Laird, M.R., Melli, G., Rey, S., Lo, R., Dao, P., Sahinalp, S.C., Ester, M., Foster, L.J., 2010. PSORTb 3.0: improved protein subcellular localization prediction with refined localization subcategories and predictive capabilities for all prokaryotes. *Bioinformatics* 26, 1608-1615.
- Yuryev, V.P., Tomasik, P., Bertoft, E., 2006. Starch: achievements in understanding of structure and functionality. In: Fiedorowicz M., Khachatryan G., Konieczna-Molenda A., Illumination of sago starch with linearly polarised visible light. Nova Science Publishers, New York, pp. 147-165.
- Zhu, M., Ajdić, D., Liu, Y., Lynch, D., Merritt, J., Banas, J.A., 2009. Role of the *Streptococcus mutans irvA* gene in GbpC-independent, dextran-dependent aggregation and biofilm formation. *Appl Environ Microbiol* 75, 7037-7043.